

STEADY STATE AND DYNAMIC BIOFILM CHARACTERISTICS
ASSOCIATED WITH PHENOL DEGRADATION
IN PULSED PLATE BIOREACTOR

Thesis

Submitted in partial fulfillment of the requirements for the degree of

DOCTOR OF PHILOSOPHY

by

VEENA B.R.



DEPARTMENT OF CHEMICAL ENGINEERING

NATIONAL INSTITUTE OF TECHNOLOGY KARNATAKA

SURATHKAL, MANGALORE-575025

AUGUST, 2016

DECLARATION

I, Veena B.R., *declare* that the Research Thesis entitled “Steady State and Dynamic Biofilm Characteristics Associated with Phenol Degradation in Pulsed Plate Bioreactor ” which is being submitted to the National Institute of Technology Karnataka, Surathkal in partial fulfillment of requirements for the award of the Degree of Doctor of Philosophy in Chemical Engineering is *a bonafied report of the research work carried out by me*. The material contained in this thesis has not been submitted to any University or Institution for the award of any degree.

VEENA B.R.

(110691CH11F02)

DEPARTMENT OF CHEMICAL ENGINEERING

Place: National Institute of Technology Karnataka

Surathkal-575025

Place: NITK-Surathkal

Date:

CERTIFICATE

This is to certify that the Research Thesis entitled “Steady State and Dynamic Biofilm Characteristics Associated with Phenol Degradation in Pulsed Plate Bioreactor ” submitted by Veena B.R. (Register Number: 110691CH11F02) as the record of the research work carried out by her, is accepted as the Research Thesis submission in partial fulfillment of the requirement of the award of degree of Doctor of Philosophy.

Research Guides

Dr. Vidya Shetty K
Associate Professor
Dept. of Chemical
Engineering
NITK, Surathkal

Dr.M.B.Saidutta
Professor
Department of Chemical Engineering
NITK, Surathkal

Chairman, DRPC

ACKNOWLEDGEMENT

I would like to express my highest gratitude to my research guides Dr. Vidya Shetty, Associate Professor, Department of Chemical Engineering, NITK Surathkal and Dr. M.B.Saidutta, Professor, Department of Chemical Engineering, NITK Surathkal for their suggestion to work on a research topic and their constant support throughout the research work for their encouragement who made me to grow as a research scientist. I am blessed to have my guides who were constantly guiding during my research work and writing of this thesis.

I would also like to thank my committee members, Dr. D V R Murthy and Dr. A. Nityananda Shetty for serving me as my committee members for their questions and valuable suggestions.

I would also express my sincere thanks to Director, NITK Surathkal. I would also thank the past and present Head, Department of Chemical Engineering, NITK Surathkal **Dr.M.B.Saidutta, Dr. K. VidyaShetty and Dr. B.Rajmohan** for providing me the necessary facilities and support during my research work.

I thank all the staff of the Department of Chemical Engineering, NITK Surathkal for their kind cooperation.

My special thanks to **P.T.RaghuRam**, Senior Scientific Officer, Department of Chemical Engineering, Indian Institute of science, who constantly supported and encouraged me during my whole research work and provided literature inputs as and when required.

My sincere thanks to **Dr. PremaChandra Sagar**, Vice Chairman for encouraging me to pursue this research work and granting me permission through QIP for doctoral programme. Also my sincere thanks to Secretary **Mr. Galiswamy** and past and present **Principal DSCE** for their moral support.

I thank all my friends at NITK , Head of the Department, Chemical Engineering, DSCE and all other colleagues at DSCE for their constant support.

A special thanks to my family. Words cannot express how grateful i am to my late father-in-law, who encouraged me in each and every aspect of my career until his last day of survival.

My deepest gratitude to my husband, Mr. **Sridhar B.T**, without his moral support and encouragement I couldnot have finished my work. My gratitude and appreciation to my dear son, Hemanth S.A., for his patience and understanding during my research work.

My sincere gratitude to Mrs. Chandrika Rao, PhD Scholar, Department of Computer Science, and Dr. Keshav Joshi, Professor and Head, Department of Chemical Engineering, SDM, Dharwad for their help and support during my research work.

My deepest gratitude to my sisters and to my brother for their endless love, prayers and encouragement. I also extend my gratitude to my brothers-in-laws, my nephews and my niece for their support in numerous ways.

I thank Dr. Ravishankar, Professor and Head, Department of Chemical Engineering, DSCE, for his constant support during my work.

Last but not least, my sincere gratitude to all my friends and other family members who supported during this journey.

Finally, I owe it all to God for giving me the strength to work beyond my limits and for fulfilling my desire.

Veena B.R.

**DEDICATED TO MY
MOTHER
AND
MY HUSBAND**

ABSTRACT

Phenol is considered to be one of the major pollutants in effluents from various industries. Biofilm reactors are the engineered systems extensively used for continuous biodegradation of phenol in wastewater. Stable and efficient operation of any biofilm reactor depends on the biofilm characteristics. The main components of biofilms are microorganisms and exopolymeric substances (EPS). The knowledge of biofilm characteristics and the factors that influence its formation and detachment behaviour would lead to better understanding, optimization, control and stability of biofilm reactors. In the present study, the steady state and start-up performance of pulsed plate bioreactor (PPBR) in continuous phenol degradation using *Pseudomonas desmolyticum* (NCIM 2112) cells immobilized on granular activated carbon (GAC) as the cell carrier material was investigated and the associated biofilm characteristics were evaluated under various operating conditions of the bioreactor such as frequency and amplitude of pulsation, cell carrier loading, dilution rate and influent phenol concentration. The physical characteristics of the biofilm such as its morphology, thickness, density and biomass dry weight; chemical characteristics such as the composition of EPS in terms of its protein, carbohydrate and humic substance content were evaluated and the effect of shear inducing conditions was investigated. Dynamics of biofilm in PPBR during the start up dominantly included three phases of accumulation, compaction and plateau. The PPBR could be continuously operated under stable conditions for degradation of phenol with influent concentration of upto 800 ppm with dilution rate of 0.33 h^{-1} at frequency of 0.08s^{-1} and amplitude of 5 cm to achieve greater than 99.5% degradation. Though stable operation of PPBR was possible at higher inhibitory concentrations of 1200 ppm, it is not recommended to operate at these concentrations owing to lower efficiency of phenol degradation. The characteristics of biofilm have been found to be influenced by the PPBR operating conditions and they play a dominant role in controlling the biofilm structure and integrity thus leading to stable operation of the bioreactor. Conditions which resulted in the formation of thinner, denser and compact biofilms with uniform and smooth surfaces have always led to better performance of PPBR in terms of phenol biodegradation. Artificial neural network model has been developed to predict the biofilm characteristics at steady state and during the start-up. The present study has successfully demonstrated that PPBR is an efficient biofilm reactor and can be employed in wastewater treatment for phenol degradation without much operational difficulties associated with controlling the biofilm thickness and stability.

Key words: biodegradation; biofilm; exopolymeric substances; phenol; pulsed plate bioreactor

TABLE OF CONTENTS

	List of Figures	
	List of Tables	
	Nomenclature	
Chapter	Title	Page Number
1	INTRODUCTION	1
1.1	Biofilm formation	2
1.2	Biofilms shearing/detachment	3
1.3	Biofilms in bioreactors	5
	Scope of the present study	8
	Research Objectives	11
	Organization of the thesis	12
2	LITERATURE REVIEW	13
2.1	Biofilm and its characteristics	13
2.1.1	Biofilm characteristics and the factors influencing them	14
2.2	Biofilm reactors	25
2.3	Phenol biodegradation in biofilm reactors	49
2.3.1	Biodegradation of phenol	49
2.3.2	Phenol biodegradation with immobilized cells	52
2.3.3	Bioreactors for phenol biodegradation	53
2.4	Pulsed plate bioreactor	59
3	MATERIALS AND METHODS	64
3.1	Microorganism	64

3.2	Materials	64
3.3	Methods	64
3.3.1	Preparation of phenol stock solution	64
3.3.2	Maintenance, subculturing and growth of the bacteria	65
3.3.2.1	Preparation of agar slant slant and subculturing of the bacteria	65
3.3.2.2	Growth of the bacterial culture in liquid media	66
3.3.3	Acclimatization of bacteria	66
3.3.4	Cell immobilization	67
3.3.5	Studies on pulsed plate bioreactor	69
3.3.5.1	Experimental setup	69
3.3.5.2	Experimental procedure	70
3.3.5.3	Experimental conditions for various studies	72
3.3.6	Extraction of EPS	73
3.3.7	Estimation of total protein concentration in EPS	73
3.3.8	Estimation of humic substance concentration in EPS	76
3.3.9	Estimation of total carbohydrate concentration in EPS	77
3.3.10	Analysis of phenol concentration	78
3.3.11	Estimation of attached biomass dryweight	80
3.3.12	Estimation of biofilm thickness and biofilm density	81
4	RESULTS AND DISCUSSION	82
4.1	Effect of dilution rate on steady state and startup performance of PBBR in terms of phenol biodegradation and biofilm characteristics	82
4.1.1	Effect of dilution rate on phenol biodegradation during start up and at steady state of PBBR	83
4.1.2	Effect of dilution rate on biofilm characteristics during startup and at steady state of PPBR	89

4.1.2.1	Chemical characteristics	90
4.1.2.2	Physical characteristics	95
4.2	Effect of influent substrate concentration on steadystate and startup performance of PPBR in terms of phenol biodegradation and biofilm characteristics.	107
4.2.1	Effect of influent substrate concentration on phenol biodegradation during startup and at steady state of PPBR	107
4.2.2	Effect of phenol concentration on biofilm characteristics during start up and at steady state of PPBR	111
4.2.2.1	Chemical characteristics	112
4.2.2.2	Physical characteristics	115
4.2.2.3	Effect of phenol loading rate on phenol removal rate	121
4.3	Effect of frequency of pulsation on steadystate and startup performance of PPBR	123
4.3.1	Effect of frequency of pulsation on phenol biodegradation during startup and at steady state of PPBR	123
4.3.2	Effect of frequency of pulsation on biofilm characteristics during startup and at steady state of PPBR	130
4.3.2.1	Effect of frequency of pulsation on chemical characteristics of EPS in biofilm during startup and at steady state of PPBR	130
4.3.2.2	Effect of frequency of pulsation on Physical characteristics of biofilm during startup and at steady state of PPBR	136
4.4	Effect of cell carrier loading on on steadystate and startup performance of PPBR in terms of phenol biodegradation and biofilm characteristics	145
4.4.1	Effect of cell carrier loading on phenol biodegradation during startup and at steady state of PPBR	147
4.4.2	Effect of cell carrier loading on biofilm characteristics during startup and at steady state of PPBR	151
4.4.2.1	Chemical characteristics	151
4.4.2.2	Effect of carrier loading on physical characteristics of biofilm	158

4.5	Effect of amplitude of pulsation on steadystate and startup performance of PPBR in terms of phenol biodegradation and biofilm characteristics at steady state and during strat-up	165
4.5.1	Effect of amplitude of pulsation on phenol biodegradation at steadystate and during startup of PPBR	165
4.5.2	Effect of amplitude of pulsation on biofilm characteristics during start up and at steady state of PPBR.	169
4.5.2.1	Effect of amplitude of pulsation on the chemical characteristics of the biofilm	169
4.5.2.2	Effect of amplitude on biofilm physical characteristics	175
5	MODELLING OF BIOFILM CHARACTERISTICS	185
5.1	Artificial Neural Networks (ANN)	187
5.2	ANN model development to predict the biofilm characteristics at steady state and during start-up of pulsed plate bioreator	190
6	SUMMARY AND CONCLUSIONS	208
	Appendix1	213
	Appendix 2	216
	REFERENCES	219
	List of publications based on research work	271
	Biodata	272

LIST OF FIGURES

Figure No.	Title	Page No.
3.1	Immobilized cells on GAC	68
3.2	Pulsed plate bioreactor	69
3.3	Calibration plot for protein using BSA as a standard	75
3.4	Calibration plot for humic substance with humic acid as standard	77
3.5	Calibration plot for carbohydrate analysis using glucose as standard	78
3.6	Calibration Plot for Phenol Estimation	80
4.1	Degradation of phenol during Start up for different dilution rates of 0.33,0.66,and 0.99h ⁻¹ with influent phenol concentration of (a) 200ppm (b)1200ppm. Conditions: f=0.08 s ⁻¹ ; A= 3.5 cm; GAC loading (S) = 80 g.	88
4.2	Performance of reactor for the removal of phenol with (a) bare GAC and (b) GAC with immobilized cells. Conditions: C _i =200ppm; A=3.5 cm; D=0.33h ⁻¹ ; S=80 g; f=0.08 s ⁻¹ ;S=80 g.	88
4.3	Effect of dilution rate on Start up time and percentage degradation at steady state with influent phenol concentration of (a) 200 ppm (b)1200 ppm.Conditions: A=3.5 cm; f=0.08 s ⁻¹ ; S =80 g.	89
4.4	Effect of dilution rate on production of (a) protein (b) carbohydrate (c) Humic substance in EPS component of biofilm during the bioreactor start-up period. Conditions: f=0.082 s ⁻¹ ; C _i = 200 ppm; A=3.5 cm; S=80 g.	93
4.5	Effect of dilution rate on production of (a) protein (b) carbohydrate (c) Humic substance in EPS component of biofilm during the bioreactor start-up period. Conditions: f=0.08 s ⁻¹ ; C _i =1200 ppm; A=3.5 cm; S =80g.	94

4.6	Effect of dilution rate on production EPS components in mg/g dry biomass, at influent phenol concentration of (a) 200ppm (b)1200ppm at steady state. Conditions: $f=0.08 \text{ s}^{-1}$; $A=3.5 \text{ cm}$; $S=80 \text{ g}$.	95
4.7	Sample cross sectional view for the measurement of biofilm thickness Conditions: $C_i=200 \text{ ppm}$; $f=0.08 \text{ s}^{-1}$; $A=3.5 \text{ cm}$; $S=80 \text{ g}$; $D=0.33\text{h}^{-1}$.	96
4.8	Effect of dilution rate on the biofilm dynamics in terms of physical characteristics (a) biofilm thickness (b) attached drybiomass (c) biofilm dry density during the start-up of bioreactor. Conditions; $C_i =200 \text{ ppm}$; $f=0.08 \text{ s}^{-1}$; $A=3.5 \text{ cm}$; $S=80 \text{ g}$.	102
4.9	Effect of dilution rate on biofilm dynamics in terms of physical characteristics (a) biofilm thickness (b) attached drybiomass (c) biofilm drydensity during the start-up of bioreactor. Conditions: $C_i =1200\text{ppm}$; $f=0.08 \text{ s}^{-1}$; $A=3.5 \text{ cm}$; $S=80 \text{ g}$.	103
4.10	Effect of dilution rate on biofilm physical characteristics at steady state for influent phenol concentration of (a)200 ppm and (b)1200 ppm . Conditions: $f =0.08\text{s}^{-1}$; $A=3.5 \text{ cm}$; $S=80 \text{ g}$	104
4.11	Morphological characteristics of biofilm during Start up for the frequency of 0.08s^{-1} and after the duration of a) 2h b) 4h c) 6h and d) 8h during the start-up of the bioreactor . Conditions: $C_i = 200 \text{ ppm}$; $f =0.08 \text{ s}^{-1}$; $A=3.5 \text{ cm}$; amount of GAC with immobilized cells=80 g.	105
4.12	Surface morphology of biofilm at steady state with different dilution ratesa) 0.33h^{-1} b) 0.66 h^{-1} c) 0.99h^{-1} at steady state. Conditions: $C_i =200 \text{ ppm}$; $f =0.08\text{s}^{-1}$; $A=3.5 \text{ cm}$; $S=80 \text{ g}$.	106
4.13	Degradation of phenol during Start up at different influent phenol concentration. Conditions: $D= 0.33 \text{ h}^{-1}$; $f= 0.08 \text{ s}^{-1}$; $A=3.5 \text{ cm}$; $S=80 \text{ g}$.	110
4.14	Effect of influent phenol concentration on percentage degradation of phenol at steady state. Conditions: $D= 0.33 \text{ h}^{-1}$; $f= 0.08 \text{ s}^{-1}$; $A=3.5 \text{ cm}$; $S=80 \text{ g}$.	111
14.15	Effect of influent phenol concentration during start-up time. Conditions: $D= 0.33 \text{ h}^{-1}$; $f= 0.08 \text{ s}^{-1}$; $A=3.5 \text{ cm}$; $S=80 \text{ g}$.	111

14.16	Effect of phenol concentration on production of (a) protein (b) humic substance and (c) carbohydrate in EPS component of biofilm. Conditions: $f=0.08\text{ s}^{-1}$; dilution rate= 0.33 h^{-1} ; $A=3.5\text{ cm}$; $S=80\text{ g}$.	114
4.17	Quantity of EPS components at steady state for various influent phenol concentraions. Conditions: Amplitude of 3.5cm ; $f=0.08\text{ s}^{-1}$; $S=80\text{g}$; $D=0.33\text{h}^{-1}$.	115
4.18	Effect of phenol concentration on the biofilm dynamics in terms of physical characteristics (a) biofilm thickness (b) attached drybiomass (c) biofilm dry density during the start-up of bioreactor. Conditions: $D=0.33\text{ h}^{-1}$; $f=0.08\text{ s}^{-1}$; $A=3.5\text{ cm}$; $S=80\text{ g}$.	118
4.19	Effect of phenol concentration on physical characteristics of biofilm at various influent phenol concentrations at steady state. Conditions: $D=0.33\text{ h}^{-1}$; $f=0.08\text{ s}^{-1}$; $A=3.5\text{ cm}$; $S=80\text{ g}$.	119
4.20	Surface morphology of biofilm at various influent phenol concentrations at steady state (a) 200ppm (b) 400ppm (c) 600ppm (d) 800ppm and (e) 1200ppm. Conditions: $f=0.08\text{s}^{-1}$; $A=3.5\text{ cm}$; $S=80\text{ g}$; $D=0.33\text{ h}^{-1}$.	120
4.21	Effect of phenol loading rate on phenol removal rate. Conditions: $D=0.33\text{ h}^{-1}$; $f=0.08\text{ s}^{-1}$; $A=3.5\text{ cm}$; $S=80\text{ g}$.	122
4.22	Degradation of phenol during Start up for different frequencies a) 0.08 s^{-1} b) 0.12 s^{-1} c) 0.16 s^{-1} . Conditions: $C_i=200\text{ppm}$; $D=0.33\text{h}^{-1}$; $A=3.5\text{ cm}$; $S=80\text{ g}$.	126
4.23	Degradation of phenol during Start up period for different frequencies frequencies a) 0.08 s^{-1} b) 0.12 s^{-1} c) 0.16 s^{-1} . Conditions: $C_i=400\text{ppm}$; $D=0.33\text{ h}^{-1}$; $A=3.5\text{ cm}$; $S=80\text{ g}$.	127
4.24	Degradation of phenol during Start up period for different frequencies frequencies a) 0.08 s^{-1} b) 0.12 s^{-1} c) 0.16 s^{-1} . Conditions: $C_i=600\text{ ppm}$; $D=0.33\text{ h}^{-1}$; $A=3.5\text{cm}$; $S=80\text{ g}$.	128
4.25	Degradation of phenol during Start up period for different frequencies frequencies a) 0.08 s^{-1} b) 0.12 s^{-1} c) 0.16 s^{-1} . Conditions: $C_i=800\text{ ppm}$; $D=0.33\text{ h}^{-1}$; $A=3.5\text{cm}$; $S=80\text{ g}$.	129

4.26	Effect of frequency of pulsation on (a) start-up time (b) steady state percentage degradation at various influent phenol concentrations. Conditions: $D=0.33 \text{ h}^{-1}$; $A=3.5 \text{ cm}$; $S=80 \text{ g}$.	129
4.27	Effect of frequency of pulsation on production of EPS component of biofilm. (a) protein (b) humic substance (c) carbohydrate content. Conditions: $C_i=200 \text{ ppm}$; $D=0.33 \text{ h}^{-1}$; $A=6.5 \text{ cm}$; $S=80 \text{ g}$.	132
4.28	Effect of frequency of pulsation on production of EPS component of biofilm. (a) protein (b) humic substance (c) carbohydrate content. Conditions: $C_i=400 \text{ ppm}$; $D=0.33 \text{ h}^{-1}$; $A=6.5 \text{ cm}$; $S=80 \text{ g}$.	133
4.29	Effect of frequency of pulsation on production of EPS component of biofilm. (a) protein (b) humic substance (c) carbohydrate content. Conditions: $C_i=600 \text{ ppm}$; $D=0.33 \text{ h}^{-1}$; $A=6.5 \text{ cm}$; $S=80 \text{ g}$.	134
4.30	Effect of frequency of pulsation on production of EPS component of biofilm. (a) protein (b) humic substance (c) carbohydrate content. Conditions: $C_i=800 \text{ ppm}$; $D=0.33 \text{ h}^{-1}$; $A=6.5 \text{ cm}$; $S=80 \text{ g}$.	135
4.31	Effect of frequency of pulsation on quantity of EPS component at different influent phenol concentrations (a) 200 ppm (b) 400 ppm (c) 600 ppm and (d) 800 ppm. Conditions: $D=0.33 \text{ h}^{-1}$; $A=6.5 \text{ cm}$; $S=80 \text{ g}$.	136
4.32	Effect of frequency of pulsation on biofilm physical characteristics during start up (a) biofilm thickness (b) attached drybiomass and (c) biofilm dry density. Conditions: $C_i=200 \text{ ppm}$; $D=0.33 \text{ h}^{-1}$; $A=3.5 \text{ cm}$; $S=80 \text{ g}$.	140
4.33	Effect of frequency of pulsation on biofilm physical characteristics during start up (a) biofilm thickness (b) attached drybiomass and (c) biofilm dry density. Condition: $C_i=400 \text{ ppm}$; $D=0.33 \text{ h}^{-1}$; $A=3.5 \text{ cm}$; $S=80 \text{ g}$.	141
4.34	Effect of frequency of pulsation on biofilm physical characteristics during start up (a) biofilm thickness (b) attached drybiomass and (c) biofilm dry density. Conditions: $C_i=600 \text{ ppm}$; $D=0.33 \text{ h}^{-1}$; $A=6.5 \text{ cm}$; $S=80$.	142
4.35	Effect of frequency of pulsation on biofilm physical characteristics during start up (a) biofilm thickness (b) attached drybiomass and (c) biofilm dry density. Conditions: $C_i=800 \text{ ppm}$; $f=0.33 \text{ h}^{-1}$; $A=6.5 \text{ cm}$; $S=80 \text{ g}$.	143

- 4.36 Effect of frequency of pulsation on physical characteristics at steady state with 144
influent phenol concentrations of (a) 200 ppm (b) 400 ppm (c) 600 ppm and (d)
800 ppm. Conditions: $C_i=800$ ppm; $f=0.33$ h⁻¹; $A=3.5$ cm; $S=80$ g
- 4.37 Morphological characteristics of steady state biofilm at different 145
frequencies (a)0.08 s⁻¹ (b)0.12 s⁻¹ and (c) 0.16 s⁻¹ and at the end of 8h.
Conditions $C_i=800$ ppm; $f=0.33$ h⁻¹; $A=6.5$ cm; $S=80$ g.
- 4.38 Variation in phenol concentration during the Start up period for different 149
cell carrier loading of a) 80g and b)120 g for various influent phenol
concentrations of 200ppm and 400ppm. Conditions: $f=0.08s^{-1}$; $D=0.33h^{-1}$;
 $A=3.5cm$.
- 4.39 Variation in phenol concentration during Start up period for different cell 150
carrier loading of a)80 g b)120 g for various influent phenol
concentraions of 600 ppm and 800 ppm. Conditions: $f=0.08$ s⁻¹; $D=0.33$
h⁻¹; $A=3.5cm$.
- 4.40 Effect of cell carrier loading on (a) Start up time (b) percentage 151
degradation of phenol at steady state for various influent phenol
concentrations. Conditions: $D=0.33$ h⁻¹; $A=3.5$ cm; $f=0.08$ s⁻¹.
- 4.41 Effect of cell carrier loading on production EPS components during start up (a) 154
protein content (b) carbohydrate content and (c) humic substance content of EPS
for influent phenol concentration of 200 ppm. Conditions: $f= 0.08$ s⁻¹; $D=0.33$ h⁻¹;
 $A=3.5$ cm.
- 4.42 Effect of cell carrier loading on production EPS components during start up (a) 155
protein content (b) carbohydrate content and (c) humic substance content of EPS
for influent phenol concentration of 400 ppm. Conditions: $f= 0.08$ s⁻¹; $D=0.33$ h⁻¹;
 $A=3.5$ c
- 4.43 Effect of cell carrier loading on production EPS components during start up (a) 156
protein content (b) carbohydrate content and (c) humic substance content of EPS
for influent phenol concentration of 600 ppm. Conditions: $f= 0.08$ s⁻¹; $D=0.33$ h⁻¹;
 $A=3.5$ cm

4.44	Effect of cell carrier loading on production EPS components during the start-up (a) protein content (b) carbohydrate content and (c) humic substance content of EPS for influent phenol concentrations of 800ppm. Conditions: $f=0.08\text{ s}^{-1}$; $D=0.33\text{ h}^{-1}$; $A=3.5\text{ cm}$.	157
4.45	Effect of cell carrier loading on quantity of EPS components at steady state with influent phenol concentration of a) 200ppm b) 400ppm c) 600ppm and d) 800ppm. Conditions: $f=0.08\text{ s}^{-1}$; $A=3.5\text{ cm}$; $D=0.33\text{ h}^{-1}$.	158
4.46	Effect of cell carrier loading on physical characteristics of biofilm during the start-up (a) biofilm thickness (b) attached dry biomass, and (c) biofilm drydensity for the influent phenol concentration of 200ppm. Conditions: $f=0.08\text{ s}^{-1}$; $A=3.5\text{ cm}$; $D=0.33\text{ h}^{-1}$.	160
4.47	Effect of cell carrier loading on physical characteristics of biofilm during the start-up (a) biofilm thickness (b) attached dry biomass, and (c) biofilm drydensity for the influent phenol concentration of 400 ppm. Conditions: $f=0.08\text{ s}^{-1}$; $A=3.5\text{ cm}$; $D=0.33\text{ h}^{-1}$.	161
4.48	Effect of cell carrier loading on physical characteristics of biofilm during the start-up (a) biofilm thickness (b) attached dry biomass, and (c) biofilm drydensity for the influent phenol concentration of 600ppm. Conditions: $f=0.08\text{ s}^{-1}$; $A=3.5\text{ cm}$; $D=0.33\text{ h}^{-1}$.	162
4.49	Effect of cell carrier loading on physical characteristics of biofilm during the start-up (a) biofilm thickness (b) attached dry biomass, and (c) biofilm drydensity for the influent phenol concentration of 800ppm. Conditions: $f=0.08\text{ s}^{-1}$; $A=3.5\text{ cm}$; $D=0.33\text{ h}^{-1}$.	163
4.50	Effect of cell carrier loading on physical characteristics of biofilm at steady state for the influent phenol concentrations of (a) 200 (b) 400 (c) 600 and (d) 800ppm. Conditions: $f=0.08\text{ s}^{-1}$; $A=3.5\text{ cm}$; $D=0.33\text{ h}^{-1}$.	164
4.51	Effect of cell carrier loading on morphological characteristics of biofilm at steady state. (a) 80 g and (b)120g of GAC loading. Conditions: $f=0.08\text{ s}^{-1}$; $A=3.5\text{ cm}$; $D=0.33\text{ h}^{-1}$; $C_i=200\text{ ppm}$.	164

4.52	Effect of amplitude of pulsation on phenol degradation for influent phenol concentration of a) 200ppm b) 400ppm c) 600ppm and d) 800ppm. Conditions: $f = 0.08 \text{ s}^{-1}$; $D=0.33 \text{ h}^{-1}$; $S=80 \text{ g}$.	168
4.53	Effect of amplitude of pulsation on (a) percentage conversion of phenol (b) Start up time. Conditions: $f=0.08\text{s}^{-1}$; $S = 80 \text{ g}$.	169
4.54	Effect of amplitude of pulsation on production of (a) Protein (b) Humic substance and (c) Carbohydrate contents of EPS during start up at influent phenol concentration of 200 ppm. Conditions: $f=0.08 \text{ s}^{-1}$; $D=0.33 \text{ h}^{-1}$; $S=80 \text{ g}$.	171
4.55	Effect of amplitude of pulsation on production of (a) Protein (b) Humic substance and (c) Carbohydrate contents of EPS during start up at influent phenol concentration of 400 ppm. Conditions: $f=0.08 \text{ s}^{-1}$; $D=0.33 \text{ h}^{-1}$; $S=80 \text{ g}$.	172
4.56	Effect of amplitude of pulsation on production of (a) Protein (b) Humic substance and (c) Carbohydrate contents of EPS during start up at influent phenol concentration of 600 ppm. Conditions: $f=0.08 \text{ s}^{-1}$; $D=0.33 \text{ h}^{-1}$; $S=80 \text{ g}$.	173
4.57	Effect of amplitude of pulsation on production of (a) Protein (b) Humic substance and (c) Carbohydrate contents of EPS during start up at influent phenol concentration of 800 ppm. Conditions: $f=0.08 \text{ s}^{-1}$; $D=0.33 \text{ h}^{-1}$; $S=80 \text{ g}$.	174
4.58	Effect of amplitude of pulsation on production of EPS components at steady state with influent phenol concentrations of a) 200 ppm b) 400 ppm c) 600 ppm and d) 800ppm. Conditions: $f = 0.08 \text{ s}^{-1}$; $D=0.33 \text{ h}^{-1}$; $S=80 \text{ g}$.	175
4.59	Effect of amplitude of pulsation on physical characteristics of the biofilm during start-up a) biofilm thickness b) attached dry biomass and c) biofilm dry density for 200 ppm of influent phenol concentration . Conditions: $f=0.08\text{s}^{-1}$; $D=0.33 \text{ h}^{-1}$; $S=80 \text{ g}$.	178
4.60	Effect of amplitude of pulsation on physical characteristics of the biofilm during start-up a) biofilm thickness b) attached dry biomass and c) biofilm dry density for 400ppm of influent phenol concentration. Conditions: $f=0.08 \text{ s}^{-1}$; $D=0.33 \text{ h}^{-1}$; $S=80 \text{ g}$.	179

4.61	Effect of amplitude of pulsation on physical characteristics of the biofilm during start-up a) biofilm thickness b) attached dry biomass and c) biofilm dry density for 600 ppm of influent phenol concentration . Conditions: $f=0.08\text{ s}^{-1}$; $D=0.33\text{ h}^{-1}$; $S=80\text{ g}$.	180
4.62	Effect of amplitude of pulsation on physical characteristics of the biofilm during start-up a) biofilm thickness b) attached dry biomass and c) biofilm dry density for 800 ppm of influent phenol concentration . Conditions: $f=0.08\text{ s}^{-1}$; $D=0.33\text{ h}^{-1}$; $S=80\text{ g}$.	181
4.63	Effect of amplitude of pulsation on physical characteristics of biofilm at steady state for various influent phenol concentration of a)200 ppm b) 400ppm c) 600ppm and d)800ppm. Conditions: $f=0.08\text{ s}^{-1}$; $D=0.33\text{ h}^{-1}$; $S=80\text{ g}$.	182
4.64	Effect of amplitude of pulsation on morphological characteristics of biofilm at steady state .(a) 3.5cm (b) 5cm and (c) 6.5 cm. Conditions:Influent phenol concentration =200 ppm $f=0.08\text{ s}^{-1}$; $D=0.33\text{ h}^{-1}$; $S=80\text{ g}$.	183
5.1	Architecture of feed forward network.	188
5.2	Neuron model	188
5.3	Output (model predicted) vs Target(experimental) values for training, testing, validation and the total data set points during Start up studies.	201
5.4	Experimental vs predicted values of the ANN model with blind data set for Start up (a)Biofilm thickness, μm (b) Biofilm density, g/cc (c)Protein content of EPS, mg/g dry biomass (d) Humic substance content of EPS, mg/ g drybiomass amd (e) Carbohydrate content of EPS, mg/g dry biomass.	202
5.5	Output(predicted) vs Target (experimental) values for training, testing, validation and the total data set points by ANN for steady state.	206

List of Tables

Table No.	Contents	Page No.
2.1	Biofilm reactors used for different applications	28
3.1	Composition of Bushnell Haas Broth Medium	65
4.1	Fig 4.21 Effect of phenol loading rate on phenol removal rate. Conditions: $D= 0.33 \text{ h}^{-1}$; $f= 0.08 \text{ s}^{-1}$; $A=3.5 \text{ cm}$; $S=80 \text{ g}$.	122
5.1	Input data for training artificial neural network system during startup period	193
5.2	Blind test data for artificial neural network system during startup period	200
5.3	Data for training artificial neural network system to predict the steady state biofilm characteristics	204

NOMENCLATURE/NOTATIONS

A	Amplitude of pulsation, cm
ATCC	American Type Culture Collection
BAS	Biofilm Airlift Suspension Reactor
BOD	Biological oxygen demand
C	Effluent phenol concentration, ppm
C:N	Carbon to Nitrogen
C:P	Carbon to Phosphorus
CH	Carbohydrate content of EPS
C _i	Influent phenol concentration, ppm
COD	Chemical oxygen demand
D	Dilution rate, h ⁻¹
DOC	Dissolve organic carbon
D _p	Diameter of particle, cm
EPS	Exopolymeric substances
f	Frequency of pulsation, s ⁻¹
G	Gram
GAC	Granular activated carbon
H	Hour
HRT	Hydraulic retention time, h
HS	Humic substance content of EPS , mg/gdrybiomass
kDa	Kilo Dalton
LPM	Litre per minute
mgL ⁻¹	Milligram per litre
N	Concentraion in Normality
NCIM	National collection of industrial microorganisms
Nm	Nanometre
N _p	Number of solid particles
P	Protein content of EPS , mg/gdrybiomass
PPBR	Pulsed Plate Bioreactor
Ppm	Parts per million

QS	Quorum Sensing
rpm	Revolution per minute
S	Solid loading to the reactor, g
SBBR	Sequential Batch Biofilm Reactor
SBR	Sequential Batch Reactor
SEM	Scanning electron microscope
VSL ⁻¹	Volatile solids per litre
W	Weight of dry attached biomass, g
w ₁	Mass of GAC withdrawn from reactor to extract EPS
w ₂	Mass of GAC withdrawn to find quantity of biomass
w ₃	Mass of biomass(g) present in w ₂ g of GAC
δ	Biofilm thickness, cm
μm	Micrometre
ρ	Density of biofilm, g/cc

CHAPTER 1

INTRODUCTION

Phenol is considered as one of the major toxic pollutants present in effluents from various industries viz., oil refineries, coal conversion, pharmaceutical and food industries etc. (Passos *et al.* 2010; Nair *et al.* 2008; Yan *et al.* 2005; Tseng and Juang 2003). Phenol containing effluents, if discharged into water bodies prior to its treatment, may pose serious health and environmental problems. Phenol is harmful if enters the body by ingestion, skin absorption or by inhalation. It causes severe eye irritation, mucous membranes, respiratory tract if exposed directly and it damages kidney and liver too. Presence phenol has serious effect on flora and fauna, animals, aquatic life and humans too, even at very low concentration (Naresh *et al.* 2012 ; ATSDR 2008; Gad and Saad 2008).

Maximum allowable phenol concentration in the industrial effluent will be specified by most of the countries. Phenol is listed as priority organic pollutant by US Environmental protection agency (EPA 2014). Central Pollution Control Board (CPCB), India, has set the maximum permissible phenol concentration as 1ppm to be discharged to water bodies (The Environment (Protection) Rules 1986a) ; World Health Organization (WHO) has set the permissible concentration of phenol as 1µg/l in drinking water (WHO 2011).

To prevent the ill effects of phenol caused by discharge of polluted water into water bodies and to meet the discharge standards specified by the regulatory bodies, it is important to treat phenol contaminated wastewaters prior to discharge. Various methods are available to treat the effluent containing phenol viz. physical, chemical and biological methods (Pishgar *et al.* 2011). Some of the physical and chemical methods of phenol removal are adsorption, incineration, extraction by using solvents, chlorination, oxidation processes, ozonation, photocatalysis, sonochemical reaction, biological oxidation process and electrochemical methods, etc. These methods seem to be either complex,

uneconomical or cause secondary pollution. In this context, biodegradation process appears to be the more promising method over the conventional methods (Shetty *et al.* 2013 ; Hsien and Lin 2005). Biological method is advantageous over other methods as complete mineralization of phenol can be achieved by this method and the process can be carried out under ambient conditions, without the use of toxic chemicals (Dey and Mukherjee 2010; Nair *et al.* 2008). In the biological methods, the various microorganisms belonging to the class of bacteria (pseudomonas species, Anthrobacter species etc.), fungi (candida species, Fusarium, Aspergillus etc.) or yeast (*Phanerochaete*, *Rhodococcus* etc.) are used to degrade phenol to simpler compounds (Basha *et al.* 2010).

Microorganisms for degrading phenol may be used in suspended form (Naresh *et al.* 2012; Agarry *et al.* 2008; Seker *et al.* 1997) or in immobilized/attached growth form (Dabhade *et al.* 2009; Nair *et al.* 2008; Shetty *et al.* 2007). The bioreactors for wastewater treatment may be suspended or immobilized cell types. Attached growth or biofilm systems are a type of immobilized cell systems. The use of biofilm reactors is generally adopted in the process of wastewater treatment (Van Loosdrecht *et al.* 1995). Biofilm is a community of microorganisms enclosed in a polymeric matrix that are adhered to living or nonliving surfaces. Biofilm reactors are advantageous compared to suspended cell reactors as they provide high biomass retention and density, higher resistance to toxicity, overcome dilution rate limitations and cell separation problems (Pellicer and Smets 2014; Shetty *et al.* 2013; Shetty *et al.* 2007), and enhance the stability of the process (Cheng *et al.* 2010) etc.

1.1 Biofilm formation

Biofilm formation is regulated by different genetic factors such as bacterial mobility, cell membrane proteins, extracellular polysaccharides, signaling molecules and environmental factors such as nutrient availability, presence of oxygen, temperature , pH, and hydrodynamics (Maric and Vranes 2007). There are number of biochemical and

genetic mechanisms involved in the process of biofilm formation. In recent studies it is learnt that one of the reasons for the formation of biofilm is based on the assumption that these structured associates are a means of protecting microorganisms from stress conditions (Nikolaev and Plakunov 2007).

Microbial cells (living or dead) and exopolymeric substances (EPS) are the main components of biofilm. Proteins, carbohydrates and humic substances are the major components of EPS and they contribute as the key components in the biofilm structure (More *et al.* 2014). The other components present in EPS are nucleic acids, lipids and other polymeric compounds. Microorganisms produce EPS to protect themselves from harsh environmental conditions and toxic substances. EPS binds the cells together forming a complex structure (Kumar *et al.* 2011). EPS are mainly responsible for the structural and functional integrity of biofilm and they play a major role in determining the physical, chemical and biological properties of biofilms (Denkhaus *et al.* 2007). Protein contributes for the adhesion and cohesion of biofilm whereas carbohydrate contributes for the structural stability and architecture of biofilm (Anderrson *et al.* 2009). EPS significantly influences the structure, adsorption ability, dehydration of the biofilm.

EPS are responsible for the formation and structure of biofilm. The composition of EPS depends on various factors viz., type of microorganisms, age of biofilm, nutrient availability, environmental conditions, shear stress, bioreactor type etc. (Sheng *et al.* 2010; Pei Shi *et al.* 2008). In depth studies on EPS is important both in understanding the biological processes and in improving the efficiency of such systems through variation of operational parameters (Sheng *et al.* 2010).

1.2 Biofilm Shearing/Detachment

The attachment of microbial cells and the production of polymeric substances helps in the formation of biofilm and the other side shear forces tend to remove certain parts of biofilm termed as biofilm detachment (Grany *et al.* 2008; Bakke *et al.* 1984). The detachment force influences the production rate of microorganisms and hence the

balance between them is an important factor to be considered for the performance (Coetser and Cloete 2005; van Loosdrecht et al. 1995; Characklis 1990).

It is shown by few of the authors that a higher detachment force would result in a stronger biofilm, however biofilm tend to form heterogeneous, porous, weaker structure when the detachment force is weak (Chen *et al.* 1998; Van Loosdrecht *et al.* 1995; Kwok *et al.* 1998; Chang *et al.* 1991; Rittmann 1982a). Liu and Tay (2001) discussed o the effect of detachment forces on the structure and metabolic behaviour of biofilms in biological systems and discussed the mechanism in response to detachment forces under hydrodynamic conditions and reported that the formation of stable biofilm was possible at higher detachment forces leading to denser biofilm. Iliuta and Larachi (2006) showed that the detachment from a surface is induced by colloidal forces in case of Brownian cells/aggregates or by the hydrodynamic forces in case of non-Brownian aggregates. Liu *et al.* (2002) showed that biofilm structure and metabolism are closely related to the interaction between detachment and growth forces. Certain components present in the microbial cell environment may inhibit the production of extracellular polymeric substances reducing microbial attachment and inducing the detachment (Xu and Liu 2011).

Hydrodynamics greatly influences mass transfer mechanisms and also creates stresses that impart direct action on biostructure deformation and detachment. The balance between the growth and detachment of the cells govern the biofilm formation. Shear and particle collision, along with growth rate of biofilms results in biofilm detachment (Garny *et al.* 2008; Villasenor *et al.* 2000). Shear stress affects the biofilm thickness, surface roughness and the biofilm density and thus is an important parameter in bioreactors (Villasenor *et al.* 2000) . The adhesion of cells depends on hydrophobicity of the microbial cells. The adhesion is poor for some of the microorganisms that are less hydrophobic in nature compared to others. Surface charge is also one of the factors influencing the attachment. Negative charge inhibits the adhesion of species whereas presence of surface cations increases adhesion of some micro-organisms. Flow of liquid is the main factor that affects behavior of micro-organisms. Oxygen concentration can

also affect bacterial adhesion. Biotic factors contribute to the degree of adhesion; e.g. for the culture of anaerobic bacteria, adhesive capacity is pronounced in early stage of logarithmic phase, decreases with age, and becomes negligibly low with depletion of nutrient in the medium (Nikolaev and Plakunov 2007).

In biofilm systems, a higher detachment force would result in a stronger biofilm, however biofilm tend to form heterogeneous, porous, weaker structure when the detachment force is weak (Chen *et al.* 1998; Kwok *et al.* 1998; Van Loosdrecht *et al.* 1995; Chang *et al.* 1991; Rittmann 1982a). The formation, structure and metabolic activity of the biofilms are closely associated with the detachment forces in the biofilm process. A more compact, stable and denser biofilm can be formed at relatively higher detachment forces. Liu and Tay (2001) worked on the effect of detachment forces on the structure and metabolic behavior of biofilms in biological systems and discussed the mechanism in response to detachment forces under hydrodynamic conditions.

Biofilm structure also depends on the type of substrate. The influence of different substrates on biofilm formation has been reported by Villasenor *et al.* (2000). Thus biofilm structure and characteristics vary with substrate, substratum (cell carrier) surface, microorganism and shear conditions in the environment.

1.3 Biofilms in Bioreactors

Biofilms are widely important in nature and in engineered processes. So a fundamental understanding of their growth and behavior is required. The Biofilm reactors are the engineered processes extensively used in waste water treatment, since (1) large volumes of dilute, aqueous solutions are to be treated and in free cell systems, the flow rates which can be handled are limited due to problems with cell washout, whereas cell washout limitations are overcome in biofilm systems (Pellicer-Nàcher and Smets 2014; Shetty *et al.* 2013; Shetty *et al.* 2007; Lopes *et al.* 2000) in comparison with most of the other industrial bioprocesses (2) natural microorganisms which readily form biofilms are used and (3) the process can be operated at high biomass concentration without requirement of separation of biomass and the treated effluent (Van Loosdrecht 1993).

Submerged filters, land treatment systems, rotating biological contactors, biological activated carbon beds and fluidized bed reactors are engineered processes that utilize biofilms (Tanyolac and Beyenal 1998). Surprisingly the formation, structure and metabolic activity of the biofilms are closely associated with the detachment forces in the bioreactors. In a biological reactor, the detachment force resulting from hydraulic shear and /or particle-particle collision is a key factor that influences formation, structure and stability of biofilm under hydrodynamic conditions. In a biofilm reactor the detachment forces are most often considered in relation to the mass transfer of the substrate. It is generally considered that substrate flux inside the biofilm would be increased with the increase of hydrodynamic conditions (Wasche *et al.* 2000 ; Furumai and Rittmann 1994; Rittmann *et al.* 1992; Trulear and Charaklis 1982). A more compact, stable, thinner and denser biofilm can be formed at relatively higher detachment force (Wasche *et al.* 2000 ; Kwok *et al.* 1998 ; Van Loosdrecht *et al.* 1995 ; Ohashi and Harada 1994; Vieira *et al.* 1993).

Garny *et al.* (2008) investigated biofilm development and detachment under different hydrodynamic conditions and at different substrate loading in rotating annular reactors. It was observed that the detachment rate was higher at higher substrate load than at lower substrate loading. Speitel *et al.* (1987) used packed bed columns with granular activated carbon as supporting material and studied biofilm shearing under dynamic conditions. They found that at rapidly changing biodegradation rate, the biofilm shearing is related to microbial growth than the amount of attached biomass. Sawyer and Hermanowicz (2000) showed that the depletion of nutrient on *Pseudomonas Aeruginosa* and *Aeromonas hydrophilla* lead to higher detachment. Knowledge of the composition of biofilms and the factors that influence the biofilm formation and detachment behaviour could lead to better understanding, optimisation and control of biofilm development or the prevention of contamination or clogging of bioreactors (Garny *et al.*, 2008).

There are a few studies on the effect of detachment forces on biofilm structure and morphology in certain bioreactors like fluidized bed bioreactors (Alves *et al.* 2002;

Chang *et al.* 1991; Rittmann 1982), differential fluidized bed biofilm reactor (Tanyolac and Beyenal 1998; Sekar *et al.* 1995), Inverse fluidized bed biofilm reactor (Nikolov and Karmanev 1990), Biofilm Airlift Suspension Reactor (Villaseñor *et al.* 2000; Kwok *et al.* 1998), rotating annular reactors and packed bed or fixed biofilm reactors (Hsien and Lin 2005; Speitel *et al.* 1987 ; Rittmann 1982). The structure of biofilm is affected by factors like detachment force and production of biopolymers in air suspension reactor as reported by Kwok *et al.* (1998). Seker *et al.* (1995) have reported the effect of biofilm thickness on density of biofilm and substrate consumption rate in differential fluidized bed reactor. The interaction between biofilm structure, formation, and detachment in rotating annular reactor has been reported by Garny *et al.* (2008). Pei-Shi *et al.* (2008) have found that shear stress influences the biofilm morphology and EPS production through their studies in suspended carrier biofilm reactor. Similar observations have been made by Mennit *et al.* (2009) in membrane biofilm reactor. Lopes *et al.* (2000) reported on chemical composition and activity of a biofilm during the Start up of an air lift reactor. Recently Begum and Radha (2015) studied the hydrodynamic effects on the performance of inverse fluidized bed biofilm reactor in terms of biofilm thickness, biofilm dry density, attached and suspended biomass concentration, using low density polystyrene as support material for the growth of bacterial *Pseudomonas fluorescens* for degradation of phenol.

For a stable operation and performance of bioreactors, morphological characteristics of the biofilm viz. biofilm thickness, biofilm density and surface characteristics are the important factors to be considered. Kwok *et al.* (1998) and Sekar *et al.* (1995) have reported that biofilm density and biofilm thickness often govern the performance of bioreactors. It is important to have knowledge on biofilm structure as it (i) helps in understanding, interpretation and prediction of the influence the biofilm may have on a system (ii) provides an ability to manipulate the biofilm structure in order to create a biofilm with the morphology and structure desired for certain applications (Picioreanu *et al.* 2000).

Scope of the present study

Biofilm composition and biofilm characteristics (physical characteristics) greatly influences the performance of a reactor. Extensive review of literature presented in Chapter 2 indicates that, most of the research papers report the physical characteristics of biofilm viz. biofilm thickness and biofilm density. Studies on biofilm morphology and composition in bioreactors are scarce. There are a very few reports on the studies on composition of biofilm and the influence of reactor conditions on the biofilm composition.

Recently pulsed plate bioreactor (PPBR) with immobilized cells has been reported to be very efficient in continuous degradation of phenol (Shetty *et al.* 2007). This bioreactor has shown the potential to be used as a bioreactor for continuous treatment of industrial effluents. It contains a reciprocating shaft with stack of perforated plates, which may offer very high shear stress on the biofilm. Presence of moving parts may impart high shear forces on the biofilm and hence may influence the biofilm structure, characteristics and composition. The high shear inducing characteristics of this bioreactor makes it an ideal candidate for studies on the effect of operating variables on the biofilm characteristics. The bioreactor operational variables such as frequency and amplitudes of pulsation may tremendously influence the shear conditions in the bioreactor and hence may affect the biofilm characteristics. Understanding the effect of these shear inducing operational variables on biofilm characteristics and its dynamics adds a new knowledge in development and operation of pulsed plate bioreactor for wastewater treatment applications and it may help in controlling the bioreactor performance. The new knowledge base can also help in providing more understanding on the influence of the operating variables on biofilm structure, morphology and composition along with its dynamic behavior during reactor start-up.

Detailed literature review on the effect of various factors influencing the biofilm formation, morphology, structure and composition in various reactors suggested that the biofilm formation, morphology, structure and composition depend on the microbial

species forming the biofilm, the support material on which the biofilm is formed, the type of substrate used and the type of bioreactor in which the biofilm is grown with the utilization of the specific substrate. Thus, during the development of any bioreactor for a specific duty of utilization of a given substrate with the cells of specific microbial species grown as a biofilm on a selected support, a detailed study on the effect of bioreactor operating variables on biofilm growth behavior in coordination with the substrate utilization, dynamics of biofilm formation during start-up, steady state biofilm characteristics is necessary (i) to facilitate a thorough understanding of the bioreactor system (ii) facilitate interpretation and prediction of the influence the biofilm may have on the bioreactor performance (iii) to provide useful information required to manipulate the biofilm structure in order to create a biofilm with the morphology and structure desired for the designated application

This thesis presents the investigations on the biofilm characteristics and the factors influencing it in pulsed plate bioreactor during continuous biodegradation of phenol by the cells of *Pseudomonas desmolyticum* strain (NCIM 2112) immobilized on granular activated carbon. *Pseudomonas desmolyticum* cells were chosen owing to their effectiveness in biodegradation of phenol as reported by Sridevi and Lakshmi (2009). Granular activated carbon was used as a support material (carrier) for biofilm in pulsed plate bioreactor, as it was earlier effectively used as a support matrix in cell immobilization for phenol degradation by Dabhade (2009) in spouted bed reactor, Wang and Li (2007) in immobilized membrane bioreactor.

The literature review also suggested that (i) the reports on the biofilm dynamics during start-up of the bioreactors are scarce (ii) limited reports are available on the effect of bioreactor operating variables on the chemical composition of the biofilm or EPS in biofilm (iii) No study is available on the detailed physical and chemical characteristics of biofilm at steady state and during start-up of pulsed plate bioreactor (iv) The studies on biofilm growth behavior in coordination with phenol degradation by the cells of

Pseudomonas desmolyticum cells, a phenol degrading bacteria are not available in literature.

Following research questions were raised based on the literature review

- (i) How effective is pulsed plate bioreactor with the cells of *Pseudomonas desmolyticum*, NCIM 2112, immobilized on activated carbon in continuous biodegradation of phenol under various pulsing and operating conditions
- (ii) How does the influent phenol concentration and dilution rate as individual factors and as combination factors in terms of substrate loading affect the physical and chemical characteristics of the biofilm associated with phenol degradation during start up and at steady state of pulsed plate bioreactor.
- (iii) How does the conditions imparting high shear forces on the biofilm such as frequency and amplitude of pulsation affect the physical and chemical characteristics of the biofilm associated with phenol degradation during start up and at steady state of pulsed plate bioreactor.
- (iv) How does the cell carrier loading affect the physical and chemical characteristics of the biofilm associated with phenol degradation during start up and at steady state of pulsed plate bioreactor.
- (v) How biofilm formation dynamics is related to phenol biodegradation during the start-up of the bioreactor.

The objectives of the research work were formulated based on extensive literature survey and the research questions

Research Objectives

The main objective of the research work is to study the degradation of phenol in wastewater and to study the biofilm characteristics such as biofilm density, biofilm thickness, biofilm structure, morphology and biofilm composition in a pulsed plate bioreactor using the bacteria *Pseudomonas desmolyticum* (NCIM 2112) immobilized on granular activated carbon.

Specific objectives are

- To study the performance of pulsed plate bioreactor for biodegradation of phenol in wastewater using *Pseudomonas desmolyticum* NCIM 2112 under various pulsing and operating conditions
- To study the individual and combined effect of dilution rate and influent phenol concentration on biofilm characteristics at steady state and during start-up of pulsed plate bioreactor
- To study the effect of pulsing conditions such as frequency and amplitude of pulsation on biofilm characteristics at steady state and during start-up of pulsed plate bioreactor
- To study the effect of cell carrier loading on biofilm characteristics at steady state and during start-up of pulsed plate bioreactor
- To study the dynamics of biofilm formation and its characteristics in coordination with the phenol biodegradation during the start-up of the bioreactor.
- To develop models to predict (i) steady state biofilm characteristics and (ii) the biofilm dynamics during the start-up of PPBR at different operating and pulsing conditions.

Organization of the thesis

The overview of the thesis is as follows

Chapter 1 presents the **Introduction**. In this chapter, the background of the research work, need for the study, gaps identified from literature review and research questions raised are presented.

Chapter 2 presents with the **Literature Review**. In this chapter, summary of the work carried out by various researchers in the area of the current study highlighting the research gaps in the existing literature is presented. The reports of various researchers which have been used in analysis and interpretation of the results of the current study are also discussed in this chapter.

Chapter 3 presents with the **Materials and Methods**. This chapter lists the materials used, followed by description of the experimental methodologies and the analytical procedures adopted in the current study.

Chapter 4 is on **Results and Discussion**. This chapter presents the results of experiments conducted in the current study along with the analysis and interpretation of the results.

Chapter 5 presents the **Modelling of Biofilm Characteristics** in pulsed plate bioreactor.

Chapter 6 presents the **Summary** of the significant findings of the present research work along with the **Conclusions** drawn.

CHAPTER 2

LITERATURE REVIEW

This chapter presents the extensive review of literature based on publications in the area of biofilm characteristics, factors affecting the biofilm characteristics, various types of biofilm reactors used for different applications, the influence of reactor conditions on biofilm characteristics and the reactor performance, studies on phenol degradation in biofilm reactors and pulsed plate column as a bioreactor.

2.1. Biofilm and its characteristics

Bacteria generally exists in planktonic form, freely existing in bulk solution and in sessile form, attached to a surface or within the biofilm (Garrett *et al.* 2008). Leeuwenhoek in 1684, was the first to investigate microbial aggregates on tooth surfaces and this resulted in identification of biofilms. The advantages of biofilm formation for the microorganisms include protection from antibiotics (Goldberg *et al.* 2002), disinfectants (Peng *et al.* 2002), and dynamic environments (Chen *et al.* 1998).

The attachment of free floating cells onto biotic or abiotic surface aids biofilm formation. Initially attachment occurs through weak, reversible adhesion with Van der Waals forces. These adhered cells produce extracellular polymeric matrix and are embedded in the same. The formation of biofilms is a multistep process (Smirnova 2010; Qureshi *et al.* 2005) and it involves various physicochemical and biological factors (Liu and Wang 1996; Rouxhet and Mozes 1990; Calleja 1984; Daniels 1980; VanLoosdrecht *et al.* 1987; Marshall *et al.* 1971). The biofilm formation has been reported to be described as a four-step process (Liu and Tay 2001). The first step is the physical movement or transport of cells from liquid to the carrier surface. It happens through hydrodynamics; diffusion; gravity force; Brownian movement and cellular mobility. The second step is the retainment of the cells on the carrier surface by various attractive

forces and promotion of stable multicellular contacts to form a monolayer of cells. The attractive forces are (i) physical such as Van der Waals force of attraction, attraction due to opposite charges; surface free energy; hydrophobicity and surface tension (ii) Chemical forces such as hydrogen bonds or formation of ionic pairs. The third step involves the maturation of attached cells, production of exopolymers, three dimensional cellular cluster growth, metabolic changes and genetic signalling induced by the environment to facilitate and strengthen the cell-cell interaction to form dense cell clusters. In the fourth step, the three dimensional structure of the immobilized cells are shaped by hydrodynamic conditions. The biofilms are finally shaped into structured community by hydraulic shear force. However, very high shear force would cause serious disaggregation and inhibition of development of biofilms.

Biofilms are complex structure composing of cells and extracellular polymeric products viz. protein, polysacchaides, DNA and humic substances (Nicolella *et al.* 2000; Charaklis 1990; Lettinga *et al.* 1980). The growth and activity of microorganisms are enhanced when adhered to some solid surface. Attachment of a cell to a substratum surface is termed adhesion, and cell-to-cell attachment is termed cohesion. Adhesive and cohesive forces exhibited a biofilm are determined by the mechanism behind these forms of attachment (Garrett *et al.* 2008).

Bacterial biofilms are ubiquitous in nature and found on any hydrated surface. They can be used in the production of valuable products or for wastewater treatment (Vanysacker *et al.* 2013). The attachment of biofilm depends upon various factors viz., solid support, hydrodynamics condition, medium characteristics etc. (Maric and Vranes 2007; Donlan 2002).

2.1.1. Biofilm characteristics and the factors influencing them

Biofilms are composed of microbial cells and exopolymeric substance (EPS) that vary in physical and chemical characteristics (Smirnova 2010; Idris and Moustafa 2004). Each biofilm community was found to be unique except having some inherent

characteristics and is composed of heterogeneous structure with mixture of high molecular weight polymers (More *et al.* 2014; Sheng *et al.* 2010; Tolker-Nielsen and Molin 2000). The microbial cells in biofilms are said to communicate through the regulatory mechanism called quorum sensing (QS) in which they exchange information through a specific signal molecules, auto inductors (Smirnova 2010; Barbara *et al.* 2009; Maric and Vranes 2007; Miller *et al.* 2001). Biofilms are generally controlled by environmental and genetic factors in which the mobility of bacteria, cell membrane proteins, extracellular polysaccharides and signaling molecules are the important factors (Maric and Vranes 2007). The Exopolymeric substances (EPS) are produced by microorganisms in order to protect themselves from various environmental conditions and toxic substances and they bind together with complex structure (Liu *et al.* 2004). Thus, the main function of EPS is to aid cell attachment on to surface of solids and protect against any environmental stress and dehydration. EPS are mainly responsible for the structural and functional integrity of biofilm and are considered as key components that determine the physicochemical and biological properties of biofilms (Denkhaus *et al.* 2007). Exopolymeric substances produced by microbial cells are mixture of complex polymers mainly consisting of proteins, polysaccharides, humic substances and lipids and these EPS components are present in the space between microbial aggregates, providing the structure and architecture of biofilms.

Various physical, chemical and biological characteristics of the biofilm play a very important role in their application in biofilm systems. The important physical characteristics of the biofilm such as biofilm density, biofilm thickness (Rim *et al.* 2004; Tanyolac and Beyenal 1998; Kwok *et al.* 1998; Payton 1996; Sekar *et al.* 1995), biofilm surface roughness and biofilm porosity which define the biofilm structure along with substratum surface coverage (Alves *et al.* 2002) influence the performance of the biofilm. The major component in the biofilm matrix is water which comprises up to 97 % (Zhang *et al.* 1998). The characteristics of the solvent trapped within the biofilm matrix are determined by the solutes dissolved in it. All major classes of macromolecules, i.e. polysaccharides, proteins, nucleic acids, peptidoglycan, and lipids can be present in a

biofilm. However, EPS are the major structural components of the biofilm matrix (Lembre *et al.* 2012). Thus, the chemical characteristics such as composition of biofilm and EPS (Bala Subramanian *et al.* 2010) along with the biological characteristics such as microbial diversity and their spatial distribution, differences in activity in terms of rates of growth, EPS production, cell death (Bishop 1995), biomass and quorum sensing also influence the performance of the biofilm in biofilm systems (Barbara *et al.* 2009; Yu Liu 2002; Liu and Tay 2001).

The structure of biofilm is a unique feature of the environment in which it develops. They are affected by various factors viz., physical factors such as hydrodynamic shear, properties of support material; environmental factors like temperature, pH; chemical factors like concentration of nutrients etc. The biological parameters are the physiology of cells, microbial population and EPS, which are related to the physical and chemical factors (Gong *et al.* 2011; Beneyal and Lewandowski 2002; Liu and Tay 2001; Van Loosdrecht *et al.* 1995; Rittmann 1982). Nutritional and physical conditions greatly affect the nature of biofilms (Stoodley *et al.* 1999a) and the biofilm structure is largely determined by the concentration of substrate. (Wimpenny and Colasanti 1997). Researchers worldwide have worked in order to understand the physical and chemical characteristics of biofilms. Various environmental factors (shear stress, surface roughness, temperature, oxygen, nutrient concentration) and genetic factors (Quorum sensing signals, activity) affect the biofilm formation and its characteristics (Kim *et al.* 2012; Chavant *et al.* 2002). The nature of support (carrier) material greatly influences the biofilm growth, oxygen mass transfer and reactor hydrodynamics. The size, shape, density and surface roughness are the most important physical characteristics of the carrier particles (Lazarova and Manen 1994; Jian-an and Nieuwstad 1992). The surface property plays an important role in the initial attachment of the cells. Pham *et al.* (2003) in their studies on the adhesion property of strain *St. guttiformis*, have found that the tendency of bacterial cells to adhere to hydrophobic surfaces to form biofilm in multilayers was greater as compared to that on hydrophilic surfaces. The hydrophilic nature of the surface along with the planktonic EPS layer adsorbed on it were reported to

inhibit the cell attachment. However, Chavant *et al.* (2002) have found the biofilm formation by negatively charged bacterial cells to be faster on hydrophilic substratum.

Substrate loading was reported to influence the density of biofilm. Higher substrate loading was found to favor the growth rate (Wijeyekoon *et al.* 2004; Van Loosdrecht *et al.* 1995). Van Loosdrecht *et al.* (1995) have reported that high substrate loading results in the the formation of less dense biofilm with more protuberances. Trulear and Characklis (1982) have reported that rate of biofilm accumulation and density increase with the increase in substrate loading. They have also reported that low density biofilms exhibit filamentous structure and high density biofilms exhibit non filamentous structure.

However, Wijeyekoon *et al.* (2004) have reported that though biofilm growth rate is positively influenced by substrate loading rate, increasingly high substrate concentrations produce increasingly compact biofilms with lower porosity. They also demonstrated that biofilm internal microstructure is affected by substrate loading. Higher specific activity was observed at slowly growing biofilms having porous structure. High substrate loading reduced the nitrification process. Their research work suggested that substrate loading is the key parameter in determining biofilm structure and function.

The effective diffusivity in the biofilm, which signifies the biofilm microstructure related parameters such as porosity and tortuosity was also found to increase with the increase in the concentration of carbon source (Beyenal and Lewandowski 2000) .

Rochex and Lebeault (2007) have shown that increasing the nutrient (carbon, nitrogen and phosphorous) concentration increases the rate and extent of biofilm accumulation. However, higher nutrient concentration above a certain limit reduced biofilm accumulation rate because of a higher detachment. Zhnag et al. (2014) have shown that nutrient depletion triggers EPS matrix production in *B.subtilis* biofilms and EPS production increases at a critical biofilm thickness and it depends on initial carbon

concentration in the environment. Tait *et al.* (1986) observed that high C : N and C : P ratios in the medium were associated with high levels of polymer production. Kwok *et al.* (1998) have reported that increase in substrate loading increases the biofilm thickness.

Detachment forces have been demonstrated to play a key role (Beyenal and Lewandowski 2000; Speitel and DiGiano 1987; Van Loosdrecht *et al.* 1995 ; Trulear and Characklis 1982) in the formation of biofilms. It was shown that the relationship between shear stress and biofilm formation was strongly linked with each other and the metabolism was influenced by the physical stress (Park *et al.* 2011). Shear stress is one of the major factors that influences the formation of stable biofilm (Fernandez *et al.* 2014; Park *et al.* 2011; Rochex *et al.* 2008; Liu and Tay 2002).

Characklis *et al.* (1990a) suggested that the detachment of biofilms could be categorised into three types, namely: erosion, sloughing and abrasion. The removal of small clusters of cells from the biofilm surface is referred as abrasion and erosion. Shear of the moving fluid on the biofilm surface causes erosion, while collision between the biofilm carrier particles as in moving bed bioreactors cause abrasion. Sloughing, refers to the detachment of relatively large portions of the biofilm wherein a fraction of the biofilm is removed down to the substratum (Morgenroth *et al.* 2000). Characklis (1990 b) referred to detachment as an interfacial transfer process, which involved the transfer of cells and other components from the biofilm compartment to the bulk liquid, with the detachment of microbial cells and related biofilm material occurring from the moment of initial attachment.

Van Loosdrecht *et al.* (1995) through their studies on Airlift suspension reactor have postulated an hypothesis saying that the structure of biofilm is determined by the ratio between the substrate surface loading on to the biofilm to shear rate and reported that a smooth and stable biofilm can be achieved with a right balance between substrate loading and shear rate. According to them, when detachment forces are relatively high

patchy biofilms are developed, whereas at low detachment forces, the biofilm becomes highly heterogeneous with many pores and protuberances.

Kwok et al. (1998) in their studies on airlift suspension reactor confirmed the hypothesis postulated by Van Loosdrecht (1995). They showed that increase in carrier loading decreased the biofilm thickness. They attributed it to increased detachment forces and decrease in biomass surface production rate, i.e. higher carrier loading provides higher biofilm surface area. These studies showed that the formation, structure and stability of biofilm is influenced greatly by detachment forces resulting from hydraulic shear or collision between the particles.

Horn and Hampel (1998) found that high substrate loading decreased biofilm density and maximized substrate conversion rate and shear effect was found to be reversed and the surface structure was influenced by shear and substrate loading. Liu et al. (2001) found that the biofilm detachment rate was higher at higher substrate loading and was related to changes in biofilm production rate, structure and composition.

Herbert-Guillou *et al.* (2001) investigated on the formation of biofilm and its mechanical properties. They found the biofilm to be elastic under the laminar and turbulent conditions. They also found that the biofilm deformation depended upon development conditions and mechanical properties of biofilm.

Beneyal and Lewandowski (2002) reported on the effect of internal and external mass transfer in biofilms that are grown at various flow velocities. Based on their investigation on the variation of effective diffusivities in the biofilm along the depth, they hypothesized that the biofilms arrange their internal architecture, that depends upon flow velocities, to control (i) rate of mass transport of nutrient and (ii) the resistance of shear stress of water flowing past them. Among these conditions, the later one will be tried by biofilms to enhance mechanical strength that can be obtained at the expense of former one.

They inferred that low velocity leads to biofilms with low density and high effective diffusivity which does not resist high shear stress, whereas high flow rate led to denser biofilm that resisted high shear stress but had lower effective diffusivity.

Flow cells that are imitation of industrial pipes were used for finding the influence of mass transfer of nutrients and shear stress on the development of biofilm (Moreira et al.2013). The biofilm formation was found to be favoured at lowest flow rates. Shear stress and mass transfer increased with increase in flow rates. It was found that shear stress was the one which controlled the biofilm and it resulted in erosion/sloughing of biofilm, whereas mass transfer promoted biofilm formation.

The initial attachment of microbial cells is an important factor and is considered as critical for the formation of biofilm. Lopes *et al.* (2000) in their studies on an airlift bioreactor with *Pseudomonas fluorescens* biofilm on basalt support have observed high production of EPS during the initial stages of biofilm formation and the majority of the protein in biofilm was mainly intracellular, thus they have reported that the bacteria produce more of exopolymeric substances when subjected to high shear stress in order to promote initial cell adhesion. The bacterial cells in biofilm rely on the interaction between them to the surface of the solid for their survival (Palmer *et al.* 2007) during the initial attachment. The factors involved in cell attachment are surface charge, mass transport, surface roughness, hydrophobicity etc. (Di Bonaventura *et al.* 2008). Substratum characteristics play an important role especially in early stages of biofilm formation. Roughness of carrier surface promotes bacterial colonisation (Gjaltema *et al.* 1997). Fox *et al.* (1990) in their studies on expanded bed reactor have hypothesized that biofilm starts growing in the crevices as they are protected from shear forces in these regions. Further the biofilm fills the crevices, forms clusters by joining with the group of cells from the neighbouring crevices. According to them, the biofilm thus matures and the rough surface is completely covered.

Various researchers have investigated on the formation of EPS in recent years (Park et al. 2011; Kumar et al. 2011). Simulation of a nitrifying biofilm with ammonia and nitrite oxidizing species to elucidate effects of EPS on biofilm structure and function was carried out by Kreft and Wimpenny (2001). They found that EPS production influenced the biofilm structure and function significantly. EPS production stimulated the growth of non producers, but decreased the growth of producers owing to energy

utilization for EPS production. Thus, the accumulation of EPS reduced with an increase in rate of production. It was observed that the roughness of biofilm with patchy area decreased and there was an increase in porosity due to EPS production.

Pei-Shi *et al.* (2008) through their studies on suspended carrier biofilm reactor, have shown that EPS secretion would be due to defensive physiological response to higher shear stress by the microorganism. In this case the sudden increase in shear stress increased the EPS-polysaccharide secretion, but had little effect on secretion of EPS-protein. Higher shear stress reduced the roughness of the biofilm thus forming flatter biofilm. Increase in shear resulted in compact and dense biofilm owing to continuous changes in pore structures and bacterial growth.

The higher shear stress reduces the surface roughness making the biofilm more compact and in turn more denser having less protuberances and the biofilm maturation slows down keeping them young when subjected to high shear stress (Rochex *et al.* 2008). Rochex *et al.* (2008) through their studies on a conical Couette-Taylor Reactor (CTR) have also shown that high shear stress reduced the biofilm diversity, slowed down the maturation of biofilm thus maintaining young biofilm. Their results also indicated the temporal variation in biofilm composition with variation in shear stress. Ochoa *et al.* (2007) have also observed the similar results in CTR and have found that the values of local shear stress were high near the wall than at the middle of the reactor which caused detachment of biofilm and hence reduction in residual biomass near the wall.

Kumar *et al.* (2011) investigated on the production of biofilm by isolated bacteria from marine water and found that a strain which showed higher production of EPS was found to possess strong adsorption bond of -OH and COOH. It was found that the attachment and growth of biofilm were dependent upon environmental conditions.

Park *et al.* (2011) in their studies on the bacterial strain *P.aeruginosa* found that morphology and dynamics of biofilm along with bacterial metabolism were altered by influence of fluid shear stress on biofilm formation. They have also reported that there exists an optimum shear stress for the formation of stable biofilm. Wang *et al.* (2011)

observed loose structure of mature biofilms at low flow rate and high substrate concentration in their studies on hydrogen production using a photosynthetic bacteria, *Rhodospseudomonas palustris* CQK01 immobilized on a glass slide in a lab-scale photoreactor. High production of hydrogen was possible with high dry weight of biofilm and at optimal porous structure.

One of the factors that influence the initial cell attachment of microbial cells is the environmental temperature to which the microorganisms are exposed. Fletcher (1977) reported that the decrease in temperature lowered the adhesive strength of a marine *Pseudomonas sp.* In contrast to this, the bacterial attachment was reported to be better at lower temperature than at high temperature for the bacteria *Listeria monocytogenes* on the surface of steel (Herald and Zottola 1988). As reported by them, the adhesion at low temperature could be due to transition from an ordered state in the presence of ions. However, as reported by Van Loosdrecht *et al.* (1995) temperature does not influence the biofilm formation on rough support material; while elevated temperature favors the biofilm formation on a smooth quartz surface. They have also concluded that, rougher the surface the stronger the attachment of biofilm and lesser the chance of detachment from the surface. The biofilm formation by the negatively charged bacterial cells was negatively correlated with growth temperature (Chavant *et al.* 2002). He *et al.* (2015) in their studies on anaerobic-anoxic-aerobic bioreactor have found that the physical characteristics viz. biofilm thickness and biofilm density on suspended carrier and the production of EPS decreased with decrease in temperature and the effect of temperature was more profound on biofilm thickness than the biofilm density.

Pellicer-Nacher and Smelts (2014) in their studies on membrane-aerated biofilm reactor have found that oxygen loading affected the biofilm parameters. At high oxygen load, increase in biofilm cohesiveness was observed, which depended on the mass of EPS and the type of shear applied. Higher content of protein in EPS was observed with increase in shear indicating strongest biofilm structure, whereas the carbohydrate content was found to be low. Also, it was observed that the outermost EPS present in strongest biofilm was hydrophobic in nature distributing around dense microbial aggregates. But in

weaker biofilm strata they were homogeneously distributed. It was observed that the oxygen penetrated fully into the depth of biofilm which avoided the anoxic biofilm zone and thinner biofilm was obtained. A porous biofilm with rough surface and lower density was observed with high oxygen load. However the higher oxygen loading did not influence the detachment rate of biofilm.

During any physical or chemical fluctuations in any biological systems, microorganisms evolve a complex decision making mechanism in response to the environmental changes and match their behaviour accordingly (Popat et al. 2015). In other words communication between bacteria occurs through chemical signalling molecules. Generally, bacteria senses the environmental effects and to overcome such effect they generate a mechanism of sensing called quorum sensing (QS), during which the bacteria releases some molecules to overcome such environmental changes. They are extremely fast decision makers in response to multiple environmental (both biotic and abiotic) challenges with gene expression.

Very few researchers have studied on the chemical composition of biofilms. Lazarova et al. (1998) treated primary and secondary effluent for nitrification process using three-phase circulating bed reactor. They observed thin biofilm formation which was below 100 μm indicating controlled development during the process. The biofilm thus formed had the composition of protein upto 35% , 58% of the biopolymers, where as the polysaccharide content was as low as less than 3%. The high nitrification was obtained during the process that could be resulted from controlled biofilm during the process by developing the bacterial cells and minimizing the production of exopolysaccharides.

Lopes et al. (2000) reported on the chemical composition of bacterial (*Pseudomonas fluorescens*) biofilm during start up of a concentric tube air lift reactor. High exopolymeric substances production was observed during early stage of biofilm formation that promoted initial cell adhesion and biofilm cohesion as well. The protein content was found to be small and the total protein was found to be intracellular. The

substrate consumption rate was reduced that could be due to reduction in cellular density within the biofilm.

Andersson *et al.* (2009) reported about the composition of extracellular polymeric substances of the denitrifying bacteria *Comamonas denitrificans* that were grown in different culture media and found that EPS consisted of 3 to 37 percent of protein, 9 to 50 percent of nucleic acids and 3 to 21 percent of carbohydrates. The release of nucleic acid was attributed to cell lysis during the extraction process. However extracellular DNA has been identified to be one of the components that provides structural strength to the biofilm.

The biofilm growth is observed since few years in industries as well domestic domains. Detrimental effects of biofilm has been observed in industries such as spoilage of food, infection etc. and blockage of pipes in various industries such as dairy (Yoo *et al.* 2002), food (Kumar *et al.* 1998), water systems (Bott *et al.* 1998), oil (Nemati *et al.* 2001), paper (Klahre *et al.* 2000), health sectors (Liesegang *et al.* 1997; Marotta *et al.* 2002; Halabi *et al.* 2001) and in households (Barker *et al.* 2000). However, the usefulness of biofilms is well known, especially in the field of bioprocesses for the production of high added value biomolecules (Zune *et al.* 2013), ethanol (Demirci *et al.* 1997), microbial fuel cells (Read *et al.* 2010), bioleaching (Olivares *et al.* 2010) and bioremediation. The microorganisms as biofilms to remove contaminants, such as metals and radio nuclides (Le *et al.* 2003; Li *et al.* 2003), oil spills (Radwan *et al.* 2002), nitrogen compounds (Zafarzadeh *et al.* 2010) and for the purification of industrial waste water (Sekoulov *et al.* 1999), are being used commonly. Biofilm characteristics majorly influence their application potential in the above said areas, thus making the study on biofilm characteristics essential.

2.2. BIOFILM REACTORS

Bioreactors play an important role in the biochemical industry. The rate of reaction and the period of operation affect the reactor productivities and the process economics (Qureshi *et al.* 2001; Maddox *et al.* 1989. Reaction rate can be increased by increasing cell mass concentration in the reactor. Cell mass concentrations can be increased with immobilized cell reactors and thus they offer high reaction rates (Tyagi *et al.* 1982).

Cells can be immobilized by entrapment and covalent bond formation, but it increases the cost of production. The adsorption technique for cell immobilization is of natural origin as cells "adsorb/and adhere" to the support naturally and firmly (Qureshi *et al.* 1987 ; Forberg *et al.* 1985; Tyagi *et al.* 1982). Adsorbed cells form layers on the support and cell mass in the bioreactor grows over time (Qureshi *et al.* 1988) to form biofilms. Formation of biofilm is an important factor to be considered in various fields viz. biotechnology, biomedical, and industrial biotechnology (Barbara *et al.* 2009; Pham *et al.* 2003; Ascon and Lebeault 1999). The biofilm reactors are engineered processes extensively used for the treatment of wastewater, production of value added products, bioremediation etc. Biofilm systems are used in various industrial applications such as in bioreactors for production of ethanol (Demirci *et al.*1997; Kunduru and Pometto 1983; Ogbonna *et al.* 1989), Butanol (Napoli *et al.* 2010), Cellulase (Hui *et al.* 2010), vinegar or acetic acid (Crueger and Crueger 1989) and wastewater treatment (Botchkova *et al.* 2014; Seyed 2011; Borkar *et al.* 2013).

Biofilm reactors are highly advantageous over suspended cell reactors in terms of (i) high cell retention, (ii) prevention of substrate inhibition and toxic effects thus allowing high substrate loading and resistance to toxic shock loading (iii) elimination of sludge formation and separation problems, (iv) preventing dilution rate limitations thus allowing for operation under high flow rate (Burghate *et al.* 2013; Shirazi 2011; Basha *et al.* 2010; Rabah *et al.* 2004; Van Loosdrecht and Heijnen 1993). In environmental

processes large quantities of dilute streams have to be treated in which biofilm process are advantageous.

From the research work carried out by Pishgar et al. (2011), on the biodegradation of phenol using suspended cell as well immobilized cells, it was reported that the time required for the degradation was shorter when immobilized cells were used and also at higher concentration of phenol (1000 mgL⁻¹), the degradation was enhanced upto 40% as compared to suspended cells. Comparison between a suspended biomass (Sequential Batch Reactor 'SBR') and immobilized biofilm reactor (Sequential Batch Biofilm Reactor 'SBBR') was carried out by Sowinska *et al.*(2016) for the treatment of wastewater. SBBR showed slower biofilm growth than SBR. The immobilized reactor improved the efficiency of sewage wastewater treatment.

Dixon and Abbas (2016) used aerated magnetic biofilm reactor with flat ring magnets as the carrier material for activated sludge in a novel aerated magnetic biofilm reactor for treating wastewater. The reactor was fed with seeding activated sludge along with Fe₃O₄ powder that acted as magnetite. A uniform magnetic biofilm was observed in reactor and the biofilm was not affected by shear due to air bubble during operating cycles. The second seeding resulted in increase of biofilm thickness which was also unaffected by shear stress due to air bubble. They attributed it to the strengthening effect of magnetite that prevented detachment of solids from the biofilm. The performance of the magnetic biofilm reactor was found more efficient than suspended growth bioreactor in nitrogen removal.

In biofilm bioreactors, microorganisms are immobilized on solid support. Different types of biofilm reactors have been used by various researchers, for the production of value added products or for waste water treatment. Biofilms can be used in various types of reactors (Cheng *et al.* 2010) such as continuous stirred tank reactors (Tyagi *et al.* 1982), packed bed reactors (Qureshi *et al.* 1988), trickling filter reactor (Wik 2003), fluidized bed reactors (Shieh *et al.* 1986), airlift reactors (Viggiani *et al.* 2006), upflow anaerobic sludge blanket (Lettinga *et al.* 1980; Lettinga *et al.* 1983)

reactors , expanded granular sludge bed (Seghezzi *et al.* 1998) reactors, rotating –disc reactor (Oliveira *et al.* 2000), spouted bed reactor (Dabhade *et al.* 2009) and membrane biofilm reactor (Clara *et al.* 2005). Table 2.1 presents various biofilm reactors used for different biotechnological applications.

Support (carrier) material for the biofilm is an important parameter to be considered in the design of biofilm reactors (Sancinetti *et al.* 2012). Biofilm formation starts with adhesion that depends on the physicochemical characteristics of the support material and its nature is considered as the design parameter to enhance biofilm formation (Habouzit *et al.* 2014). It was shown that the carrier surface roughness increased biofilm formation and this factor is dominant than the physico-chemical characteristics (VanLoosdrecht 1998; Mulder *et al.* 1988; VanLoosdrecht 1995). Choice of support material plays vital role for the successful operation of the bioreactor (Garcia *et al.* 2008).

Different inert carrier materials for cell immobilization were used by various researchers viz. granular activated carbon (Dabade *et al.* 2009 ; Fan *et al.* 1987); hydrophobic polystyrene, charged SiO₂ plate, hydrophilic Duropore (Shreve *et al.* 1991); polyvinyl chloride (PVC), polyethylene terephthalate (PET) (Sancinetti *et al.* 2012); plastic composite-support made of agricultural material like oat hulls or soybean hulls (Demirci *et al.* 1997); glass beads and activated alumina beads (Shetty *et al.* 2007) and calcium alginate beads (Pishgar *et al.* 2011; Abd-El-Haleem *et al.* 2003).

Wilderer *et al.* (2000) used four types of biofilm carrier materials such as: clay granules, GAC, zeolite and plastic rings in SBBR and found that substrate was temporarily stored in the carrier material by means of adsorption, ion exchange and absorption processes. They have reported that as the reaction phase proceeded, the bulk liquid concentration dropped leading to dominance of desorption processes followed by metabolic reactions. They concluded that thick biofilms and the biofilm carrier particles with high adsorption capacities are favorable to withstand fluctuations in peak loads and to keep the effluent concentrations within stipulated levels.

Table 2.1 Biofilm reactors used for different applications.

Reactor type	Support Material	Substrate used	Application	Organism Used	Reference
Packed bed reactor	Polypropylene	Glucose	Ethanol production	<i>Zymomonas mobilis</i>	Khunduru and Pometto (1983)
Fluidized bed reactor	Sand	Acetic acid	Bio-methanation of acetic acid	Bacteria from methane fermenter	Fidel Toldra et al. (1986)
Packed column	Granular activated carbon	Phenol, p-aminophenol	Biomass loss due to shearing effect study	Not specified	Spietel et al. (1987)
Trickle bed reactor	Beech wood shavings	Ethanol	Acetic acid production	Acetic acid bacteria	Crueger and Crueger (1990)
Fermenter	Plastic composite support	---	Ethanol production	<i>Saccharomyces Cerevisia</i>	Demirci (1997)
Rotating disc biofilm reactor	Plexiglass disc	Molasses	Denitrification	Secondary effluent inoculum	Boaventura and Rodrigues (1997)
Differential fluidized bed reactor	Activated carbon	Phenol	Phenol degradation and Prediction of average biofilm density of bioparticle	<i>Pseudomonas putida</i>	Tanyolac (1998)
Bioreactor	Flexible brush	Activated sludge	oxidation of ammonia	Anammox bacteria	Botchkova et al. (2014)
Fixed biofilm reactor	Polyurethane foam sponge cube	Phenol	Biodegradation of phenol	Bacteria from recycled sludge	Hsien and Lin (2005)

Reactor type	Support Material	Substrate used	Application	Organism Used	Reference
Pulsed plate column	Glass beads	Phenol	Degradation of phenol	<i>Nocardia hydrocarbonoxydans</i>	Shetty et al. (2007)
Packed bed bubble column	Silicon coated rings	Glycerol	Di-hydroxyacetone Production	<i>Glucono bacteroxydans</i>	Hekmat et al. 2007
Tubular membrane reactor	Silicon tubing	Styrene	S-Styrene oxide	<i>Pseudomonas species</i>	Gross et al. (2007)
Stirred vessel	None; bacteria create cellulose granules	D-alanine	Pyruvic acid production	<i>Recombinant acetobacter xylinum</i>	Setyavati et al. (2009)
Spouted bed contactor	Granular activated carbon	Phenol	Phenol degradation	<i>Nocardia hydrocarbonoxydans</i>	Dabhade et al. (2009)
Packed bed bioreactor	Tygon rings	Synthetic cheese whey	Butanol manufacture	<i>Clostridium acetobutylicum</i>	Napoli et al. (2010A)
Moving Bed Biofilm Reactor	Polyethylene cylinders	Glucose	Partial nitrification/ denitrification process	Heterotrophs and nitrifiers	Zafarzadeh et al. (2010)
Gas lift reactor	Pumice stone	Semi-synthetic effluent	removal of organic waste and sulphate	Sulfate reducing bacteria and methanogenic archaea	Pizarro et al. (2011)
Fixed-Bed Biofilm Reactors	Woven polypropylene (PP) fiber sheets	Synthetic wastewater with ammonium chloride and sodium acetate	Nitrification	nitrifying biofilms.	Elawwad et al. (2012)

Reactor type	Support Material	Substrate used	Application	Organism Used	Reference
Horizontal flow biofilm reactor	horizontal plastic sheets	Methane and Liquid nutrient feed	Methane removal from gas mixture	methanotroph-rich biomass capable of methane oxidation	Kennelly et al. 2012
fixed bed biofilm reactors	plastic media	Biodegradable ozonation byproducts	Ozonation byproduct removal	----	McNaught et al. 2015
Moving-Bed Biofilm Reactor	----	Simulated wastewater containing PCBs	Biodegradation of Polychlorinated Biphenyls (PCBs)	----	Dong et al. 2015
Packed bed biofilm reactor	Tygon rings	glucose and lactose	Butanol production	<i>Clostridium acetobutylicum</i>	Raganati et al. 2016
Moving bed biofilm reactor	Cubic-shaped polyurethane sponges	Organics in waste water	Domestic wastewater treatment	Microbial consortia	Zhang et al. 2016

Dimitrov *et al.* (2007) through their studies on growth of two bacterial strains viz., *Pseudomonas aeruginosa* O1 and *Bacillus subtilis* CIP 5265 on powdered activated carbon with polymer coating have found that the biofilm development rate can be improved by modifying the surface properties of the carrier material with polymers.

Yotova et al. (2009) studied on the dynamics of the formation of biofilm by the strain *Artrobacter oxydans* 1388 immobilized on two newly synthesized carrier materials. The immobilization was done using two methods viz. covalent bonding and adhesion to different polymeric matrixes. The base of copolymer acrylonitrile with acrylamide was mixed with cellulose acetate butyrate to obtain the matrices of high mechanical stability. The covalent binding was proved to be more effective among the two types of immobilization. The formation of biofilm was better on the polymer matrix composed of Polyacrylonitrile and polyacryl amide.

Habouzith *et al.* (2014) studied the effect of solid support material on biofilm development during start up with methanogenic bacteria in anaerobic biofilm reactor using different solid support materials such as polypropylene, polyethylene and polyvinyl chloride. They found that the composition of biofilm was dependent upon the size of inoculum irrespective of nature of support material or organic loading, but archaeal population were dependent highly on the support material. The start-up of reactor was shown to be affected by the nature of the support material.

Xiao and Chu (2015) developed a novel biofilm carrier (Bamboo Fibre Biofilm Carrier, BFBC) material using bamboo fibre as raw material and used in bio-contact oxidation reactor (BCOR) to investigate the characteristics, specific surface area, hydrophobicity, and adsorption capacity of carrier material that was prepared. For comparison purpose, in another set a combined carrier material support made of bamboo fibre mixed with polyester fiber was used in the reactor. The reactor started more rapidly when filled with BFBC than when filled with combined carrier and also the efficiency of the reactor was significantly higher in case of BFBC than combined carrier loading. BCOR was more efficient in removing pollutant and was resistant to load variations and more efficient to remove total nitrogen and to reduce COD to a required level in municipal waste water treatment plant.

Granular activated carbon (GAC) is generally used as an adsorbent in wastewater treatment and considered as one of the most efficient adsorbent due to availability of

large surface area and well developed pores which provides more active sites for adsorption (Annadurai *et al.* 2000b). Herzberg *et al.* (2004) through their studies on atrazine degradation using *Pseudomonas sp.* strain in a fluidized bed biofilm reactor have reported higher stability with GAC as a biofilm carrier as compared to a reactor with non-adsorbing carrier. Internal flux of desorbed atrazine from the GAC to the base of the biofilm was found to increase the active biofilm surface area. Formation of biofilm on GAC was reported to provide better efficiency in removal or biodegradation of organic compounds (Gibert *et al.* 2013). Several researchers (Dabhade *et al.* 2009; Prieto *et al.* 2002; Pai *et al.* 1995) have shown that the microbial cells immobilized on Granular activated carbon could degrade phenol very efficiently. Thus, in the present investigation *Pseudomonas desmolyticum* (NCIM 2112) was immobilized on GAC and used in the bioreactor.

Biofilm reactors have found numerous applications in recent years. In several cases the principles of their design and operation are known or are largely based on several thumb rules. But, the systematic information is lacking. The structure and composition of biofilm are crucial for (i) better understanding, interpretation and prediction of the influence a biofilm may have on a system (Stoodley *et al.* 1997) and (ii) the ability to manipulate the biofilm structure, in order to create the biofilm desired in a certain application. The performance of a biofilm reactor is affected by the biofilm structure and composition. The studies on structure and composition of biofilm are important to ensure the formation of biofilm and its applicability.

According to Picioreanu *et al.* (2000), the biofilm structure can affect the (i) Overall transformation rates in a bioreactor. (ii) Stability of bioreactor operation (iii) Fluid frictional resistance (iv) Biofilm detachment and (v) Biofilm ecology.

The morphological characteristics of biofilms such as: biofilm thickness, biofilm density and biofilm surface shape affect the biomass hold-up and mass transfer in a biofilm reactor (Garrido *et al.* 1997; Tijhuis *et al.* 1995) and play a significant role in determining the overall performance of a biofilm reactor. Biofilm density affects the

achievable biomass concentration and the overall substrate conversion rate. For aerobic processes, thin biofilms ($< 150 \mu\text{m}$) are favorable (Tijhuis *et al.* 1994). Thick biofilms lead to presence of a high fraction of non-active biomass in the reactor due to limited substrate penetration depth. The shape of biofilm surface affects the external mass transfer resistance and thus influences the mass transfer of nutrients to biofilm cells (Bishop *et al.* 1997; De Beer *et al.* 1994, 1995, 1996; Yang and Lewandowski 1995; Zhang *et al.* 1994;). Porosity of the biofilm and composition of the matrix affect the resistance to transport of solutes within the biofilm interiors by influencing the effective diffusivities within the biofilm matrix (Stewart 1998).

The control of biofilm thickness is an important aspect for a stable operation of biofilm reactors, as phenomena like sloughing may occur with thicker biofilms (Beefink 1987). In particle biofilm processes such as fluidized bed bioreactors, may become unstable due to fluffy biofilms and outgrowth which may cause difficulties in separation of biofilm particles from water (Tijhuis *et al.* 1995). Thus, biofilm surface shape is also an important parameter for the stability of reactor. Formation of filamentous biofilms or very thick biofilms and the sloughing of parts of the biofilms from the carrier surface often results in lower effluent quality.

Stooley *et al.* (1999b) through their studies on biofilms in flow channels, proposed that in the event of the presence of isolated cell clusters on the surface, the velocity profile in the vicinity of the cell cluster resembles that of the empty channel. When cell clusters are close enough, each cluster is influenced by the flow wakes generated by other clusters. However, no vortices are formed when the biofilm completely covers the carrier surface, and thus the flow "skims" over the biofilm surface. In turbulent conditions, filamentous structures may be developed in the biofilm and these filamentous forms freely oscillate in flowing conditions (Stoodley *et al.* 1998). Stoodley *et al.* (1999b) hypothesized that the detachment of individual clusters from the biofilm may be dependent on their shape and location. Continuous superficial erosion may lead to loss of biomass from uniform and thick biofilms (Picioreanu 1999). Ohashi and Harada

(1994, 1996) and Ohashi *et al.* (1999) found that increase in biofilm dry density increases the biofilm strength. If due to starvation and ageing, the cells decay in deep biofilm layers, the adhesive strength of the biofilm reduces leading to faster biofilm detachment rates.

Biological characteristics of microorganisms forming a biofilm affect the biofilm accumulation in biofilm reactors. Biofilm characteristics viz. biofilm density and biofilm thickness, are important parameters and the overall reaction critically depends on these parameters (Karel *et al.* 1985; Grady 1985; Andrews 1982). According to Bhamidimarri (1988), the general consensus is that the biofilm dry density increases as the biofilm thickness increases up to a certain thickness beyond which it begins to decrease and with different reactor configuration and substrates, the biofilm thickness varied between 0.01-0.1 cm and a biofilm dry density from 0.033 to 0.11 g/cm³.

Under similar of temperature and shear in airlift reactor, the slow growing nitrifiers were found to form biofilms with higher density than the fast growing heterotrophs (Tijhuis *et al.* 1994, 1995). However, hydrodynamics is reported to influence the emerged structures more profoundly. The flow pattern determines the rate of external mass transfer of nutrients and products to and from the biofilm. The higher the liquid velocity, the higher the mass transfer rate which leads to the faster rate of biofilm accumulation. Higher liquid velocities also imply larger shear forces at the biofilm surface, leading to higher biofilm detachment rate. The experiments by Stoodley *et al.* (1999a) demonstrated that the polymeric matrix of *Pseudomonas* biofilms underwent permanent strain when subjected to variable fluid shear. The balance between the rate of biofilm growth and detachment determines the biofilm formation. Thus, it is important to analyze the effects of availability of nutrients and hydrodynamics on biofilm structure together.

Fennell *et al.* (1992) developed a biofilm of Methane utilizing bacteria on diatomaceous earth and granular activated carbon in a fluidized bed bioreactor and obtained a steady growth of biofilm in spite of low influent methane concentration. They

obtained biofilm thickness of 160 μm and biofilm densities of 120 to 190 g VSL^{-1} . The total suspended solids varied from 5 to 74 mgL^{-1} .

It is reported that in rotating cylinder and in tubular reactors under steady state conditions with constant substrate loading rate, the biofilm density increased (Christensen and Characklis 1990; Characklis *et al.* 1982) and biofilm thickness decreased (Characklis 1981) with increasing fluid shear stress. Under constant shear conditions, the biofilm density (Characklis *et al.* 1982) and maximum biofilm thickness (Characklis 1981) increased with an increasing substrate loading rate.

Trulear and Characklis (1982) through their studies on annular reactor have found that detachment increases with fluid velocity and mass of biofilm. Higher fluid velocities led to reduction in hydraulic retention time which caused a high biomass loss coefficient due to shearing forces during bioremediation of acetic acid in fluidized bed bioreactor (Fidel Toldra *et al.* 1986).

Fan *et al.* (1987) used immobilized cells of mixed microbial cells with *Pseudomonas putida* as dominant microorganism on polymethylmethacrylate as support material in a draft tube gas-liquid-solid fluidized bed reactor for degrading phenol and studied the dynamics of biofilm. It was observed that the biofilm thickness increased steadily till certain time and later the increase in thickness was drastic with bulky and loose filamentous matrix that could be due to the switch over of activity of microorganism from non-filamentous to filamentous with decrease in rate of phenol degradation. At the same time the density increased with increase in thickness and decreased with further increase in biofilm thickness indicating loose structure of biofilm when the activity changed from non filamentous to filamentous. The necessity of biofilm control in the reactor when the thickness increased drastically was evident in their work.

Chang *et al.* (1991) have reported that the particle-particle collision and hydrodynamics influences the biofilm detachment rate. On comparison of biofilms in

fluidized and non-fluidized reactor systems, they found the formation of smoother biofilms in non fluidized reactor and rougher biofilms in fluidized reactor. Their studies also showed higher detachment rates in fluidized systems, confirming influence of shear and hydrodynamics on biofilm structure and detachment. Their studies showed that increased particle-particle collision and turbulence resulted in thin and dense biofilms. Hence the turbulence and attrition between particles during fluidization was considered to be a dominant detachment mechanism.

The detachment rate was related directly to biofilm growth rate by Peyton and Charaklis (1993) in their studies on a Rotor Torque Biofilm reactor with glucose as a substrate for the growth of *Pseudomonas aeruginosa* and mixed population of microorganisms and they found the detachment rate to be lower at the factors which limited the growth rates.

Tijhues *et al.* (1994) observed three stages of biofilm formation during the studies on dynamics in concentric-tube Biofilm Airlift Suspension Reactor (BAS reactor) using a mixed culture grown on basalt carrier. During first stage, initial attachment occurred by adsorption on surface and in the cavities in which shear was lower. It helped in the formation of micro colonies during second stage and thirdly, continuous development of microcolonies that led to a continuous biofilm covering the entire surface at steady state. It is reported that for continuous biofilms and for high biomass concentration, a hydraulic retention time should be lower than the inverse of maximum growth rate of suspended biomass. When retention time was longer, lesser quantity of attached biomass can be present as patchy biofilm. The amount of biomass per biofilm particle remained constant on reducing the bare carrier concentration during start up at short hydraulic retention times(HRT). Substrate loading rate affected only the amount of biomass on biofilm particles. Thicker biofilms were formed at higher substrate loading. During start up studies it was found that the detachment rate per biofilm area to be independent of substrate loading rate, but dependent on the concentration of bare carrier material. Choi and Tijhuis *et al.* (1994) have studied the effect of HRT in a biofilm airlift suspension

reactor with heterotrophic biofilms and found that to achieve high biomass concentrations in the reactor and for the formation of biofilms, HRT must be shorter than the reciprocal of the maximum growth rate of suspended bacteria.

Choi *et al.* (1995) studied the effect of hydraulic loading on biofilm characteristics in Inverse fluidized bed reactor. The reactor was stable for HRT of 2 h and for 4.5 kg COD m⁻³ day⁻¹ and they observed abrupt growth of filamentous microorganisms beyond this value. It was found from the experiments that the optimum thickness to be 200 μm and biofilm dry density to be 0.08 g cm⁻³.

The performance of Biofilm Airlift Suspension reactor was found to be good at shorter retention time than maximum growth rate of suspended microorganisms to washout suspended microorganisms, where a stable continuous biofilm was formed (Tijhuis *et al.* 1994).

Sekar (1995) studied the effect of biofilm thickness on biofilm density and substrate consumption rates under pseudo-steady state in differential fluidized bed biofilm reactor. They observed parabolic increase in the substrate consumption rates with increase in biofilm thickness. The consumption rates increased with increase in biofilm density due to enhanced rate of reaction, but decreased after 78 g/dm³ of biofilm density. The critical thickness of biofilm in their work was found to be 90 μm and the biofilm density increased up to critical biofilm thickness and then decreased slowly.

Zhang *et al.* (1995), investigated the influence of the structure of biofilm on mass transport and transformation processes in a laboratory scale rotating drum biofilm reactors during biodegradation with autotrophic and heterotrophic biofilms. Experiments revealed non-uniform spatial distribution of biofilm properties. The substrate/nutrient transformation and diffusion processes were affected by decrease in metabolically active biomass and increase in porosity within the depth of biofilm. Through the biofilm modelling studies, they found that the ratio of effective diffusivity to that in bulk of liquid (D_e/D_b) could decrease from 50-81% at the top of biofilm layer and 20-50% at the bottom of the layer. This reduction was found to be dependent on various factors like

density of biofilm, porosity, etc. They found that the biofilm structure and the performance was affected by biofilm thickness. Biofilm thickness was found to be strongly influenced by the biofilm density. However, the relationship was found to be non-uniform.

Peyton (1996) studied the effect of substrate loading and shear stress on the biofilm thickness, density and roughness using *Pseudomonas aeruginosa* in an annular reactor. It was found from this study that the biofilm thickness showed significant increase up to a value of 30 μ m with an increase in substrate loading, but shear stress did not show any change in thickness. It was observed that there was an increase in roughness with increase in thickness.

Tanyolac and Beneyal (1996) studied the degradation of phenol in a continuous fluidized bed bioreactor using *Pseudomonas putida*. The cells were pre immobilized on granular activated carbon under batch conditions for the formation of a biofilm layer and then used in continuous reactor. They reported biofilm thickness as the main parameter that affected the degradation of phenol. They have found an increase in the performance of fluidized bed reactor with optimum average density of biofilm.

Boaventura *et al.* (1997) used Rotating Disk Biofilm Reactor to study denitrification using inoculum from secondary effluent of a domestic sewage treatment plant. They obtained biofilms of varying thickness and density with variations in feed nitrate concentration and feed flow rates. They found biofilm wet density decreasing linearly with the biofilm thickness, upto 622 μ m thickness and then remain constant with further increase in thickness. The biofilms were found to be fully penetrated in cases with kinetic controlled regime and partially penetrated biofilms in diffusion controlled regime.

Kwok *et al.* (1998) observed the dependencies of biofilm structural parameters with varying substrate loading rates in terms of COD and carrier concentration in biofilm airlift suspension reactor (BAS) with basalt carrier particles. High biomass

content and low biomass yield were obtained at lower substrate loading. Biofilm thickness decreased with a decreasing substrate loading rate and with increasing carrier concentration signifying higher detachment forces generated by particle-particle collisions. They found that with growing biofilms the detachment of biomass is lower at higher carrier concentration. In growing systems, the detachment decreased with increasing detachment force. Smoother, denser, thinner and compact biofilms were formed as the biomass surface production rate decreased and/or shear force increased. Their results also showed the formation patchy biofilm at high detachment forces and highly heterogeneous biofilm with more voids and protuberances at low detachment force. Their results contradicted the general belief that high detachment force is not desirable for a stable biofilm formation. They hypothesized that by a high detachment force, the surface growth is controlled and thus more substrate diffuses into the biofilm and leads therefore, to a higher biofilm density. Higher resistance of dense biofilms against detachment forces was attributed by Kwok *et al.* (1998) to the fact that a dense biofilm is generally smoother and therefore less susceptible for detachment forces. They concluded that a higher carrier loading, which results in higher biofilm density and higher biomass concentration is desirable. Increase in biofilm density with increasing carrier concentration have been observed in BAS reactors (Kwok *et al.* 1998) with heterotrophic organisms, in fluidised bed reactors (Chang *et al.* 1991) and in BAS reactors with nitrifying biofilms (Van Benthum *et al.* 1997).

Horn and Hempel (1998) studied on mass transfer and substrate utilization in the boundary layer of biofilm systems during biodegradation of acetate and succinate and their studies showed the limitation of biofilm thickness to be 800µm in the reactor for the Reynolds No. exceeding 3000-4000 and also it was shown that there is a decrease in biofilm density and maximum conversion rate with increase in substrate loading, whereas with high shear the density had increased.

Casey (1999) has reported a faster growth of biofilm in terms of its thickness at higher oxygen concentration and at higher flow velocity, during biofilm development in membrane-aerated biofilm reactors.

Hirata et al. (1999) studied the dynamics of completely mixed three phase fluidized bed reactor for waste water treatment with coal ash as support material with a mixed culture of microorganisms for step change in the influent concentration. The sudden shock to the microorganisms in terms of change in initial concentration of feed slowed down the activity of microbial cells during which the concentration of BOD accumulated in the reactor and hence the outlet concentration reached a peak value under transient conditions. Once the cells regained their activity, the concentration reduced and reached a new steady state value. However, they observed that the biofilm surface area remained almost constant during the transient period following a step increase or decrease in the influent concentration.

Biofilm characteristics such as the activity in terms of substrate consumption rate and composition in terms of exopolymeric substances (polysaccharides and proteins), attached biomass and thickness were studied by Lopes *et al.* (2000), during the start-up in an Airlift Reactor. *Pseudomonas fluorescens* bacteria was used in this study with glucose as a substrate. Extracellular proteins and polysaccharides increased with time to reach a peak in the beginning of the start-up period, but further decreased to reach a lower and more stable value. High polymer production during initial stages of biofilm was found favourable in promoting initial cell adhesion and cohesion. They attributed it to high turbulence and strong abrasion condition in the reactor during the initial stages. Decrease in exopolymer production in later part was attributed to diminishing of abrasion effect of particle collisions. The total protein content was found to be very high compared to extracellular proteins, thus indicating that biofilm proteins were mainly intracellular. The biofilm accumulation caused high activity, however the activity was found to be decreased due to reduction in cell density within the biofilm. The biofilm formation included three stages starting with a bare carrier with initial cell attachment, formation of microcolonies with patchy biofilm and then a continuous biofilm on the carrier surface.

Nam *et al.* (2000), worked on fluidized bed reactors to study the effect of sand size and location on biofilm characteristics. The effective diameter of sand used for their study was 0.23 and 0.60 mm. A thinner and smoother biofilm was observed in the sand size of 0.6mm which was due to the higher shear environment and a thick, rough, and porous biofilm was observed on 0.23 mm sand particles. Also, variations in biofilm thickness were observed with distance in the reactor. A thinner biofilm was observed at the base of the reactor that had high turbulence than the samples that were taken from less turbulence regions. However it was observed that the biofilm surface area per unit biofilm volume remained almost constant irrespective of sand size and sampling location.

The effect of different substrates (Formate, formaldehyde, and methanol) on biofilm formation was studied using air lift suspension reactor by Villasenor (2000) and they reported that the biofilm formation depends upon the type of substrate. The biofilms were denser with low substrate concentrations and the detachment of biofilms was larger in growing biofilms than in non-growing biofilms subjected to same detachment forces.

Liu and Tay (2001) reported on the effect of shear stress on metabolic response of biofilm in terms of growth yield and dehydrogenase activity and biofilm structure using rotating disc annular reactor. The bacteria for the growth of biofilm was obtained from a steady state laboratory scale, aerobic-settling-anaerobic reactor. High shear stress led to dense, smooth and stable biofilm and at the same time the dehydrogenase activity was higher and on the other hand increase in shear stress decreased the growth yield. The authors concluded that biofilms may respond to shear stress by regulating metabolic pathways associated with the substrate flux. Dissociation of catabolism from anabolism would occur at high shear stress. They proposed a hypothesis that the proton translocation across the cell membrane is stimulated by shear-induced energy spilling, which favours formation of a stronger biofilm.

Liu and Tay (2002) have also reported that aerobic biofilms can metabolically respond to hydrodynamic shear force, in turn favouring the formation of a strong and

stable biofilm under stressful hydrodynamic conditions. They concluded that shear force has significant influences on the structure, mass transfer, production of exopolysaccharides, metabolic/genetic behaviours of biofilms and recommended that a biological process can be engineered by manipulation of hydrodynamic shear force, as a control parameter to enhance process efficiency.

The influence of the composition of the medium, in terms of carbon/nitrogen ratio and sulfur concentration, on characteristics of biofilm used for denitrification using *Alcaligenes denitrificans* (Alves et al. 2002) was studied in a fluidized bed reactor. It was observed that there was steady increase in biofilm thickness even after the attainment of steady state. The biofilm density was found to be independent of loading conditions and it was observed that there was composition of proteins and polysaccharides in biofilm with change in C/N ratio and phosphorous concentration. The higher denitrifying activity and higher production of protein was observed with increase in phosphorus concentration since there was shifting of metabolism from carbohydrate to protein content. The biofilm thickness and density were related to shear stress in the reactor. Choi et al. (2003) in their studies on annular reactor have reported that the bifilm strength is governed to a significant degree by the very recent history of shear conditions.

Rabah et al.(2004) reported on the characteristics of biofilm (biofilm thickness and bed porosity) and biomass concentration with varying height in a fluidized bed biofilm reactor (FBBR). The biomass concentration in the reactor decreased with increase in nitrogen loading rate and the highest biomass concentration was observed at the bottom of the column, whereas the biofilm thickness increased from the bottom to the top signifying the stratification of the growth medium in the reactor and increase in bed porosity from bottom to top of the reactor. It was reported that the variation in biofilm dry density could be due to variations in physical conditions and the characteristics of microorganisms in the reactor. Also the average biomass concentration per unit volume of reactor decreased with increase in superficial velocity which was attributed to increase

in bed porosity leading to lower concentration of bioparticles per unit volume of reactor and due to high shear that could have resulted in detachment of biomass.

Ebrahimi and Piciooreanu (2005) observed biofilm formation at high shear region initially in honeycomb monolith which they attributed to the balance between biofilm growth and detachment due to shear stress induced erosion. According to them, in the early stages, the biofilm growth in the low shear regions was strongly limited by external substrate transfer resistance. As the biofilm grows in thickness, the passing gas bubbles induce mechanical forces which leads to the formation of a more regular biofilm shape even in the low shear regions.

Cresson et al. (2006) studied biofilm formation during the start-up of an anaerobic three phase inverse turbulent bed biofilm reactor for COD removal to reduce the time of colonization during start-up phase. In their work, low density particles were used as support material for biofilm formation. Organic loading rate was increased stepwise from 0.5 to 20 gCOD L⁻¹ day⁻¹ and the COD removal rate was maintained at 80%. They recommended the operation of the reactor at short hydraulic retention time, so that the suspended cells wash out and only the attached cells grow to favour biofilm accumulation.

The rotating annular reactor was used by Garny et al. (2008) in order to understand the interaction between biofilm development, structure, and detachment of biofilm. In their experiments, they varied nutrient load keeping constant hydrodynamic condition. A larger impact on biofilm structure was observed for mixed culture than single ones. The detachment was found to be higher at high substrate loading and it was related with biofilm production rate, structure and composition.

Andersson et al. (2009) used denitrifying organism *Comamonas denitrificans* for waste water treatment and studied the characteristics of exopolymeric substances. Their results showed lower production of exopolysaccharides when the organisms were provided with lower concentration of limiting nutrients indicating higher cell concentration in biofilm matrix in contrast to normal belief on the production of high EPS

at low concentrations of limiting nutrient. They found that the production of EPS was less with more cells leading to thinner biofilm when treated with wastewater that was rich in nitrogen content and poor in carbon content. The extracellular protein was found to be abundant in EPS from biofilm.

Pizarro et al. (2011) used a gas lift reactor for the removal of organic waste and sulphate and proposed a strategy to obtain a well-established biofilm. The performance of the reactor was evaluated in terms of shear force. Biogas recirculation was provided for shear effects. During the first stage of start-up, colonization was observed along with the presence of extracellular polymeric substances. The biofilm development did not have any adverse effect with increase in gas flow. According to their strategy, gradual increase in gas flow and organic loading rate leads to well established active biofilm and it is essential to have a proper start-up procedure for better performance of a reactor.

Sarti *et al.* (2011) studied the biofilm characteristics and performance of a full scale anaerobic sequencing batch biofilm reactor used for sulfate rich waste water treatment with mineral coal as support material for the growth of microorganisms. Operational stability (sulfate removal) was achieved after 71 cycles (steady-state period) following the changes in operating conditions, thus indicating the high capacity of the mineral coal to retain the biomass. The biofilm formation was found to have two different patterns, one initial colonization and other one of a mature biofilm. Low adhesion of microbial cells on support material and low suspended solids removal efficiency was observed during the start-up period. The higher efficiencies were attained by increasing the recirculation flow rate and the COD/sulfate ratio. According to them, the strategy of high COD/sulfate ratio and high recirculation flow rate allowed a greater availability of organic matter or electron donor for sulfate reduction and a reduced influence of the liquid-phase mass transfer resistance respectively.

Langer et al. (2014) studied dynamics of biofilm formation during anaerobic digestion of organic waste in biogas reactor. The maturation and maintenance of biofilms was found to vary during the batch fermentation process due to decreasing substrate

availability. This study demonstrated that the digestion of organic waste can be enhanced and positive effects on biogas production could be brought about with biofilms of high cell densities.

Fernandez et al. (2014) grew *Pseudomonas fluorescens* bacteria on polyvinyl chloride surface in a simple flow cell reactor and found that the fluid shear stress and salinity influenced Anammox biofilm formation. The high ionic strength was said to cause the reduction in electrostatic repulsive forces that encouraged strong Anammox biofilm formation without appreciable biofilm detachment.

The effect of low carbon to nitrogen (C/N) ratio and temperature on microbial structure and biofilm was investigated by He et al. (2015) in a suspended carrier biofilm reactor with polypropylene spheres as the carrier material. The objective of the study was to assess how design and operation of the bioreactor might improve pollutant removal and maintain the stability of biofilm structures. The production of extracellular polymeric substances, biofilm thickness and biofilm density decreased with increase in temperature and low temperature favored the EPS production. Low temperature rather than low nutrient supply stimulated the filamentous bacteria growth as indicated by bulking and dispersed growth at lower temperatures. Stable operation of the reactor was found to be beneficial in terms of lower carbon requirements for the removal of organics and nitrogen.

Tang et al. (2016) studied the adhesion characteristics of a biofilm in an integrated moving bed biofilm reactor–membrane bioreactor. They found that the maturity of a biofilm may be evaluated by its roughness and the stability of biofilm is determined by tightly-bound protein and polysaccharide. They have also reported three stages in the development of a biofilm.

Application of biofilms in bioreactors are beneficial and are becoming more popular for wastewater treatment and for the production of desired products (Ochoa 2007; Rittmann 1982; Cheng *et al.* 2010). The biofilm structure depends on physical phenomena (substrate transport, biomass production, shear stress) and chemical

processes (metabolism) occurring in the reactor and are governed by the concentration of substrate, composition of biofilm, EPS production, shear force etc. (Cheng *et al.* 2010). Hydrodynamics strongly affects the structure and activity of biofilm (Ochoa *et al.* 2007; Liu and Tay 2002 ;Van Loosdrecht 1995; Rittmann 1982). Literature indicates that the biofilm thickness and biofilm density are the main design parameters which evaluate the rate of consumption of substrate and in turn the performance of a bioreactor (Andrews *et al.* 1982). For stable operation of any bioreactor, parameters such as biofilm thickness, biofilm density should be controlled (Alves 2000).

The operating conditions which influence the performance of any biofilm reactors are influent concentration, flow rate of liquid and air, cell carrier loading and the speed of moving parts which bring about the mixing and mass transfer. Grabow and Hamoda (1998) have studied the performance of a pilot-scale four-stage aerated submerged fixed film (ASFF) process for treating domestic wastewater in terms of the organic removal rates and reported that the organic (BOD and COD) removal rate was influenced by the hydraulic loadings applied.

Kargi and Eker (2003) treated high strength synthetic wastewater in a Rotating Perforated Tubes Biofilm Reactor at different operating conditions and studied the effect of flow rate of wastewater and COD concentration on the performance of the reactor in terms of COD removal. COD removal efficiency increased with the specific biofilm surface area and the rotational speed, but decreased with increasing COD loading rate in rotating perforated tubes biofilm reactor during biological wastewater treatment.

Sokol *et al.* (2003) worked on three phase fluidized bed bioreactor for treating refinery wastewater with inoculum from activated sludge grown on propylene solid support and optimized the ratio of bed volume to reactor volume and air velocity for maximum COD removal.

Rabah and Dahab(2004) investigated denitrification of waste water containing high-nitrate with specific emphasis on the effect of nitrogen loading rate and the

superficial velocity. The maximum efficient loading rate to meet the required effluent quality was found to be dependent on the superficial velocity. With increase in superficial velocities, the optimum maximum loading rate dropped and higher denitrification rates were achieved at relatively lower velocities. However, they found that below a particular minimum superficial velocity biomass agglomeration would occur.

The performance of anaerobic, packed-bed bioreactors treating leachate from potato waste was evaluated in terms of organic loading rate (OLR) as well as the recirculation flow rate by Mshandete *et al.* (2004). The bioreactor with the lower recirculation flow rate showed operational stability when a high OLR was applied, while the one with high recirculation flow rate became overloaded.

Effect of major operating variables such as hydraulic retention time (HRT), disc submergence and disc rotational speed on COD removal in Rotating biological contactor (RBC) were examined by Najafpour (2006) for the treatment of food canning wastewater. COD removal efficiency was increased with increase in HRT, disc submergence and rotational speed. The rotational speed helps in enhancing the oxygen and nutrient transfer required for the cell growth in the biofilm. Rotational speed of the discs can be manipulated to control the biofilm thickness and the dissolved oxygen (Del Borghi *et al.* 1985). However, the treating capacity is not always changed by changing rotational speed but it affects the power requirement. Thus, high power economy can be obtained by operating the RBC at minimum rotating speed (Fujie *et al.* 1983). Optimization of rotational speed is thus necessary.

Aygun *et al.* (2008) studied the performance of moving bed biofilm reactor (MBBR), and found that the organic removal efficiency decreased with increase in organic loading rate.

El-Naaz *et al.* (2010) worked on degradation of phenol present in waste water using Spouted bed reactor with *Pseudomonas putida* immobilized on polyvinyl alcohol. It was found that the rate of degradation of phenol increased with increase in air flow rate upto certain limit, which could be due to mass transfer resistance in bulk of the liquid at lower flow rates and also increase in dissolved oxygen when flow rate was increased.

On the other hand when the flow rate was higher than a certain limit, the degradation reduced with increase in air flow rate due to air bubble coalescence.

A fluidized bed reactor with low density polypropylene as support material was used by Haribabu and Sivasubramanian (2014) for treating wastewater. They reported that the percentage COD reduction increased with increase in superficial gas velocity and decreased with increase in inlet concentration. The decrease in percentage reduction with increase in inlet concentration of wastewater would be due to increase in organic loading that leads to increase in viscosity of wastewater providing less air holdup. On the other hand, increase in COD reduction with superficial gas velocity was attributed to increase in air holdup which enhances the rate of mass transfer.

Barwal and Chowdhary (2014) through their studies on moving bed biofilm reactor (MBBR), have found that the reactor performance depends on the amount and surface area of biocarrier, organic loading and dissolved oxygen. The performance of MBBR in terms of BOD and COD removal has been reported to be dependent on retention time.

Literature review suggests that the performance of any continuous bioreactor depends upon various operating conditions, mainly. (i) influent concentration of substrate which determines the substrate (organic) loading and substrate limitation conditions governing the growth rate of the microorganisms, (ii) influent stream flow rate which determines the dilution rate or hydraulic retention time (HRT) of the liquid in the reactor, substrate availability, the mass transfer characteristics and biofilm detachment rate in the reactor (iii) cell carrier loading which determines the detachment rate by attrition and biomass hold up and (iv) the speed of motion of the shear inducing components in the reactor which determine the biofilm detachment rates in the bioreactor and the mass transfer characteristics in the reactor. These operating conditions in turn influence the biofilm characteristics viz. physical characteristics like biofilm thickness, biofilm density, biofilm morphology and chemical composition of EPS (protein, carbohydrate, humic substance etc.) and these biofilm characteristics govern the overall biochemical reaction

(Karel *et al.* 1985; Grady 1983; Andrews 1982) and the performance of the bioreactor. The nature of the substrate strongly affects the production of exopolymeric substances that play key role in biofilm formation. Thus, studies on biofilm characteristics (physical and chemical) are important in biofilm reactors. Hence in the studies pertaining to any bioreactor, the investigations on the effect of operating conditions on biofilm characteristics should be carried out to understand how the performance of the reactor may be improved by controlling these characteristics.

The characteristics of biofilms mostly in terms of biofilm thickness and density in different types of bioreactors are reported in literature. Although EPS is an important factor to be considered for the better performance and for design aspects, they are poorly understood, especially in terms of chemical composition of biofilm matrix (Marvasi *et al.* 2010). To the best of our knowledge, the research on the behavior/characteristics of biofilm in terms of chemical composition in biofilm reactors are scarce. High shear bioreactor such as pulsed plate bioreactor is a true candidate for studies on biofilm characteristics. The study on the behaviour of biofilms in this bioreactor may be useful in the design and analysis of this bioreactor when used for waste water treatment.

2.3. PHENOL BIODEGRADATION IN BIOFILM REACTORS

2.3.1. Biodegradation of Phenol

Phenol is considered as one of the major organic pollutants. Industries that are producing the phenolic wastes are steel plants, petroleum refineries, synthetic chemicals, pulp and paper industries, etc. Phenol greatly affects the plants, animals, human beings, aquatic animals and microorganisms even at lower concentrations (Pishgar *et al.* 2011). Hence there is a need to treat industrial waste water for the removal of phenol and to reduce the concentration below the permissible limits before its discharge into the environment.

Various methods for treatment of phenol containing waste are classified as physical, chemical and biological processes. The methods for removal of phenol include processes like adsorption (Yousef *et al.* 2011), incineration (Medel *et al.* 2012), extraction by using solvent (Yang *et al.* 2006), photocatalysis (Choquette-Labbé *et al.* 2014), sonochemical reaction (Lesko *et al.* 2006), oxidation processes (Yavuz *et al.* 2007), biological oxidation process (Scott and Ollis 1995), electrochemical methods (Pimentel *et al.* 2008), ozonation (Moussavi *et al.* 2009) etc. The processes such as adsorption and extraction do not lead to mineralization of phenol, but transfer it from one phase to another (Shah 2014). Incineration of phenolic waste leads to generation of toxic gaseous compounds (Medel *et al.* 2012). Wet oxidation process needs high temperature and pressure conditions (Fajerwerg *et al.* 1997). Electrochemical or Fenton oxidation processes lead to sludge generation and thus sludge disposal problems arise (Pimentel *et al.* 2008). Photocatalysis process encounter scale up difficulties (Wang *et al.* 2005). Most of these processes are either of high cost or cause secondary pollution. Among these biological degradation is considered most effective due to low cost, complete mineralization of phenol producing innocuous end products and can be brought about under ambient conditions (Shetty *et al.* 2013; Dey and Mukherjee 2010; Dabhade *et al.* 2009; Goudar *et al.* 2000; Chang *et al.* 1998). Biodegradation method is based on microbial activity that requires carbon and energy source. Thus the majority of organic chemicals, serve as carbon and energy source and they may be specific to certain types of microorganisms. In this method the organic pollutants are mineralized to carbon dioxide, water and other inorganic forms. Biological degradation of phenol follows either aerobic or anaerobic pathways (Basha *et al.* 2010; Krug *et al.* 1985). The aerobic process, unlike the anaerobic process utilizes oxygen during metabolism. The aerobic process for degradation is more preferred than anaerobic (Basha *et al.* 2010; Shetty *et al.* 2007) due to certain advantages viz. low cost, fast growth of microbial cells, etc. (Al-Khalid and Muftah 2012).

It is observed by many researchers that the efficiency of degradation depends not only on the type of pollutant and nature of microorganism but also on mechanism of

degradation. The mechanism depends on aerobic or anaerobic degradation conditions (Sridevi *et al.* 2012). In aerobic condition, phenol ring is first monohydroxylated by monooxygenase phenol hydroxylase at ortho position to form catechol which is the main intermediate (Gauthami and Vidya 2016). Then the catechol undergoes cleavage either at ortho or meta position. Thus, metabolic pathway for phenol degradation follows either ortho (Paller *et al.* 1995) or meta (Shetty *et al.* 2016, Mahiudddin and Fakhruddin 2012) cleavage path way to accomplish complete mineralization into CO₂ and H₂O.

Many microorganisms like bacteria, fungi, algae and yeasts use phenol as a sole source of carbon and degrade them. A large number of phenol degrading microorganisms are isolated and characterized at the genetic level. Aerobic biodegradation of phenol has been studied as early as in the 19th century (Chang *et al.* 1998; García *et al.* 1997).

Studies have shown that phenol can be aerobically degraded by a wide variety of microorganisms of genera *Pseudomonas* (Ahmed *et al.* 1995), *Acinetobacter* (Ying *et al.* 2007), *Alcaligenes* (Jiang *et al.* 2007), *Arthrobacter* (Unell *et al.* 2008; Karigar *et al.* 2006; Kar *et al.* 1997), *Bacillus* (Banerji *et al.* 2010), *Nocardia* (Shetty *et al.* 2007; Dabhade *et al.* 2009), *Candida* (Chang *et al.* 1998), *Fusarium sp.* (Cai *et al.* 2007); *Phanerochaete chrysosporium* (Kennes and Lema 1994) and fungus *Rhodococcus* (Prieto *et al.* 2002; Hidalgo *et al.* 2002). However, bacteria of the genera *Pseudomonas* has been widely reported based on their versatility to use wide range of aromatic substrates which makes their selection more impressive for wastewater treatment systems (Sridevi *et al.* 2012; Basha *et al.* 2010; Nair *et al.* 2008; Annadurai *et al.* 2000). They have been used for aerobic phenol biodegradation (Kotresha and vidyasagar 2007; Annadurai *et al.* 2007; Monteiro *et al.* 2000) and has been found to be very efficient phenol degraders. *Pseudomona desmolyticum* has also been reported to degrade phenol effectively. Effect of temperature, carbon source, pH and inoculum size on phenol degradation by *Pseudomona desmolyticum* (NCIM 2028) has been reported by Sridevi and Chandana Lakshmi (2009). However, to date no study has been reported on continuous biodegradation of phenol using *Pseudomona desmolyticum* cells.

2.3.2. Phenol biodegradation with immobilized cells

Several researchers have studied phenol biodegradation both in suspended cell systems (Chen et al. 2007; Liu et al. 2009) and in immobilized cell or biofilm systems (Chen et al. 2007; Prieto et al. 2002; Shetty et al. 2007). Immobilized cell systems have always been preferred over the suspended cell systems in continuous biodegradation. Immobilization is an approach in utilizing cell biomass in engineering systems (Annadurai 2000). Substrate inhibition of microbial growth occurs when cells are used in suspension during phenol degradation and immobilization is one of the methods to overcome substrate inhibition. Some of the advantages of cell immobilization are high productivity, tolerance to high toxic substances, blockage problems, downstream process like separation, repeated use of cells, cell stability, low cost, etc. (Shreve et al. 1991; Kourkoutas et al. 2004). Immobilization is proved to be more effective (Liu et al. 2009) over suspended cells in terms of degradation (Pishgar et al. 2011; Liu et al. 2009). Immobilized cell systems can overcome dilution rate limitations.

Gonzalez et al. (2001) studied on biodegradation of phenol using pure culture immobilized by entrapment in calcium alginate gel beads in both batch and continuous mode. It was possible to degrade phenol concentration up to 1000 mgL⁻¹, when microorganisms are adopted to the toxic compound. It was found that immobilized cells performed better than the suspended biomass.

Prieto et al. (2002) used suspended and immobilized cells of *Rhodococcus erythropolis* UPV-1 for degrading phenol both under discontinuous and continuous mode in an air stirred reactor. In this work, diatomaceous earth was used as support material on which acclimated cells were immobilized. It was found that the immobilized cells were able to degrade phenol completely in synthetic waste water containing phenol at a volumetric loading of 11.5 kg m⁻³ day⁻¹.

Acinetobacter sp. Strain W-17 (Abd-El-Haleem et al. 2003), degraded phenol completely in suspended cell condition up to 500 mgL⁻¹ after incubation of 120 h using

mixed nitrogen sources. When the same strain was immobilized, the time for degradation reduced to 24 h in minimal salt medium and to 15 h in simulated wastewater. The strain was tolerant to high concentrations of ammonium and Nitrate sources. The immobilized cells were used five times without loss of activity.

Karigar et al. (2006) isolated *Arthrobacter citreus* from hydrocarbon contaminated site and used for phenol degradation studies. The organism was immobilized in alginate and was found to be efficient.

Ying et al.(2007) isolated phenol degrading bacteria from activated sludge of a waste water treatment plant in china. The bacteria in free suspended form was efficient to remove 99.6% of phenol within 9 h and could metabolize phenol up to 1100 mgL⁻¹. It was found that the immobilized strain was tolerant to higher phenol concentration, indicating good potential in the treatment of phenol containing waste water.

2.3.3. Biofilm reactors for phenol biodegradation

Biofilm systems with the cells immobilized on solid support seems to be more popular due to its simplicity (Dabhade et al. 2009; Kourkoutas et al. 2004) and these biofilm systems may offer less diffusional transfer resistance than the entrapped cell systems. Thus biofilm reactors are widely used for continuous phenol biodegradation.

Molin and Nilsson(1985) grew *Pseudomonas putida* (ATCC 11172) in a continuous culture in which phenol was used as the only carbon and energy source. Experiments were conducted on phenol removal rate without and with biofilm formation at different surface area/volume ratios. The biofilm increased the maximum phenol removal rate keeping maximum suspended cell concentration to be almost same in the effluent at 5.5 cm² of biofilm surface per millilitres of reactor volume. The biofilm tolerated higher value of influent phenol concentration upto 3 gL⁻¹ whereas the non-biofilm tolerated upto 2.5 gL⁻¹ indicating that biofilms can tolerate higher phenol

concentrations than the suspended cells in continuous culture and it enhances the aerobic degradation of phenol compound.

Mixed culture having *Pseudomonas putida* as predominant species immobilized on spherical activated carbon as support material was used for degradation of phenol in a draft tube gas-liquid-solid fluidized-bed bioreactor (Fan et al. 1987). It was observed from their experiments that the biofilm formed was thin, uniform and dense. The biofilm dry density increased during initial stages of biofilm formation reaching a maximum and decreased further with increase in biofilm thickness thus indicating loose and bulky matrix of filamentous microorganisms.

Tang et al. (1987) studied biofilm characteristics in terms of biofilm dry density and thickness along with volumetric oxygen mass transfer coefficient and phenol removal rates in a draft tube gas-liquid-solid fluidized bed reactor(DTFB) under different operating conditions. It was concluded that DTFB was able to degrade phenol efficiently at the rate as high as $18 \text{ kg/m}^3\text{-day}$ with an effluent phenol concentration less than 1 g/m^3 .

Speitel et al. (1987) studied biofilm shearing under dynamic conditions in a packed column with granular activated carbon as support used for phenol and para nitrophenol (substrates) degradation. The biofilm shearing was found to be closely related to the microbial growth rate than the amount of attached biomass under the condition of rapid biodegradation rate. Through model development and simulation they found that the value of the growth-related shearing parameter significantly depended on the substrate. Substantial biofilm shearing occurred during periods of rapid biodegradation, which demonstrated the importance of biofilm shearing in attached growth reactors.

Livingstone and Chase (1989) studied phenol degradation by bacteria immobilized onto particles of calcined diatomaceous earth in a draft-tube, three-phase fluidized-bed reactor. They used the data on steady-state degradation to calculate biofilm substrate diffusivities which were found to decrease as the biofilm density increased.

They also determined a critical ratio of phenol/dissolved oxygen concentration at which a transition from phenol to oxygen-limiting biofilm kinetics occurred.

A mixture culture isolated from soil was used by Koch *et al.* (1991) for degradation of mixture of 22 phenols in an air lift loop bioreactor. The culture was immobilized on particles of sand and activated carbon. During experimentation the dissolved organic carbon (DOC) was varied. The removal of DOC was constant when sand particles were used as support material, whereas the biomass concentration was increased proportionately with DOC loading rate and reached a plateau at loading rates above 200 mgL⁻¹ h⁻¹. The biomass concentration was higher when activated carbon was used as carrier support under the same conditions. However the removal of DOC decreased during operation.

Seker *et al.* (1995), studied the effect of biofilm thickness on biofilm density and substrate consumption rate in a differential fluidized bed biofilm reactor (DFBBR 1995) during biodegradation of substrates viz. glucose and ammonium chloride and oxygen. In their studies biofilm of *Zoogloea ramigera* was developed on spherical activated carbon support material. Biofilm thickness was estimated using a “diffusion and reaction model” with biofilm density depending upon simultaneous diffusion coefficients. They observed that the consumption rate increased parabolically with biofilm thickness up to some critical value. The increase in consumption rate was due to increase in amount of biomass and decrease was due to dominating effect of diffusion. It was also observed that there was an increase in biofilm density during the growth of microorganism till some critical thickness and later the decrease in biofilm density enabling better substrate transport to the inner regions.

Tanyolac and Benryal (1996) worked on phenol degradation to predict the density of fully active bioparticles. In this study the biofilm thickness varied from 24.5 to 220.4 µm for the substrate concentration of 0.0164 to 0.0087 kg/m³ respectively. The experimental values of biofilm thickness were same as that of model values for fully active biofilm but varied for inactive core for the same surface concentration values.

Tanyolac and Beneyal (1998) worked with a differential fluidized bed reactor for degradation of phenol using *Pseudomonas putida* immobilized on carbon particles. They demonstrated the dependency of effective diffusion coefficient of substrate on biofilm density. By simulation of a diffusion and reaction model, they concluded that the internal structure of biofilm gets rearranged to attain the maximum substrate consumption rate.

Kryst and Karamanev (2001) used inverse fluidized-bed biofilm reactor for the continuous aerobic biodegradation of phenol in water and found the reactor to be very stable because of the efficient control of the biofilm thickness. From the studies on the effect of dilution rate on biodegradation rate, they found that the degradation rate passed through a maximum at a specific dilution rate.

Quan *et al.* (2004) studied biodegradation of 2,4-dichlorophenol and phenol in an airlift inner-loop bioreactor packed with honeycomb-like ceramic as the carrier to immobilize *Achromobacter sp.* Their results showed that with the increase of phenol loading rates, the removal efficiency of 2,4-DCP reduced, while that of phenol remained at about 99.6%. Thus, Phenol was found to inhibit the biodegradation of 2,4-DCP and the major carbon source shifted from 2,4-DCP to phenol on addition of phenol.

A three-phase fluidized bed reactor was used for degrading phenol using polypropylene as biomass support material (Sokol and Korpál 2004). The reactor was operated for various operational parameters viz. air velocity, residence time and bed volume to reactor volume (V_b/V_r) ratio and COD removal was determined for the same. Maximum removal was obtained for $(V_b/V_r) = 0.5$; air velocity (u) = 0.041 ms^{-1} ; residence time = 45 h. COD reduction was around 98%.

Hsien *et al.* (2005) adopted a fixed film bioreactor for treating phenolic wastewater. 94 percent degradation of phenol was achieved and the biofilm density was found to be 10.64 mg VSS/L. The authors concluded that the fixed biofilm reactor can be employed for biodegradation of phenolic wastewater from oil refining industries.

Dabhade et al. (2009) reported the effect of shock load on the reactor stability using spouted bed bioreactor in which the actinomycetes *Nocardia hydrocarbonoxydans* (NCIM 2386) was immobilized on granular activated carbon and on polymer beads. The microorganisms immobilized on granular activated carbon was found to take shock load when the phenol concentration was 50 to 500 mgL⁻¹. Higher dilution rate and higher phenol loading resulted in increase in effluent phenol concentration which was attributed to biomass washout.

Spouted bed column was used to study phenol degradation using *Pseudomonas putida* immobilized in a polyvinyl alcohol gel by El-Naas et al. (2009). High concentration of phenol inhibited the activity of microbial cells. But at the lower concentration, rate of degradation increased with decrease in particle size .

Sancinetti *et al.* (2012) studied phenol degradation in anaerobic fluidized bed reactors (AFBR) packed with polymeric particulate supports with influent phenol concentrations ranging from 100 to 400 mg/L and HRT of 24 h. The formation of extracellular polymeric substances was better with the polyvinyl chloride particles, but deformations in these particles proved detrimental to reactor operation. Polystyrene was found to be the best support for biomass attachment for phenol removal. The phenol removal efficiency was 100% using these support materials for influent phenol concentration of upto 400 ppm.

Vijayagopal and Sabarathinam (2012) have studied biological treatment of phenolic wastewater in a three phase draft tube fluidized bed bioreactor containing biofilm and it was proven that almost 100% phenol removal could be attained at a specific biofilm surface area per volumetric phenol loading rate exceeding 132 m²/kg phenol/day. Bioparticle diameter and bioparticle hold-up were found to be the decisive factors for the removal of phenol in this bioreactor

Begum and Radha et al. (2013) used indigenous pure culture of *Pseudomonas fluorescence* bacteria immobilized on low density support particles for the degradation of phenol in a three phase inverse fluidized bed biofilm reactor and studied the biofilm

characteristics viz. suspended and attached biomass concentration, biofilm thickness, bioparticle density. Complete degradation of phenol occurred with the maximum COD removal of 97.9% with the time duration of 110 h. Substrate inhibition effect could be overcome by biofilms.

Ghannadzhadeh *et al.* (2015) studied on phenol removal rate from synthetic wastewater in a fixed bed reactor with upflow sludge blanket filtration (FUSBF) to compare with usual USBF reactor. The effect of initial phenol concentrations on the phenol removal and COD removal efficiency at hydraulic retention time of 12 h and solid retention time (SRT) of 20 days was investigated for both the systems. The FUSBF was found to have better phenol and COD removal than USBF and can be used for treating industrial waste containing organic compounds.

Inverse fluidized bed biofilm reactor was used by Sabarunisha Begum and Radha (2015) to study hydrodynamic behaviour during phenol degradation (1200 ppm) using *Pseudomonas fluorescens* by varying Settled bed volume to working volume in the reactor. The optimum value of this ratio was found to be 0.2 for optimal superficial velocity of 0.22 ms^{-1} and the COD reduction efficiency was found to be 98.5%. The biomass and biofilm characteristics viz. biofilm dry density, biofilm thickness, bioparticle density, suspended and attached dry biomass, were evaluated under the optimal conditions. It was observed that the biofilm thickness and bioparticle density decreased with increase in superficial air velocity but an increase in biofilm dry density and suspended biomass concentration was observed. However the outgrowth of biofilm was not controlled by detachment forces beyond optimum superficial velocity and the thickness of biofilm increased rapidly with decrease in suspended biomass concentration. The optimum superficial velocity for efficient biodegradation of phenol were found to increase with the particle sizes.

Slamet *et al.* (2015) used *Acinetobacter sp.* and cow's stomach bacteria consortium to develop biofilm on pumice stone. Large quantity of exopolymeric substances were observed in the formed biofilm. These biofilms were tested for phenol degradation. The

source of phenol was waste from batik industry. The *Acinetobacter sp.* was able to degrade around 77% 10 ppm phenol whereas the cow's stomach consortium was able to degrade 89% of phenol.

It is apparent from the literature review that the performance of any biofilm reactor in terms of phenol biodegradation is determined by the operating conditions such as HRT or dilution rate as determined by the influent flow rate; phenol loading or influent phenol concentration and carrier loading etc. The biofilm characteristics in these reactors are governed by the shear inducing parameters and in turn influence the diffusional mass transfer characteristics. However, detailed studies on biofilm characteristics with emphasis on chemical characteristics in bioreactors degrading phenol are scarce. Limited studies on physical characteristics of biofilm associated with phenol biodegradation are reported in literature. The optimum values of bioreactor operating variables or the biofilm characteristics, for maximum phenol biodegradation varies with the type of reactor, the microorganism and the support material. Thus, it is important to study the biofilm characteristics associated with phenol degradation in any bioreactor to develop an adequate operational strategy and to engineer the process for its stable operation.

2.4. PULSED PLATE BIOREACTOR

In any aerobic biofilm reactor the substrate, nutrients and oxygen are to be transferred from the bulk to the surface of biofilm and then diffuse through the biofilm where biochemical reaction is aided by the microorganisms and the products of the reaction should diffuse back into the bulk (Shetty et al. 2010; Livingstone and Chase 1989). These processes involve external and diffusional mass transfer resistances. For efficient operation, a biofilm reactor should be designed to eliminate any such mass transfer limitations. Widely used bioreactors such as packed bed reactors offer mass transfer limitations. Though fluidized bed reactors are known to eliminate mass transfer limitations, particle attrition may lead to high biofilm shearing.

Mass transfer limitations in reactors are known to be eliminated and mixing is improved by pulsation technique (Roca et al. 1994). Sanromen et al (1994) used a pulsing device with a packed bed reactor for alcoholic fermentation and concluded that the improvements of the process are attributable to a mechanical effect rather than to physiological changes of microorganisms. Roca et al (1994) used elastic membrane pulsator with packed bed column for ethanol production using yeast *Saccharomyces cerevisiae* immobilized in calcium alginate and found that the ethanol yield enhanced by pulsed feed.

Van Dijk, in 1935, developed Reciprocating plate column or pulsed plate column and these columns were further used for liquid–liquid extraction operations (Yung *et al.* 2012; Smith *et al.* 2008 ; Shen *et al.* 1985; Karr 1959) and solid liquid extraction operations (Landau et al. 1973). Reciprocating plate column has exhibited good mixing (Srinikethan et al. 1987; Stevens *et al.* 1990) and liquid-liquid (Stella *et al.* 2008; Shen et al. 1985) and gas liquid mass transfer characteristics (Rama Rao and Baird 2003). Gas hold up in a reciprocating plate column depends on the column geometry (diameter and column height, the number of perforated plates and the diameter of the holes on the plate), as well as on the operating conditions (vibration intensity, superficial velocity of the gas and liquid phase (Lounes and Thibault 1993; Sundaresan and Varma 1990; Yang et al. 1986; Rama Rao et al. 1988 ; Rama Rao *et al.* 1983). Gas hold up in a three phase reciprocating plate column was found to be better than the two phase columns (Skala 2005).

The performance of a reciprocating bioreactor was evaluated in terms of axial dispersion coefficient and was found to be dependent upon the reciprocating speed but was not influenced by the flow rate of air and oxygen mass transfer coefficient was found to be higher when compared to other types of mixing devices for the same power input (Lounes and Thibault 1993). The substrate utilization (glycerol and water) by yeast *Aureobasidium* was efficient in an reciprocating plate bioreactor that resulted in higher production of extracellular polysaccharide indicating good performance of the reactor (Lounes *et al.* 1995).

Multiphase reactors have been extensively used in chemical industries on gas-liquid-solid catalytic processes. These systems are receiving increasing attention in biochemical industries and in wastewater treatment plants (Vicente et al. 2001; Siegel *et al.* 1988). The development of efficient bioreactors meeting the need for process enhancement is certainly an up-to-date task that needs to be continued.

Several researchers have worked on pulsed plate columns for various biotechnological applications.

A reciprocating plate bioreactor was used for the fermentation of polysaccharide and the influence of molecular weight and the concentration of polysaccharide on oxygen mass transfer coefficient (K_{LA}) was reported by Audet et al. (1996). The mass transfer coefficient was affected significantly by dissolved biological macromolecules due to their effect on rheology of the medium and also effect on gas liquid interface.

It was reported by Wiczorek and Brauer (1997) that the performance of the reactor was influenced by availability of nitrogen concentration for the production of citric acid using fungus *Aspergillus niger*.

Nitrification and COD oxidation of actual wastewater was carried out in a reciprocating jet bioreactor having three stages by Brauer and Annachhatre (1992) and the growth parameters were investigated. They reported the yield coefficient to be 0.3329 kg Biomass per kg COD and decay coefficient was reported as 0.0032 h^{-1} . On the other hand the same author designed a novel pilot plant reciprocating jet bioreactor that consisted of three stages. The nitrification and denitrification stage followed the COD destruction stage with residence time of 3-4.5 h, 0.3 h and 1-3 h respectively that led to greater than 90% conversion of COD, $\text{NH}_4^+\text{-N}$, and $\text{NO}_3^-\text{-N}$.

Pulsed plate column or reciprocating plate column was used as a biofilm reactor with immobilized cells by Shetty et al. (2007a,b) for phenol biodegradation. The column with the immobilized cells in the space between the pulsing plates was proved to be very efficient in phenol degradation. Such a three phase aerobic bioreactor exhibited very

good solid-liquid and oxygen mass transfer characteristics. Kodialbail and Srinikethan (2011) performed mixing and solid liquid mass transfer studies in three phase pulsed plate column with packed bed of solids in interplate spaces, with potential use as a aerobic immobilized cell bioreactor. They found that increase in liquid superficial velocities, frequency of pulsation, amplitude of pulsation and the vibrational velocities enhance the soli-liquid mass transfer coefficient and dispersion. The mixing behaviour in this contactor approximated a mixed flow behaviour.

Shetty and Srinikethan (2010) reported that that the volumetric oxygen mass transfer coefficient values in the three-phase pulsed plate column are similar or higher than the literature reported values for conventional two-phase pulsed plate columns. The values of volumetric oxygen mass transfer coefficients in the three-phase pulsed plate column were found to be higher order of magnitude than the literature reported values of volumetric oxygen mass transfer coefficient for many other three-phase gas-liquid-solid reactors.

Shetty *et al.* (2007 a) worked on biodegradation of phenol in Pulsed plate bioreactor by using *Nocardia hydrocarbonoxydans*, immobilized on glass beads. It was observed that the non-pulsed condition lead to higher biofilm thickness and the thickness reduced with pulsation but biomass dry weight remained constant. The percentage degradation of phenol was found to increase with increase in frequency of pulsation and was completely degraded at an frequency of pulsation greater than 05s^{-1} and the biofilm thickness remained almost constant. Influence of dilution rate and influent phenol concentration on phenol degradation was also studied by Shetty *et al.* (2007b) in the same reactor. It was observed that the time required to reach steady state increased with increase in dilution rate and influent phenol concentration. The percentage degradation was found to decrease with increase in dilution rate. It was possible to obtain almost 100% of phenol degradation for influent phenol concentrations of 300 and 500 ppm at dilution rate of 0.4094 h^{-1} and more than 99% at higher dilution rates. But the percentage degradation was reduced at higher dilution rate of 1.0235 h^{-1} and at influent phenol

concentrations of 800 and 900 ppm. It was observed that the attached biomass dry weight, biofilm thickness and biofilm density were also influenced by dilution rate and influent phenol at steady state condition. Frequency and amplitudes of pulsation were found to combinedely affect the biodegradation of phenol in the pulsed plate bioreactor and hence the vibrational velocity (amplitude*frequency) was found to influence the bioreactor performance (Shetty et al. 2008). It was found that optimum vibrational velocities need to be fixed for maximum removal efficiency of the bioreactor depending on the influent phenol concentration. Shetty et al. (2011) by modeling phenol biodegradation in a pulsed plate bioreactor have found that the performance of the cells in the biofilm, biodegradation rate and hence the reactor performance are mainly governed by internal diffusion limitations,rather than the external mass transfer resistance.

Shetty *et al.* (2013) also studied the effect of cell carrier loading and number of packed stages during start-up and at steady state on phenol biodegradation in a pulsed plate bioreactor for treating wastewater containing phenol with *Nocardia hydrocarbonoxydans*. Increase in cell carrier loading and number of stages improved the performance of the reactor during Start up and at steady state. It was found that the start up time may be decreased with increase in pre-acclimatization steps for the cells to adapt to new environment.

Pulsed plate bioreactor has been proved to be an efficient bioreactor. Hence in the present study pulsed plate column was selected for phenol degradation using *Pseudomonas desmolyticum* bacteria immobilized on granular activated carbon as solid support. Detailed studies on biofilm formation and characteristics with a due focus on physical structure of the biofilm and chemical composition of extracellular polymeric substances in pulsed plate bioreactor has not been reported in literature. Thus, the present study focuses on the effect of various operating conditions on the biofilm characteristics associated with continuous phenol degradation in pulsed plate bioreactor during the reactor start up and at steady state.

CHAPTER 3

MATERIALS AND METHODS

This chapter presents the materials used and the detailed methodology adopted to achieve the stated objectives of the research work.

3.1. Microorganism

Pseudomonas desmolyticum (NCIM 2112) was chosen for phenol biodegradation and was procured from National Collection of Industrial Microorganisms (NCIM), Pune, India in a lyophilized form.

3.2 Materials

Phenol (Analytical grade), Copper sulphate, Potassium ferricyanide and Humic acid were procured from Loba Chemie, (India) Ltd., Mumbai; Disodium tartrate, Sodium hydroxide from Merk (India) Ltd., Mumbai; Ammonium chloride, Sodium carbonate and granular activated carbon (GAC) from NICE Chemicals, (India) Ltd., Cochin; 4-Aminoantipyrene from Spectrochem Pvt. Ltd., (India), Mumbai; Bushnell and Haas media, Nutrient Agar and Nutrient media from HI-Media, (India) Ltd., Mumbai.

3.3. Methods

3.3.1. Preparation of phenol stock solution

Stock of 10 000 ppm phenol solution was prepared by dissolving 10 g of phenol and making the total volume of solution to 1000 mL in a standard flask using distilled water.

3.3.2. Maintenance, Sub culturing and growth of the bacteria

3.3.2.1. Preparation of agar slant and subculturing of the bacteria

28 g of nutrient agar powder was suspended in 1 litre of distilled water. The mixture was heated stirring constantly until the powder dissolved completely. The mixture was autoclaved at a temperature of 121⁰C at 1.5 kg/cm² gauge pressure for 20 minutes. The nutrient agar was later cooled retaining liquid state and kept in a slant position until the agar solidified. The slants thus prepared were used for subculturing of *Pseudomonas desmolyticum* cells.

The initial culture of *Pseudomonas desmolyticum* cells in lyophilized form was obtained from NCIM. The ampoule was marked near the middle of the cotton wool with sterile sharp file. The outer surface was disinfected with 70% alcohol. The ampoule was wrapped with sterile cotton and was cut open at the marked area. The pointed top was removed gently and cotton plug was removed carefully. To this 0.3 mL of Bushnell Haas broth (Bushnell and Haas 1941) in distilled water, having composition as presented in Table 3.1, was added to make a suspension of culture.

Table 3.1. Composition of Bushnell Haas Broth Medium in distilled water

Ingredients	gL ⁻¹
MgSO ₄	0.2
CaCl ₂	0.02
KH ₂ PO ₄	1.0
K ₂ HPO ₄	1.0
NH ₄ NO ₃	1.0
FeCl ₃	0.05

Using a sterile loop, a loopful of the suspension was taken and streaked on previously prepared agar slant and incubated at 30°C for 24 hours. The slants thus prepared were covered with aluminium foil and refrigerated until use. The cells were subcultured fortnightly.

3.3.2.2 Growth of the bacterial culture in liquid media

The bacterial culture was further grown in liquid medium, containing phenol as sole carbon source for the growth of *Pseudomonas desmolyticum* cells as follows:

99mL of Bushnell Haas broth in distilled water (Table 3.1) was taken in a 250 mL conical flask and the flask was sterilized along with the mineral medium for 20 minutes in an autoclave at 1.5 kg/cm² gauge pressure and cooled to room temperature. One millilitre of 10 000 ppm phenol solution was added to this sterilized medium in a laminar flow chamber in order to obtain 100 ppm of phenol concentration and total volume of 100 mL. This media was inoculated with two loopful of organisms from the freshly subcultured slant. This inoculated culture was kept in an incubator shaker for about 24 h at 30°C and 120 rpm. This served as a primary culture and was used as the inoculum for acclimatization.

3.3.3 Acclimatization of bacteria

For any microorganism to degrade phenol from the aqueous environment, it should be able to grow in that environment. Thus, in order to enable the growth of bacteria at high phenol concentrations, the acclimatization of the bacteria to phenol is required. Thus, *Pseudomonas desmolyticum* (NCIM 2112) cells were acclimatized to phenol. The acclimatization procedure is as follows:

For the acclimatization of bacteria, to 94 mL of sterilized media 1 mL of 10 000 ppm phenol stock solution was added. 5 mL of primary culture was used to inoculate the aqueous media. Thus, 100 mL of the media containing 100 ppm phenol and the bacterial inoculum was shaken in an incubator shaker at 30°C and 120 rpm speed for 24 h

incubation time. This formed a secondary acclimatized culture. Same procedure was followed for the third and fourth acclimatization, using the second acclimatized culture and third acclimatized culture as the inoculums respectively and each time using 24 h incubation time. The culture obtained by the above said procedure has been thus acclimatized to 100 ppm phenol. Further acclimatization to 200, 300, 400, 500, 600, 700, and 800 ppm phenol were done gradually using the above procedure.

The solution of various phenol concentrations of 200,300, 400,500,600,700 and 800ppm in mineral media were obtained by mixing 2,3,4,5,6, 7, and 8mL of 10 000 ppm phenol stock solution to 250 mL flask containing 93, 92, 91, 90, 89, 88 and 87 mL of the sterilized mineral media solution respectively and on inoculation with 5 mL of the culture to make a total volume of 100 mL.

The successive acclimatization to higher phenol concentrations were done, using 5 mL of cultures acclimatized to immediate lower concentration, as the inoculum, e.g. when a culture need to be acclimatized to 400 ppm phenol, then the inoculum used was the one which had undergone acclimatization at 100, 200, and 300 ppm phenol successively. Cultures acclimatized to the required phenol concentration were stored at 4°C for further use in the experiments.

3.3.4 Cell Immobilization

In the present study pulsed plate column was used with the cells of *Pseudomonas desmolyticum* immobilized on Granular activated carbon (GAC) as the carrier material. The following method was adopted to immobilize the phenol acclimatized *Pseudomonas desmolyticum* cells on the GAC.

Cell culture suspension was prepared by growing the cells in the media containing the required concentration of phenol for 24 h in an incubatory shaker. Cell suspension cultured for 24 h was prepared from the culture acclimatized to the required phenol concentration and was used for immobilization of microbial cells on GAC. For 100 mL of 24 h grown cell suspension, 20 g of GAC was added and was refrigerated at 4°C for 48 h with occasional stirring. After 48 h, the GAC particles with the immobilized

cells were separated from the broth by filtration, washed and then used in continuous bioreactor experiments. The GAC particles with the immobilized cells are herein after referred as bioparticles.

In order to confirm the immobilization of microbial cells on GAC, following experiment was conducted. Initially 100 mL culture in 250 ml of flask was prepared having known concentration of phenol in mineral medium. The initial absorbance of the culture thus prepared was noted at absorbance of 610 nm. To this, 20g of GAC was added and refrigerated at 4°C for immobilization to occur. At regular time interval liquid sample was taken for measuring the absorbance. The absorbance kept on decreasing with time and reached a constant value confirming the cell attachment on GAC. The final value indicated the equilibrium value. The immobilization of microbial cells on GAC was also confirmed using Scanning electron microscope (Fig.3.1) where a layer of attached cells on the surface was visible.

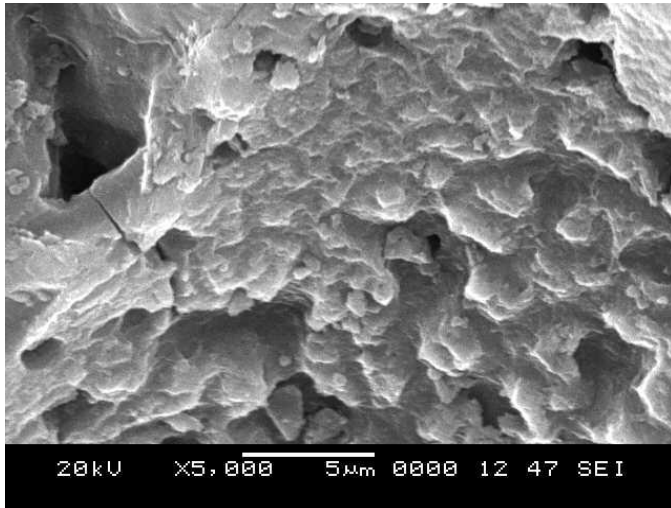


Fig.3.1. Immobilized cells on GAC

3.3.5 STUDIES ON PULSED PLATE BIOREACTOR

3.3.5.1 Experimental Setup

The experimental pulsed plate bioreactor used in the present study is shown in Fig.3.2. It consisted of a perspex column of 6.8 cm inner diameter, 7.5 cm outer diameter and 56 cm height. The plate stack consisted of number of perforated brass plates of 6.4 cm diameter, 1.5 mm thick mounted over a central steel rod of 1 cm diameter through a hole at the centre of each plate. The spacing between plates was set to 3cm. Each plate consisted of 88 holes of 2 mm diameter drilled on a triangular pitch. The fractional free area available on the plate was 0.086.

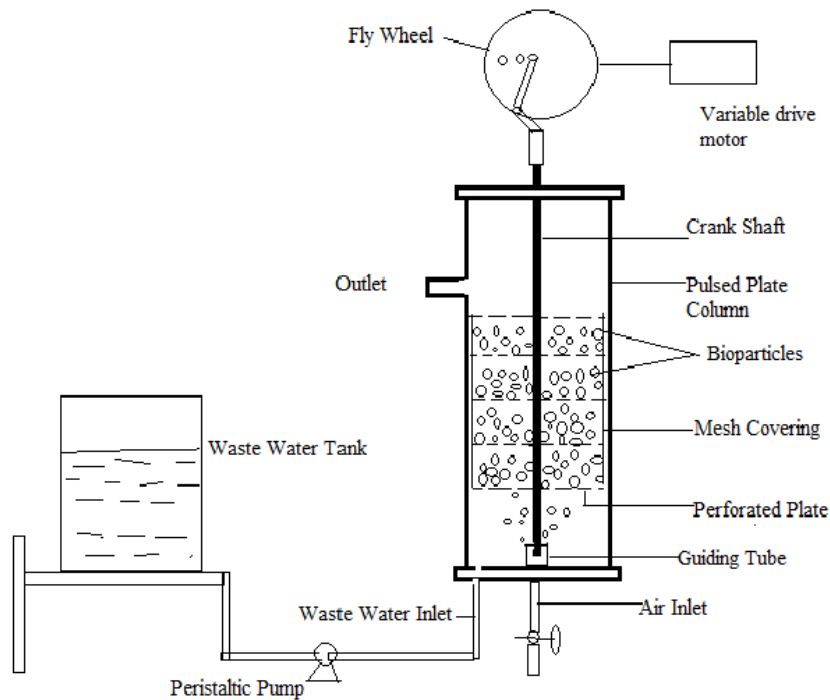


Fig.3.2. Pulsed Plate Bioreactor

The periphery of the plate stack was covered with a nylon mesh having a thickness of 0.5 mm. The space between any two consecutive plates formed a stage in the bioreactor. Known quantity (as per the requirement for the present study) of carrier

particles (GAC) immobilized with *Pseudomonas desmolyticum* (NCIM 2112) cells, was packed in each stage of the bioreactor. The bioreactor contained a plate stack with five plates, thus forming four stages. The whole set i.e. central rod with the packed stages, was inserted into the column with the bottom portion of the rod positioned in the guiding tube. The central steel rod with the plates was connected at the top to a slider and the slider in turn was connected to the crank shaft. The crank shaft was positioned on to one of the holes in the flywheel to set a required amplitude of pulsation.

The pulsing action to the plates was provided by running the flywheel using a variable speed motor with gear reduction and frequency controller, through the slider/crank arrangement. The required frequency and amplitude of pulsation was obtained through this arrangement. The amplitude of the pulsing motion is the distance between the neutral position to the maximum displaced position of the plate stack. The frequency of pulsation was measured by counting the number of oscillations for a given period of time. Water and air inlet ports are provided at the bottom of the column. The outlet for the effluent port was provided on the column wall at 37 cm from the bottom of the column. Four nozzles were provided at the bottom portion of the guiding tube in the column in order to disperse small bubbles of air. The reactor working volume was 1.34 L.

3.3.5.2 Experimental Procedure

The experimental setup was assembled as shown in Fig. 3.1 Each stage was filled with a known quantity of GAC particles (as per the requirement of the study) with the cells of *Pseudomonas desmolyticum* immobilized on them and then covered with a nylon mesh along the whole periphery of the plates. Synthetic phenol solution was prepared using tap water with required phenol concentration and nutrients as given in Table 3.1, and the pulsed plate bioreactor was filled with this solution upto the reactor outlet port at 37 cm. Variable speed regulator was used to set the required frequency of pulsation and the required amplitude was set by changing the position of the crankshaft. Peristaltic pump was used to pump the synthetic waste water from the bottom of the column at the required flow rate and compressed air was passed continuously from the bottom of the

column through air pressure regulator equipped with a filter and a rota meter and an airflow rate of 1.7-1.8 LPM was maintained to ensure proper supply of oxygen to the microorganisms. The water samples were drawn at the outlet of the column at regular intervals of time and were analyzed for phenol concentration during the Start up until steady state was reached and the steady-state condition was considered when the concentration of phenol remained almost constant for about 10–12 h. Then the experiment was stopped.

The time taken to reach steady state (start-up time) was determined for each of the continuous column experiment conducted at a fixed set of conditions viz. frequency and amplitude, influent phenol concentration, dilution rate and the GAC loading. The total time was split into equal time intervals. The experiment was run for each of the pre-calculated times with the fresh bioparticles. The experiment under a fixed set of conditions was performed for a fixed pre-calculated time period. The experiment was stopped after this time and the bioparticles were withdrawn from the reactor for further analysis. The effluent from the reactor was collected and the phenol concentration was determined by using the methodology described in Section 3.10. Percentage Degradation of phenol was calculated using Eq.3.1.

$$\text{Percentage degradation of phenol} = \frac{C_i - C}{C_i} 100 \dots\dots\dots 3.1$$

A sample of bioparticles from the reactor were dried using the methodology presented by Schadler *et al.* (2008). The biofilm thickness of dried particles were measured using scanning electron microscope at its cross section and the biomass dry weight was determined by using the procedure given in Section 3.3.11. A sample of the bioparticles were used for the extraction of EPS. EPS extraction from the bioparticles was carried out as described in Section 3.3.6 and the EPS was analyzed for determining the composition of EPS in terms of protein, carbohydrate and humic substance as described in Section 3.3.7 to 3.3.9. During all the experiments, the dilution rate (D= volumetric flow rate/volume of the reactor) based on liquid flow rate, influent phenol

concentration, frequency of pulsation and amplitude of pulsation were set at the required values.

3.3.5.3 Experimental conditions for various studies

The PPBR was operated at influent phenol concentrations in the range of 200 to 1200 ppm, dilution rate(D) in the range of 0.33 h^{-1} to 0.99 h^{-1} , frequencies of pulsation (f) in the range of 5 to 10 per minute (0.08 s^{-1} to 0.16 s^{-1}), amplitudes of pulsation (A) in the range of 3.5 cm to 6.5 cm and GAC loading of 80 g (20 g per stage) and 120 g (40 g per stage). To study the effect of dilution rate on phenol removal and biofilm characteristics, reactor was operated with different dilution rates viz. 0.33 , 0.66 and 0.99 h^{-1} with amplitude of pulsation as 3.5 cm, cell carrier loading as 80g of bioparticles. The effect of dilution rate was studied at influent phenol concentration of 200 ppm and 1200 ppm at frequency of pulsation of 0.08s^{-1} , 0.12s^{-1} and 0.16s^{-1} .

To study the effect of frequency of pulsation, the reactor was operated with different frequencies of 0.08 s^{-1} , 0.12 s^{-1} and 0.16 s^{-1} keeping dilution rate of 0.33 h^{-1} , amplitude of pulsation as 3.5 cm and cell carrier loading as 80 g of bioparticles. these experiments were carried out at influent phenol concentration of 200 ppm, 400 ppm and 800 ppm . To study the effect of influent phenol concentration, the reactor was operated with different influent phenol concentrations of 200, 400, 600 and 800 ppm with dilution rate of 0.33 h^{-1} , amplitude of pulsation as 3.5 cm, and cell carrier loading as 80 g of bioparticles. These experiments were carried out at frequencies of 0.08s^{-1} , 0.12s^{-1} and 0.16s^{-1} . To study the effect of influent phenol concentration of 1200 ppm, the reactor was operated with amplitude of pulsation as 3.5 cm, cell carrier loading as 80 g of bioparticles and at frequency of pulsation of 0.08s^{-1} . These experiments were carried out at dilution rates of 0.33h^{-1} , 0.66h^{-1} and 0.99h^{-1} .

Similarly the effect of amplitude of pulsation was studied by operating the reactor with different amplitudes of pulsation of 3.5, 5, and 6.5 cm with dilution rate of 0.33 h^{-1} , frequency of pulsation as 0.08 s^{-1} and cell carrier loading as 80 g of bioparticles.

These experiments were carried out at influent phenol concentrations of 200 ppm to 800 ppm.

The effect of cell carrier loading was studied by operating the reactor with different carrier loadings of 80 and 120 g GAC with dilution rate of 0.33 h^{-1} , frequency of pulsation as 0.08 s^{-1} , amplitude of pulsation as 3.5 cm. these experiments were carried out at influent phenol concentrations of 200 ppm to 800ppm.

3.3.6 Extraction of EPS

The bioparticles were withdrawn from the reactor after the calculated time interval and were washed with distilled water to remove the loose cells. Small portion of the bioparticles were taken for the extraction of EPS and rest were used for finding the dry weight of attached biomass, biofilm thickness and to study the morphology of microorganisms. EPS extraction was carried out by following the methodology adopted by Liu and Fang (2002) with modification. For the extraction of EPS, the cells were fixed first by adding 8mL of formaldehyde to 20g of bioparticles and refrigerated for 1h followed by addition of 1N NaOH solution to the sample and refrigerated at 4°C for 3h. The sample was then subjected to sonication and vortexing in series for about 8 min (precalculated to ensure complete extraction of EPS) and then the liquid was centrifuged for 20 min at 20000 g at 4°C . The supernatant containing the EPS was then purified by using dialysis membrane of 3.5 kDa at 4°C for 24 h. The sample was used to analyze the composition of EPS in terms of protein, carbohydrate and humic substance as described in Section 3.3.7, 3.3.8 and 3.3.9 respectively.

3.3.7 Estimation of Total protein concentration in EPS

Total protein in the exopolymeric substances was determined by Lowry's method (Lowry *et al.* 1951). The following reagents were prepared.

Solution A : 500mL of aqueous solution containing 2.8598 g of NaOH and 14.3084 g of Na_2CO_3

Solution B: 100 mL of aqueous solution containing 1.4232 g of CuSO_4

Solution C: 100 mL of solution containing 2.85299 g disodium tartrate dihydrate

Lowry's solution was prepared by mixing solution A, solution B and solution C in volume ratio of 100:1:1

Folin's reagent: 5 mL of 2 N Folin's reagent was added to 6 mL of double distilled water.

Preparation of Standard Solution: Bovine Serum Albumin (BSA) was used as standard. 0.1 mg/mL of BSA was prepared as standard stock solution. 2, 4, 6, 8 and 10 mL of standard stock solutions were taken in 15 mL test tubes and the total volume was made upto 10 mL by adding distilled water that gave 0.02, 0.04, 0.06, 0.08 of 0.1 mg/mL of standard BSA. Distilled water was taken as blank for the analysis.

Protein analysis: 0.5 mL of sample or the standard was taken and to this 0.7 mL of Lowry's solution was added and mixed in vortex mixer. This solution was incubated at room temperature in dark for 20 minutes and later 0.1 mL of Folin's reagent (freshly prepared) was added and mixed in vortex mixer. The solution was then incubated for 30 minutes and the absorbance was measured at 750 nm using UV-VIS spectrophotometer (Labomed NCR III 40) against reagent blank. A calibration curve was plotted using the measurements for the standard solutions and is shown in Fig 3.3. The concentration of protein in the sample was found by using the calibration curve from the absorbance values.

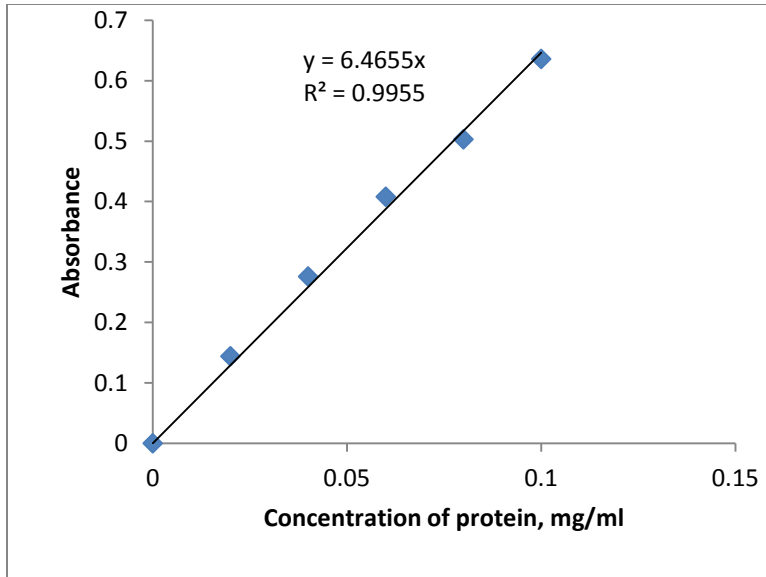


Fig 3.3. Calibration plot for protein using BSA as a standard

The amount of protein in the EPS of the biofilm per unit mass of the biomass, P was calculated by using Eq.3.2

$$P = \frac{p_1}{(w_1 \times w_3) / w_2} \quad (3.2)$$

Where

P is the mg protein in the EPS of the biofilm per unit mass of the biomass, mg protein /g of biomass

p_1 = mg of protein present in w_1 g of GAC = Concentration of protein in mg/mL obtained from the calibration plot \times Volume of sample obtained after dialysis in mL

w_1 = mass of GAC (g) withdrawn to extract EPS for protein/humic acid /carbohydrate analysis

w_2 = mass of GAC (g) withdrawn to find the quantity of biomass

w_3 = mass of biomass (g) present in w_2 g of GAC.

3.3.8 Estimation of humic substance concentration in EPS

Humic substance in EPS was estimated by modified Lowry's method (Frolund et al. 1995).

Solution A and Solution B as described in Section 3.7 were prepared. Lowry's solution for modified Lowry's method was prepared by mixing solution A and solution B in volume ratio of 100:1. Folin's reagent was prepared by adding 5 mL of 2 N Folin's reagent to 6 mL of double distilled water

Preparation of Standard Solution: In this method humic acid was used as the standard. 1 mg/mL of humic acid was prepared as standard stock solution. 2, 4, and 6 mL of standard stock solution was taken in 15 mL test tubes and the total volume was made upto 10 mL by adding distilled water that gave 0.2, 0.4, and 0.6 mg/mL of standard humic acid. Distilled water was taken as blank for the analysis. The method of analysis is similar to that used for protein estimation (Section 3.7), but without the addition of Solution C (CuSO₄). The absorbance was measured at 750 nm using UV-VIS spectrophotometer against reagent blank with distilled water. A calibration curve was plotted using the measurement for the standard solutions and is shown in Fig 3.4. The concentration of humic acid in the sample was found by using the calibration curve from the absorbance values. The amount of humic acid present in the EPS per unit mass of the biomass, C_{HA} was calculated using Eq.3.3.

$$C_{HS} = \frac{HS}{(w_1 \times w_3) / w_2} \quad (3.3)$$

Where

C_{HS} is the humic substance content in EPS of the biofilm in mg per gram of biomass,

Hs = mg of humic acid present in w₁ g of GAC = Concentration of humic acid in mg/mL obtained from the calibration plot × Volume of sample obtained after dialysis in mL,

w₁, w₂ and w₃ are as defined earlier in Section 3.3.7.

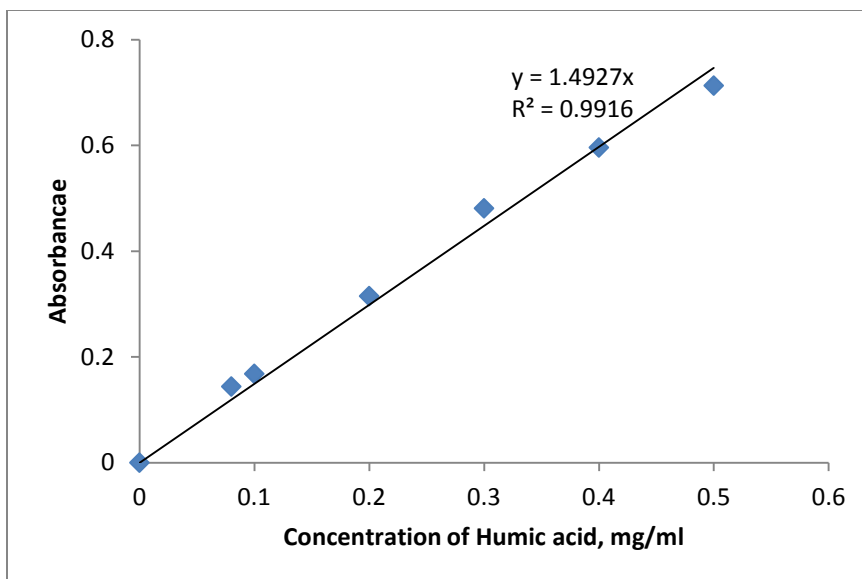


Figure 3.4. Calibration plot for humic substance with humic acid as standard

3.3.9 Estimation of Total Carbohydrate Content

Total carbohydrate was estimated by Dubois method (Duboi *et al.* 1956).In this method, Phenol (5%) and sulphuric acid (97%) were used as the reagents.

Preparation of Standard Solution: 0.1 mg/mL of glucose solution was prepared as a stock solution. 2,4,6 and 8 mL of the stock solutions were taken in a test tube and diluted to 10 mL using distilled water to prepare standard solutions of various concentrations viz. 0.02, 0.04, 0.06, 0.08 mg/mL.

Carbohydrate analysis: 2 mL of the standard or the sample was taken and 1 mL of 5% aqueous solution of phenol was added. Further, 5mL of concentrated sulphuric acid was added and kept for incubation at room temperature for 10 minutes and then kept in water bath at 30° C for about 30 minutes and finally absorbance was noted at 490 nm using UV-Vis Spectrophotometer against reagent blank with distilled water. The calibration curve

of absorbance vs. glucose concentration of standard solutions in mg/mL was plotted and is shown in Fig 3.5. The concentration of Carbohydrate in the sample was found by using the calibration curve from the absorbance values. The amount of Carbohydrate present in the EPS per unit mass of the biomass was calculated using Eq.3.4

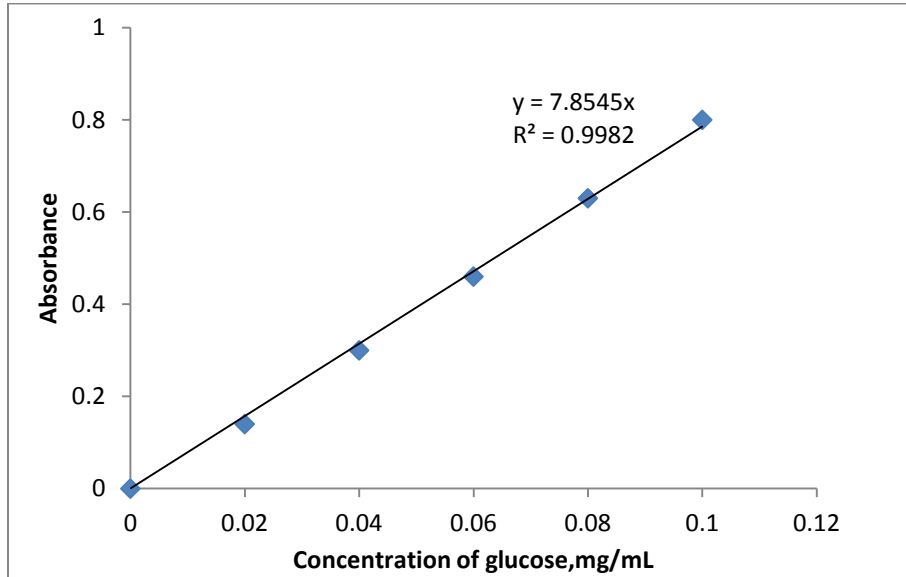


Figure 3.5. Calibration plot for carbohydrate analysis using glucose as standard

$$C_{CH} = \frac{CH}{(w_1 \times w_3) / w_2} \quad (3.4)$$

Where

C_{CH} is the carbohydrate content in EPS of the biofilm in mg per gram of biomass.

CH = mg of carbohydrate present in w_1 g of GAC = Concentration of carbohydrate in mg/mL obtained from the calibration plot \times Volume of sample obtained after dialysis in mL and w_1, w_2 and w_3 are as defined earlier in Section 3.3.7.

3.3.10 Analysis of phenol concentration

The analysis of phenol the present investigation was carried out by 4-aminoantipyrene method (APHA 1995). This method is based on rapid condensation of

phenol with 4-aminoantipyrine, followed by oxidation with potassium ferricyanide under alkaline conditions to form a red colored antipyrine dye.

1 mL of 10 000 ppm stock phenol solution was diluted to 100 mL in a standard flask to obtain 100ppm of phenol solution.

Reagents for analysis were prepared as follows :

Ammonium chloride solution: Ammonium chloride solution was prepared by dissolving 20 g NH_4Cl in distilled water and making volume upto 1000 mL.

Ammonium hydroxide solution: NH_4OH having specific gravity of 0.91 was used.

4-aminoantipyrine solution: This solution was prepared by dissolving 2 g of 4-antiaminopyrine in distilled water and making volume up to 100 mL. A fresh solution was prepared for each day of use.

Potassium ferricyanide solution: This solution was prepared by dissolving 8 g of $\text{K}_3\text{Fe}(\text{CN})_6$ in distilled water and making volume up to 100 mL. Fresh solution was prepared for each week of use.

Preparation of standard solutions of phenol :A series of 100 mL phenol standards of 1,2,3,4, and 5 ppm concentration were prepared by adding 1,2,3,4, and 5 mL of 100 ppm phenol solution into a standard volumetric flask and diluting to 100 mL by distilled water.100 mL of distilled water was taken for blank.

Phenol analysis: The standards measuring 100 mL each or a known volume of the sample diluted to 100 mL with distilled water were treated with the reagents as follows: 5 mL of ammonium chloride solution was added to each flask and the pH was adjusted to 10.0 ± 0.2 with 0.5 mL of ammonium hydroxide solution. Then 2.0 mL of 4-aminoantipyrine solution was added and mixed in a vortex mixer. Finally 2.0 mL of potassium ferricyaanide solution was added and mixed well. After 15min of incubation at room temperature, absorbance of each solution was measured in UV/VIS spectrophotometer against the reagent blank at 510 nm . A calibration of absorbance vs.

phenol concentration was plotted and is shown in Fig. 3.6. The samples from the reactor were centrifuged at 15 000g before phenol analysis to remove any biomass present in the sample. Suitable volume of the sample was taken and diluted to 100 mL with distilled water to bring the concentration of phenol below 5 ppm. The reagents were added to the solution as previously described and the absorbance was measured against the reagent blank at 510 nm. The concentration of phenol in the sample was obtained by calculating the concentration corresponding to the absorbance from the calibration graph and then multiplying it by the dilution factor.

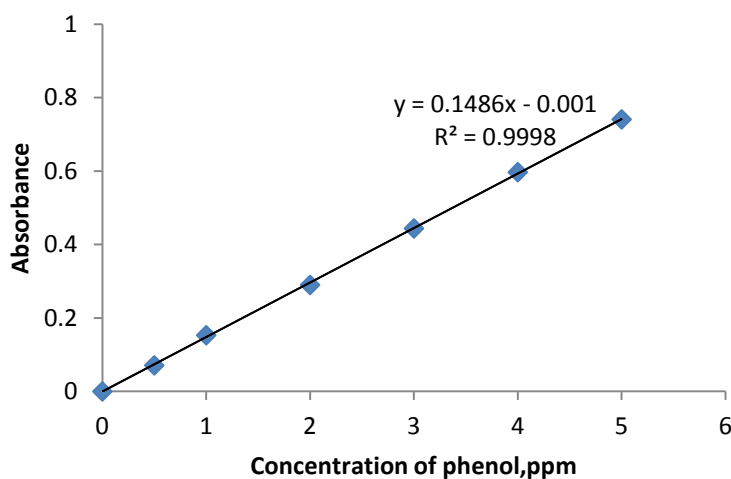


Figure 3.6. Calibration Plot for Phenol Estimation

3.3.11 Estimation of Attached Biomass Dry Weight .

The bioparticles from the reactor were washed with distilled water to remove free cells and dried in an oven at 105 °C for 24 hours and weighed. Then the biofilm was removed completely from solid particles by treating with hot 0.25 N NaOH solution. Then the solid particles were washed with distilled water, dried at 105°C for 24 h and

weighed. This procedure of heating, washing and drying was continued until constant weight was obtained. The dry biomass weight of known amount of particles was obtained by subtracting the weight of dried bioparticles from the weight of dry solid (GAC) particles after removal of biomass (Tang and Fan 1987). As the total weight of dry GAC particles taken for analysis was known, attached dry weight in the entire reactor was calculated.

3.3.12 Estimation of Biofilm Thickness and Biofilm Density

The bioparticles were dried (Schadler *et al.* 2008), gold sputtered and the average biofilm thickness was estimated at its cross section by using scanning electron microscope (JEOL JSM-6380LA).

The biofilm density was calculated by using Eq. 3.5. (Tang and Fan, 1987).

$$\rho = \frac{W}{N_p \left(\frac{\pi}{6} \right) [(d_p + 2\delta)^3 - d_p^3]} \quad \text{-----3.5}$$

Where

ρ – biofilm density, g/cc

W- weight of dry attached biomass, g

N_p -number of particles

d_p -equivalent diameter of the particle, cm

δ -thickness of biofilm, cm

CHAPTER 4

RESULTS AND DISCUSSION

4.1. Effect of dilution rate on steady state and Start up performance of PPBR in terms of phenol biodegradation and biofilm characteristics

This chapter presents the results of the experiments conducted to study the effect of dilution rate, influent phenol concentration, frequency and amplitude of pulsation and cell carrier (GAC) loading on steady state and start up performance of Pulsed Plate BioReactor with *Pseudomonas desmolyticum* cells in terms of phenol biodegradation and biofilm characteristics.

Biofilm characteristics are presented in terms of physical characteristics such as biofilm thickness, biofilm dry density, attached dry biomass and morphology along with chemical characteristics such as composition of EPS in terms of the amount of protein, carbohydrate and humic substances.

Dilution rate is considered as one of the factors which affect the performance of a reactor for a given duty. Hence in the currently reported study, the effect of dilution rate on steady state and Start up performance of PPBR in biodegradation of phenol was studied.

The biofilm matrix strength is influenced by the amount and composition of extracellular polymeric substances (EPS) present in the biofilm and it governs the biofilm detachment rates. The hydrodynamic conditions in the column exerts shear on the biofilm and detachment is thus also governed by these conditions. Surface erosion must be considered as being triggered when the shear forces exceeds the adhering force of the individual cell. Again, the adhering force is governed by the amount of EPS, and the composition of polymers (Kommedal and Bakke 2003).

Thus, knowledge of nature and characteristics of biofilm in terms of its major constituents becomes important in optimal performance of biofilm reactors (Cortez *et al.* 2008). The morphological and physical characteristics of the biofilm are influenced by the hydrodynamic conditions and it in turn dictates the stable operation of the bioreactor.

Thus, the effect of dilution rate on the composition of EPS in biofilm and physical characteristics of the biofilm at steady state in pulsed plate bioreactor during biodegradation of phenol was studied. The effect on biofilm dynamics in terms of its physical and morphological characteristics during the reactor start-up was also studied.

In the present study, the effect of dilution rates in the range of 0.33, 0.66, and 0.99 h⁻¹ are considered. For the given reactor configuration the minimum flow rate was 0.33 h⁻¹ below which the liquid present in the reactor was almost stagnant or the residence time was too long and above 0.99 h⁻¹ the residence time in the reactor was too small for the degradation to take place. Hence the above range was considered for the present study.

4.1.1. Effect of dilution rate on phenol biodegradation during Start up and at steady state of PPBR.

The degradation of phenol during the Start up and steady state was studied under the conditions when the reactor was operated at a frequency (f) of 0.08 s⁻¹ and with a total of 80 g of GAC (S) (20 g in each stage) with immobilized cells; influent phenol concentrations of (C_i) 200 ppm and 1200 ppm; at an amplitude (A) of 3.5 cm and at various dilution rates (D) of 0.33 h⁻¹, 0.66 h⁻¹ and 0.99 h⁻¹. The results are presented in Fig. 4.1.

It can be observed from Fig. 4.1 that the Start up behavior of PPBR in terms of change in effluent phenol concentration during phenol biodegradation consists of three phases. During the initial stage there is a sudden decrease in phenol concentration. This sharp decrease may be due to adsorption of phenol on to the free surface of GAC during

initial stage of the operation and simultaneous consumption of phenol by the attached bacteria on the surface of GAC. The rate of biological degradation during the initial periods may be slow due to insufficient biofilm formation. Thus the phenol concentration increases slightly after an initial sudden decrease. The initial sudden decrease is due to adsorption on the free GAC surface, which is a fast process. But once the free surface of GAC is saturated with phenol, the rate of phenol removal becomes slower owing to slower degradation process by a thin monolayer of cells on GAC surface. Thus, the second phase of a slight increase in phenol concentration occurs after an initial sudden decrease. In the second phase the rate of removal may be lower than the rate at which phenol enters the reactor, thus leading to phenol accumulation in the reactor which resulted in an increase in phenol concentration. But with the passage of time, the cells on the GAC surface consume phenol, grow and the biofilm develops. Biomass growth rate increases and phenol removal rate by biodegradation also increases. During this period there may be fluctuations in phenol concentrations owing to growth and detachment of biofilm. In the third phase, since the microbial cells are active, the growth and detachments may be equal, thus leading to constant biofilm thickness and the concentration of phenol reaches almost a constant value indicating a steady state. At steady state the volumetric net phenol removal rate from the reactor is equal to the rate of phenol biodegradation, and the concentration attains a constant value. Hence, in the third stage the removal of phenol could be solely due to microbial activity or biodegradation than adsorption that had happened during initial stage of removal of phenol. These three phases were observed during start up with influent phenol concentrations of 200 ppm and 1200 ppm and at all the dilution rates studied.

In order to understand whether adsorption of phenol on GAC occurring during the continuous removal of phenol in PPBR contribute for phenol removal during the start-up, continuous phenol removal experiments were conducted using bare GAC and GAC with the immobilized cells in the pulsed plate column under same set of experimental conditions as : influent phenol concentration of 200 ppm; GAC loading of 80 grams of GAC; dilution rate of 0.33 h^{-1} , frequency of pulsation of 0.08s^{-1} ; and amplitude of pulsation of 3.5 cm. The percentage removal

of phenol during the Start up and steady state were determined under these conditions. The results are presented in Fig. 4.2. It may be observed from Fig.4.2 that, when only GAC was used as an adsorbent, the concentration of phenol decreased suddenly to a very low value initially and then increased slowly. During the initial time period owing to adsorption of phenol onto GAC surface, the phenol concentration reduces drastically. However, as portions of GAC bed get saturated with passage of time, the concentration of phenol in the effluent goes on increasing. Given enough time and continuous flow, the bed may get saturated entirely with the effluent concentration reaching the influent value indicating the complete saturation of GAC bed. However, when the GAC immobilized with the cells were used for phenol removal under the similar set of experimental conditions, the concentration of phenol decreased initially at a very fast rate, then increased slightly but with the passage of time attained a steady value. The initial sudden decrease in concentration at the similar rate as it occurred with bare GAC, confirmed that adsorption onto the surface of GAC uncovered with the cells by ex-situ pre-immobilization procedure is the dominant mechanism for phenol removal in this phase. But, when the uncovered surface of GAC is saturated partly, the phenol concentration in the effluent increased. The growth of cells on the surface may be very less even when the bed portions start saturating, to contribute for phenol removal by biodegradation, thus leading to increase in phenol concentration at the effluent. However, as discussed earlier in this section, with the passage of time the cells grow to form considerable biomass to bring about biodegradation and thus the system attains a steady value. It confirms that during the initial period of start-up, adsorption is the dominant phenol removal mechanism and later biodegradation contributes largely in phenol removal, with it being the dominant phenomena during the steady state operation of the bioreactor.

From Fig.4.3(a) and 4.3 (b), it may be observed that the time taken to reach steady state (start up time) increased with the increase in dilution rates in the range of 0.33 to 0.99 h⁻¹ at both 200 ppm and 1200 ppm influent phenol concentrations. However, the effect of dilution rate on start-up time for low influent phenol concentration of 200 ppm was found to be very predominant (Fig.4.3a) when compared with that at influent

phenol concentration of 1200 ppm, as evidenced by only a marginal increase in start-up time with increase in dilution rates (Fig.4.3b). The start up time increased from 12 to 37 h with 200 ppm influent phenol concentration, whereas the increase was from 47 to 55 h with 1200 ppm influent phenol concentration as the dilution rate was increased from 0.33 to 0.99 h⁻¹. During the Start up, biofilm formation takes place. Biofilm formation phase involves growth of biofilm and the detachment of biofilm. Owing to reduced contact time at higher dilution rates, the rate of growth of biofilm is slower. Higher dilution rate causes higher rates of detachment of biomass due to shear caused by the fluid flowing at high velocities. Hence reduced growth rates and increased detachment rates cause longer time for the attainment of steady state biofilm thickness and thus increases the Start up period with increase in dilution rates.

As presented in Fig. 4.3(a) with influent phenol concentration of 200 ppm, the percentage degradation of phenol at steady state was above 99% for the dilution rate of 0.33 h⁻¹, however steady state percentage degradation reduced to 93% when the dilution rate was increased to 0.66 h⁻¹ and further decreased to 73% at a dilution rate of 0.99 h⁻¹. When the concentration was increased to 1200 ppm, the degradation of phenol at steady state at a dilution rate of 0.33 h⁻¹ was 76% and the percentage degradation reduced to 55% with dilution rate of 0.66 h⁻¹ and was still decreased to 27% at dilution rate of 0.99 h⁻¹ as shown in Fig. 4.3(b). From Fig.4.3, it is observed that there is a reduction in steady state percentage phenol degradation with an increase in dilution rate and this could be due to decrease in residence time of phenol in the reactor, which in turn reduces the contact time period between microorganisms in the biofilm and the phenol present in the medium. As the dilution rate increases the volumetric phenol loading to the reactor also increases, residence time provided in the reactor reduces and not enough time is available for diffusion of phenol through the biofilm. It reduces the availability and utilization of phenol by the cells in the interior of biofilm. If the external mass transfer rate was the controlling factor, then the percentage degradation would have increased with the increase in dilution rate owing to increased flow velocity which decreases the mass transfer resistance and thus increasing the external mass transfer coefficient. But

decrease in percentage degradation with increase in dilution rate shows that external mass transfer resistance is not the governing resistance. It may be as a result of the high rate of mass transfer achievable in the reactor, which is caused by high mixing and turbulence created due to pulsation of plates.

On comparison of the steady state percentage phenol degradations obtained with influent phenol concentration of 200 ppm and 1200 ppm, as shown in Fig.4.3 (a) and 4.3(b), it is observed that the steady state percentage degradation decreased with the increase in influent phenol concentration. It could be due to the inhibitory effect of phenol on microbial activity at higher phenol concentration. The volumetric loading of phenol is higher at higher phenol concentration and hence this could also contribute to the reduction in percentage degradation of phenol (Shetty *et al.* 2007). At the dilution rate of 0.99 h^{-1} and at the influent phenol concentration of 1200 ppm, both the factors, i.e. erosion of biofilm and phenol inhibition would act simultaneously leading to a very low percentage degradation.

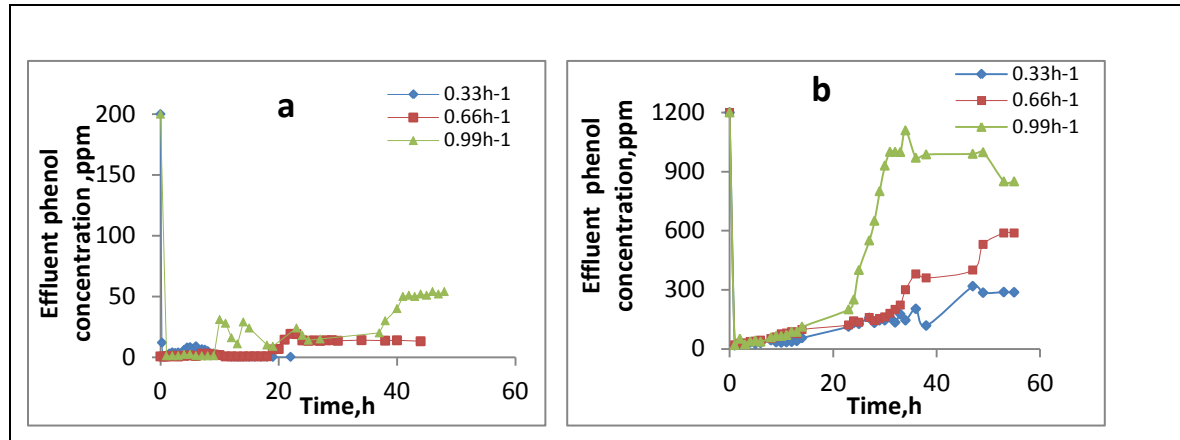


Fig4.1 Degradation of phenol during Start up for different dilution rates of 0.33,0.66,and 0.99h⁻¹ with influent phenol concentration of (a) 200ppm (b)1200ppm. Conditions: $f=0.08\text{ s}^{-1}$; $A= 3.5\text{ cm}$; GAC loading (S) = 80 g.

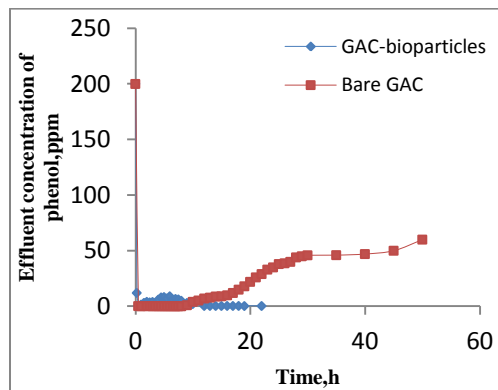


Fig.4.2 Performance of reactor for the removal of phenol with (a) bare GAC and (b) GAC with immobilized cells. Conditions: $C_i=200\text{ ppm}$; $A=3.5\text{ cm}$; $D=0.33\text{ h}^{-1}$; $S=80\text{ g}$; $f=0.08\text{ s}^{-1}$; $S=80\text{ g}$.

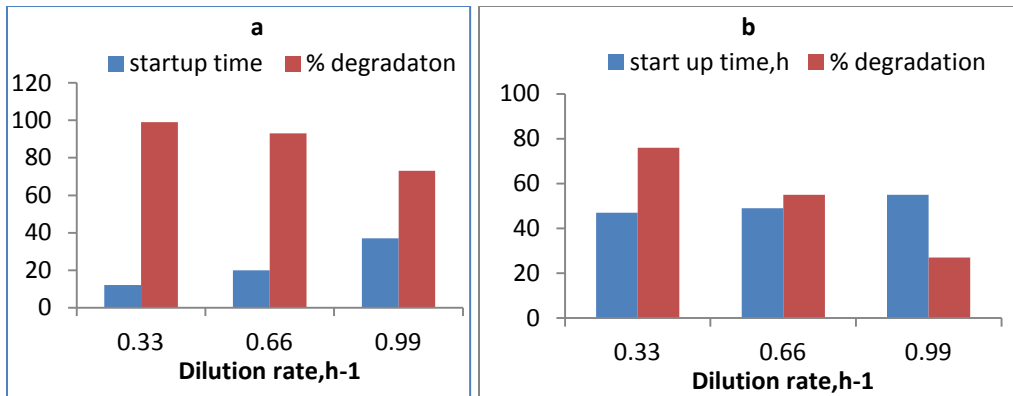


Fig.4.3 Effect of dilution rate on Start up time and percentage degradation at steady state with influent phenol concentration of (a) 200 ppm (b)1200 ppm. Conditions: A=3.5 cm; f=0.08 s⁻¹; S =80 g.

4.1.2 Effect of dilution rate on biofilm characteristics during start up and at steady state of PPBR.

Through the results of experiments on steady state and start up performance of PPBR in terms of phenol biodegradation, the start up time for the bioreactor under different dilution rates could be determined. These studies have helped in designing the experiments for studies on variation of biofilm characteristics during start-up. Once the start-up time was determined, each experimental run under given set of conditions of dilution rate and influent phenol concentration were split into equal time intervals and each experiment was run for a known interval of time. For example, the start-up time for dilution rate of 0.33 h⁻¹ was 12 h and corresponding time intervals were 2, 4, 6, 8, 10, and 12 h. The reactor was operated for various pre-calculated time period for the Start up studies at each dilution rate. The reactor was stopped after the said time period and the bioparticles were drawn for the analysis. A part of bioparticles were taken for the extraction of EPS component and the extracted EPS component was analyzed for protein, carbohydrate, and humic substance contents. The rest of the sample was taken for the analysis of physical characteristics of biofilm viz., biofilm thickness, and biofilm dry density that may be obtained from the attached dry biomass weight analysis. The reactor was operated at a frequency of 0.08 s⁻¹ and with

total amount of 80g of GAC with immobilized cells; influent phenol concentrations of 200 ppm and 1200 ppm; at an amplitude of 6.5 cm and at various dilution rates of 0.33 h^{-1} , 0.66 h^{-1} and 0.99 h^{-1} and the chemical and physical characteristics of biofilm was studied during the Start up and steady state. the results are discussed in the following sections.

4.1.2.1 Chemical characteristics

The results of the effect of dilution rate on the composition of EPS produced during the start up period of the bioreactor are presented as time course variation of protein, carbohydrate and humic substance content of EPS in Fig.4.4 and Fig.4.5 respectively for 200 ppm and 1200 ppm influent phenol concentrations.

As mentioned in Section 4.1, during the first phase of start-up of the bioreactor, majority of phenol may adsorb on to surface thus leading to phenol removal by physical phenomenon rather than the biological degradation and hence the rate of production of EPS components in terms of its individual components as protein, carbohydrate and humic substance are lower initially as evidenced in Fig. 4.4 (a), (b) and (c) when compared to high initial rate of phenol removal shown in Fig.4.1 (a) and (b).

During initial stages microorganisms tend to produce EPS component to protect themselves from high shear environment and the EPS component, thus formed during the initial stages may be by the fraction of adsorbed microbial cells or from patchy biofilm formed during ex-situ immobilization. As observed in Fig. 4.4 (a), (b) and (c), the composition of EPS in terms of protein, carbohydrate and humic substance concentration have increased with time during the start-up.

The rate of production of protein is low initially, as during this phase predominantly the bacterial monolayer forms by lateral growth of the bacteria to cover the surface of GAC. The bacteria may not secrete EPS proteins at a high rate in this region as EPS protein is required only for adhesion of the bacteria onto the GAC surface, but not for cohesion. During second stage, the

cells on GAC surface grow and biofilm develops forming multiple layers of cells with a production of more amount of EPS protein that may be required for adhesion and cohesion in order to maintain the structure of biofilm, and hence increase in EPS protein quantity with time was observed . A loose and fluffy biofilm formed during the initial phase may tend to detach easily during the second phase. As more of the biomass gets formed, in order to resist the shear and to reduce the effect of detachment forces, the bacteria try to compact themselves by cohesion, requiring EPS protein production at higher rate. Thus, EPS protein may be produced at higher rate during this phase. Compaction of biofilm occurs in this region, which enhances the requirement for EPS protein and thus EPS protein production increases rapidly. During last stage, the detachment force would balances with biofilm formation leading to constant EPS protein content as shown in Fig.4.4(a).

The protein content is required for adhesion and cohesion during all the stages of biofilm formation and the carbohydrate content is important to maintain structure and architecture of biofilm (More *et al.* 2014; Marvasi *et al.* 2010; Andersson 2009; Flemming *et al.* 2001). The production of EPS by cells may also be to protect themselves from exposed phenol environment. The carbohydrate content in EPS increases with time to impart structural integrity to the biofilm. The rate of production of protein is slower initially as compared to that of carbohydrates and humic substances. This may be attributed to the fact that the EPS production by microbial cells depends on the carbon and nitrogen availability in the culture medium. The microorganisms utilize carbohydrates as their carbon and energy source and ammonium salts as their source of nitrogen (Czaczyk *et al.* 2003 ; Looijesteijn *et al.* 1999; Gandhi *et al.* 1997) .

The high content of nitrogen sources in the medium induces extracellular protein production by microbial cells. Carbohydrate production in EPS is favored under nitrogen source limiting conditions in the medium. The ratio of carbon to nitrogen source dictates the production of carbohydrates and proteins in EPS (Czaczyk and Myszka 2007). In the PPBR influent, the inorganic nitrogen sources are provided as nutrients and phenol serves as the carbon source. As the availability of carbon in phenol is much higher as compared to the nitrogen availability with

the nutrient media, the initial rate of production of proteins may be slower than that of carbohydrates in EPS. The cells on GAC surface grow and biofilm develops producing more amount of EPS and hence the EPS component increases with time as evidenced by increase in its individual components [Fig.4.4(a), (b), (c) and Fig.4.5 (a), (b), (c)].

As the bacteria grow and tend to form biofilm, they need to secrete EPS containing protein and carbohydrates, which helps in their adhesion on the substratum and cohesion among themselves. It may be observed from Figure 4.4 and 4.5 that the humic substance is appreciable in quantity. Release of humic substance is a result of decomposed microbial cells (More *et al.* 2014). However, with further increase in time the rate of production of EPS components seems to have decreased as indicated by slower increase in the EPS components at later times. The role of EPS components, mainly polysaccharides and proteins in biofilm formation is to hold the biofilm together by adhesion and cohesion and to retain water in biofilm matrix (Denkhaus *et al.* 2007; Flemming *et al.* 2001). Hence the structure of biofilm is influenced by EPS production (More *et al.* 2014).

During the last stage, the detachment rate would balance with biofilm formation rate leading to constant amount of each of the EPS components as shown in Fig.4.4 and 4.5 This indicates that when the bioreactor attained a steady state, content of each of the EPS components reached a constant value. It may be observed from Figure 4.6 that the production of protein, carbohydrate and humic substances at steady state decreases with increase in dilution rate. As the dilution rate increases, residence time in the reactor for phenol decreases, leading to reduced contact between the cells and phenol. This provides not enough time for the diffusion of phenol through the biofilm. This may result in deficiency of substrate availability to the microorganisms and growth rate decreases leading to porous biofilm with lower production of EPS components. Increase in dilution rate increases the fluid flow velocity and this would lead to erosion of biofilm and thus reduce the EPS component in the biofilm.

As presented in Figure 4.6(b), the concentration of protein, carbohydrates and humic substances in EPS component of the biofilm are lower at 1200 ppm influent phenol concentration

as compared to those at 200 ppm influent phenol concentration. The lower amount of EPS component at higher influent phenol concentration of 1200 ppm would have resulted due to inhibitory effect of phenol causing lower growth and EPS component production.

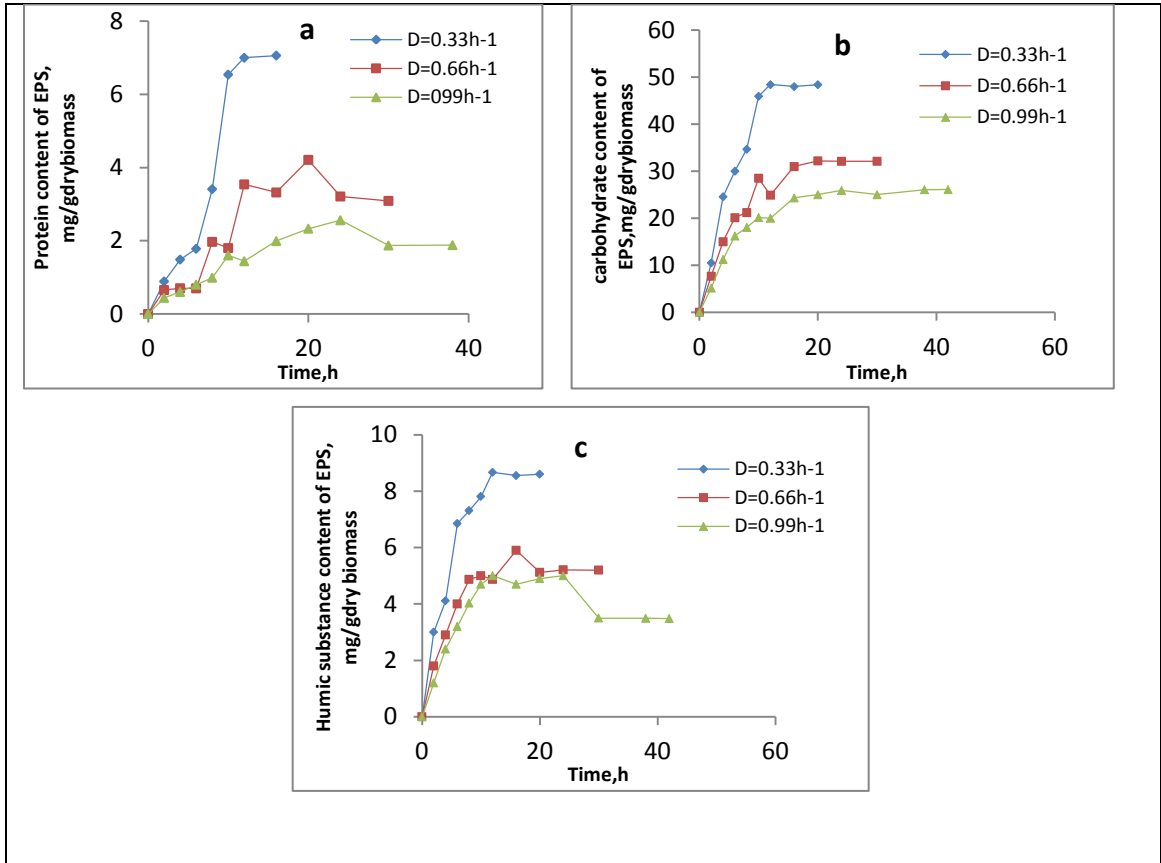


Fig.4.4 Effect of dilution rate on production of (a) protein (b) carbohydrate (c) Humic substance in EPS component of biofilm during the bioreactor start-up period. Conditions: $f=0.082 \text{ s}^{-1}$; $C_i=200 \text{ ppm}$; $A=3.5 \text{ cm}$; $S=80 \text{ g}$.

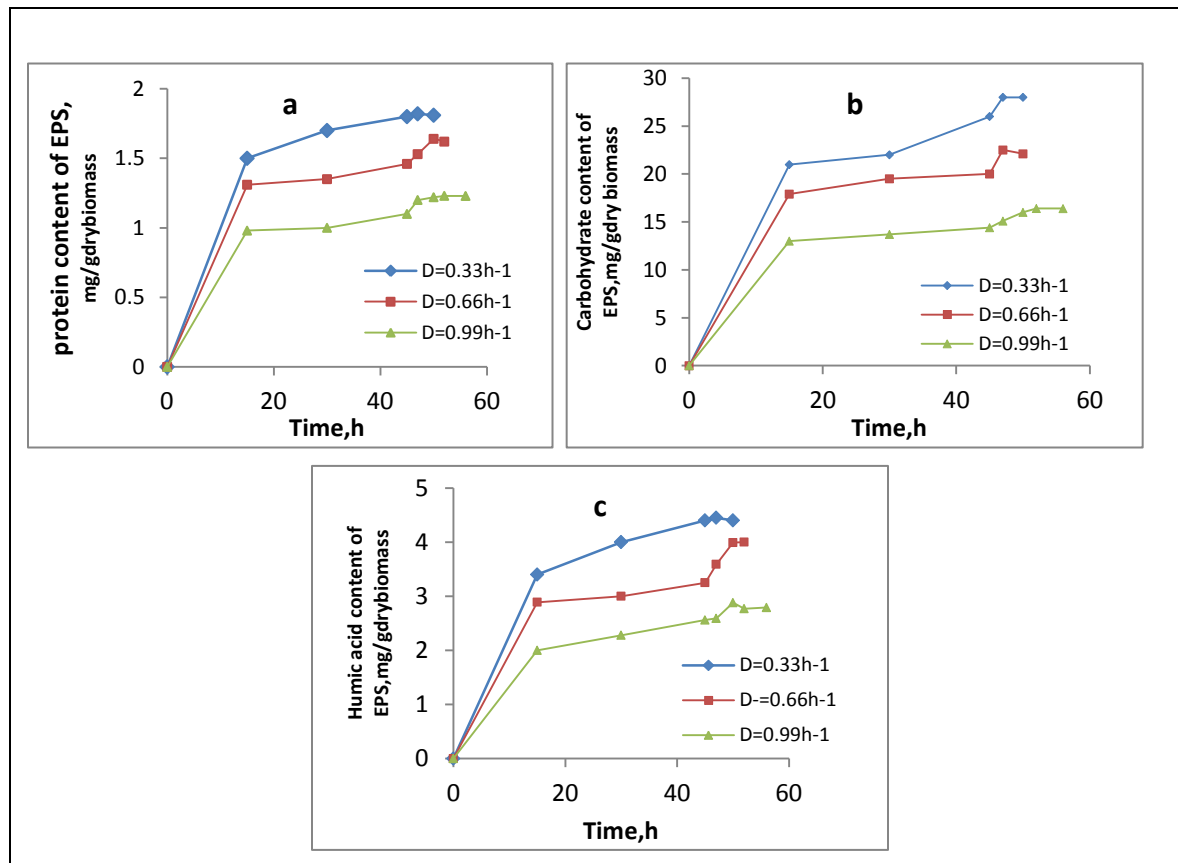


Fig. 4.5 Effect of dilution rate on production of (a) protein (b) carbohydrate (c) Humic substance in EPS component of biofilm during the bioreactor start-up period. Conditions: $f=0.08 \text{ s}^{-1}$; $C_i=1200 \text{ ppm}$; $A=3.5 \text{ cm}$; $S=80\text{g}$.

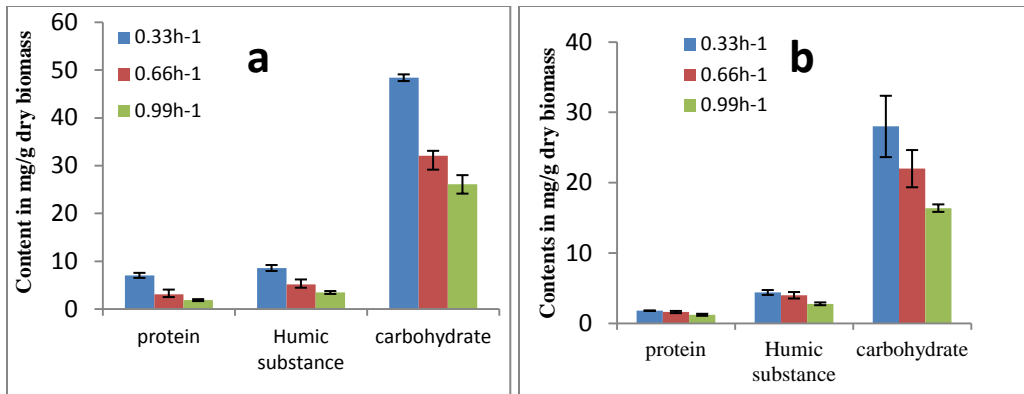


Fig. 4.6 Effect of dilution rate on production EPS components in mg/g dry biomass, at influent phenol concentration of (a) 200ppm (b)1200ppm at steady state. Conditions: $f=0.08 \text{ s}^{-1}$; $A=3.5 \text{ cm}$; $S=80 \text{ g}$.

4.1.2.2 Physical characteristics

The variation in morphological characteristics, average biofilm thickness and the biofilm dry density of the biofilm on the particles were analyzed during the start up of the bioreactor at different frequencies of pulsation. The sample sectional view of the biofilm for the measurement of biofilm thickness is shown in Fig.4.7. Four bioparticles from each stage of Pulsed Plate column were withdrawn from the reactor after each experimental run and the average thickness was calculated

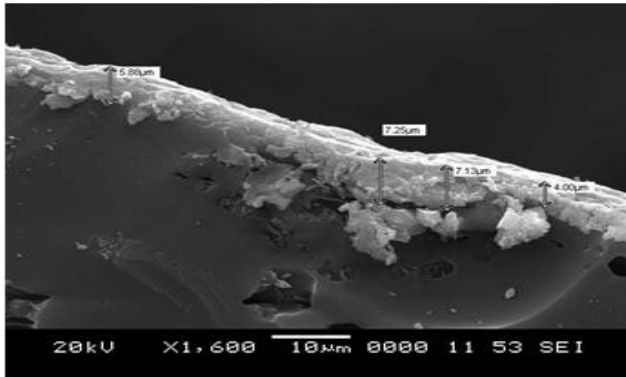


Fig.4.7 Sample cross sectional view for the measurement of biofilm thickness
Conditions: $C_i=200$ ppm; $f=0.08$ s⁻¹; $A=3.5$ cm; $S=80$ g; $D=0.33$ h⁻¹.

Fig.4.8 (a) ,(b) and (c) show the variation in a) biofilm thickness, b) attached dry biomass weight and c) biofilm dry density as a function of time during the start-up of the bioreactor at various dilution rates with 200 ppm influent phenol concentrations. The biofilm physical characteristics during the start-up for 1200 ppm influent phenol concentrations are presented in Fig.4.9(a), (b) and (c). The biofilm thickness during start up of the reactor at 200 and 1200 influent phenol concentrations, presented in Fig.4.8 (a) and 4.10 (a) respectively, show that there is an increase in thickness of biofilm up to a certain value, referred as active or critical thickness (Tanyolac and Beneyal 1998; Sekar *et al.* 1995), and thereafter a decrease with time is observed, further reaching almost a constant value.

As reported by Trulear and Characklis(1982), the biofilm development can be divided into three phases (i) induction (ii) accumulation and (iii) plateau. Induction period may not be observed in the present case, as the carrier particles with pre-immobilized cells were used in the reactor initially. During the initial stages, the GAC particles consist of only the bacteria which were previously immobilized on them by ex-situ immobilization. These preimmobilized bacteria consume phenol in the bioreactor and grow. During the initial stages of biofilm formation the microorganisms would grow on the surface of GAC, laterally to cover all the GAC surface. Hence the thickness seems to be less during the initial stages. Later, the biofilm tend to grow layer by layer and the thickness increases. The EPS

component production increases during the biofilm formation so as to bind the bacteria within the biofilm matrix. The bacterial growth and detachment occurs during the entire period of start-up. The increase in biofilm thickness with time shows the accumulation phase indicating that the biofilm growth rate is higher than the detachment and decay rates in this phase. There was an increase in biofilm density with time as observed in Fig.4.8 (c) and 4.9 (c) during this phase, though the biofilm thickness increased. This indicates that the microorganisms not only grow at a fast rate in this phase, but also try to compact themselves in the biofilm matrix with the secretion of EPS components. First critical thickness may be reached when polycell layer is formed from the monocell layer. In this phase, the fixed cells reproduce and biodegradation occurs without internal diffusion limitations. In processing technologies like in wastewater treatment- biofilm thickness should be controlled at the critical value (by adequate design of the reactor). Further the fixed cell productivity continues, biofilm grows, biodegradation of phenol occurs by the fixed cells and the film is stable. But internal diffusion limitation may exist in the zone beyond the critical thickness. When the thickness further increases, cells near the carrier surface may decay and lysis may occur, owing to formation of cavities and then detachment. But in the present case, the biofilm thickness being very less, internal diffusion limitation may not cause cell lysis in the interior of the biofilm. So the point of maximum biofilm thickness is the critical thickness. In the present case, the biofilm thickness has decreased with increase in time after the critical thickness. This decrease in thickness may not be attributed to detachment, as we find that the biomass dry-weight increases with the increase in time initially during the accumulation phase and then remains almost constant in the phase after the critical thickness as shown in Fig 4.8(b) and 4.9(b). Detachment rate may still be lower. As more and more microorganisms are produced in the biofilm due to growth, they tend to secrete more of the EPS components owing to the stress conditions that exist due to shear caused by pulsation in the reactor. In resistance to the shear, the microorganisms tend to tightly adhere to each other forming a compact film. In the initial time period of increasing thickness, the EPS component formation may be lesser, so the film may be loose but thicker. The rate of compaction

may be lesser than the rate of growth, thus leading to increase in thickness. But in the later period of decreasing thickness, the rate of compaction may outperform the rate of growth, thus leading to decrease in thickness. Further, the biofilm thickness appears to be nearly remaining constant representing a plateau. In this phase, the rate of growth may be compensated by the rate of compaction and rate of detachment, if any. Thus, the formation of biofilm in PPBR dominantly included three phases of accumulation, compaction and plateau.

It is said that the physical phenomenon contributes to morphological changes i.e. biofilm structure and the detachment in biofilms rather than biological phenomenon (Liu and Tay 2001). It may be observed from Fig. 4.10(a) and (b) that the thickness of biofilm at steady state decreased with increase in dilution rate. High dilution rate would impart high shear on biofilm due to fluid moving at high velocities. The shear effect of the fluid on the biofilm surface may lead to larger detachment rate causing the erosion of biofilm, thus reducing the biofilm thickness. High dilution rate would lead to liquid shear and abrasion due to particle-particle collision, or interaction between particle and reactor wall and hence reduction in thickness of biofilm (Lopes *et al.* 2000). Nicolella *et al.*(2000) have also reported that increase in dilution rate could cause erosion i.e. removal of small parts of biofilm from the surface of biofilm which in turn causes reduction in attached biomass and biofilm thickness. As discussed earlier, though higher dilution rate results in higher phenol loading, the contact time between cells and phenol reduces due to decreased residence time. This reduces the availability of phenol to cells in the interior of the biofilm owing to biofilm diffusional limitations. This decrease in the availability of phenol results in lower growth of biofilm at higher dilution rates. The low growth rates and higher detachment rates results in thinner biofilms as observed by decrease in thickness with increase in dilution rate as shown in Fig.4.11(a) and (b).

It may be observed from Fig.4.10(a) and (b) that the biofilm dry weight and biofilm dry density at steady state decreased with increase in dilution rate. Increase in dilution rate would have reduced the growth of microbial cells as discussed earlier and hence resulted in reduction of attached biofilm weight and decrease in biofilm density (Shetty *et al.* 2007). The erosion occurring as a result of high detachment rates at high dilution rates may also cause reduction in

attached dry biomass (Shetty *et al.*2007; Rahab *et al.*2004). Higher velocity was shown to exert a profound influence on the amount of attached biomass in three phase fluidized bed reactor (Cheng *et al.* 1997). They have attributed it to the abrupt intensification of shear stress and frictional forces both acting on the bioparticle surfaces at high velocities. The morphological characteristics of biofilm as observed in SEM are shown in Fig.4.11. It is observed from the figures that, during the initial stage of biofilm formation, i.e. at 2nd h, the GAC surface is not uniformly covered by the cells. The cell clusters are localized. At the 4th h the GAC surface is covered by biomass layer, but the biofilm surface is rough and seem to consist of more of exopolymeric substances than the microbial cells. The entire surface is not covered, as visible from the uncovered patches. At 6th h, it is observed that more number of microorganisms is produced and rough poly layer of cells have been formed with distinct micro pores. At 8th h, the biofilm seems to be dense and smooth with no distinct visible micro pores and has more sophisticated structure.

The surface morphology of steady state biofilms at various dilution rates is shown in Fig. 4.12. It is observed from the figure that the surface of biofilm is uniform with smoother surface at lower dilution rate of 0.33h^{-1} . But as the dilution rate increased, the biofilm seems to be with more uneven and rough surface. Uneven surface represents that higher dilution rates may have resulted in erosion of biofilm from the surface. Erosion is caused by shear forces of the moving fluid in contact with the biofilm surface and is assumed to be effective over the entire surface of the biofilm (Choi and Morgenroth 2003). The existence of several deeper troughs on biofilm surface at higher dilution rates showed that abrasion would have resulted at high dilution rates. Abrasion is the detachment by collision of cell carrier medium (Choi and Morgenroth 2003). With increase in dilution rate the fluid velocity increases. Higher fluid velocity leads to higher detachment and thus leading to erosion of the biofilm from the surface. The possibility of particle-particle collision is also higher at higher fluid velocities due to slow movement of cell carrier particles (GAC) within the bed. It would have resulted in abrasion of the biofilm, leading to rough surface. It is found that, at higher flow rates due to high shear rates, the biofilm growth becomes very non-uniform and forms patches rather than coating the surface continuously. At small shear rates, an

increase in shear rate increases the flux of nutrients to the the biofilm surface, thus increasing the rate of reaction, whereas too high flow rates causing high shear rate discourages reaction because of insufficient residence time and detachment of bacterium from the biofilm. Advective flow velocity dominantly controls shear force in flow reactors. However, the local surface velocity field on the biofilm is not only determined by the bulk flow velocity, but also strongly on the biofilm surface morphology (Kommedal and Bakke 2003). According to DeBeer and Stoodley (1995), at higher bulk liquid velocities the mass transfer boundary layer and thus the local velocity field in the biofilm, closely followed the local biofilm surface morphology and at lower flow rates the velocity field followed the substratum morphology. Thus, biofilm erosion and transport of dissolved substrates into the biofilm are strongly controlled by bulk flow velocity (Lewandowski *et al.* 1994). The combined effect of increased local erosion rates and increased substrate transport, and thus higher local growth rate, indicates a local negative feedback regulation of biofilm thickness at varying shear rates. Thus, that biofilm thickness is by large dominated by the interactive effect of bulk velocity on biofilm erosion and growth rate (Tijhuis *et al.* 1996). Kwok *et al.* (1998) also recognize these processes to dominate the morphology and structure of the biofilm.

Several physical, biological, and chemical factors have the potential to influence Quorum Sensing (QS) in biofilm systems (Horswill *et al.* 2007). Bacteria use quorum sensing or intercellular signaling to coordinate gene expression according to the density of their local population (Fuqua *et al.* 2001). The hydrodynamic environment is one such factor with the potential to influence QS in several ways. Kirisits *et al.* (2007) have found that hydrodynamic environment can impact QS induction in biofilms. Signal produced in the biofilm diffuses into the bulk fluid and is washed away by advection at high dilution rates. Thus, all of the signals does not remain in the local environment causing lower attached biomass at high dilution rates. Mass transfer also can produce substrate and nutrient gradients, and the nutritional environment has been shown to influence QS (Bollinge *et al.* 2001; Duan *et al.* 2007) .

Trulear and Characklis (1982) in their studies on annular reactor have also found that detachment increases with fluid velocity and mass of biofilm. Cheng *et al.* (1997) through their investigation in the three-phase fluidized bed bioreactor for the nitrification process have demonstrated that the biofilm formation was significantly affected by the mean liquid velocity. Moreira *et al.* (2013) through their studies on biofilm formation in a flow cell reactor under turbulent conditions have reported that if the biofilm formation is favored at the lowest flow rates, then shear stress effects are more important than mass transfer limitations. Detachment by abrasion has successfully been exploited to control biofilms in moving bed and biofilm airlift suspension reactors (Tijhuis *et al.* 1996; Gjaltema *et al.* 1995; Gjaltema *et al.* 1997). In the current study, lower dilution rate has favored the formation of uniform and thick biofilm in PPBR. It implies that in pulsed plate bioreactor shear stress effects are more important than mass transfer limitations.

It may be concluded that the chemical and physical characteristics of the biofilm in pulsed plate bioreactor during start-up and at steady state are strongly influenced by the dilution rate.

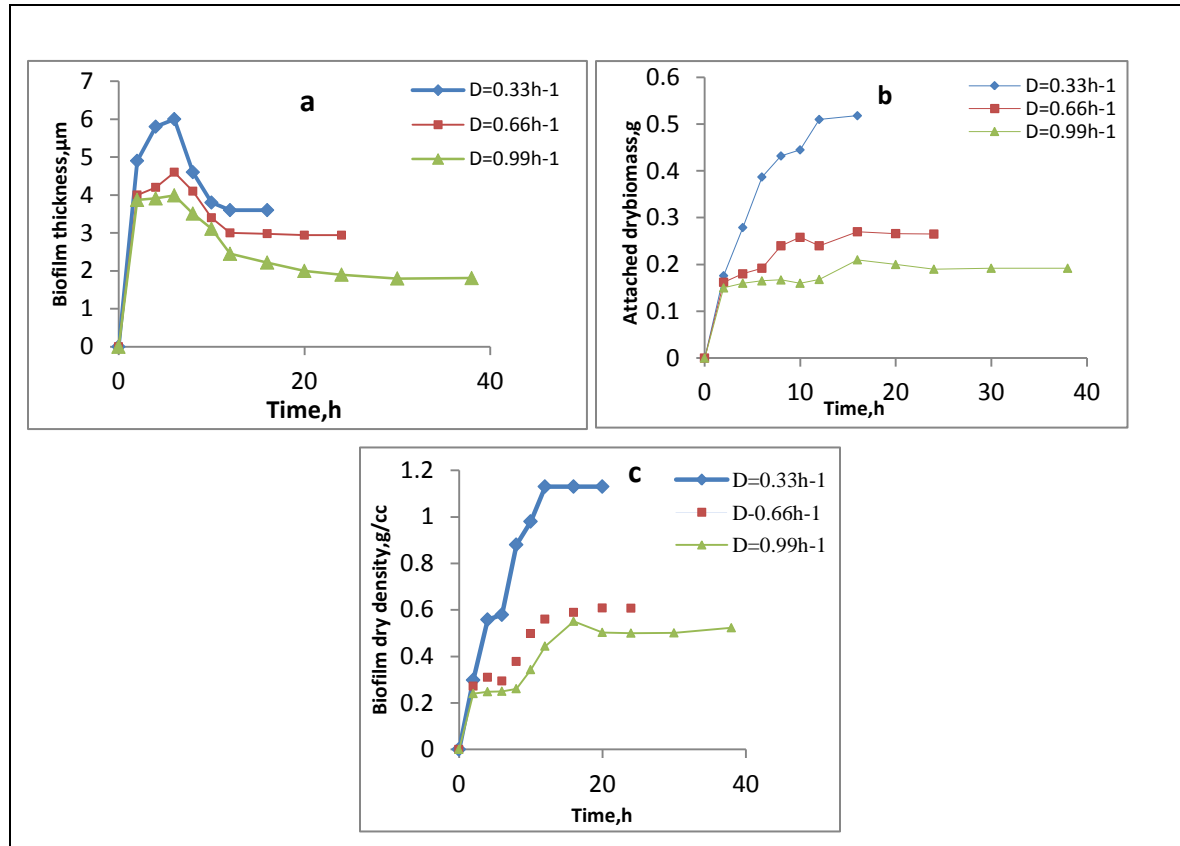


Fig.4.8 Effect of dilution rate on the biofilm dynamics in terms of physical characteristics (a) biofilm thickness (b) attached drybiomass (c) biofilm dry density during the start-up of bioreactor. Conditions; $C_i=200\text{ ppm}$; $f=0.08\text{ s}^{-1}$; $A=3.5\text{ cm}$; $S=80\text{ g}$.

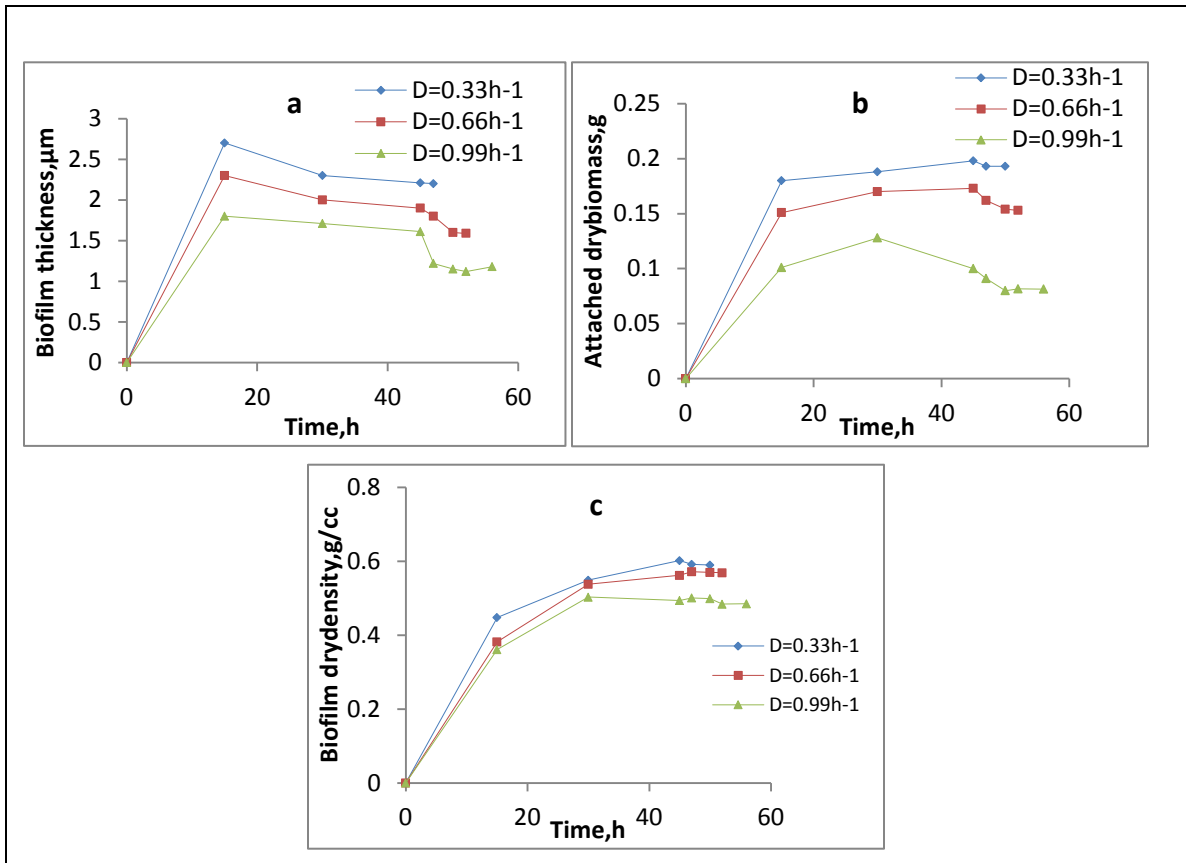


Fig.4.9 Effect of dilution rate on biofilm dynamics in terms of physical characteristics (a) biofilm thickness (b) attached dry biomass (c) biofilm dry density during the start-up of bioreactor. Conditions: $C_i = 1200 \text{ ppm}$; $f = 0.08 \text{ s}^{-1}$; $A = 3.5 \text{ cm}$; $S = 80 \text{ g}$.

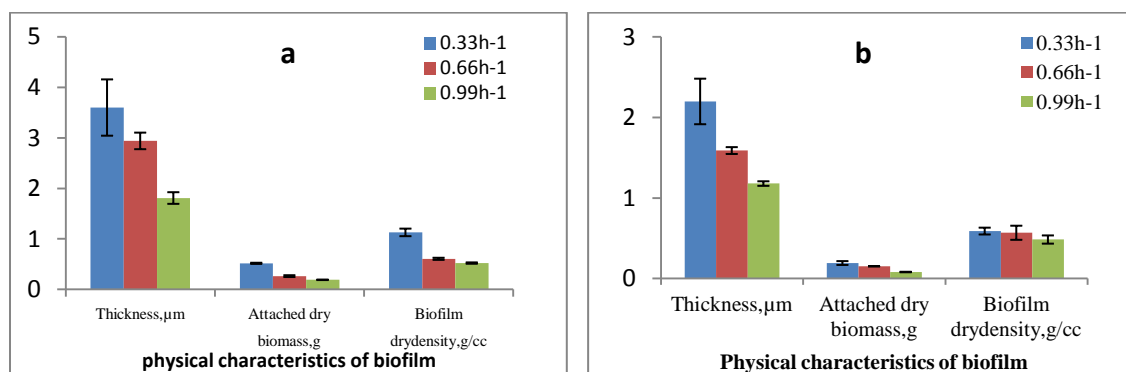


Fig. 4.10 Effect of dilution rate on biofilm physical characteristics at steady state for influent phenol concentration of (a)200 ppm and (b)1200 ppm . Conditions: $f = 0.08s^{-1}$; $A = 3.5$ cm; $S = 80$ g.

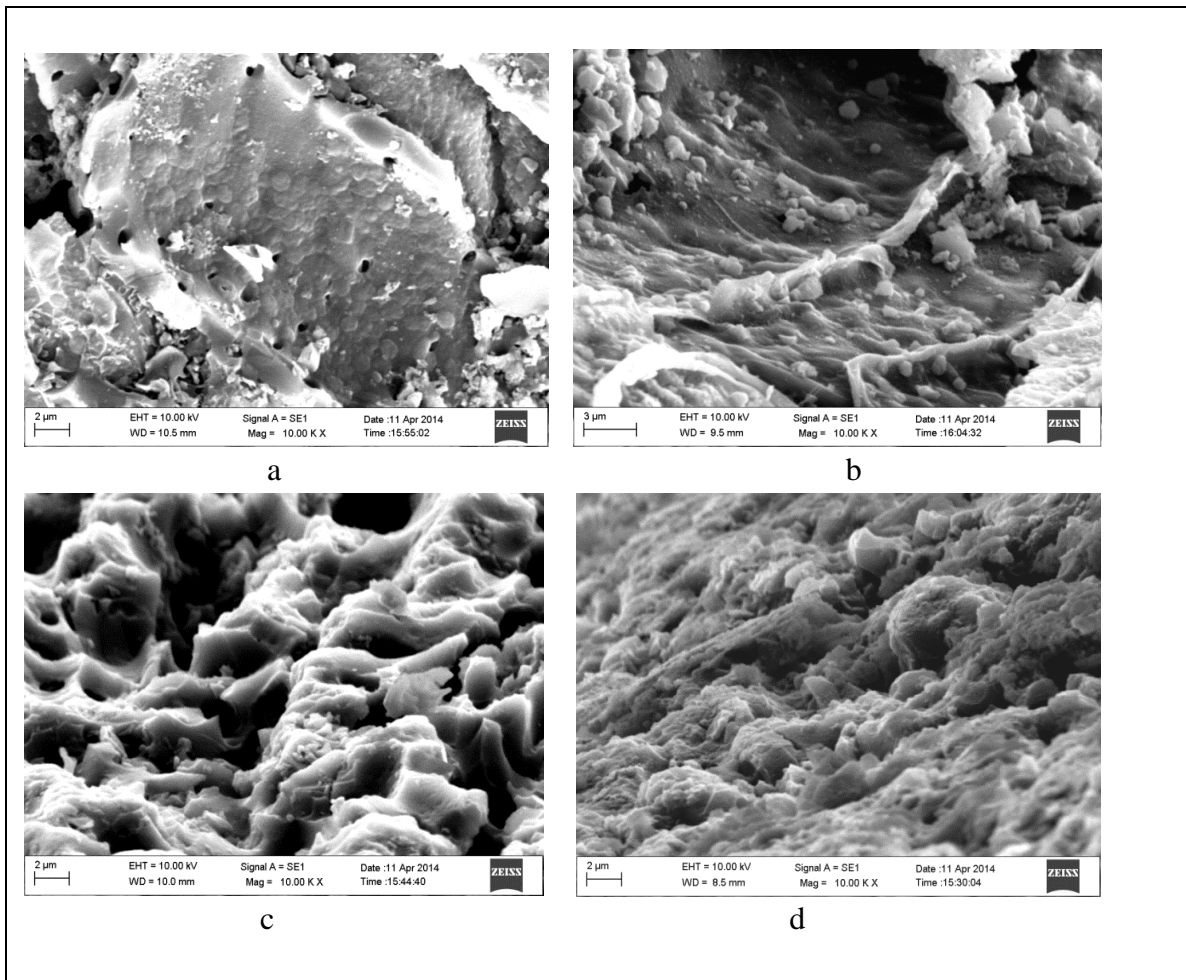


Fig.4.11. Morphological characteristics of biofilm during Start up for the frequency of $0.08s^{-1}$ and after the duration of a) 2h b) 4h c) 6h and d) 8h during the start-up of the bioreactor . Conditions: $C_i = 200$ ppm; $f = 0.08 s^{-1}$; $A = 3.5$ cm; amount of GAC with immobilized cells = 80 g.

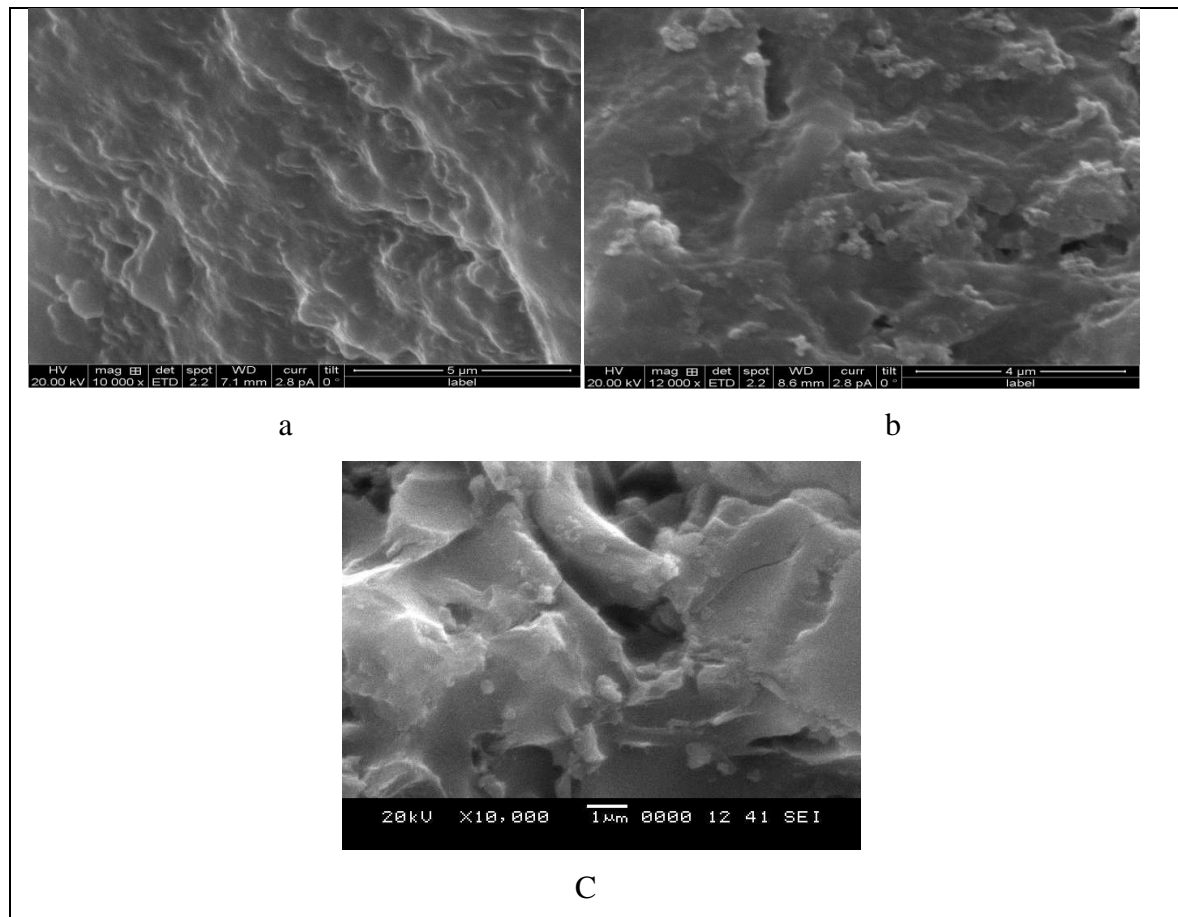


Fig.4.12 Surface morphology of biofilm at steady state with different dilution rates a) $0.33h^{-1}$ b) $0.66 h^{-1}$ c) $0.99h^{-1}$ at steady state. Conditions: $C_i = 200$ ppm; $f = 0.08s^{-1}$; $A = 3.5$ cm; $S = 80$ g.

4.2 Effect of influent substrate (Phenol) concentration on steady state and Start up performance of PPBR in terms of phenol biodegradation and biofilm characteristics.

Conceptually, removal of substrate from the aqueous phase requires all the metabolic reactants like the substrate, nutrients and oxygen to diffuse into the biofilm, metabolism by the microbes followed by diffusion of metabolic products out of the biofilm into the aqueous phase (Williamson and McCarty 1976). The substrate flux in the biofilm is influenced by the biofilm structure. The effective diffusivity of the substrate in the biofilm is governed by the biofilm structure. Substrate concentration was reported to influence the effective diffusivity to a much larger extent than the flow velocity (Beyenal and Lewandowski 2000). In practice the growth rate of biofilm in bioreactors depend on the substrate loading rate and is considered as the growth force for biofilm formation. At a fixed dilution rate, the substrate loading rate is proportional to the influent substrate concentration. Thus, in the present work, the effect of influent phenol concentration in the range of 200 ppm to 1200 ppm on phenol biodegradation and biofilm characteristics was studied. The influent phenol concentration above 1200ppm was found to be toxic to the bacteria and didnot facilitate the growth.

4.2.1. Effect of influent substrate concentration on phenol biodegradation during Start up and at steady state of PPBR.

The degradation of phenol was studied during the Start up of PPBR, when it was operated at the dilution rate of 0.33h^{-1} with cell carrier loading (S) of 80g with various influent phenol concentrations of 200, 400, 600, 800 and 1200 ppm and at an amplitude of 3.5cm, frequency of 0.08 s^{-1} . The variations in effluent phenol concentrations as a function of time during the start-up of the bioreactor at different influent phenol

concentrations are presented in Fig.4.13. As observed in Fig.4.13 (a) to (d) with their corresponding insets and in Fig 4.13(e), it is found that the phenol concentration decreases suddenly due to adsorption, followed by an increase due to saturation of GAC surface, further decrease in concentration indicating the effect of biodegradation and finally a steady state value of effluent phenol concentration indicating balance between biofilm formation and detachment rates. Fluctuations were observed during the second phase, indicating continuous detachments along with the growth. The fluctuations observed with very high influent phenol concentrations of 800 ppm and 1200 ppm are higher than those at lower influent phenol concentrations. This may be attributed to the occurrence of higher detachments due the fluffy and very porous biofilms that would have formed as a result of lower growth rate caused by phenol inhibition or toxic effects of phenol at higher concentrations involved during start-up. During the start-up of the bioreactor after the bed saturation phase begins, the concentrations in the bioreactor may be at levels higher than the inhibitory concentration of phenol to the bacteria. Thus, the bacteria on the GAC may get exposed to inhibitory levels of phenol. The inhibitory levels of phenol lead to lower growth of the bacteria. This results in more time to achieve the formation of sufficient biofilm on GAC surface. Even when the bacteria grow at a slower rate to form polylayers of cells the outermost cells get exposed to higher concentrations of phenol which may be inhibitory, though the inner layers are exposed to lower concentrations of phenol. Thus, the inner layers of cells grow at a faster rate and form dense film, whereas the outerlayers grow at a slower rate owing to inhibitory effect of phenol. Thus, the outer layers may be fluffy and loose with low strength structure, being more prone to erosion by the fluid movement. Thus, when the influent phenol concentrations are very high, the detachment rates are higher and detachment continuously competes with growth, resulting in domination of each rate over the other at certain time periods. Thus, high fluctuations in bulk phenol concentration was observed when the influent concentrations were high, i.e 800 ppm or above. Owing to continuous growth and detachment, the development of steady biofilm takes a longer time at high concentrations. However, once developed, a steady-state biofilm can tolerate

high bulk substrate concentrations, because the inner layers of the biofilm are exposed to lesser substrate concentrations due to mass transport resistance and substrate utilization in the outer layers of the biofilm. In such situations, maximal rates of substrate utilization and microbial growth occur in the middle or at the inner surface of the steady-state biofilm (Ganlzer 1989).

It may be observed from Fig. 4.14 that the degradation of phenol at steady state was above 99% for the initial phenol concentration of upto 600 ppm and the degradation was around 98% for 800ppm influent phenol. However the degradation reduced further to 75% for influent phenol concentration of 1200 ppm as shown in Fig.4.14. The reduction in phenol degradation for influent phenol concentration of 800 ppm and above could be due to high volumetric loading of phenol. When the overall rate of degradation of phenol is less than the rate of volumetric phenol loading, the percentage degradation reduces owing to the limited metabolic activity of the microorganisms. As shown in Fig.4.15, the Start up period is 12h for all phenol concentrations upto 800ppm and increased to 47 h for 1200 ppm. Since there may be high inhibitory effect of phenol at influent concentration of 1200 ppm, the microbial cells would require longer time to balance growth and detachment rates and hence require longer Start up period. Once the growth and detachment forces had balanced, the system reached a steady state. These studies indicate that, stable operation of pulsed plate bioreactor is possible even at high influent concentrations of upto 1200 ppm. However, high phenol degradation efficiency was possible only upto around 800 ppm phenol, indicating that the volumetric substrate loading upto this concentration level is favorable in PPBR operating at a dilution rate of 0.33h^{-1} .

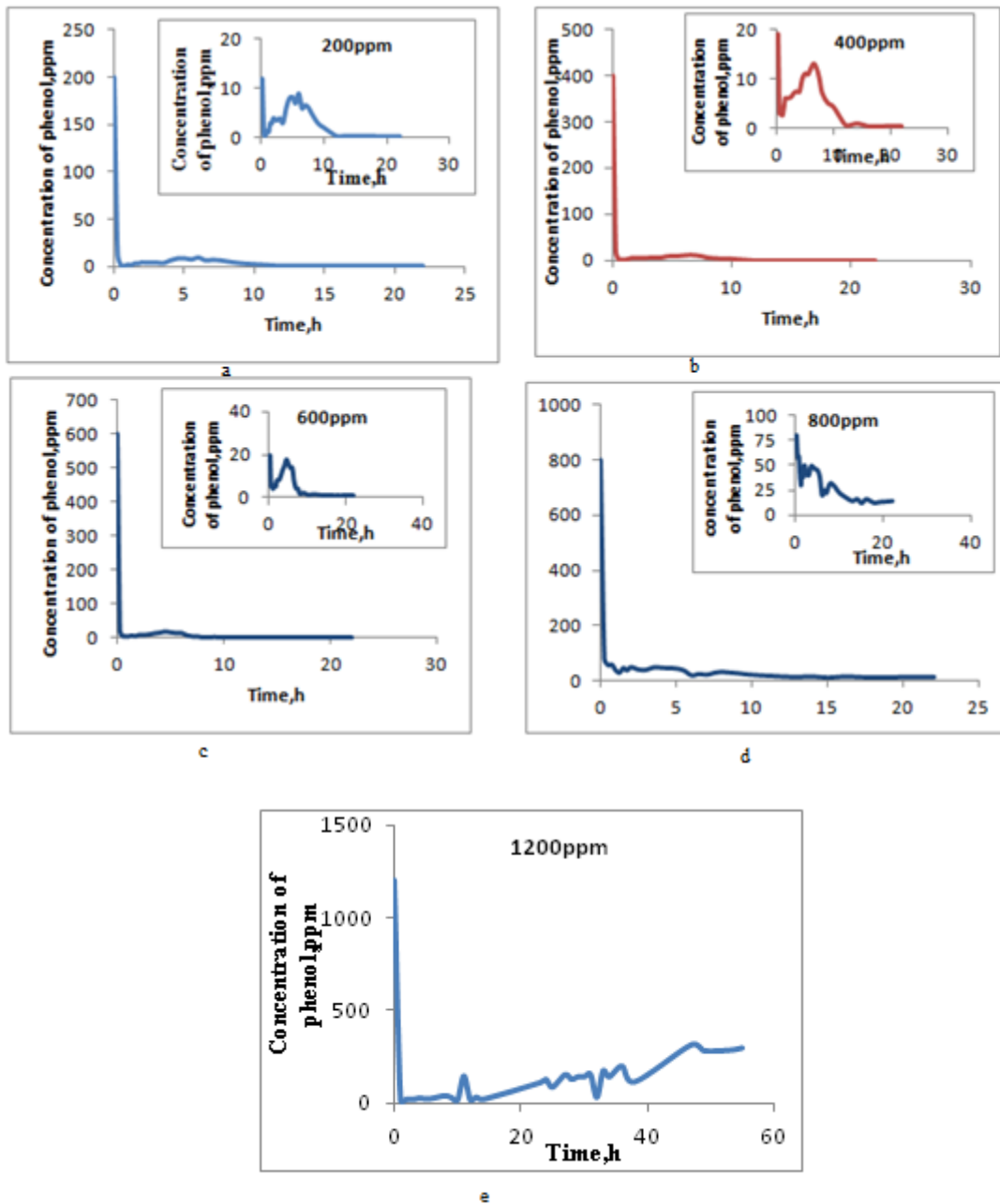


Fig 4.13. Degradation of phenol during Start up at different influent phenol concentration. Conditions: $D= 0.33 \text{ h}^{-1}$; $f= 0.08 \text{ s}^{-1}$; $A=3.5 \text{ cm}$; $S=80 \text{ g}$.

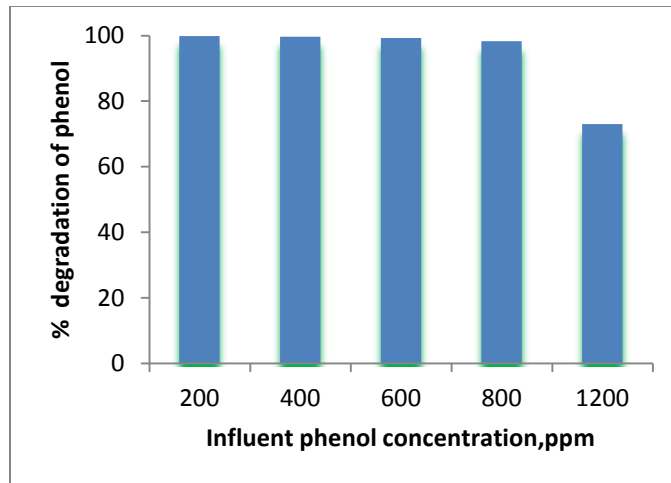


Fig.4.14 Effect of influent phenol concentration on percentage degradation of phenol at steady state. Conditions: $D= 0.33 \text{ h}^{-1}$; $f= 0.08 \text{ s}^{-1}$; $A=3.5 \text{ cm}$; $S=80 \text{ g}$.

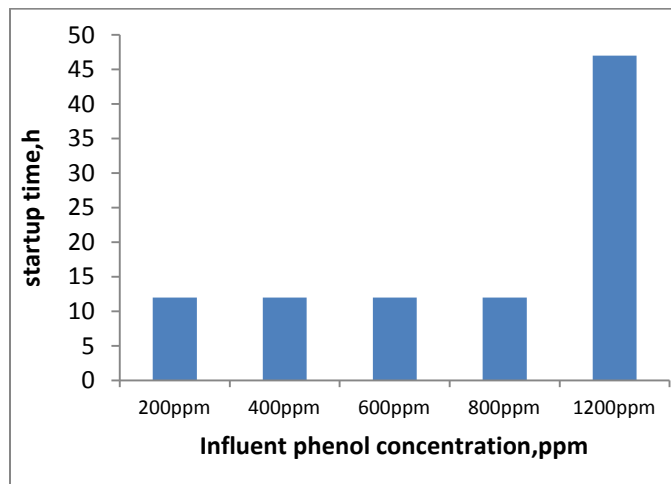


Fig.4.15. Effect of influent phenol concentration during start-up time. Conditions: $D= 0.33 \text{ h}^{-1}$; $f= 0.08 \text{ s}^{-1}$; $A=3.5 \text{ cm}$; $S=80 \text{ g}$.

4.2.2 Effect of phenol concentration on biofilm characteristics during start up and at steady state of PPBR

As discussed in Section 3.3.5.2 and 4.1.2, the continuous phenol degradation experiments were conducted with different influent phenol concentrations for different time periods during the bioreactor start-up and the physical and chemical characteristics

of the biofilm were determined during the start-up period till the attainment of steady state and at steady state. The experiments were conducted for different initial phenol concentrations viz., 200, 400, 600, 800 and 1200 ppm and for different frequencies of 0.08 s^{-1} , 0.12 s^{-1} and 0.16 s^{-1} at a fixed amplitude of 3.5 cm with GAC loading of 80 g. The results on the characteristics of biofilm during the Start up and steady state are discussed in the following sections.

4.2.2.1 Chemical characteristics

The experiments were conducted to study the biofilm characteristics during start up as described in section 3.3.5.2 for various influent phenol concentrations viz., 200, 400, 600, 800 and 1200 ppm keeping all the other parameters constant. The procedures for the EPS extraction and determination of chemical characteristics in terms of EPS composition are explained in detail in section 3.3.6 to 3.3.9

The results on the composition of EPS component of biofilm produced during the start up period of the bioreactor are presented as time course variation of protein, carbohydrate and humic substance content of EPS at different influent phenol concentrations in Fig.4.16 (a), (b), (c) respectively. The composition of EPS component in terms of protein, carbohydrate and humic substance concentration have increased with time during the start-up. As discussed in section 4.1.2.1, during initial stages microorganisms tend to produce EPS component to protect themselves from high shear environment and since the surface of GAC is not entirely covered with biofilm, the quantities of each of the components of EPS are less. During second stage, the cells on GAC surface grow and biofilm develops forming multiple layers of cells with a production of more amount of EPS protein required for adhesion and cohesion of the cells in the biofilm and carbohydrates for structural strength. During the bioreactor start-up the cell growth occurs along with the biofilm detachment and decay. Humic substance is the cell debris formed after death of the cells. As the cell death and decay occurs during the entire period of start-up, the humic substance content increases with time slowly. However, these humic substances may also help in cohesion of cells (Frolund *et al.* 1995) in the biofilm by increasing

the structural integrity of EPS component and thus the strength of the biofilm formed. Thus, EPS components are produced at higher rate during the second phase followed by constant values in the last stage, wherein the detachment rate is balanced by biofilm formation rate indicating the steady state as shown in Fig.4.16.

From Fig.4.17 it may be observed that the protein, carbohydrate and humic substance quantities at steady state increased with increase in influent phenol concentrations upto 800 ppm and further when the phenol concentration was increased to 1200ppm, production of these substances reduced drastically. The increase in production of EPS component and its components may be due to increase in availability of phenol or improvement of phenol supply to the microorganisms at higher influent phenol concentrations (Wang *et al.* 2011).

When the bulk concentration of phenol is lesser than the inhibitory concentrations, the growth rates are higher, thus the bacterial cell population is higher. The EPS component production is higher when the cell populations are higher. The amount of EPS components such as protein and carbohydrates required for the formation of biofilms involving larger bacterial populations is higher, which indicate that the cells would have secreted large amount of EPS component necessary for their structural integrity and cohesion when the phenol concentration is higher.

However, the increase in quantities of EPS components even when the influent concentration was increased to 800 ppm indicate that the inhibitory effect seems to be not predominant at this concentration.

When the influent concentration of phenol was increased to 1200 ppm, the bulk concentration would have been greater than the inhibitory phenol concentration to the cells or it could be due to high phenol concentration in the bulk during start up wherein the phenol would have penetrated deep in to the biofilm rendering inhibitory effect on the cells in the biofilm (Shetty *et al.* 2007). It implies that the biomass produced may be lesser with 1200 ppm influent phenol and biofilms formed at steady state, may be thin,

loose and porous with very less EPS. Thus, the biofilm may not be compact and strong. A similar trend of effect of increase in the influent concentrations was observed at other frequencies of 0.12s^{-1} and 0.16s^{-1} .

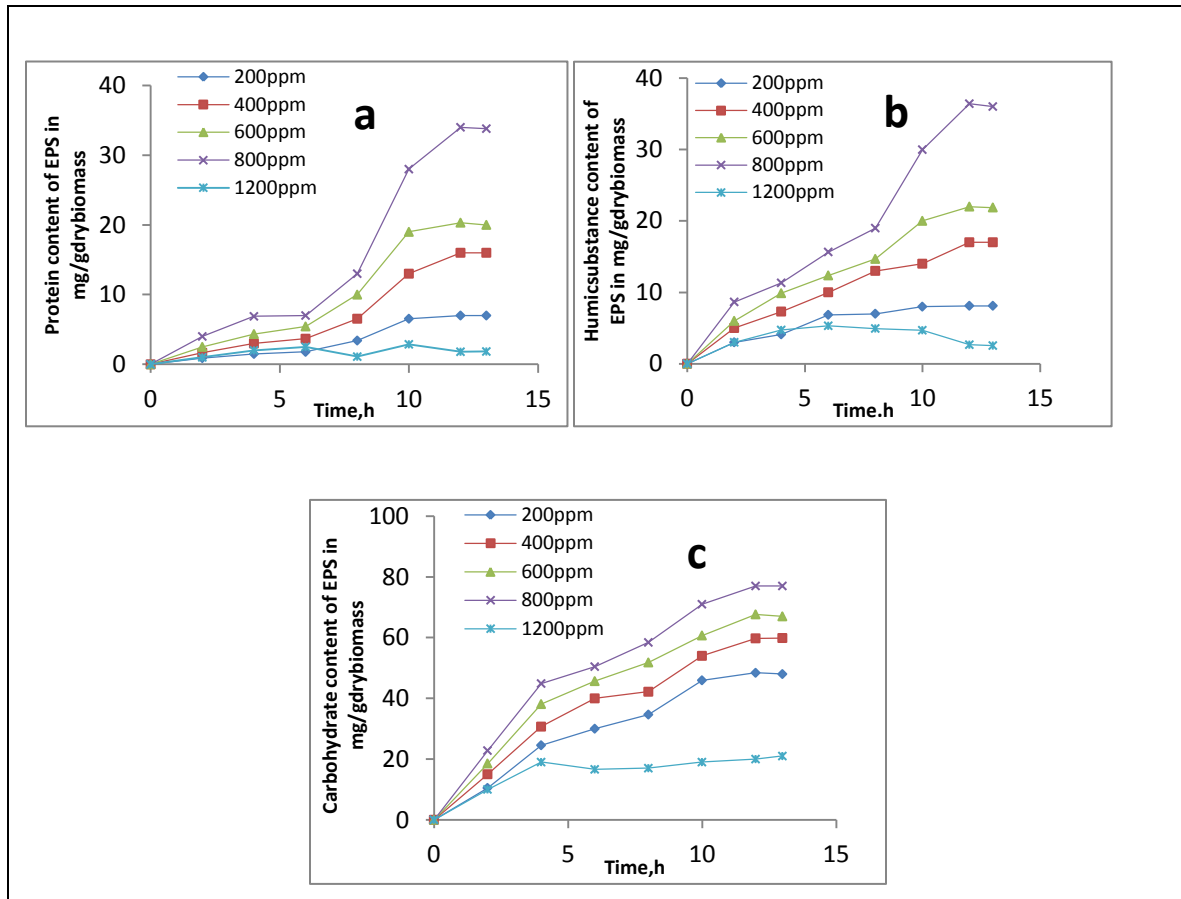


Fig.4.16 Effect of phenol concentration on production of (a) protein (b) humic substance and (c) carbohydrate in EPS component of biofilm. Conditions: $f=0.08\text{ s}^{-1}$; dilution rate= 0.33 h^{-1} ; $A=3.5\text{ cm}$; $S=80\text{ g}$.

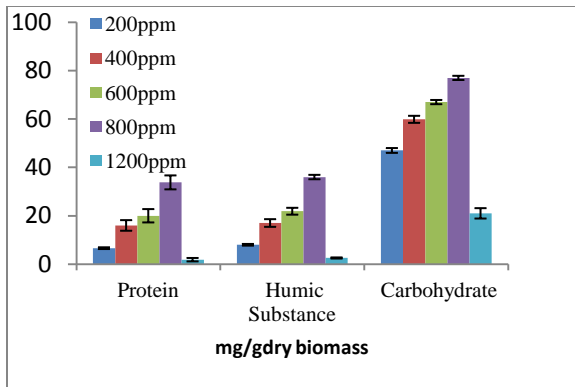


Fig.4.17 Quantity of EPS components at steady state for various influent phenol concentrations. Conditions: Amplitude of 3.5cm; $f=0.08\text{ s}^{-1}$; $S=80\text{g}$; $D=0.33\text{h}^{-1}$.

4.2.2.2 Physical characteristics

The physical characteristics of the biofilm, during the start-up period for various influent phenol concentrations viz., 200, 400, 600, 800 and 1200 ppm were determined. The physical characteristics such as biofilm thickness, attached dry biomass, and biofilm dry density as a function of time during the start-up of the bioreactor for various influent concentrations of phenol are presented in the Fig. 4.18 for frequency of 0.08s^{-1} . From Fig.4.18 (a) it is observed that the thickness of biofilm has increased with increase in time, reached a maximum value and then decreased to remain constant. This trend has been observed at all the influent phenol concentrations and the biofilm growth characteristics during the start-up has already been explained in Section 4.1.1.2. The attached biomass also increased with time, before it reached a constant value as observed in Figure 4.18(b). The reason for the trend is explained in Section 4.1.1.2.

As observed in Fig.4.18 (a), the biofilm thickness increased with increase in influent phenol concentrations of upto 800 ppm. It is known from the literature that high phenol loading leads to faster growth of biofilm. The mass transfer of substrate (phenol) from the bulk to the surface of biofilm occurs followed by diffusion through the biofilm and its conversion leads to growth of biofilm. But at higher influent phenol concentrations, the biofilm surface concentrations of phenol are higher, which results in

faster outgrowth of biofilm from the surface. Biofilms may grow to macroscopic structure under their beneficial conditions.

VanLoosdrech *et al.*(1995) have reported that the faster outgrowth of biofilms occur at higher surface substrate loading . When biofilm is exposed to low substrate loading, the cells grow slowly, thus the protuberances in biofilm may erode before the formation of macroscopic structure (Van Loosdrecht *et al.*1995). Substrate flux plays an important role in biofilm formation and the biofilm thickness is also affected by substrate load (Van Loosdrecht *et al.*1995). At higher phenol concentrations upto the limits of 800ppm influent phenol concentration, the microbial activity may be dominating than the substrate flux that would lead to protuberances in biofilm (outgrowth of biofilm). The faster outgrowth of biofilms occur at higher surface substrate loading that forms less denser biofilms (VanLoosdrech *et al.*1995). The development of protuberances increases the biofilm thickness but, results in filamentous fluffy structure which are not denser (Pellicer and Smets 2014). From Fig.4.18 (b) it can also be observed that the attached dry biomass increased with increase in phenol concentration upto 800 ppm influent phenol concentration. However, Fig.4.18(c) shows that the biofilm dry density decreased with the increase in influent phenol concentration, indicating the formation of loose and more porous structured biofilm at higher phenol concentrations. At high phenol concentration, the growth of biofilm becomes rapid, increasing the biomass but forms loose structure leading to decrease in density (Wang *et al.* 2011; Horn and Hampel 1998; Tanyolac and Beneyal 1997; Peyton 1996; Howell and Atkinson 1976). The loose structure was formed at higher phenol concentrations, due to faster rate of growth of the biofilm, which allows lower degree of compacting of the biofilm. At higher phenol concentrations, the protuberances in biofilm (outgrowth of biofilm) are formed which inturn increases porosity of biofilm thus reducing the density of the biofilm or in other words low compaction of biofilm. When the phenol is consumed by microorganisms present in protuberances, phenol may not reach the base of the biofilm thus leading to lower growth at the biofilm base and reducing the biofilm density. In case, if these protuberances are removed due to shear, the substrate can penetrate into the base of

biofilm leading to increase in density (Van Loosdrecht *et al.* 1995). However, in this case the rate of detachment of the protuberances from the biofilm surface due to erosion by the existing shear conditions may be much lower than the rate of outgrowth of biofilm from the surface due to higher substrate concentrations. The phenol would not have diffused to the base of the biofilm as it is consumed by the cells in the protuberances, thus leading to lower biofilm density at higher influent phenol concentration. However at a influent concentration of 1200 ppm, the reduction in biofilm thickness, biomass dry weight and biofilm dry density occurred as shown in Fig.4.18, may be due to the phenol inhibitory and toxic effect on microbial activity leading to reduced growth of biofilm at higher phenol concentration.

It may be observed from Fig. 4.19 that the biofilm dry density at steady state decreased with increase in substrate concentration, but attached dry biomass increased with substrate concentration upto 800 ppm and decreased with further increase in substrate concentration. Similarly the biofilm thickness increased with increase in substrate concentration upto 800 ppm and decreased with further increase in substrate concentration. These results follow the similar trend as the effect of phenol concentration on biofilm characteristics during the start up.

The morphological characteristics of biofilm with increase in influent concentration are shown in Fig.4.20. The SEM images also show the denser, compact and smoother biofilms at lower influent phenol concentrations. As the phenol concentration increases, the biofilm surface is rough and non uniform. Presence of microbial outgrowths is observed at higher concentrations of 600 and 800 ppm, confirming the results on biomass weight and density. The SEM image for the biofilm at 1200 phenol reveals nonuniform biofilm with highly uneven surface and large troughs.

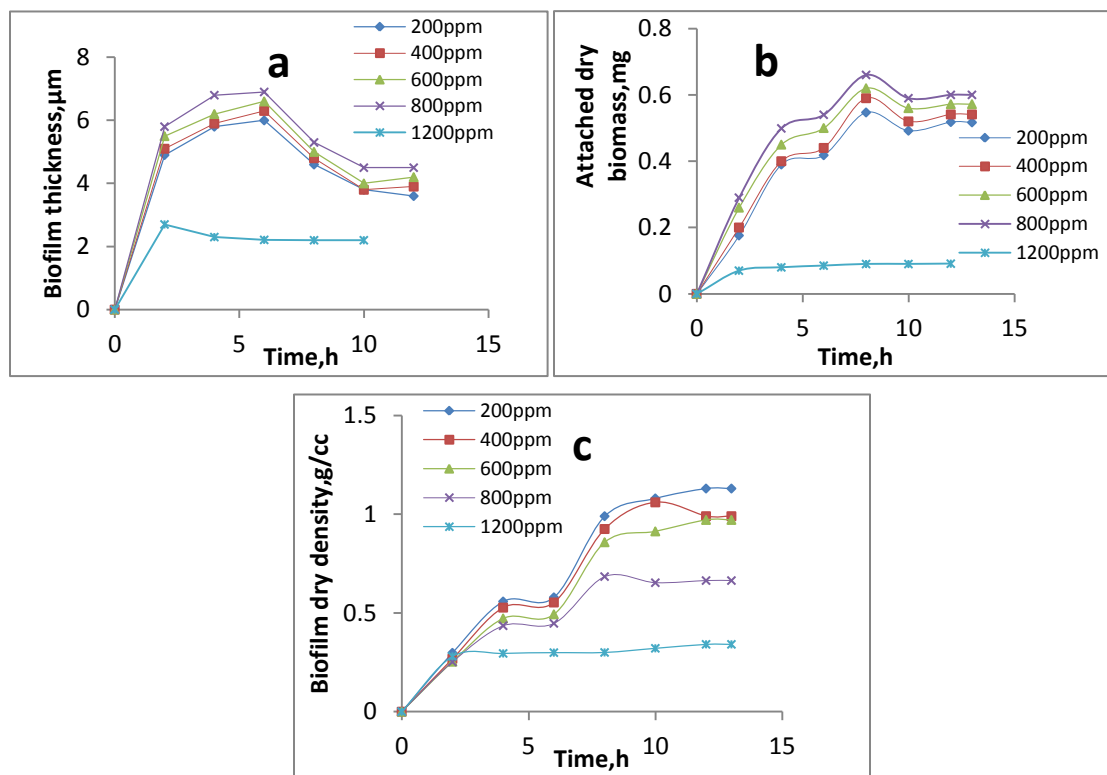


Fig.4.18 Effect of phenol concentration on the biofilm dynamics in terms of physical characteristics (a) biofilm thickness (b) attached drybiomass (c) biofilm dry density during the start-up of bioreactor. Conditions: $D=0.33 \text{ h}^{-1}$; $f=0.08 \text{ s}^{-1}$; $A=3.5 \text{ cm}$; $S=80 \text{ g}$.

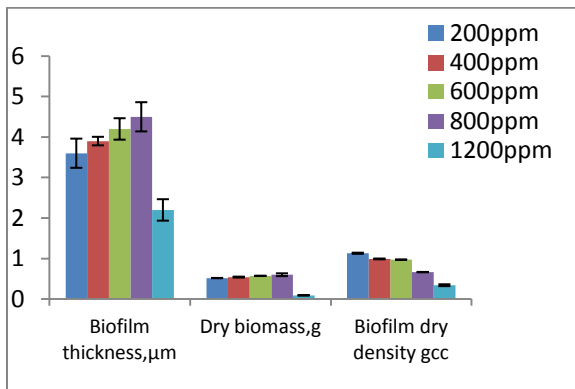


Fig.4.19 Effect of phenol concentration on physical characteristics of biofilm at various influent phenol concentrations at steady state. Conditions: $D=0.33 \text{ h}^{-1}$; $f=0.08 \text{ s}^{-1}$; $A=3.5 \text{ cm}$; $S=80 \text{ g}$.

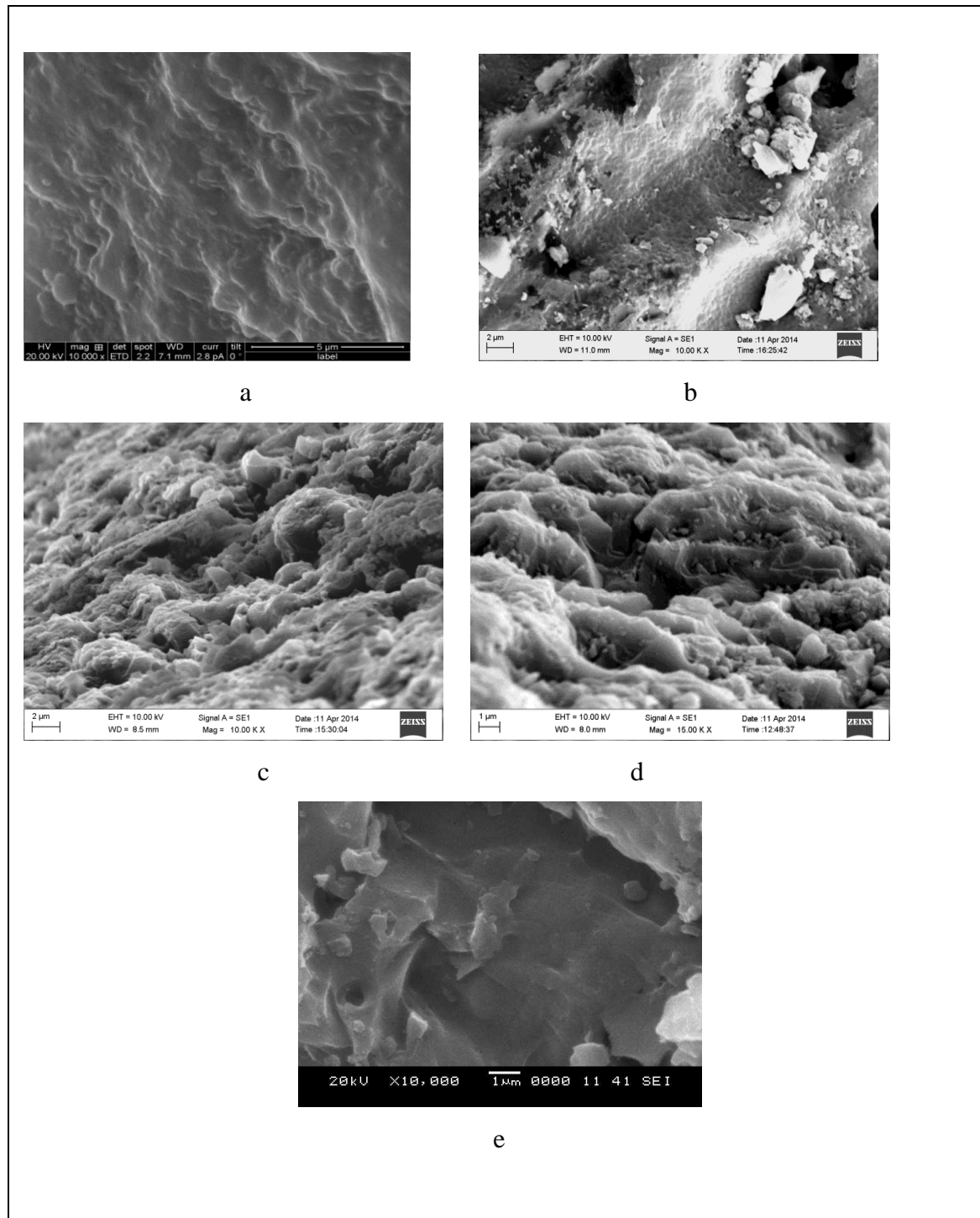


Fig.4.20 Surface morphology of biofilm at various influent phenol concentrations at steady state (a) 200ppm (b) 400ppm (c) 600ppm (d) 800ppm and (e) 1200ppm. Conditions: $f=0.08s^{-1}$; $A= 3.5\text{ cm}$; $S=80\text{ g}$; $D=0.33\text{ h}^{-1}$.

These studies have shown that the physical and chemical characteristics vary with the influent phenol concentration, thus influencing the performance of the bioreactor. Lower concentrations always favor the formation of dense and compact biofilm, whereas higher concentrations favor the biomass growth and EPS production. However, concentrations upto 800ppm are favorable in terms of biofilm formation, biomass growth and phenol degradation. Though, the biofilm operation is stable even at 1200 ppm influent phenol concentration, inhibitory effect at this concentration is too high and thus the biomass growth is not favored leading to lower EPS production and phenol degradation efficiency. Thus the operation of PPBR at very high influent phenol concentrations is not recommended from the technological and economical perspective.

4.2.2.3 Effect of phenol loading rate on phenol removal rate

To study the combined effect of dilution rate and the phenol concentration, the results of the experiments conducted at various dilution rate and influent phenol concentration were analyzed in terms of phenol loading rate (DC_i) to the reactor and phenol removal rate $[D(C_i-C)]$ from the reactor at steady state.

As shown in Fig.4.21 and Table 4.1, the phenol removal rate increased with the phenol loading rate of upto $792 \text{ mgL}^{-1}\text{h}^{-1}$ of phenol loading and then decreased with further increase in phenol loading. The phenol loading rate of $792 \text{ mgL}^{-1}\text{h}^{-1}$ correspond to influent phenol concentration of 1200 ppm with dilution rate of 0.66 h^{-1} . This shows that maximum phenol removal could be obtained even when the influent phenol concentration is inhibitory. Thus, maximum rate of phenol removal in PPBR may be obtained, if the bioreactor is operated at phenol loading rate of $792 \text{ mgL}^{-1}\text{h}^{-1}$ irrespective of the levels of influent concentration and dilution rate. However toxicity of phenol on the cells may limit the maximum allowable influent concentration.

Table.4.1 Phenol loading rate and phenol removal rate for various influent phenol concentrations and dilution rates. Conditions: $f=0.08\text{ s}^{-1}$; $A=3.5\text{ cm}$; $S=80\text{ g}$.

Influent phenol concentration, ppm	Dilution rate, h^{-1}	$D C_i$, $\text{mgL}^{-1}\text{h}^{-1}$	$D(C_i-C)$, $\text{mgL}^{-1}\text{h}^{-1}$
		0	0
200	0.33	66	65.9
400	0.33	132	131.8
600	0.33	198	97.76
800	0.33	264	258.7
1200	0.33	396	301.0
200	0.66	132	123.0
1200	0.66	792	403.9
200	0.99	198	144.5
1200	0.99	1188	346.5

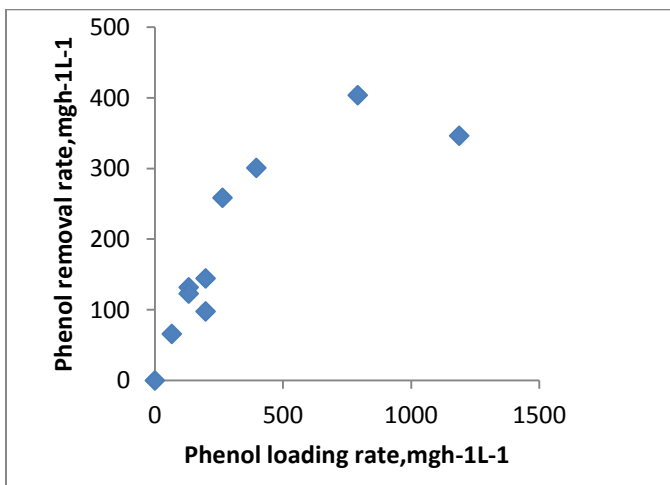


Fig 4.21 Effect of phenol loading rate on phenol removal rate. Conditions: $D=0.33\text{ h}^{-1}$; $f=0.08\text{ s}^{-1}$; $A=3.5\text{ cm}$; $S=80\text{ g}$.

4.3 Effect of frequency of pulsation on steady state and start up performance of PPBR

The formation, structure and metabolic activity of the biofilms are closely associated with the detachment forces in the bioreactors. In bioreactors, the detachment force resulting from hydraulic shear, particle-particle collision or moving parts is a key factor that influences formation, structure and stability of biofilm. In biofilm reactors the mass transfer of the substrate within the biofilm is also governed by the detachment forces. Biofilm characteristics are influenced by shear conditions in bioreactors. The performance of the bioreactor is governed by biofilm density and biofilm thickness. Shear stress is an important parameter that affects biofilm density and thickness and in turn the bioreactor performance. Presence of, moving parts may impart high shear forces on the biofilm and hence may influence the biofilm structure, characteristics and composition. The PPBR under study contains a reciprocating shaft with stack of plates, which may offer very high shear stress on the biofilm. The PPBR operational variables such as frequency and amplitudes of pulsation may tremendously influence the shear conditions in the bioreactor and hence may affect the biofilm characteristics. Understanding the effect of these shear inducing operational variables on biofilm characteristics may help in controlling the bioreactor performance. Thus, the effect of frequency of pulsation on the bioreactor performance was studied in terms of phenol biodegradation and biofilm characteristics.

4.3.1. Effect of frequency of pulsation on phenol biodegradation during Start up and at steady state of PPBR.

The degradation of phenol was studied during the Start up when the reactor was operated at various frequencies viz. 0.08 s^{-1} , 0.12 s^{-1} and 0.16 s^{-1} , with cell carrier loading of 80 g of GAC and at various influent phenol concentrations of 200,400,600 and 800 ppm, at dilution rate of 0.33 h^{-1} and at an amplitude of 3.5 cm. The change in effluent phenol concentration as a function of time during the start-up of the bioreactor at

different frequencies and at influent phenol concentrations of 200 ppm, 400 ppm, 600 ppm and 800 ppm are presented in Fig. 4.22 to 4.25 respectively.

As described in Section 4.1, during the start up period there exists three phases. These three phases were observed during the start up with influent phenol concentrations of 200, 400, 600, and 800 ppm and at all the frequencies under consideration. As observed from the insets to the plots of phenol concentration vs time shown in Fig. 4.22, 4.23, 4.24 and Fig. 4.25, the variation in phenol concentration with time is more oscillatory at higher frequencies owing to growth and detachment of biofilm. It indicates that at higher frequencies the detachment forces are strong and they compete with the biomass attachment forces induced by the biomass growth and secretion of EPS for biofilm compaction, leading to continuous and frequently varying rates of attachment and detachment of the biofilm before the attainment of steady state. Continuous attachment and detachment of biofilm leads to variation in biofilm structure during the start-up, thus altering the substrate flux. The variation in substrate flux through the biofilm results in variation in the overall rate of phenol degradation and thus resulting in fluctuating effluent phenol concentrations during the bioreactor start-up.

Fig. 4.26(a) shows the effect of frequency on the start up time for the bioreactor at different influent phenol concentrations. The start up time has decreased with increase in frequency of pulsation. The start-up time has reduced from 12 h to 8h as the frequency was increased from 0.08s^{-1} to 0.16s^{-1} at all the influent phenol concentrations. The resistance to mass transfer for the transfer of phenol and oxygen to the biofilm reduces with increase in frequency. This results in higher mass flux across the film. Thus, the rate of phenol transfer from the bulk liquid to the surface of biofilm increases. The biofilm surface concentration comes closer to the bulk concentration. Thus higher substrate and oxygen concentrations are available in the neighbourhood of the microorganisms for their growth (Shetty *et al.* 2007a). This enhances the rate of utilization of phenol and the rate of biomass growth. Thus the biofilm develops at a faster rate forming sufficient biomass to cause biodegradation of phenol, thus reducing the start-up period.

The variations of percentage degradation of phenol at steady state with change in frequency are presented in Fig.4.26 (b) for all the influent phenol concentrations. The percentage degradation was found to marginally increase with the increase in frequency at phenol concentrations of 200 to 600 ppm. More than 99% degradation was achieved at steady state with lower phenol concentrations of 200 to 600 ppm. However with higher influent phenol concentration of 800 ppm, the increase in steady state percentage degradation with increase in frequency was found to be of higher magnitude depicting that the influence of frequency is higher at higher phenol concentrations. With the increase in frequency, the turbulence in the column increases leading to thinning of the external liquid film around the biofilm which increases the rate of mass transfer of phenol from the bulk to the biofilm surface thus making the phenol readily available for the microorganisms to consume. The high rates of mass transfer at high frequencies make the concentration at the biofilm surface to come closer to the bulk concentration, making higher substrate and oxygen concentrations available in the vicinity of the microorganism for their growth. This enhances the percentage degradation with increased frequency.

Since at higher frequencies, the micro-organisms are exposed to higher stress owing to high shear conditions, they try to protect themselves from the high shear environment. Thus, they produce more EPS to compact themselves. Production of more EPS is led by higher rates of consumption of the substrate phenol. Since there was an increase in the rate of consumption of phenol, the percentage of degradation increased with the increase in frequency of pulsation. However, at lower phenol concentrations, the volumetric phenol loading rates to the bioreactor are lower and the residence time provided in the reactor is sufficiently high enough to achieve phenol removal rate almost equated with the phenol loading rate in the bioreactor. Thus, the frequency was found to have marginal influence on percentage degradation at lower influent phenol concentrations.

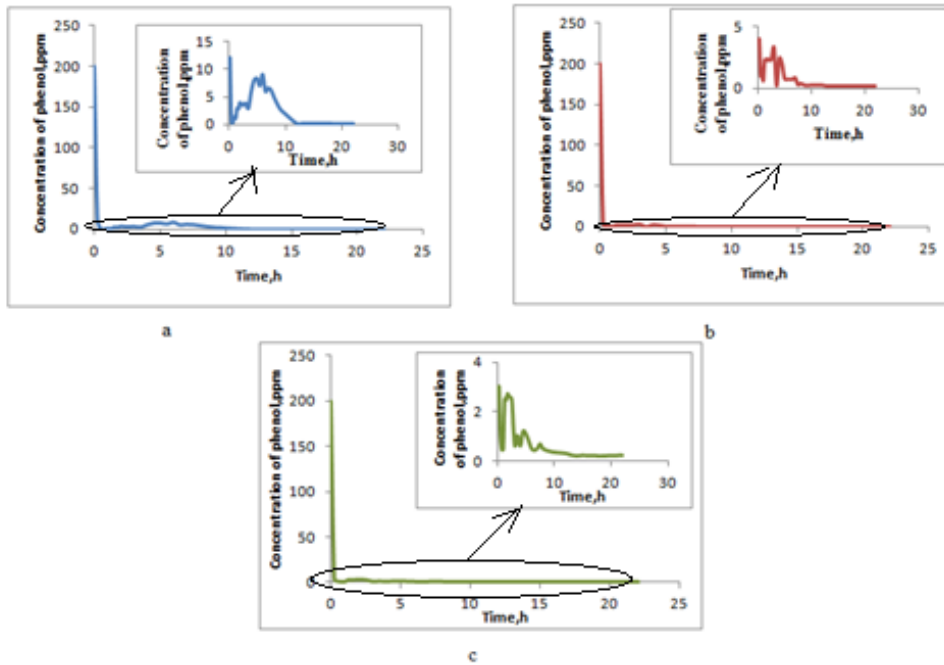


Fig.4.22 Degradation of phenol during Start up for different frequencies a) 0.08 s^{-1} b) 0.12 s^{-1} c) 0.16 s^{-1} . Conditions: $C_i = 200 \text{ ppm}$; $D = 0.33 \text{ h}^{-1}$; $A = 3.5 \text{ cm}$; $S = 80 \text{ g}$.

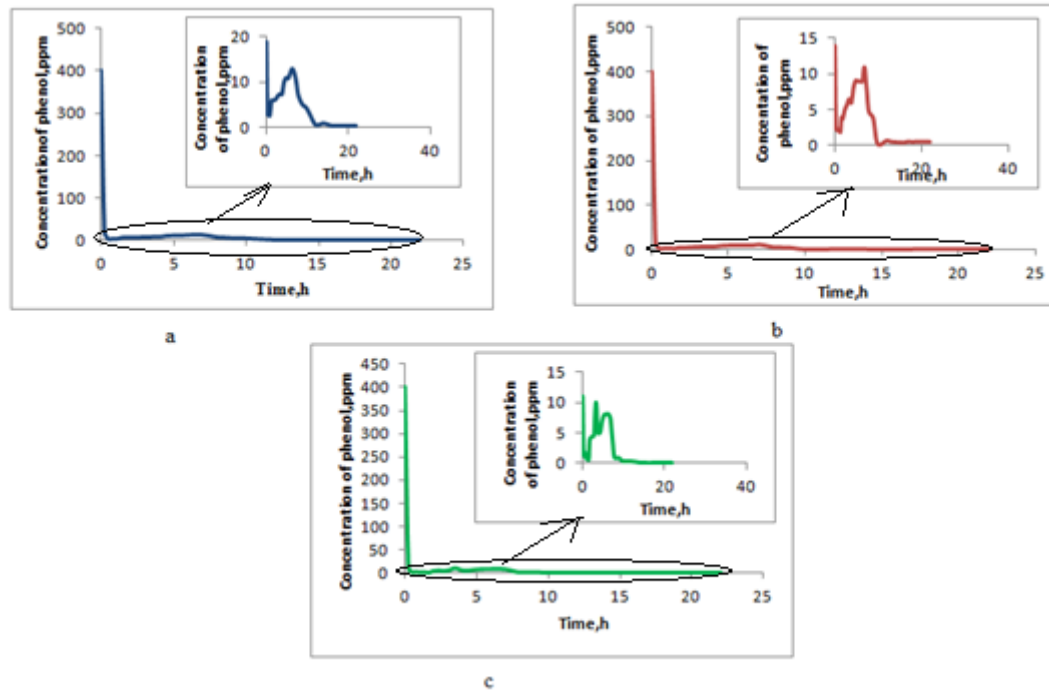


Fig.4.23. Degradation of phenol during Start up period for different frequencies frequencies a) 0.08 s^{-1} b) 0.12 s^{-1} c) 0.16 s^{-1} . Conditions: $C_i= 400\text{ppm}$; $D = 0.33 \text{ h}^{-1}$; $A=3.5 \text{ cm}$; $S=80 \text{ g}$.

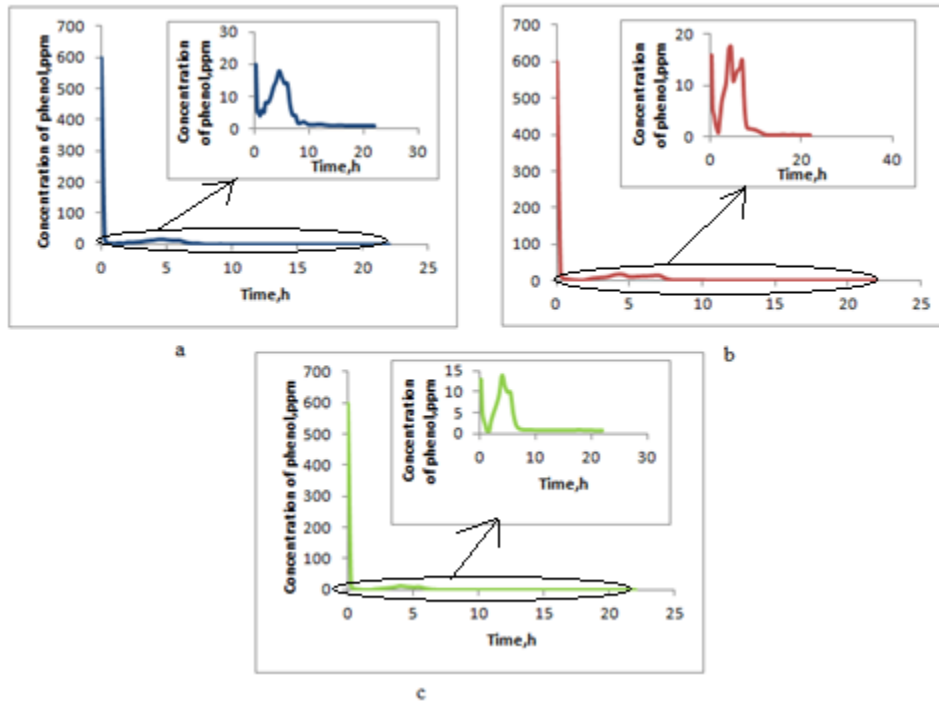


Fig.4.24. Degradation of phenol during Start up period for different frequencies frequencies a) 0.08 s^{-1} b) 0.12 s^{-1} c) 0.16 s^{-1} . Conditions: $C_i= 600 \text{ ppm}$; $D=0.33 \text{ h}^{-1}$; $A=3.5\text{cm}$; $S=80 \text{ g}$.

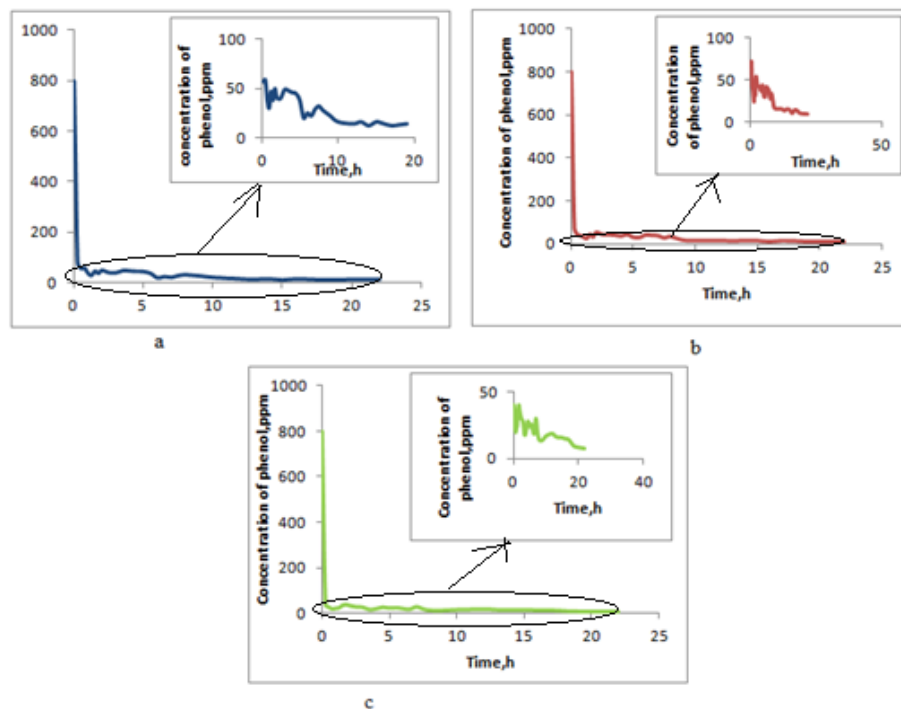


Fig.4.25. Degradation of phenol during Start up period for different frequencies frequencies a) 0.08 s^{-1} b) 0.12 s^{-1} c) 0.16 s^{-1} . Conditions: $C_i=800\text{ ppm}$; $D=0.33\text{ h}^{-1}$; $A=3.5\text{ cm}$; $S=80\text{ g}$.

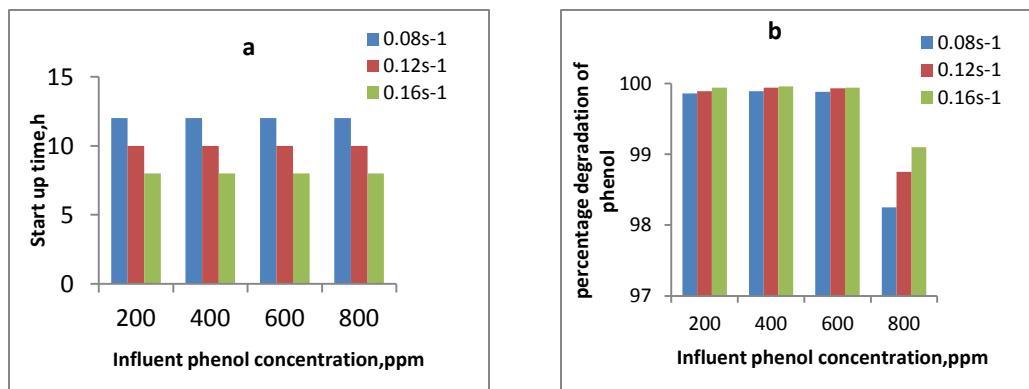


Fig. 4.26 Effect of frequency of pulsation on (a) start-up time (b) steady state percentage degradation at various influent phenol concentrations. Conditions: $D=0.33\text{ h}^{-1}$; $A=3.5\text{ cm}$; $S=80\text{ g}$.

4.3.2 Effect of frequency of pulsation on biofilm characteristics during Start up and at steady state of PPBR

Shear stress is considered to be one of the important factors responsible in construction of stable biofilm (Park *et al.*2011). Detachment rate governs the biofilm characteristics and thus the start-up and steady state performance of bioreactor. Thus, in the present study the effect of frequency of pulsation on the chemical and physical characteristics of the biofilm in PPBR during the start-up and steady state were studied. Continuous phenol biodegradation experiments were conducted at various frequencies viz., 0.08 s^{-1} , 0.12 s^{-1} and 0.16 s^{-1} , with cell carrier loading of 80 g as bioparticles at various influent phenol concentrations of 200, 400, 600 and 800 ppm and at an amplitude of 3.5 cm. The reactor was operated for various pre-calculated time period for the Start up studies as described in described in Section 3.3.5.2 of Chapter 3 and in Section 4.1 at each experimental set of condition. The biofilm characteristics were determined at various time periods during the start-up and at steady state.

4.3.2.1. Effect of frequency of pulsation on chemical characteristics of EPS in biofilm during Start up and at steady state of PPBR.

The variation of the EPS component composition in terms of protein, carbohydrate and humic substances (as mg per g of dry biomass) during the start up period of the bioreactor for each frequency and at various influent phenol concentrations of 200 ppm, 400 ppm, 600 ppm and 800 ppm are shown in Fig. 4.27 to 4.30 respectively. It can be observed that the quantities of protein, carbohydrate and humic substances increase with increase in time during the start-up. As the bacteria grow and tend to form biofilm, they need to secrete EPS containing protein and carbohydrates, which helps in their adhesion on to the substratum and cohesion among themselves. Release of humic substance is probably a result of decomposed microbial cells (More *et al.*2014). It can be observed from Fig 4.27 to 4.30 that the production of protein, carbohydrate and humic substances increase with increase in frequency. The higher production of EPS components with increased frequency are also achieved at steady state

as observed in Fig 4.31(a) to (d). Similar effect of shear were reported by Pei-Shi *et al.* (2008). Higher frequencies would lead to high shear. The microorganisms may attempt to protect themselves when they are exposed to high external shear stress by producing more exopolymers substances. This probably would have led to higher production of exopolymers at higher frequencies. Metabolic pathways of microbial cells may be regularised in response to shear stress to balance external detachment force (Liu and Tay 2001) and shear stress maintains young biofilm by slowing down biofilm maturation (Rochex *et al.* 2008), hence there may be increase in production of EPS component. Increased EPS synthesis has also been reportedly observed as part of a major change in gene expression in the biofilm state for a number of bacterial species (Sutherland 2001). The increase in EPS component components with respect to increase in frequency in the range studied, was 9-13 folds for protein, 4-20 for humic substance and 3-5 for carbohydrate. Since under higher shear stress, detachment rate is higher, microorganisms produce more EPS component to keep the biofilm structure stronger, leading to increase in protein content (Pellicer and Smets 2014) and carbohydrate content with increase in frequencies. Comparing Fig. 4.27(a), (b), and (c) , it is observed that the humic substance quantity is also a major constituent in the EPS that would have resulted from cleavage of protein, lipid or carbohydrate molecules (Wawrzynczyk *et al.* 2007).

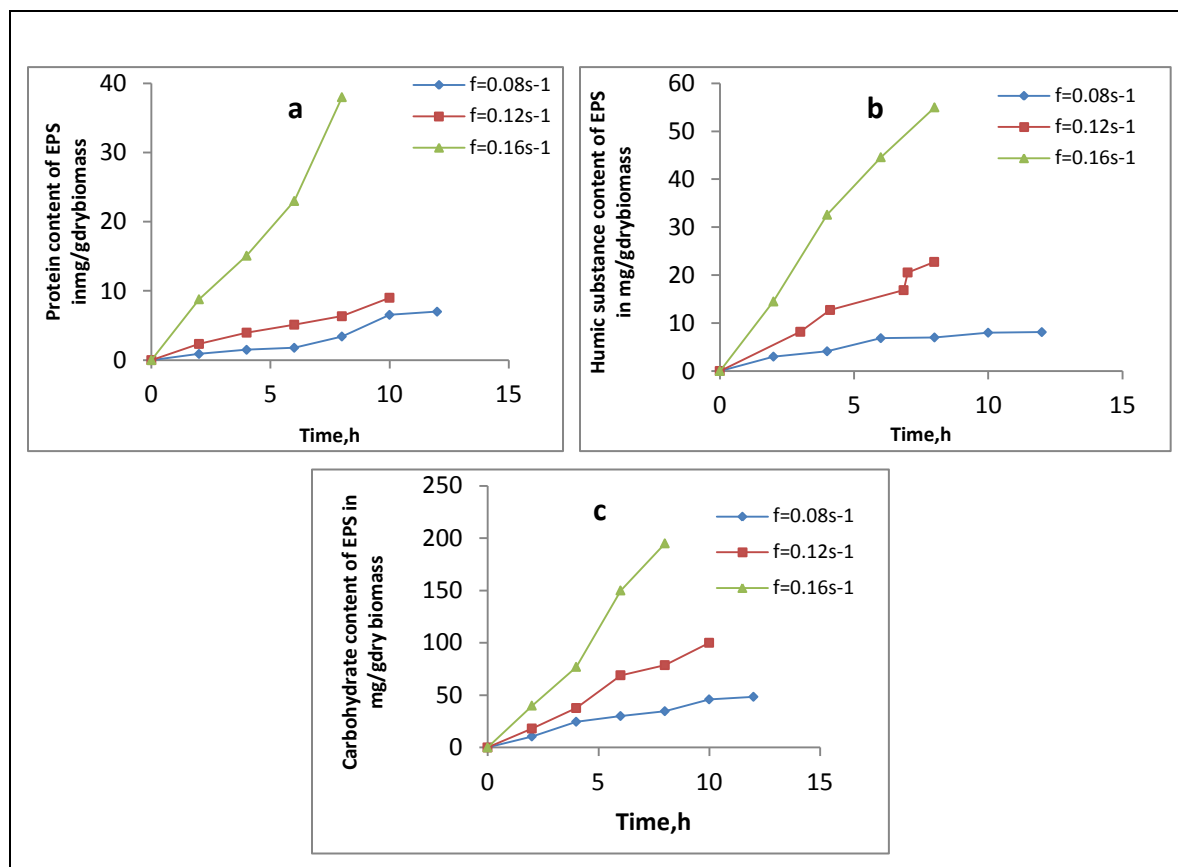


Fig.4.27. Effect of frequency of pulsation on production of EPS component of biofilm. (a) protein (b) humic substance (c) carbohydrate content. Conditions: $C_i=200$ ppm; $D=0.33$ h⁻¹; $A=6.5$ cm; $S=80$ g.

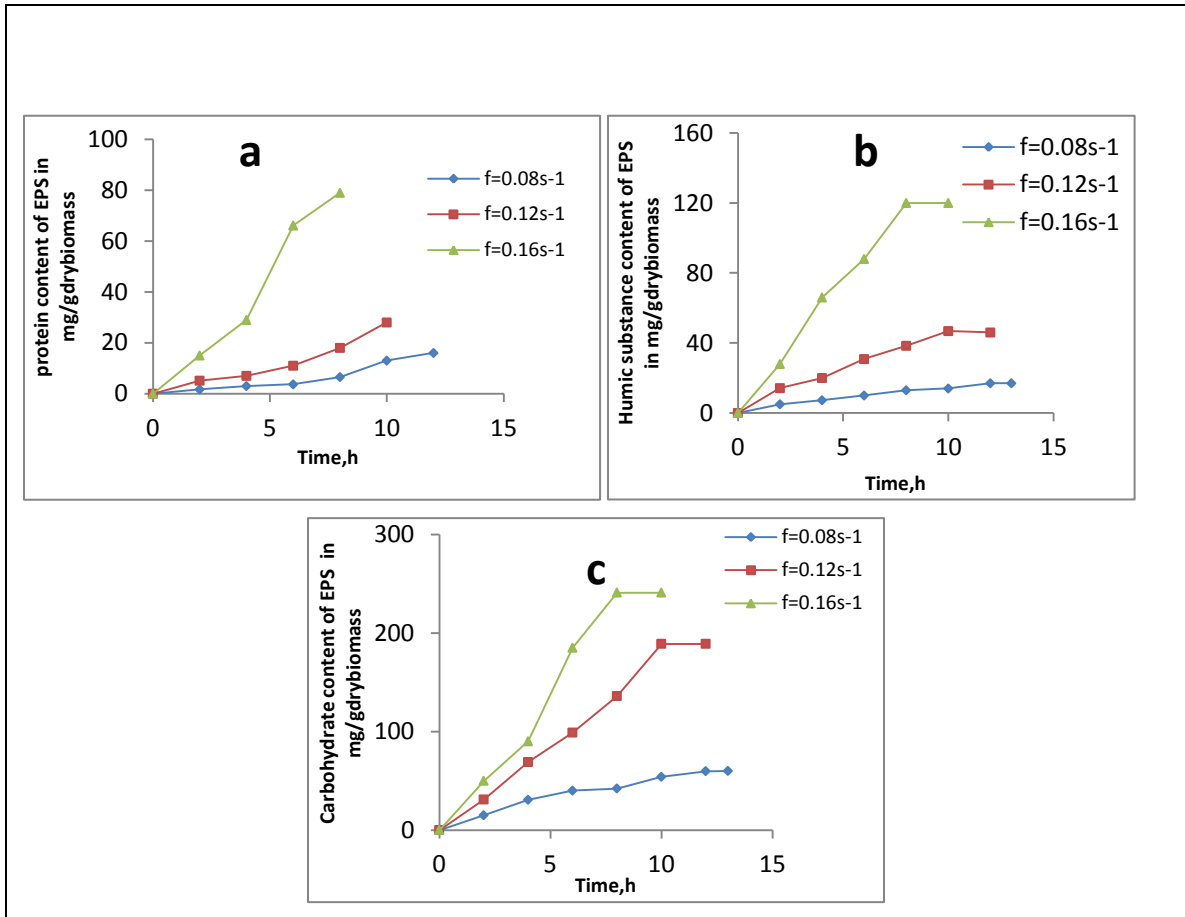


Fig.4.28. Effect of frequency of pulsation on production of EPS component of biofilm. (a) protein (b) humic substance (c) carbohydrate content. Conditions: $C_i = 400$ ppm; $D = 0.33 \text{ h}^{-1}$; $A = 6.5 \text{ cm}$; $S = 80 \text{ g}$.

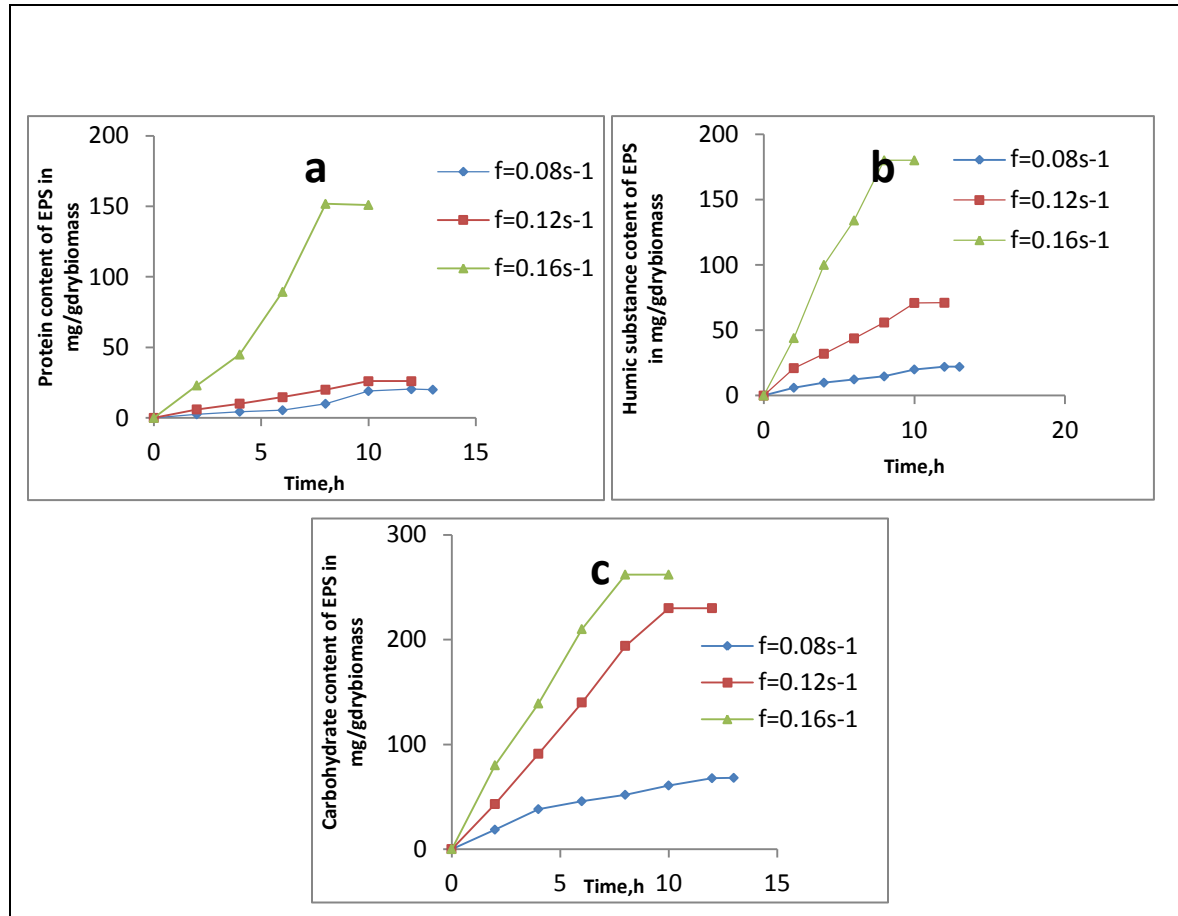


Fig.4.29 Effect of frequency of pulsation on production of EPS component of biofilm. (a) protein (b) humic substance (c) carbohydrate content. Conditions: $C_i = 600$ ppm; $D = 0.33 \text{ h}^{-1}$; $A = 6.5$ cm; $S = 80$ g.

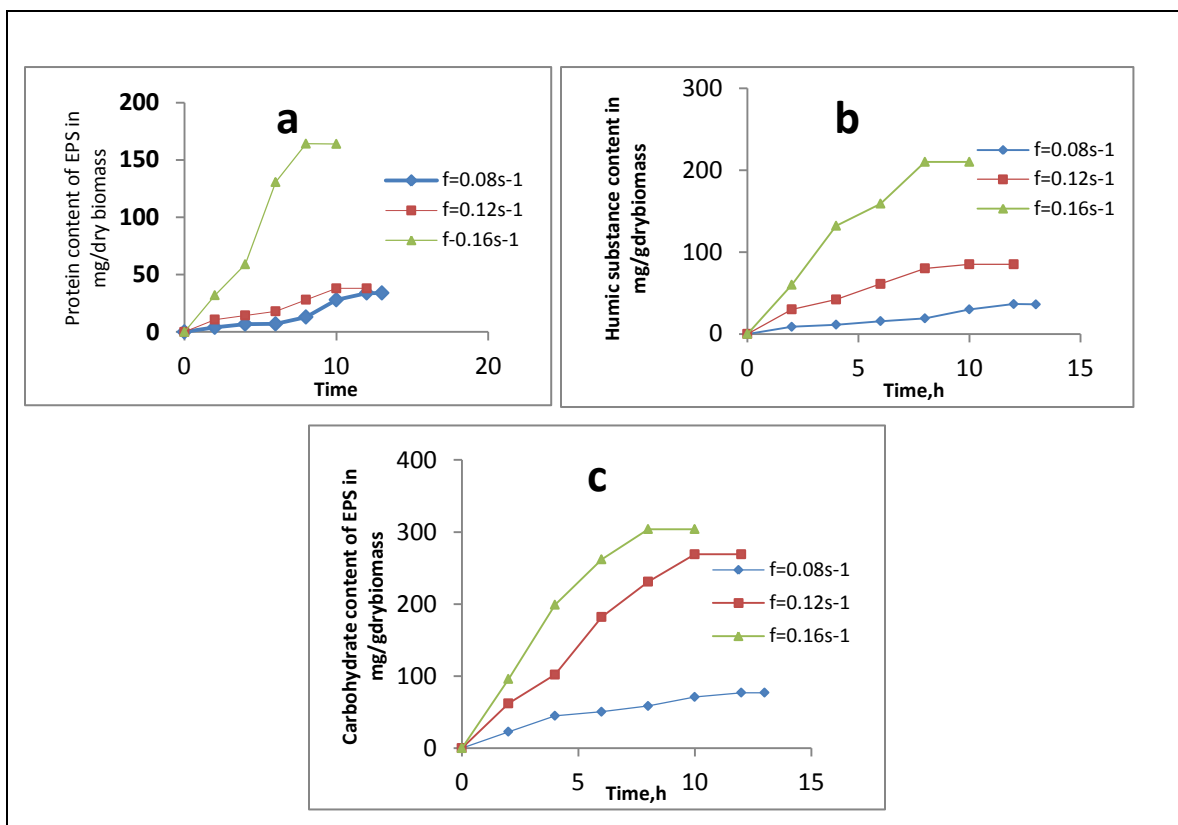


Fig.4.30. Effect of frequency of pulsation on production of EPS component of biofilm. (a) protein (b) humic substance (c) carbohydrate content. Conditions: $C_i = 800$ ppm; $D = 0.33 \text{ h}^{-1}$; $A = 6.5 \text{ cm}$; $S = 80 \text{ g}$.

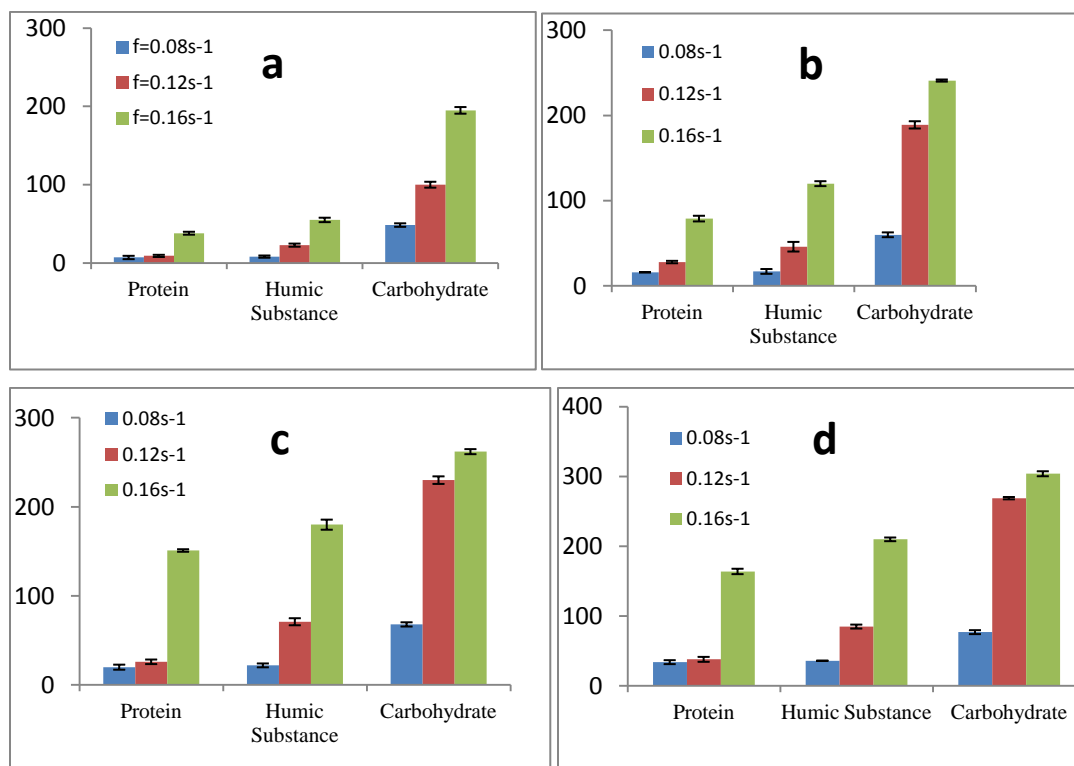


Fig 4. 31. Effect of frequency of pulsation on quantity of EPS component at different influent phenol concentrations (a) 200 ppm (b)400 ppm (c) 600 ppm and (d) 800 ppm. Conditions: $D=0.33 \text{ h}^{-1}$; $A=6.5 \text{ cm}$; $S=80 \text{ g}$.

4.3.2.2 Effect of frequency of pulsation on physical characteristics of biofilm during Start up and at steady state of PPBR

The variation in biofilm thickness, attached dry biomass and biofilm dry density were analyzed during the start up of the bioreactor at different frequencies of pulsation. The variation of biofilm thickness during the Start up period is shown in Fig.4.32a, Fig. 4.33a,

4.34a and 4.35a for the influent phenol concentrations of 200 ppm, 400 ppm, 600 ppm and 800 ppm respectively. It can be observed that there is an increase in thickness of biofilm up to a certain value, referred as active or critical thickness (Fernandez *et al.* 2014; Sekar *et al.* 1995; Tanyolac and Beyenal 1998), and thereafter a decrease with time is observed, further reaching almost a constant value. The detailed discussion on time course variations of biofilm thickness in PPBR during the start-up are discussed in Section 4.1.2.2. However, as indicated in Fig. 4.32(a) to 4.35 (a), the variation in thickness with time was found to be in a narrow range at higher frequencies, but at the lowest frequency of 0.08 s^{-1} , the biofilm thickness varied from $4.9 \text{ }\mu\text{m}$ to a maximum of $6 \text{ }\mu\text{m}$ and then decreased to around $3.6 \text{ }\mu\text{m}$ when the steady state was reached. The attached dry biomass also increased with time as indicated in Fig. 4.32(b) to 4.35(b) at all the frequencies and influent phenol concentrations under study, indicating microbial growth due to phenol utilization by the immobilized cells during start-up. Increase in biofilm density with time [Fig. 4.32(c) to 4.35(c)] at all the frequencies and influent phenol concentrations was observed indicating the EPS production during start-up causing the cell cohesion and formation of denser biofilm.

It can be observed from Fig. 4.32(a) to 4.35(a), that the biofilm thickness decreased with increase in frequency. As observed in Fig 4.36 (a) to (d) the biofilm thickness at steady state decreased with increase in frequency at all the influent phenol concentrations under study. The decrease in thickness of biofilm with increase in frequency may be due to erosion or sloughing of biofilm at high shear stress (Choi and Morgenroth 2003). However, in the present study it is observed that the attached biomass dryweight and the biofilm dry density increased with the increase in frequency of pulsation as observed in Fig. 4.32b to 4.35 b and Fig. 4.32c to 4.35 c respectively at all the influent phenol concentrations. Reduction in thickness in spite of increase in attached biomass dry weight has resulted in increase in density of the biofilms with increase in frequency of pulsation. It indicates that the biofilm becomes stable and compact with increase in shear (Pei-shi *et al.* 2000; Villasenor *et al.* 2000; Vieira *et al.* 1993). Increase in frequency of pulsation, increases the hydrodynamic turbulence. Increased turbulence leads to thinner hydrodynamic boundary layer and thus lower film mass transfer resistance for the transfer of substrate to the biofilm surface. Thus the substrate flux increases with the increase

in frequency of pulsation. Increased substrate flux leads to higher growth and thus would lead to higher EPS production. As a response to high shear conditions, the cells are stressed and they secrete more of EPS as a response to resist shear. Higher EPS production results in more adhesion and cohesion leading to thinner but denser biofilm. The correlation between production of EPS and biofilm density was noticed by Tsuneda et al. (2003). Fleming and Wingender (2001) also have reported that the detachment forces lead to a thinner and denser biofilm. However, these interactions are physical rather than biological. Similar observations of an increase in substrate flux with an increase in hydrodynamic turbulence indicating the biofilm to be thinner and the denser has been reported by Trulear and Charaklis (1982) and Wasche *et al.*(2000).

Detachment by abrasion has successfully been exploited to control biofilms in moving bed and biofilm airlift suspension reactors (Gjaltema *et al.* 1997; Tijhuis *et al.* 1996; Gjaltema *et al.* 1995). In pulsed plate column, stable biofilms are formed at frequencies upto 0.16 s^{-1} , indicating that detachment by abrasion due to the moving plates or the particle –particle collision and erosion due to moving fluid would result in biofilm detachment and the rate of detachment is balanced by the growth rate to form a stable biofilm at steady state. The formation of stable biofilm also indicates the absence of sloughing. Sloughing generally appears as release of large particles due to local rupture of the extra cellular network in deeper parts of biofilms (Kwok et.al, 1998). The stable operation of the PPBR under the frequencies of upto 0.16 s^{-1} indicate that the strain force is uniform throughout the biofilm and is lower than the tensile strength of the polymer matrix and thus avoiding the breakage of the matrix.

The morphological characteristics of steady state biofilm obtained at influent phenol concentration of 200ppm, as observed in SEM are shown in Fig. 4.37(a) to (c) at frequencies of 0.08 s^{-1} to 0.16 s^{-1} respectively. It is observed from Fig. 4.37 that the surface is rough for the lower frequency and becomes smoother as the frequency increases. At lowest frequency of 0.08 s^{-1} , valleys and peak structure was observed with large troughs and many numbers of micropores with varying sizes on the surface. However, at a frequency of 0.12 s^{-1} , the surface is more uniform with a very few uniform sized micropores. With increase in frequency to 0.16 s^{-1} , the biofilm surface seems smooth, uniform, dense and compact. A small sized pores are rarely visible. More number of micro pores is observed at lower frequency. At

the highest frequency of 0.16 s^{-1} , the micro pores are smaller and lesser. It indicates the formation of a more compact and dense film at higher frequencies. Similar results were observed by Pei-shi *et al.*(2008).

Thus, from the studies on the effect of frequency of pulsation it was found that the higher frequencies favor biodegradation at higher influent phenol concentrations. However more than 98% degradation of phenol could be achieved at all influent phenol concentrations even at the lowest frequency of 0.08 s^{-1} . However, the biofilm characteristics are greatly influenced by the frequency of pulsation. More compact and dense biofilms are formed at higher frequencies. Though the frequencies lower than 0.16 s^{-1} were found to be suitable for the stable operation of PPBR, higher frequency of 0.16 s^{-1} was found to enhance the bioreactor stability by forming thin and dense biofilms which are more stable. But owing to marginal influence of increasing the frequency of pulsation on phenol biodegradation efficiency, lowest frequency of 0.08 s^{-1} was used for further studies.

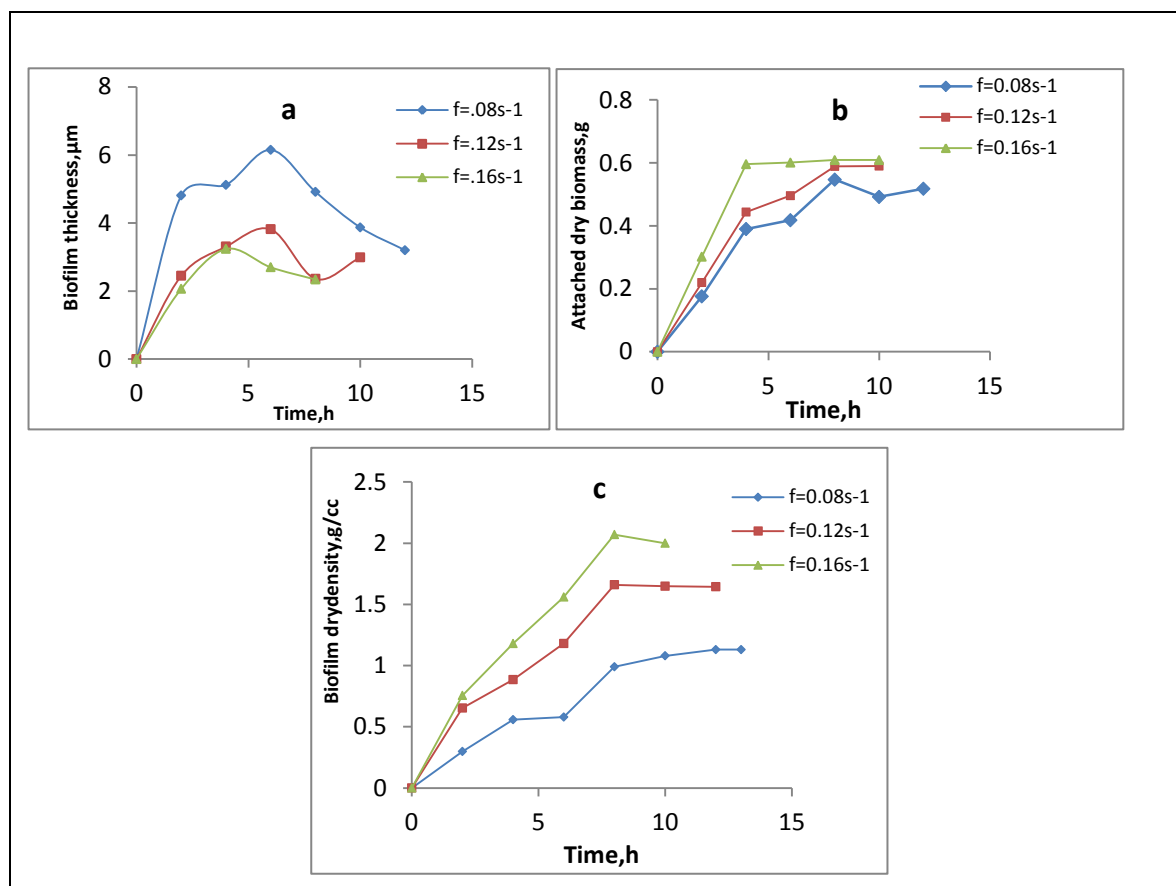


Fig.4.32. Effect of frequency of pulsation on biofilm physical characteristics during start up (a) biofilm thickness (b) attached drybiomass and (c) biofilm dry density. Conditions: $C_i=200$ ppm; $D=0.33$ h⁻¹; $A=3.5$ cm; $S=80$ g.

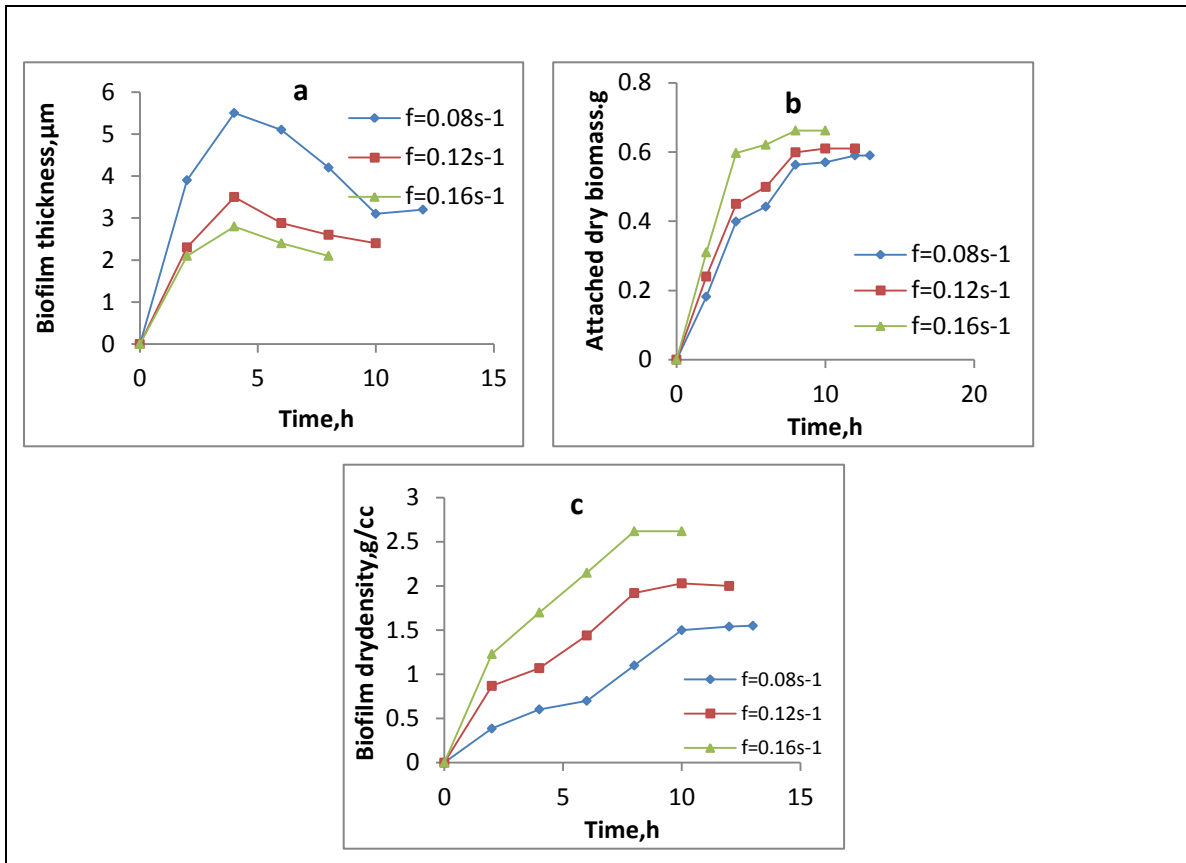


Fig.4.33 Effect of frequency of pulsation on biofilm physical characteristics during start up (a) biofilm thickness (b) attached drybiomass and (c) biofilm dry density. Condition: $C_i = 400$ ppm; $D=0.33\text{ h}^{-1}$; $A=3.5\text{ cm}$; $S=80\text{ g}$.

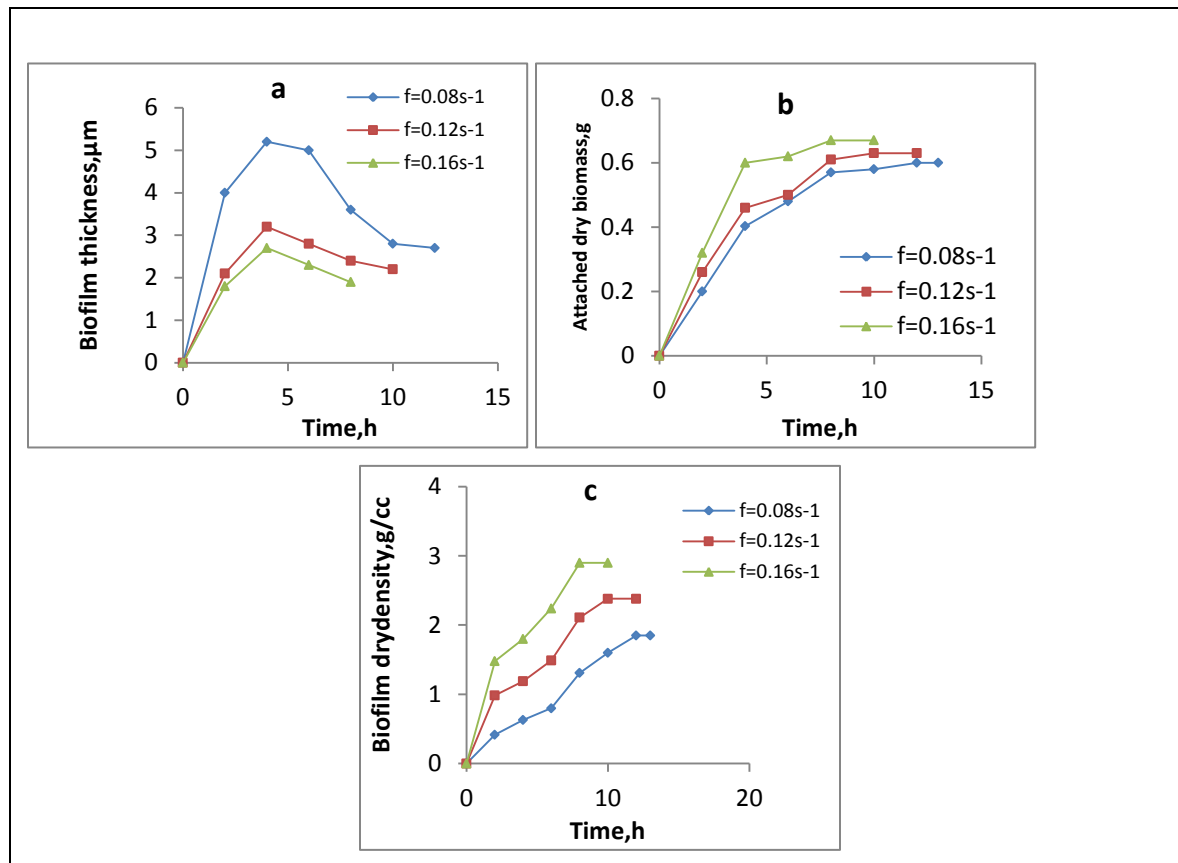


Fig.4.34 Effect of frequency of pulsation on biofilm physical characteristics during start up (a) biofilm thickness (b) attached drybiomass and (c) biofilm dry density. Conditions: $C_i = 600$ ppm; $D = 0.33 \text{ h}^{-1}$; $A = 6.5 \text{ cm}$; $S = 80$.

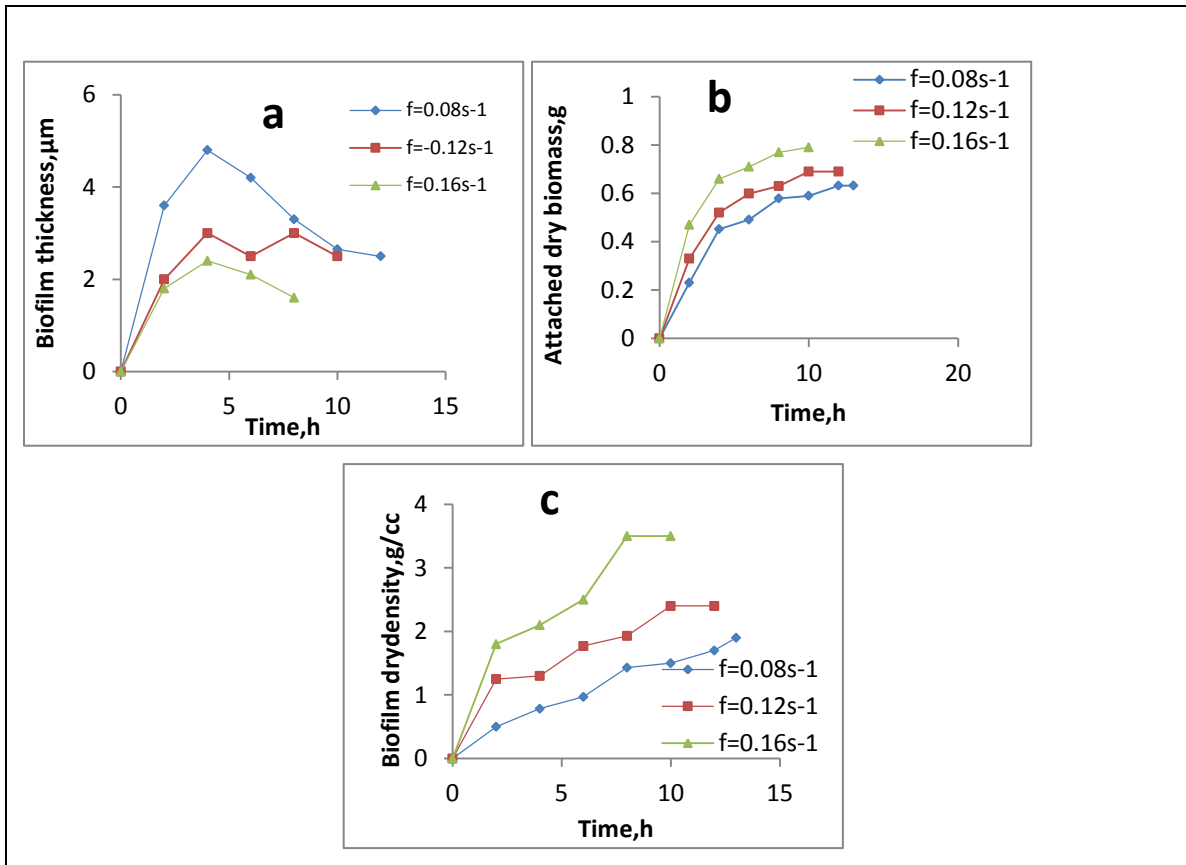


Fig.4.35. Effect of frequency of pulsation on biofilm physical characteristics during start up (a) biofilm thickness (b) attached drybiomass and (c) biofilm dry density. Conditions: $C_i = 800$ ppm; $f = 0.33 \text{ h}^{-1}$; $A = 6.5 \text{ cm}$; $S = 80 \text{ g}$.

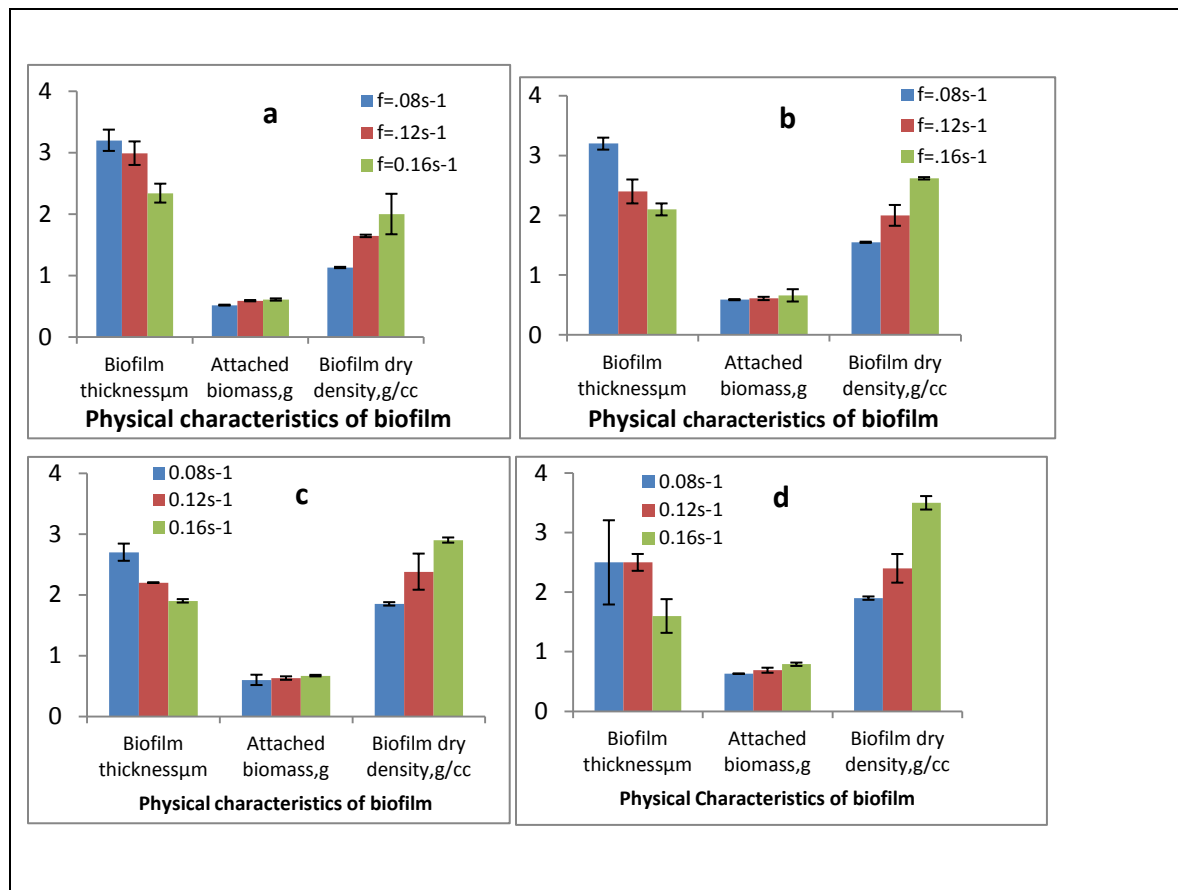


Fig.4.36. Effect of frequency of pulsation on physical characteristics at steady state with influent phenol concentrations of (a) 200 ppm (b) 400 ppm (c) 600 ppm and (d) 800 ppm. Conditions: $C_i = 800$ ppm; $f=0.33 h^{-1}$; $A=3.5$ cm; $S=80$ g.

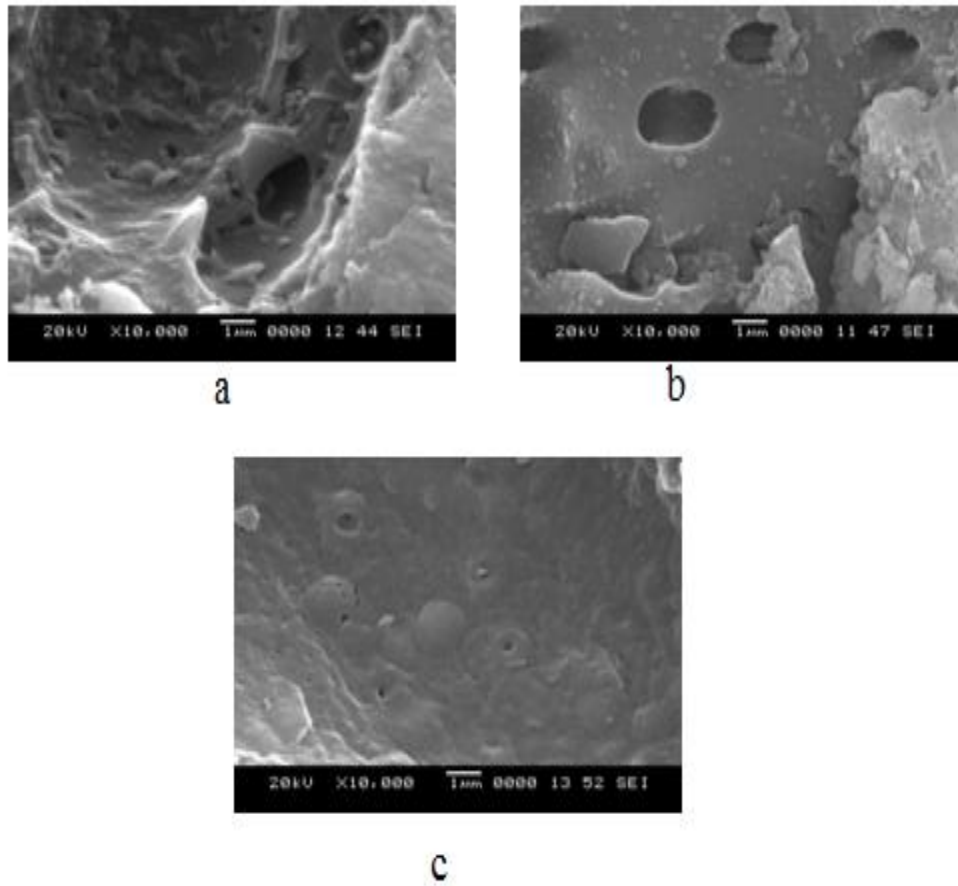


Fig.4.37. Morphological characteristics of steady state biofilm at different frequencies (a) 0.08 s^{-1} (b) 0.12 s^{-1} and (c) 0.16 s^{-1} and at the end of 8h. Conditions $C_i = 800 \text{ ppm}$; $f = 0.33 \text{ h}^{-1}$; $A = 6.5 \text{ cm}$; $S = 80 \text{ g}$.

4.4. Effect of cell carrier loading on on steady state and Start up performance of PPBR in terms of phenol biodegradation and biofilm characteristics

Variation in cell carrier loading varies the solid loading in the bioreactor. The solid loading in the bioreactor may influence the mass transfer characteristics in any three phase bioreactor involving a solid phase. The local velocity field in the tortuous channels in the bed of solids may vary in the bioreactor leading to slow movement of the particles in the bed. This may influence the fluid-solid mass transfer. Presence of solids was found

to decrease the air bubble diameter and increase the liquid phase dispersion in three phase fluidized bed reactor (Kawase and Uchiyama 1993). Oxygen mass transfer was found to increase with an increase in solids loading in inverse fluidized bed reactor (Haribabu and Sivasubramanian 2013). In air lift reactor the gas hold up decreased with the increase in solid-hold up (Freitas and Teixeira 1998). Increase in solid loading was found to cause a decrease in liquid circulation velocities in suspended bubble columns and air lift reactor (Immich and Onken 1992), draft tube spouted bed reactor (Fan *et al.* 1984). Thus the mixing and mass transfer characteristics were found to be influenced by the solid loadings in bioreactors. The performance of any three phase bioreactor is closely related with its mixing, solid-liquid and gas-liquid mass transfer characteristics. High solid loadings are necessary to achieve a high conversion in a continuous bioprocess (Klein *et al.* 2002). Cell carrier loading may also influence the biofilm detachment rate owing to particle-particle collision.

The cell carrier(solid) loading has been found to influence performance of three phase PPBR (Shetty *et al.* 2013). Thus in the present study, the effect of cell carrier loading in the bioreactor on phenol biodegradation by the immobilized cells of *P.desmoliticum* and biofilm characteristics during start-up and at steady state were studied.

The effect of cell carrier loading on the degradation of phenol in PPBR during the Start up and at steady state were studied under the conditions when the reactor was operated at a frequency of 0.08 s^{-1} ; dilution rate of 0.33 h^{-1} ; at an amplitude of 3.5 cm and at different cell carrier (GAC) loadings of 80 g and 120 g with immobilized cells. The initial biomass loading in the reactor was 0.184 and 0.276 mg with 80 and 120 g of GAC loading. These experiments were conducted at various influent phenol concentrations of 200 ppm to 800 ppm.

4.4.1. Effect of cell carrier loading on phenol biodegradation during Start up and at steady state of PPBR

The time course variations of phenol concentration during the start-up of PPBR with 80 and 120 g of cell carrier loading are presented in Fig. 4.38 (a) and (b) for influent phenol concentrations of 200 and 400 ppm. Similar plots for influent phenol concentrations of 600 and 800 ppm are presented in Fig 4.39 (a) and (b) respectively. The insets in the figures indicate the dynamics during the start-up till the achievement of the steady state.

As explained in Section 4.1, there exists three stages of change in effluent phenol concentration during the Start up. The fluctuating behavior of the concentration variations during start up was found to be similar at both the cell carrier loading indicating that start-up behavior was not influenced by the cell carrier loading at all the concentrations. As observed in Fig 4.40, the start-up time has reduced from around 12 h to 10 h when the cell carrier loading increased from 80 to 120 g. This trend has been observed at all the influent phenol concentrations studied. When the number of carrier particles increased, available surface area increases and in turn the initial number of immobilized cells increase, which means the inoculum size increases. With large number of cells present in the reactor initially, the rate of phenol consumption increases, leading to faster growth of the cells. Increased rate of cell growth and phenol consumption results in reduction in Start up time (Shetty *et al.* 2013). It can be observed from Fig4.40(b), the steady state percentage degradation for 80 g GAC was found to be around 99% and was > 99.9% when the carrier loading was increased to 120 g of GAC upto 600 ppm of influent phenol concentration. The percentage degradation for 80 g GAC was found to be around 98% and was > 99 % when the loading was increased to 120 g of GAC for 800 ppm of influent phenol concentration. So it can be observed that, the steady state percentage degradation increased marginally with the increase in cell carrier loading. With larger carrier loading, a larger number of GAC particles with immobilized cells were used in the reactor, and hence more total surface area was available for the transfer of substrate and oxygen between the liquid and the biofilm and also for the biochemical

reaction. This results in increase in the net removal rate of phenol, leading to increased percentage degradation with the increase in carrier loading (Shetty *et al.* 2013).

The solid loading increases the gas holdup in the three-phase reciprocating plate column (Nikolić *et al.* 2005; Skala *et al.* 1993). The gas holdup greatly affects both the interfacial area and the oxygen mass transfer rate in multiphase reciprocating or pulsed plate columns (Stamenković *et al.* 2005), thus influencing the oxygen mass transfer in PPBR.

However, in the present study, the increase in percentage degradation with the increase in carrier loading was found to be marginal at the influent phenol concentrations of 200 ppm to 600 ppm. The surface available for the biochemical reaction with 80 g of GAC may itself be abundant for the degradation of phenol loaded into the reactor at lower influent phenol concentrations and the variations in mass transfer characteristics with increase in solid loading may not be very predominant, thus the further increase in carrier loading to 120 g would have resulted only in marginal increase in percentage degradation. However, at influent phenol concentration of 800 ppm, the percentage degradation at steady state increased from 98.25 % to 99.71 %, bringing in large increase in net removal rate of phenol showing the positive influence of increase in cell carrier loading at high influent phenol concentrations. When the cell carrier loading in the bioreactor was 80 g the loading per stage was 20 g. At lower carrier loading per stage, the local fluidization of bioparticles occur between the plates leading to slow movement of particles within the bed. Though the fluidization of the whole bed was not observed, the particles tend to move locally around their own regime. This may result in enhanced mass transfer of phenol and oxygen to the biofilm. However, it is observed that at lower cell carrier loading the percentage biodegradation and net phenol removal were lower. The effect of enhancement in mass transfer due to particle movement seems marginal as compared to the effect of reduced biodegradation owing to lower surface area and lower biomass available for biodegradation at lower cell carrier loading, thus resulting in lower biodegradation of phenol.

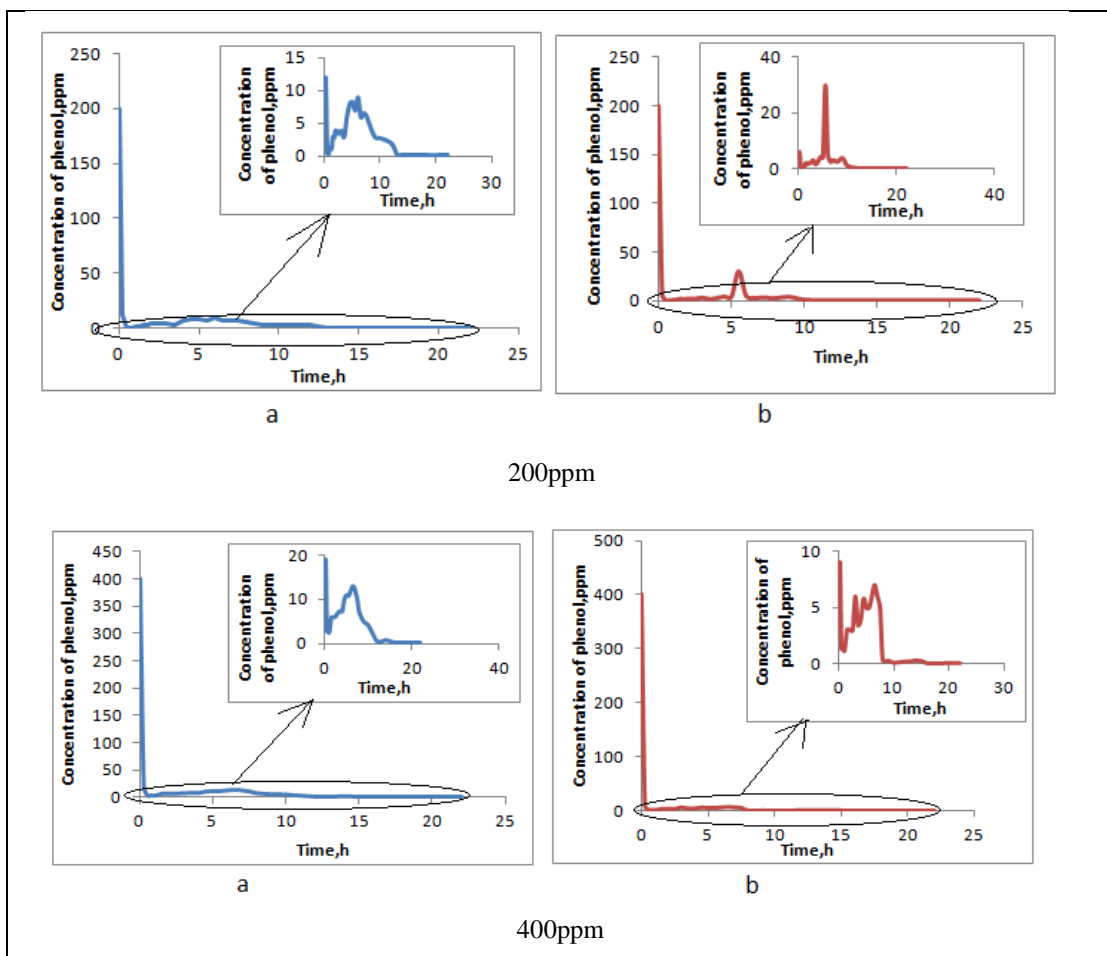


Fig.4.38. Variation in phenol concentration during the Start up period for different cell carrier loading of a) 80g and b)120 g for various influent phenol concentrations of 200ppm and 400ppm. Conditions: $f=0.08s^{-1}$; $D=0.33h^{-1}$; $A=3.5cm$.

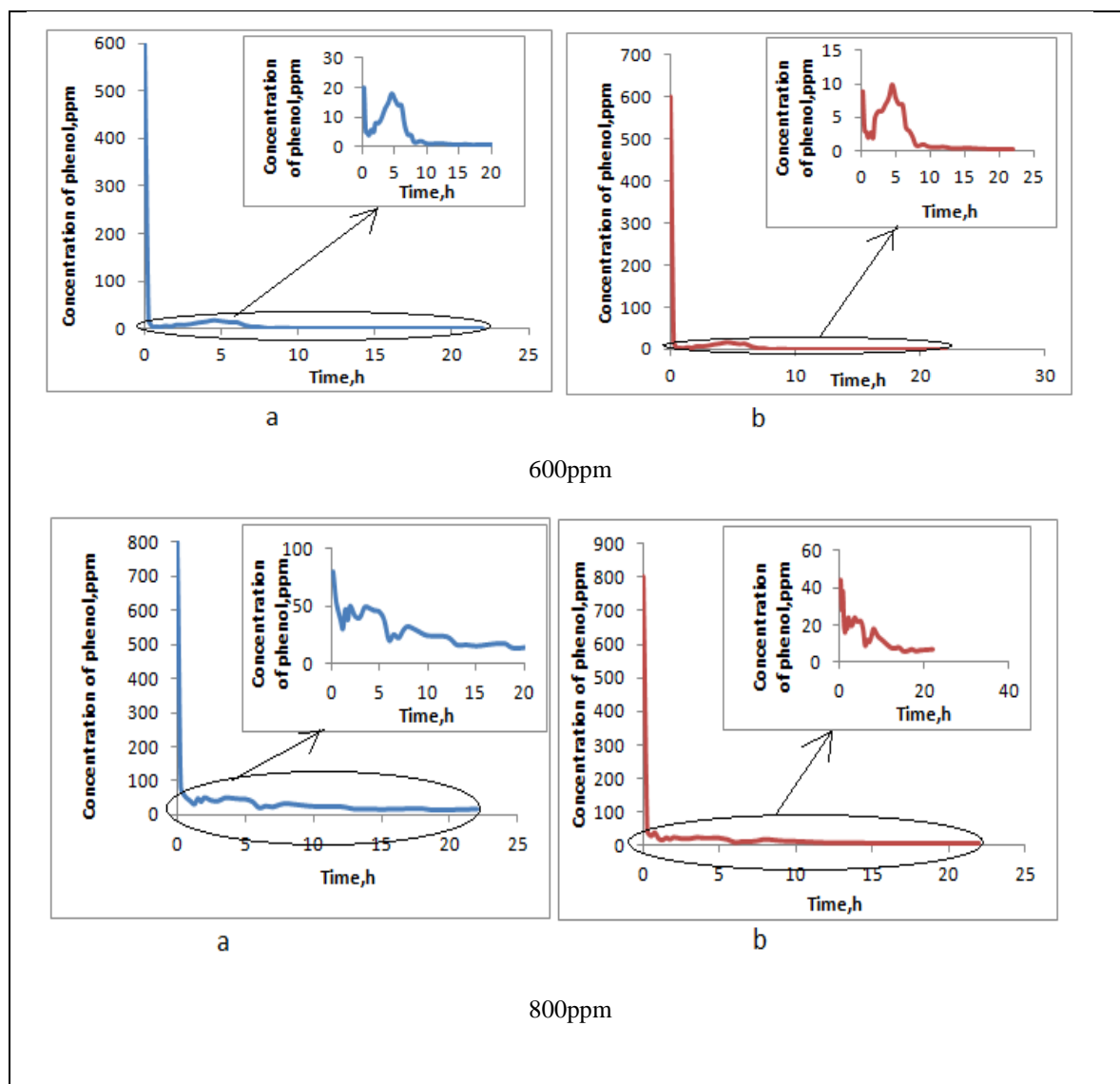


Fig.4.39. Variation in phenol concentration during Start up period for different cell carrier loading of a)80 g b)120 g for various influent phenol concentraions of 600 ppm and 800 ppm. Conditions: $f=0.08 \text{ s}^{-1}$; $D=0.33 \text{ h}^{-1}$; $A=3.5\text{cm}$.

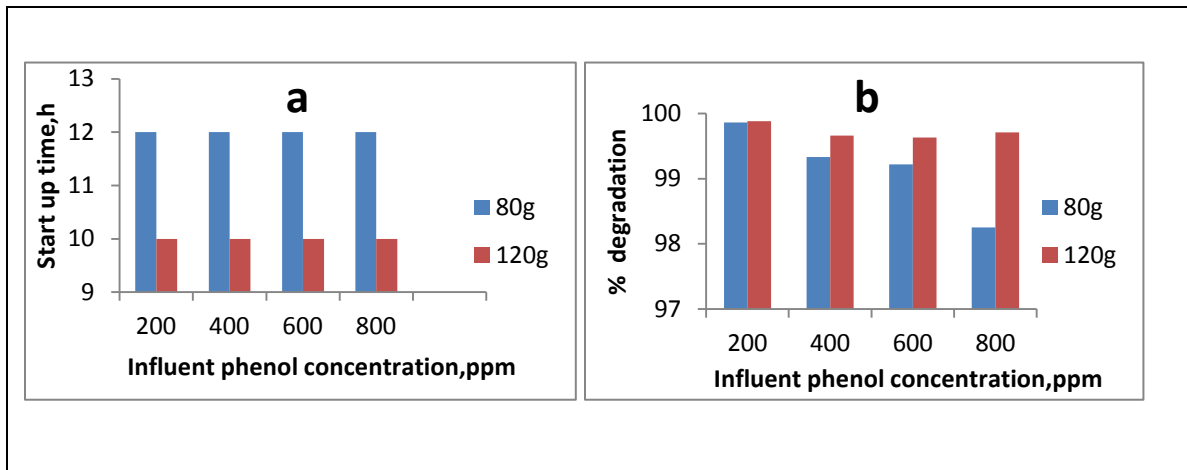


Fig.4.40. Effect of cell carrier loading on (a) Start up time (b) percentage degradation of phenol at steady state for various influent phenol concentrations. Conditions: $D=0.33 \text{ h}^{-1}$; $A=3.5 \text{ cm}$; $f=0.08 \text{ s}^{-1}$.

4.4.2 Effect of cell carrier loading on biofilm characteristics during Start up and at steady state of PPBR

As mentioned in Section 3.5.2 the experiments were conducted to study the effect of cell carrier loading on the biofilm characteristics under frequency of 0.08 s^{-1} ; dilution rate of 0.33 h^{-1} ; at an amplitude of 3.5 cm and at different cell carrier (GAC) loadings of 80 g and 120 g. The start-up behavior of the bioreactor was studied as mentioned in Section 3.5.2. The biofilm characteristics were determined and results are presented in the following sections.

4.4.2.1 Chemical characteristics

The results of the effect of cell carrier loading on the composition of EPS produced during the start up period of the bioreactor are presented as time course variation of protein, carbohydrate and humic substance content of EPS in Fig.4.41 to Fig.4.44 for

200, 400, 600 and 800 ppm influent phenol concentrations respectively.

As shown in Fig.4.41 to Fig.4.44, the protein, humic substance and carbohydrate content in EPS increased with time and reached a steady value both with 80 and 120 g of cell carrier loading. On comparison of the time for achievement of steady state for phenol degradation (Fig.4.40a) and EPS component contents (Fig.4.41 to Fig.4.44), it is observed that the EPS composition also attained a steady value at the same time when the phenol concentration attained steady state confirming the steady state behavior of the bioreactor. When the cell carrier loading was increased, the protein, humic substance and carbohydrate content of EPS were found to increase. As observed in Fig.4.41 to Fig.4.44, the protein, humic substance and carbohydrate content at any time during start-up are higher with 120 g than with 80 g cell carrier loading, indicating that the rate of increase in protein, humic substance and carbohydrate content increase with the increase in cell carrier loading. This could be due to high total surface area available for adsorption of phenol and the higher number of immobilized cells present in the reactor during the initial stage of reactor start-up operation which leads to enhanced rate of phenol consumption and microbial growth with simultaneous EPS component production. As the cells grow in the biofilm, the protein, carbohydrate and humic substance content in the EPS increase at a faster rate to facilitate the adhesion and cohesion of the cells in the biofilm and to provide strength to the biofilm (Liu *et al.* 2004; Sutherland 2001).

Fig 4.45 shows that the protein, carbohydrate and humic substance content in EPS at steady state increased with increase in cell carrier loading at all the initial phenol concentrations studied. The protein, carbohydrate and humic substance content in EPS have increased considerably with the increase in cell carrier loading, though the increase in percentage degradation is only marginal. Though the variation in percentage degradation is marginal, the net phenol removal rate is substantial at higher cell carrier loading.

Owing to larger surface available for microbial adhesion and cohesion at higher cell carrier loading, the EPS component required for the biofilm is also higher. Thus the bacteria secrete more EPS at steady state at higher cell carrier loading. Higher percentage degradation achieved also indicates that the net phenol removal rate increased with the increase in cell carrier loading. Higher removal rate is owing to the higher utilization or degradation of phenol by the cells in the biofilm. Higher degradation results higher bacterial growth rate thus, increasing the EPS production in biofilm. Higher biomass necessitates the production of large amount of protein and carbohydrate content of EPS to facilitate the adhesion and cohesion of cells in the biofilm. Higher growth rate also leads to rise in the number of dead cells and thus increases the humic substance content of the EPS.

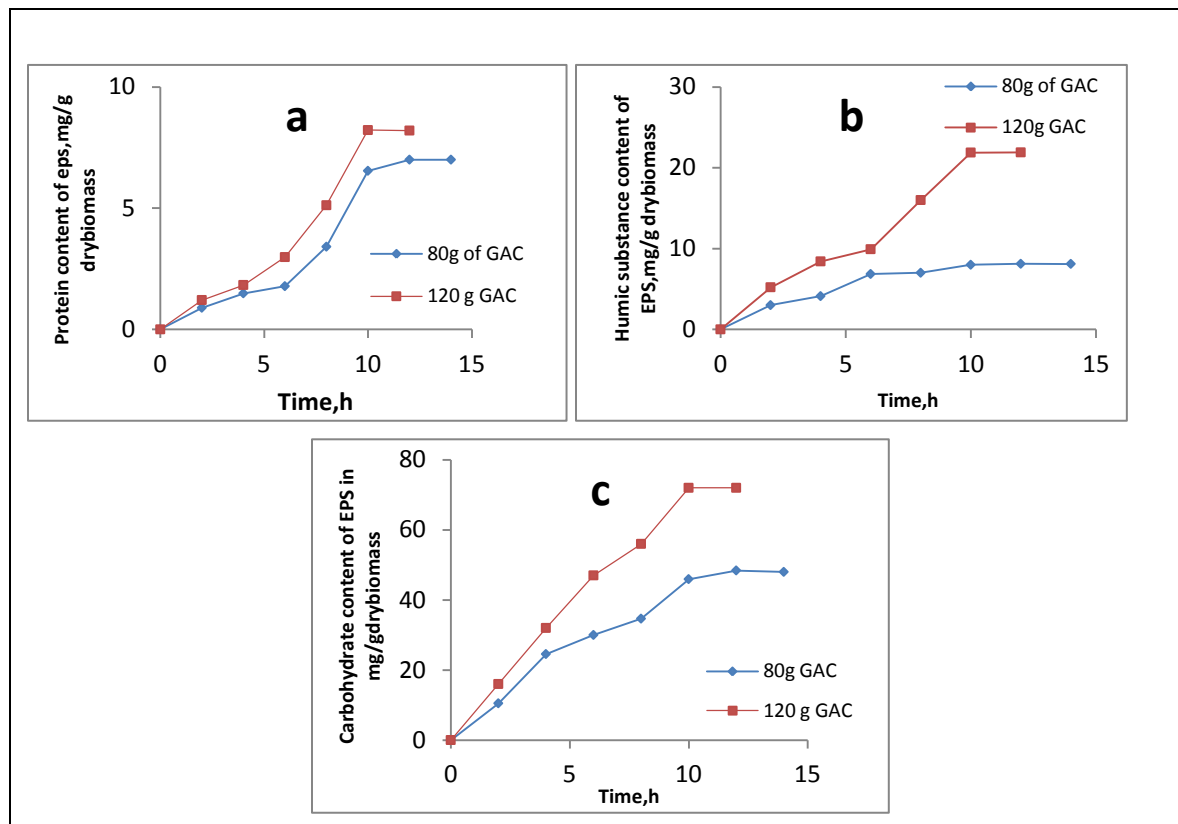


Fig.4.41. Effect of cell carrier loading on production EPS components during start up (a) protein content (b) carbohydrate content and (c) humic substance content of EPS for influent phenol concentration of 200 ppm. Conditions: $f= 0.08 \text{ s}^{-1}$; $D=0.33 \text{ h}^{-1}$; $A=3.5 \text{ cm}$.

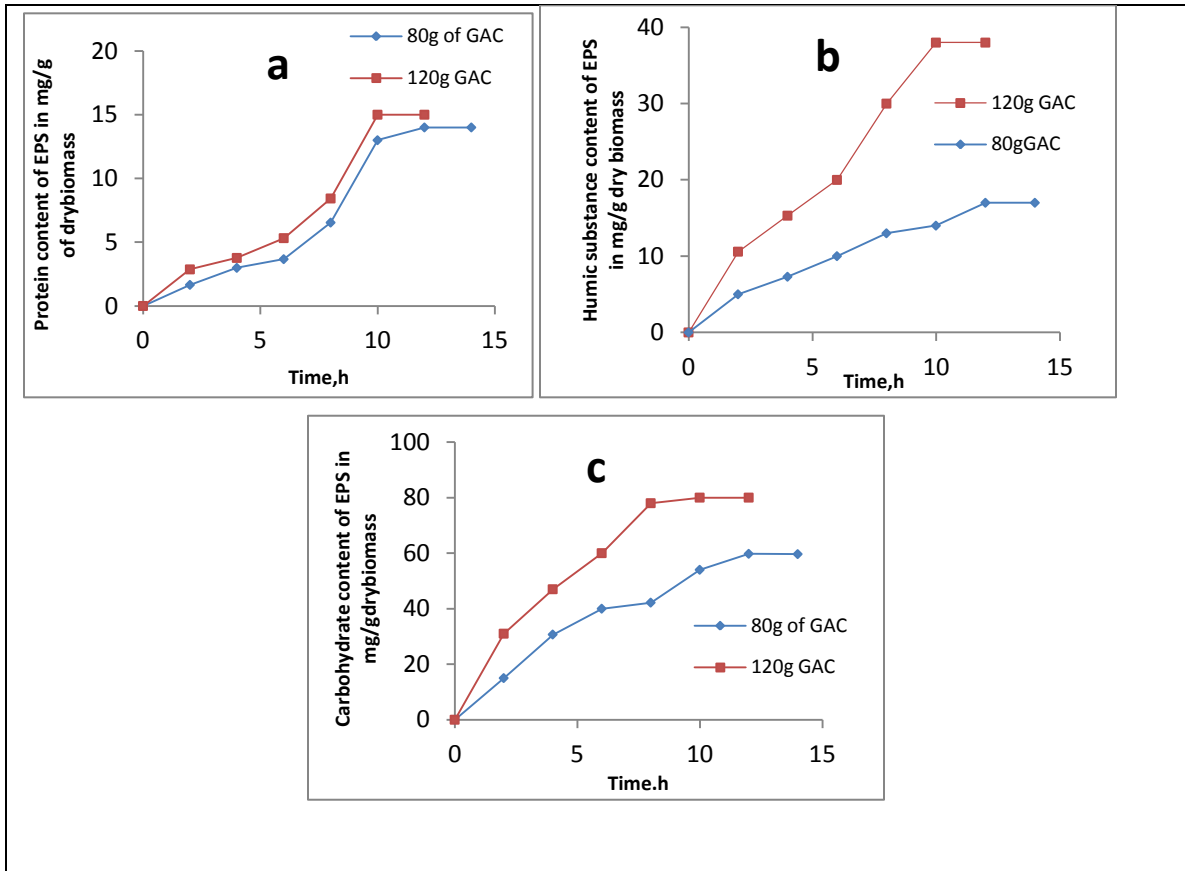


Fig.4.42. Effect of cell carrier loading on production EPS components during start up (a) protein content (b) carbohydrate content and (c) humic substance content of EPS for influent phenol concentration of 400 ppm. Conditions: $f= 0.08 \text{ s}^{-1}$; $D=0.33 \text{ h}^{-1}$; $A=3.5 \text{ cm}$

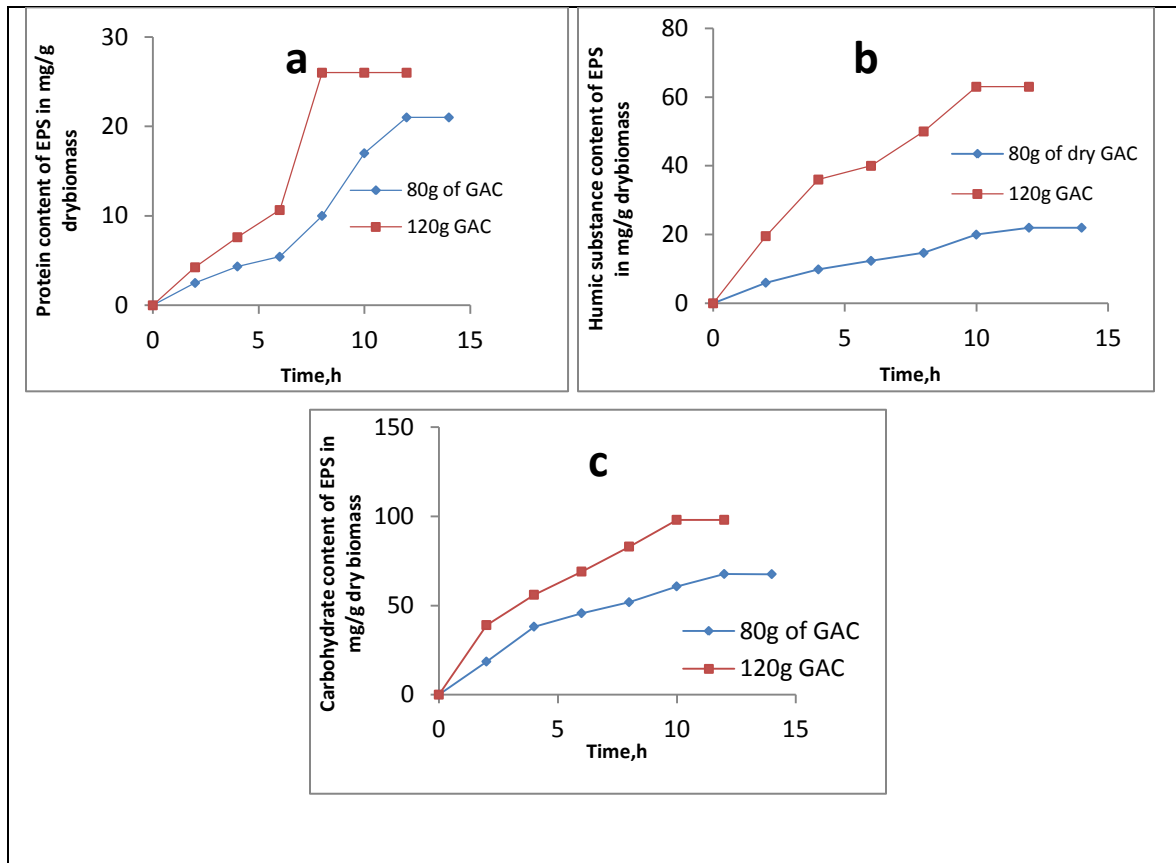


Fig.4.43. Effect of cell carrier loading on production EPS components during start up (a) protein content (b) carbohydrate content and (c) humic substance content of EPS for influent phenol concentration of 600 ppm. Conditions: $f= 0.08 \text{ s}^{-1}$; $D=0.33 \text{ h}^{-1}$; $A=3.5 \text{ cm}$

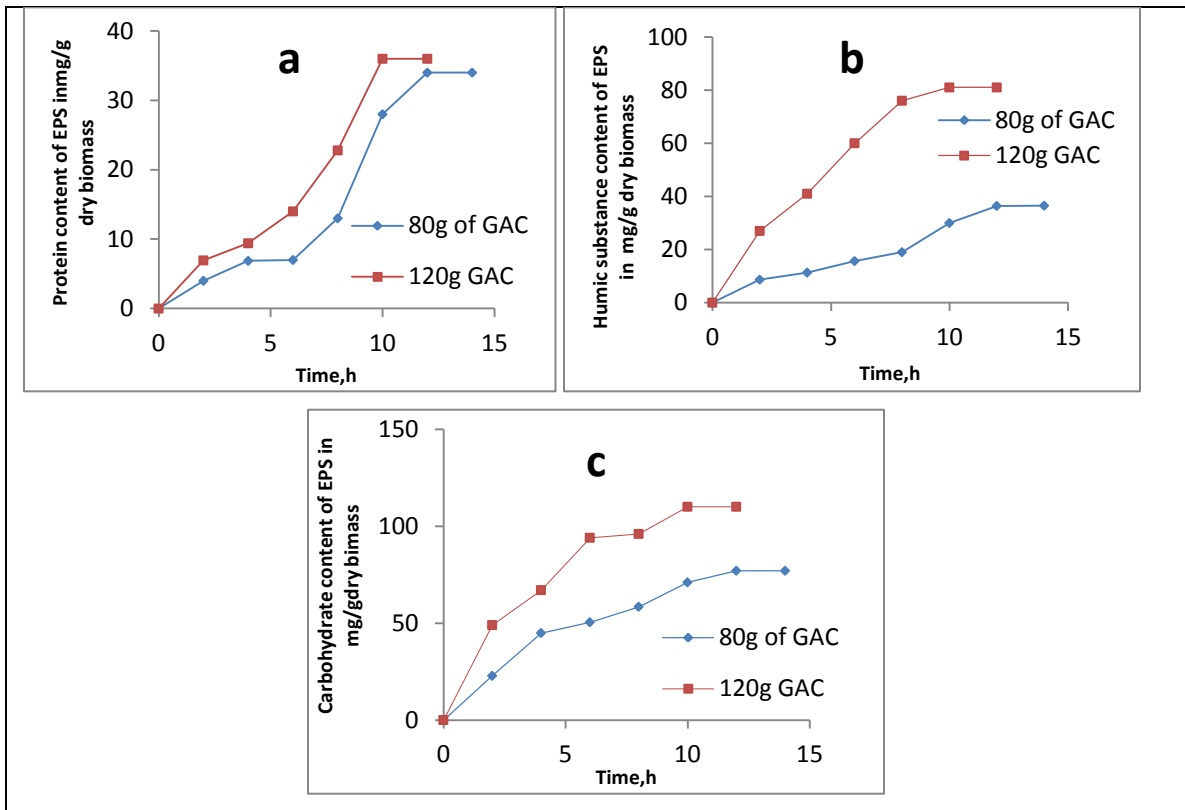


Fig.4.44. Effect of cell carrier loading on production EPS components during the start-up (a) protein content (b) carbohydrate content and (c) humic substance content of EPS for influent phenol concentrations of 800ppm. Conditions: $f=0.08\text{ s}^{-1}$; $D=0.33\text{ h}^{-1}$; $A=3.5\text{ cm}$.

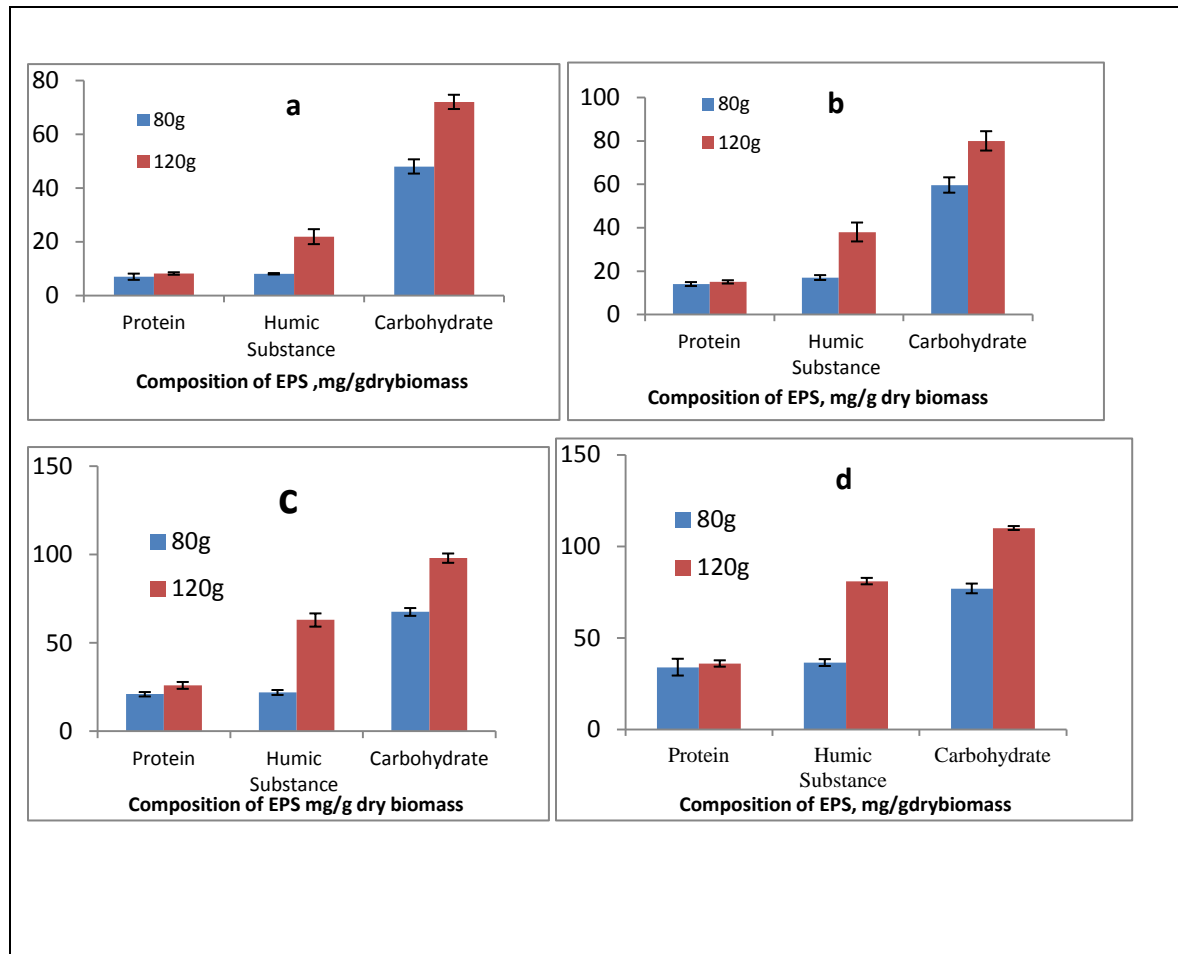


Fig.4.45 Effect of cell carrier loading on quantity of EPS components at steady state with influent phenol concentration of a) 200ppm b) 400ppm c) 600ppm and d) 800ppm. Conditions: $f = 0.08 \text{ s}^{-1}$; $A = 3.5 \text{ cm}$; $D = 0.33 \text{ h}^{-1}$.

4.4.2.2 Effect of cell carrier loading on physical characteristics of biofilm.

The effect of cell carrier loading on physical characteristics of biofilm during start-up studied at different influent concentrations of 200 ppm to 800 ppm. The variation in physical characteristics of the biofilm such as biofilm thickness, dry biomass and biofilm dry density with time can be explained as discussed in Section 4.3.1.2 .

The effect of carrier loading on biofilm characteristics during start up at different influent phenol concentrations are shown in Figure 4.46 to Figure 4.49. It can be observed from Fig.4.50, that at steady state, the biofilm thickness decreased and the biomass dry weight increased with increase in cell carrier loading resulting in increased biofilm dry density of the biofilm. With increased cell carrier loading, the amount of immobilized cells initially present in the reactor was higher. With higher amount of cells being available per unit volume of the reactor, the rate of cell growth may be higher with utilization of phenol. Increased cell growth rate leads to higher biomass dry weight in the reactor when the cell carrier loading was higher. Thus, the rate of growth is higher at high carrier loadings. As discussed in earlier sections, the enhanced rate of phenol consumption and microbial growth with simultaneous EPS component production occurs when higher cell carrier loading was used owing to higher number of cells initially immobilized on the surface of the carrier particles and larger biofilm surface area available (Kwok *et al.* 1997). Enhanced rate of EPS component production at high cell carrier loading would have led to stronger and tighter cohesion of the cells in the biofilm resulting in the formation of denser biofilm with reduced thickness. Thus, the biofilm thickness decreased and biofilm density increased with increase in carrier loading into the reactor. The local movement of particles within the bed at lower cell carrier loading may result in increased cell detachment rates and enhanced mass transfer of phenol and oxygen to the biofilm. However, it is observed that at lower cell carrier loading the attached biomass dry weight is lower and the biofilm thickness is higher. Higher biofilm thickness at lower cell carrier loading indicates that the detachment rate due to particle movement does not have profound influence on the biofilm. The attached biomass was lower at lower cell carrier loading showing that the effect of enhancement in mass transfer due to particle movement seems marginal as compared to the effect of lower surface area available for phenol biodegradation and biomass production at lower cell carrier loading.

Lower attached biomass dryweight and higher biofilm thickness with lower biofilm density indicates that the biofilm may be loose and porous in structure at lower carrier loadings as compared to that at higher carrier loading. The morphological

characteristics of biofilm with different cell carrier loading are shown in images of Fig.4.51. The comparison of biofilm morphological features shown in Fig 4.51(a) and (b) at carrier loadings of 80 g and 120 g indicates that the biofilm formed at 80 g carrier loading are with rough and uneven surface with larger and non uniform pores indicating their loose structure. The biofilm formed at 120 g cell carrier loading is with smooth and compact surface consisting of uniform sized small micropores. The morphological characteristics support the results on biofilm thickness and density. However, more number of single loose cells are observed on the biofilm at cell carrier loading of 120 g which seem to be on the verge of colonization. However, the number of loose cells on the biofilm at 80 g cell carrier loading are fewer indicating that the slow particle movement may lead to detachment of loose cells easily at lower cell carrier loadings. However owing to marginal influence of increase in the cell carrier loading on biodegradation, lower loading of 80 g GAC was further used in the experiments.

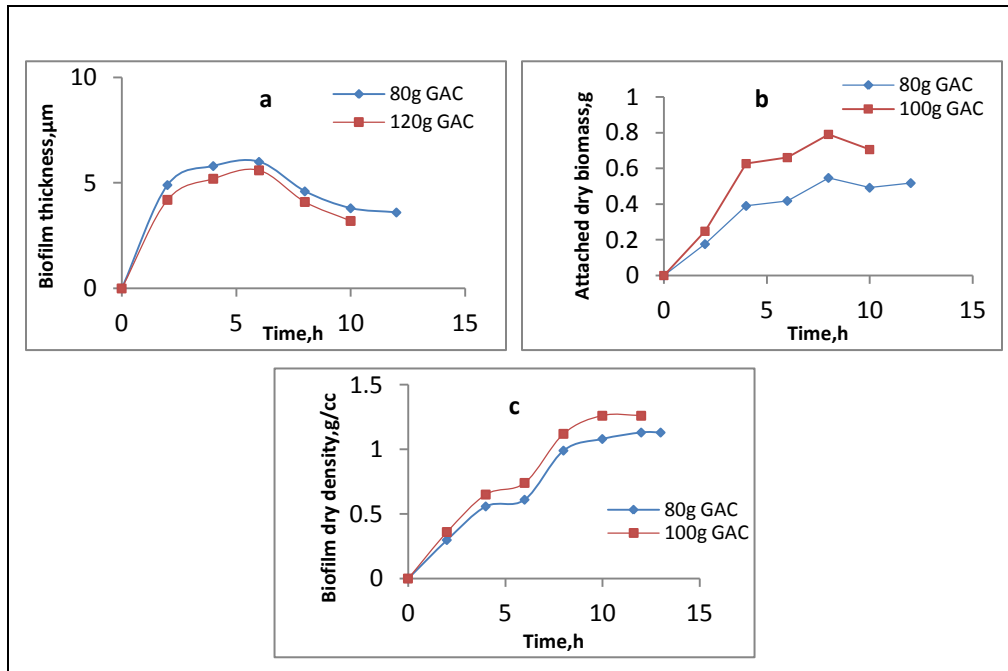


Fig.4.46 Effect of cell carrier loading on on physical characteristics of biofilm during the start-up (a) biofilm thickness (b) attached dry biomass, and (c) biofilm drydensity for the influent phenol concentration of 200ppm. Conditions: $f=0.08 \text{ s}^{-1}$; $A=3.5\text{cm}$; $D=0.33 \text{ h}^{-1}$.

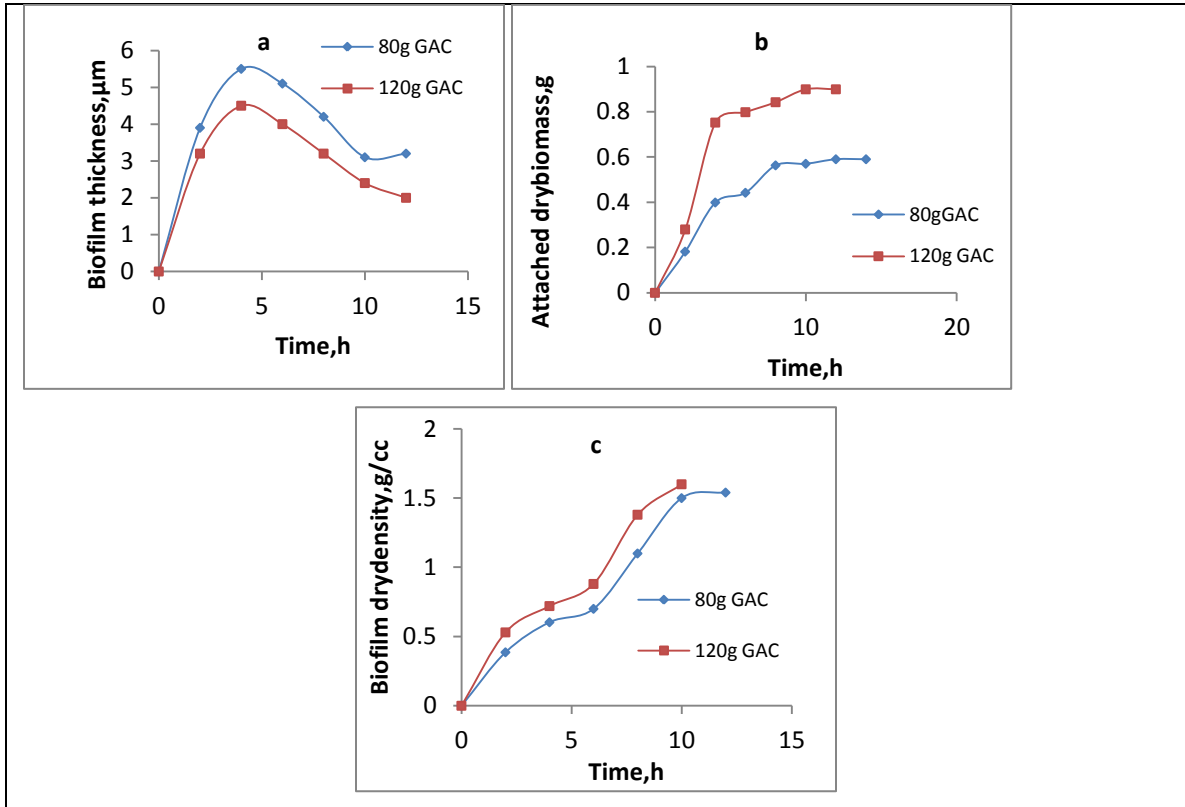


Fig.4.47 Effect of cell carrier loading on on physical characteristics of biofilm during the start-up (a) biofilm thickness (b) attached dry biomass, and (c) biofilm drydensity for the influent phenol concentration of 400 ppm. Conditions: $f=0.08 \text{ s}^{-1}$; $A=3.5 \text{ cm}$; $D=0.33 \text{ h}^{-1}$

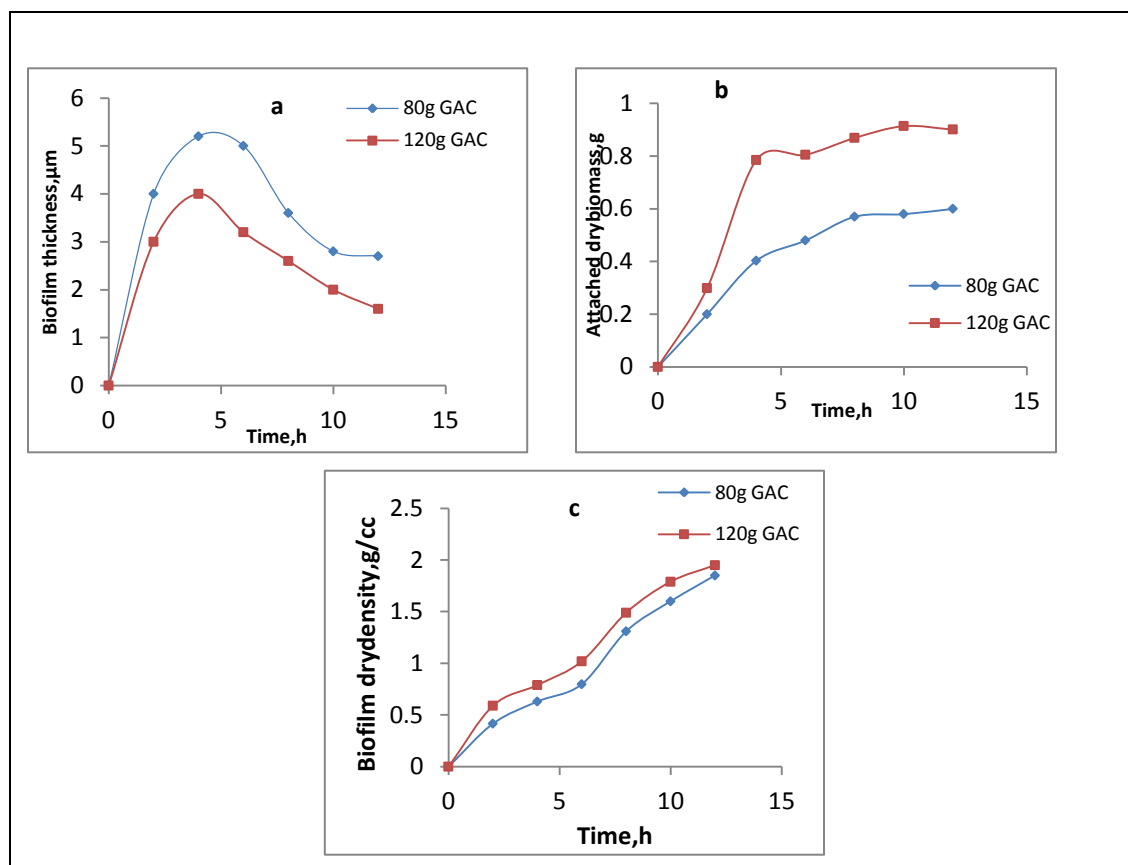


Fig.4.48 Effect of cell carrier loading on on physical characteristics of biofilm during the start-up (a) biofilm thickness (b) attached dry biomass, and (c) biofilm drydensity for the influent phenol concentration of 600ppm . Conditions: $f=0.08 \text{ s}^{-1}$; $A=3.5 \text{ cm}$; $D=0.33 \text{ h}^{-1}$.

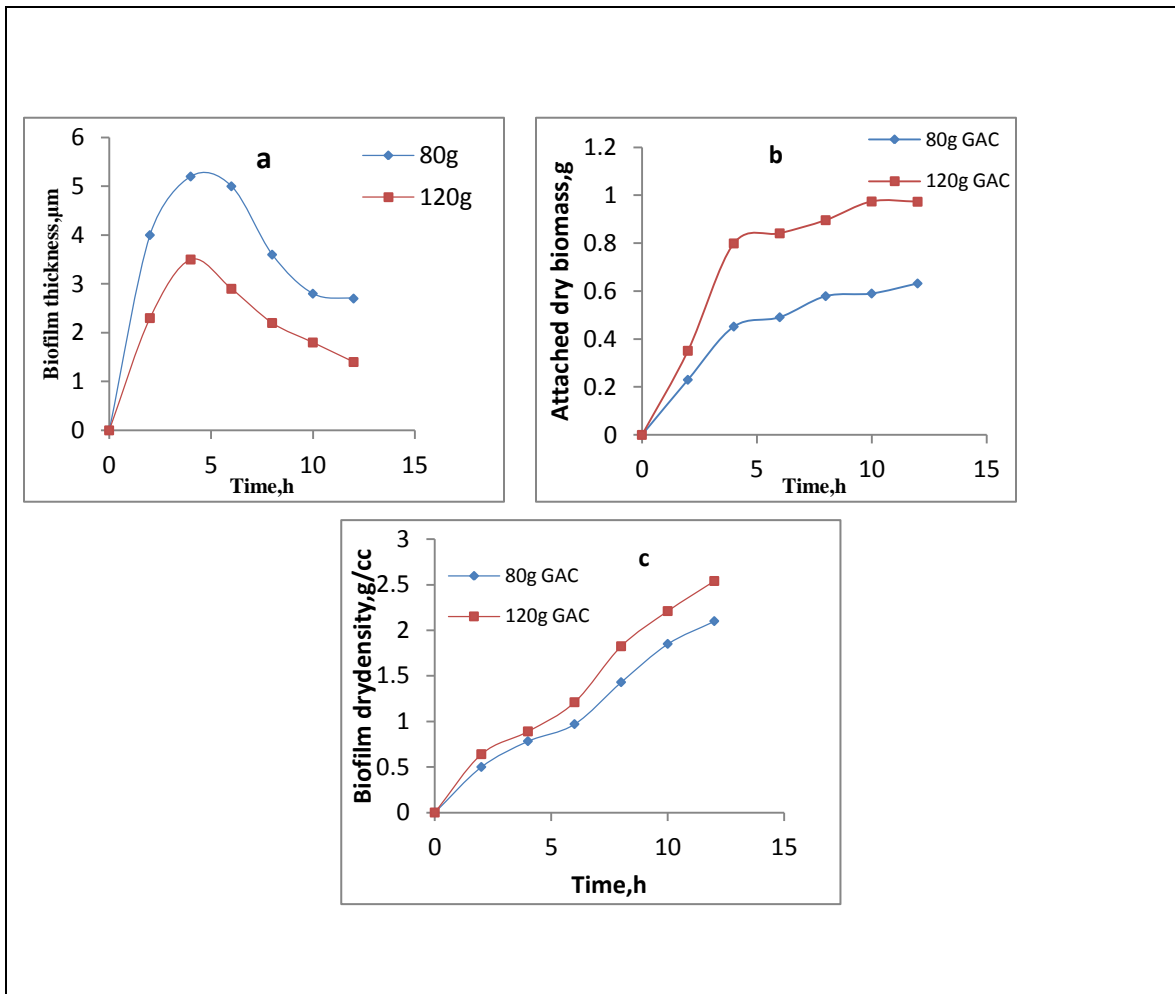


Fig.4.49 Effect of cell carrier loading on physical characteristics of biofilm during the start-up (a) biofilm thickness (b) attached dry biomass, and (c) biofilm drydensity for the influent phenol concentration of 800ppm. Conditions: $f=0.08 \text{ s}^{-1}$; $A=3.5 \text{ cm}$; $D=0.33 \text{ h}^{-1}$.

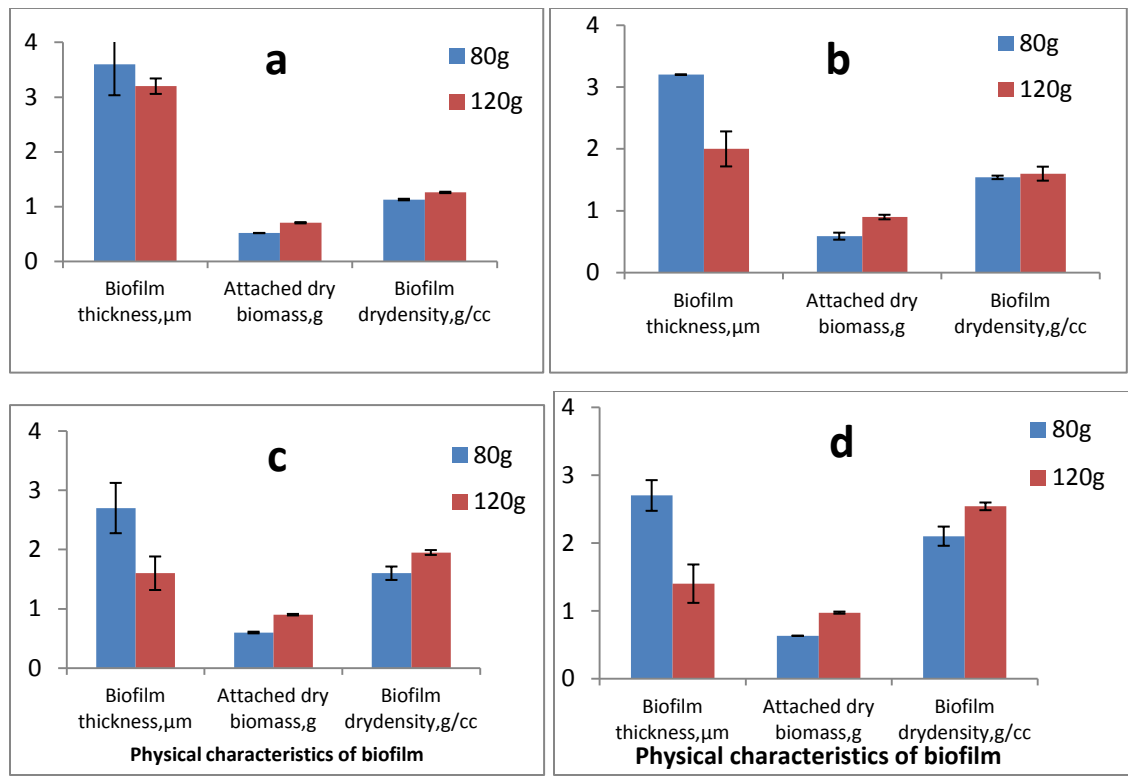


Fig.4.50 Effect of cell carrier loading on physical characteristics of biofilm at steady state for the influent phenol concentrations of (a) 200 (b) 400 (c) 600 and (d) 800ppm. Conditions: $f=0.08 \text{ s}^{-1}$; $A=3.5 \text{ cm}$; $D=0.33 \text{ h}^{-1}$.

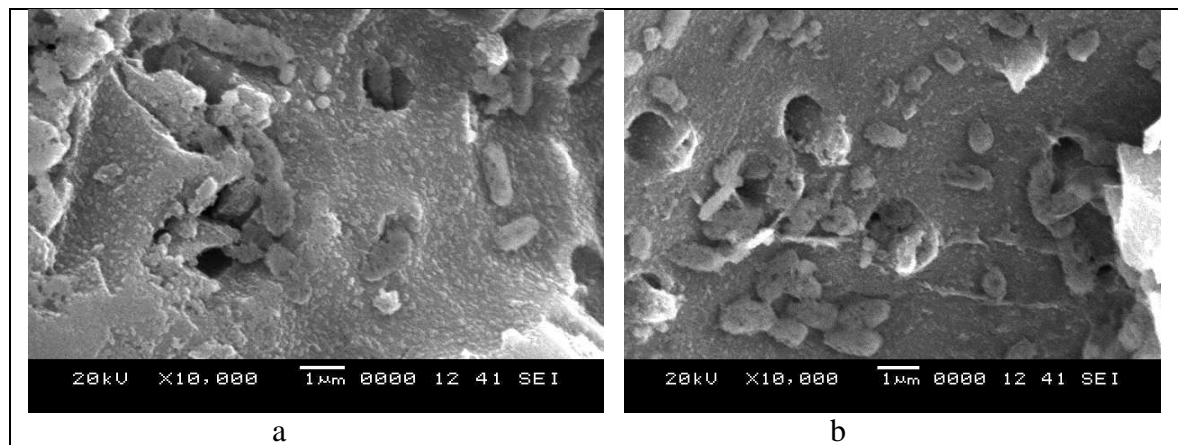


Fig.4.51 Effect of cell carrier loading on morphological characteristics of biofilm at steady state. (a) 80 g and (b)120g of GAC loading. Conditions: $f=0.08 \text{ s}^{-1}$; $A=3.5\text{cm}$; $D=0.33 \text{ h}^{-1}$; $C_i =200 \text{ ppm}$.

4.5 Effect of amplitude of pulsation on steady state and Start up performance of PPBR in terms of phenol biodegradation and biofilm characteristics at steady state and during strat-up.

As discussed in Section 4.3, amplitude of pulsation is one of the shear inducing operational variable in PPBR and the shear inducing parameters influence the performance of the bioreactor by controlling the mixing, mass transfer characteristics and the biofilm characteristics in the bioreactor . Thus, understanding the effect of amplitude of pulsation on biofilm characteristics may help in controlling the bioreactor performance.

The degradation of phenol and biofilm characteristics during the Start up and steady state was studied at various influent phenol concentrations of 200 ppm to 800 ppm under the conditions when the reactor was operated at a frequency of 0.08 s^{-1} and with cell carrier loading of 80g as bioparticles at a dilution rates of 0.33 h^{-1} and at various amplitude of pulsation of 3.5, 5.0, and 6.5cm.

4.5.1. Effect of amplitude of pulsation on phenol biodegradation at steady state and during Start up of PPBR.

Fig.4.52 (a) - (d) show the variation of effluent phenol concentration with time for different amplitudes of pulsation and at influent phenol concentrations of 200ppm, 400ppm, 600ppm and 800 ppm respectively. It may be observed from the figure that there is decrease in effluent phenol concentration with increase in amplitude. The biofilm formation phase is extended with the decrease in amplitude of pulsation. The increase in effluent phenol concentration after the beginning of GAC saturation phase is higher at lower amplitudes of pulsation and the phase of increase in effluent concentration also extends for a longer period. Further the concentration decreases for a longer period of time before the steady state is achieved. It indicates that at lower amplitude of 3.5 cm, the time taken for the development of biofilm on the GAC surface is higher. The time for biofilm formation decreases with the increase in amplitude. The overshoot in effluent phenol

concentration also increases with the increase in amplitude of pulsation. It shows that the adsorption remains the dominant phenol removal phenomena for a longer time during the start-up at lower amplitudes of pulsation. At lower amplitude of pulsation the mass transfer rate for phenol and oxygen are lower thus, the rate of growth of biomass is slower. Thus, the large portion of GAC particles remain uncovered with the biomass. The cells which are initially immobilized may be present as individual cells or as distinct colonies not covering the entire GAC surface. Owing to reduced availability of substrate and oxygen at lower amplitudes as compared to that at higher amplitude, the biofilm growth rate is lower and longer time is taken for the production of sufficient EPS and abundant biomass to form a biofilm. Thus, phenol removal mainly occurs by adsorption on GAC bare surface till the biofilm is formed covering the entire GAC surface. The decrease in phenol concentration at later phase before the attainment of steady state is an indication of biodegradation being the dominant removal mechanism and it takes longer time to achieve this phase if the amplitude is lower.

As shown in Fig.4.53 (a), there is increase in percentage degradation of phenol at steady state with increase in amplitude of pulsation. The increase in percentage degradation with increase in amplitude of pulsation is not very pronounced at lower influent phenol concentrations of 200 to 600 ppm. However, the percentage degradation increased by marginal extent from 98% to almost complete degradation as the amplitude was increased from 3.5 cm to 6.5 cm. The amplitude of pulsation shows a profound effect at higher influent phenol concentrations. However, as observed in Fig. 4.53(b) the start up time has decreased from 12 to 8 h with increase in amplitude of pulsation from 3.5 cm to 5 cm. However, further increase in amplitude of pulsation has not resulted in any change in the start-up time. As the amplitude was increased, the region of influence of turbulence caused by plate pulsation enhances leading to more intense mixing in the reactor. Thus, at the higher amplitudes which leads to high turbulence cause higher volumetric rate of movement of liquid in the reactor, thus enhancing the mixing of liquid in the reactor (Shetty *et al.* 2011). The higher turbulence and mixing intensities enhance the rate of mass transfer of phenol from the

bulk liquid phase to the cells by improved solid-liquid mass transfer characteristics (Shetty *et al.* 2011) and the oxygen mass transfer characteristics in the bioreactor (Shetty and Srinikethan 2010) thus leading to the higher rate of degradation of phenol. Amplitude increases the pulsation intensity ($A \cdot f$). Usmaan *et al.* (2009) have reported that the increase in pulsation intensity is a function of energy added to the column contents. The increase in energy content increases the mixing intensity. The oxygen mass transfer coefficient also increases with increasing pulsation intensity (Vasić *et al.* 2007).

Thus, enhanced mixing and mass transfer characteristics are brought about by increasing the amplitude leading to higher rate of phenol degradation. Higher rate of degradation results in reduced Start up time as the amplitude was increased. However, the amplitudes of 5 cm and above could facilitate to effectively overcome any mass transfer limitations in the bioreactor (Gomma and Taweel 2005; shetty *et al.* 2008), thus leading to almost complete degradation of phenol at all the influent phenol concentrations studied.

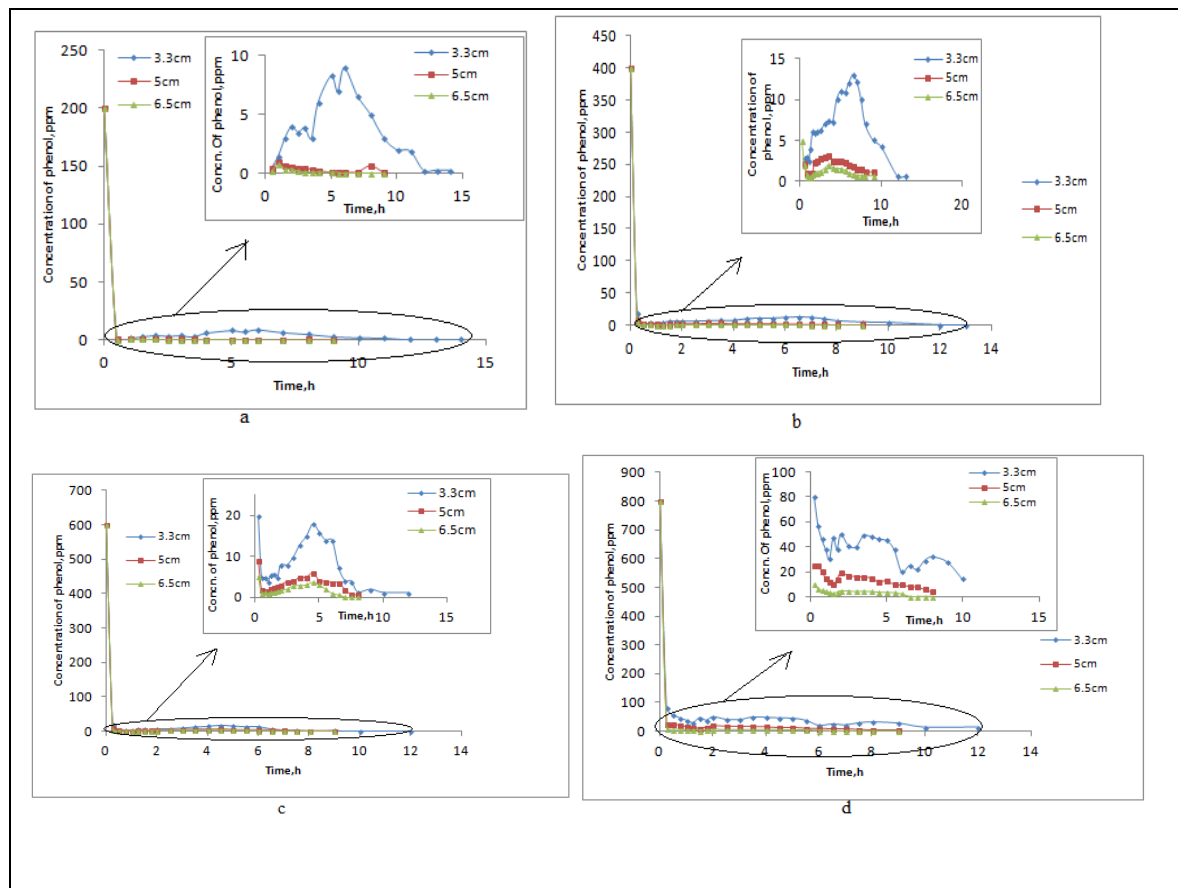


Fig.4.52 Effect of amplitude of pulsation on phenol degradation for influent phenol concentration of a) 200ppm b) 400ppm c) 600ppm and d) 800ppm. Conditions: $f = 0.08 \text{ s}^{-1}$; $D=0.33 \text{ h}^{-1}$; $S=80 \text{ g}$.

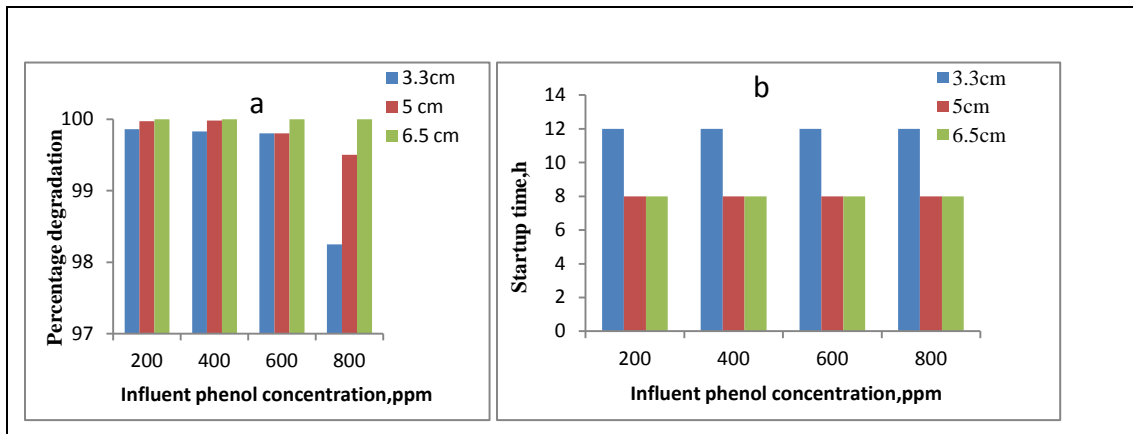


Fig.4.53 Effect of amplitude of pulsation on (a) percentage conversion of phenol (b) Start up time. Conditions: $f=0.08s^{-1}$; $S = 80 g$.

4.5.2 Effect of amplitude of pulsation on biofilm characteristics during start up and at steady state of PPBR.

The characteristics of biofilm in PPBR was studied during the Start up and at steady state under different influent phenol concentrations of 200, 400, 600 and 800 ppm, with frequency of pulsation of 0.08 s⁻¹, dilution rate of 0.33 h⁻¹, GAC loading of 80 g at different amplitude of pulsatio.

4.5.2.1. Effect of amplitude of pulsation on the chemical characteristics of the biofilm

The results of the effect of amplitude of pulsation on the composition of EPS produced during the start up period of the bioreactor are presented as time course variation of protein, carbohydrate and humic substance content of EPS in Fig.4.54,4.55, 4.56 and 4.57 for influent phenol concentrations of 200, 400, 600, and 800 ppm respectively. It is observed from these figures that, the protein, carbohydrate and humic substance content increased with time and then reached a steady value as discussed earlier in Section 4.1.1.1.

As seen in Fig.4.54 to Fig 4.57, the components of EPS increased with increase in amplitude from 3.5 cm to 5 cm during start-up. Similar trend was observed in Fig.4.58 (a),(b),(c) and (d) which shows the influence of amplitude on the protein, carbohydrate and humic substance content of EPS component at steady state. The increase in the amount of protein, carbohydrate and humic substance in EPS were of appreciable amount when amplitude was increased from 3.5 cm to 5 cm. The increase in EPS components with increase in amplitude from 3.5cm to 5 cm could be due to availability of more nutrients to the microorganisms caused by enhanced mixing of liquid in the bioreactor and better mass transfer rate from bulk of the fluid to the solid surface. As discussed in Section 4.1.1.1, enhanced protein content of EPS component would result in enhanced adhesion and cohesion of the cells in the biofilm and carbohydrate content provides structural integrity along with cohesion properties, whereas the humic substances also provide strength to the biofilm (Frolund 1995). However the increase in the quantity of EPS components with increase in amplitudes from 5 cm to 6.5 cm is not very significant in the present study. The mass transfer resistance would have reached to a negligible level for the amplitude of 5 cm, thus mass transfer rate no further remains as the rate limiting step in the process of phenol biodegradation and hence further increase in amplitude did not make much difference in the production of EPS component. The same trend is observed at the influent phenol concentrations of 400, 600, and 800 ppm.

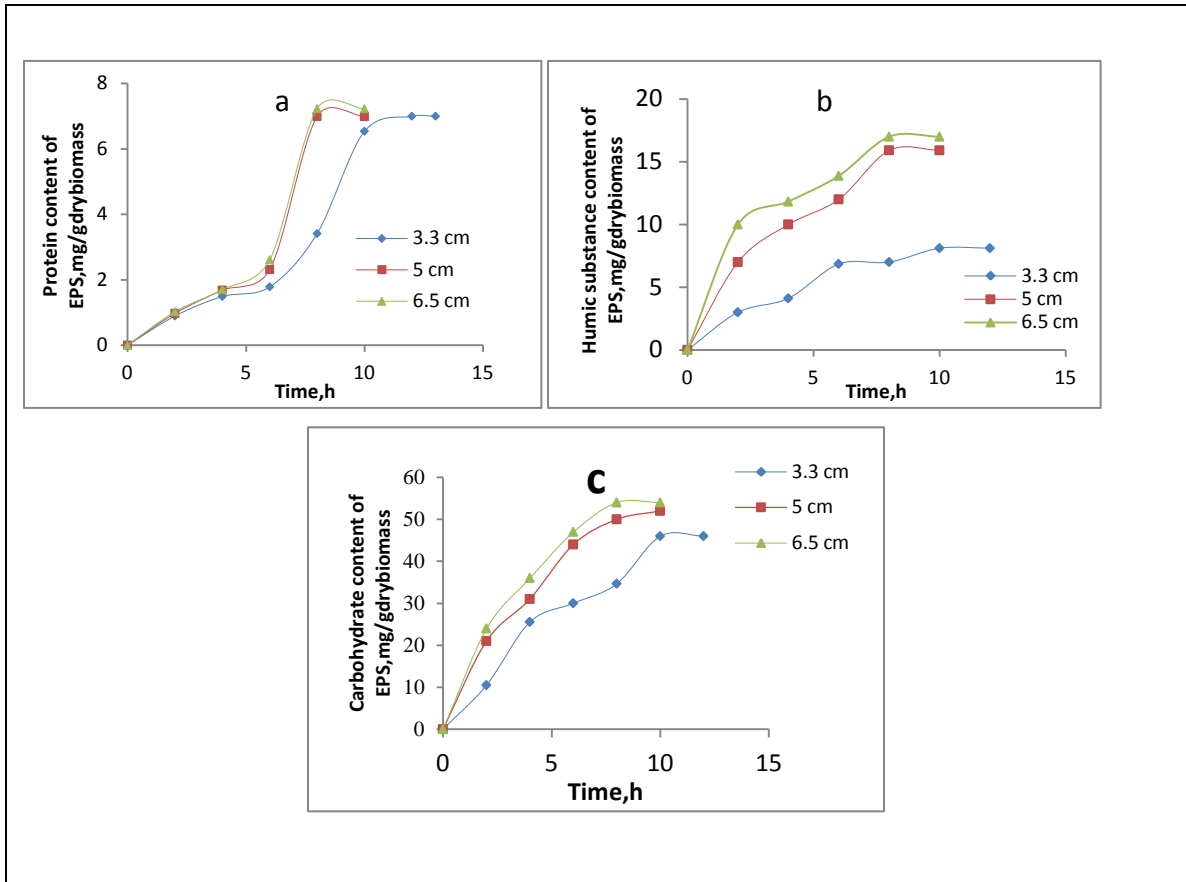


Fig.4.54 Effect of amplitude of pulsation on production of (a) Protein (b) Humic substance and (c) Carbohydrate contents of EPS during start up at influent phenol concentration of 200 ppm. Conditions: $f=0.08 \text{ s}^{-1}$; $D=0.33 \text{ h}^{-1}$; $S=80 \text{ g}$.

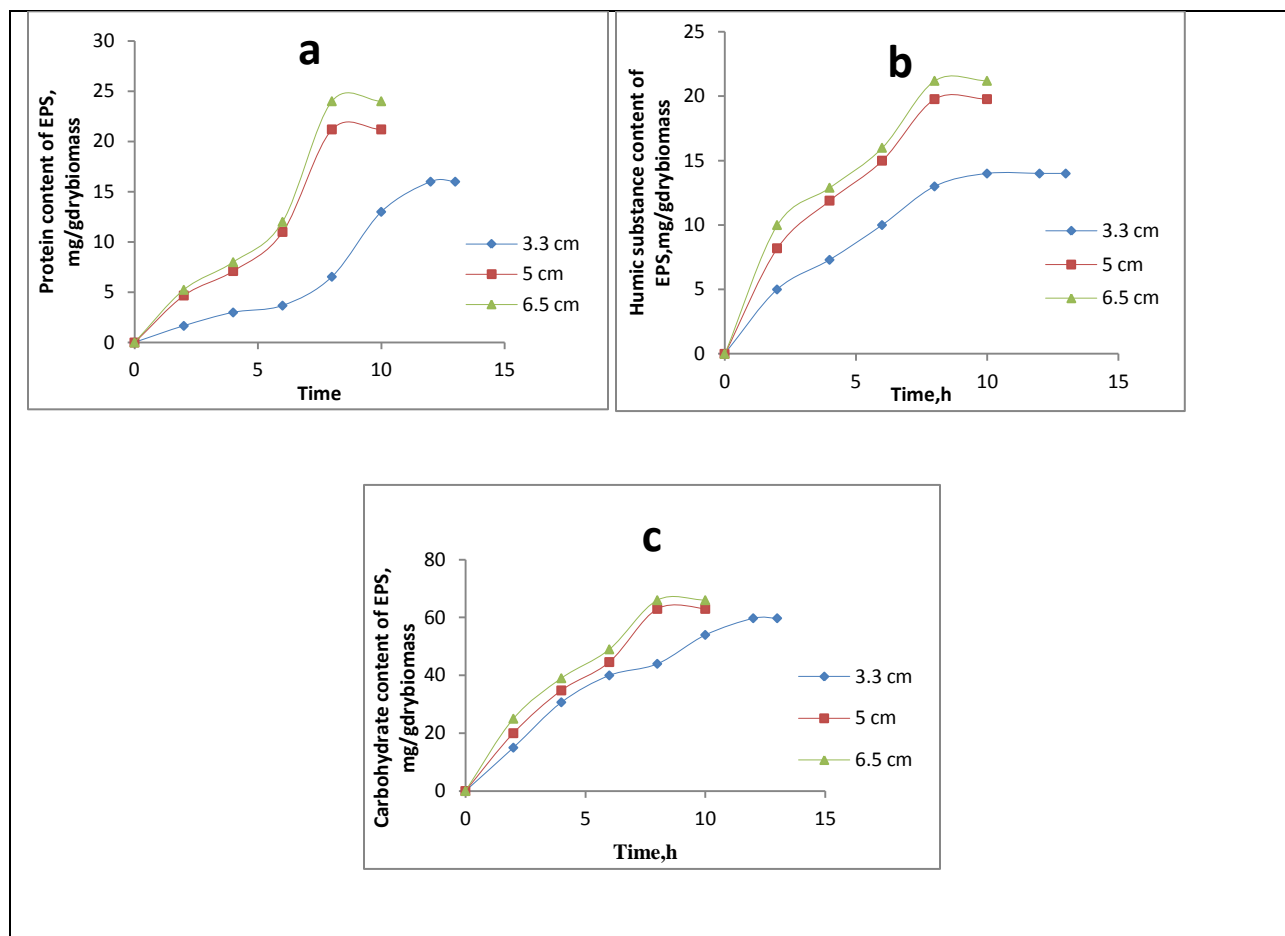


Fig.4.55 Effect of amplitudet of pulsation on production of (a) Protein (b) Humic substance and (c) Carbohydrate contents of EPS during start up at influent phenol concentration of 400 ppm. Conditions: $f=0.08 \text{ s}^{-1}$; $D=0.33 \text{ h}^{-1}$; $S=80 \text{ g}$.

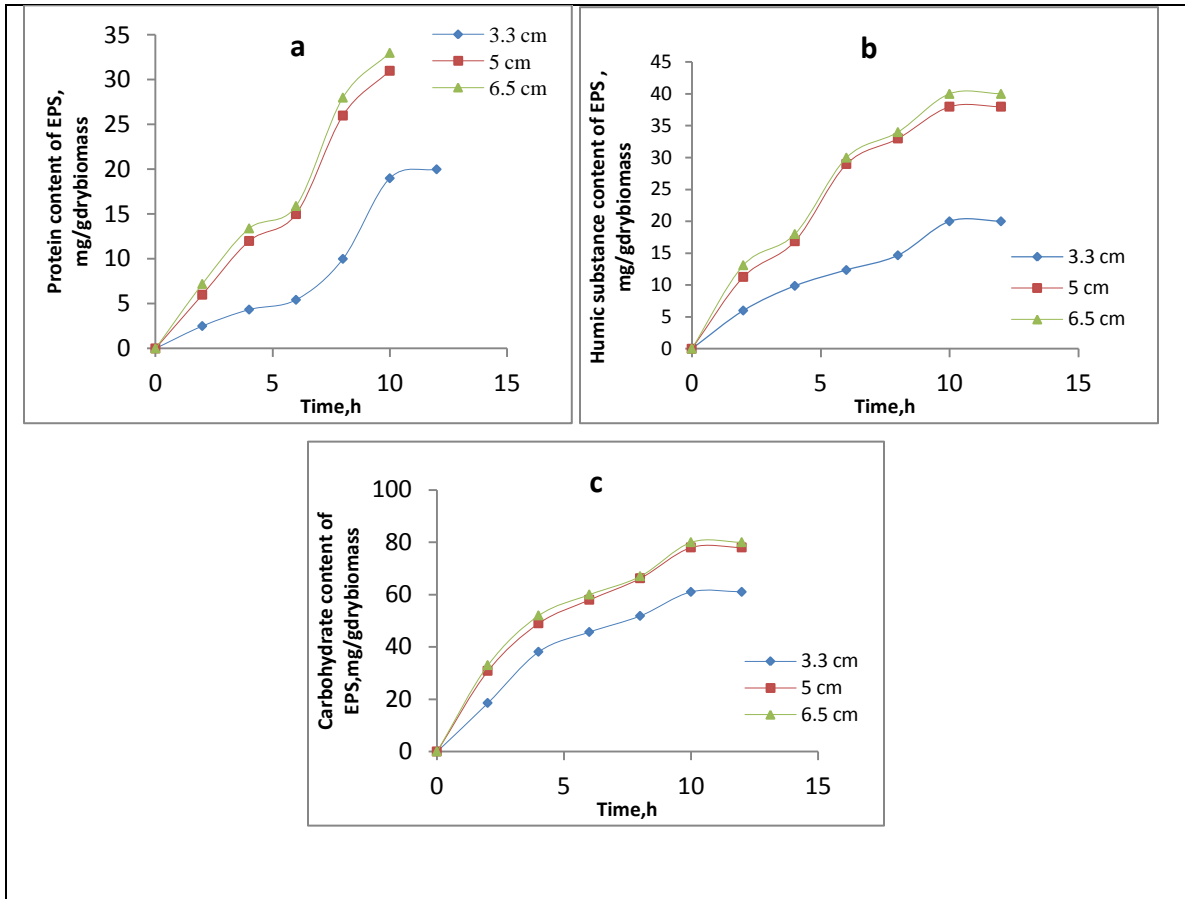


Fig.4.56. Effect of amplitude of pulsation on production of (a) Protein (b) Humic substance and (c) Carbohydrate contents of EPS during start up at influent phenol concentration of 600 ppm. Conditions: $f=0.08 \text{ s}^{-1}$; $D=0.33 \text{ h}^{-1}$; $S=80 \text{ g}$.

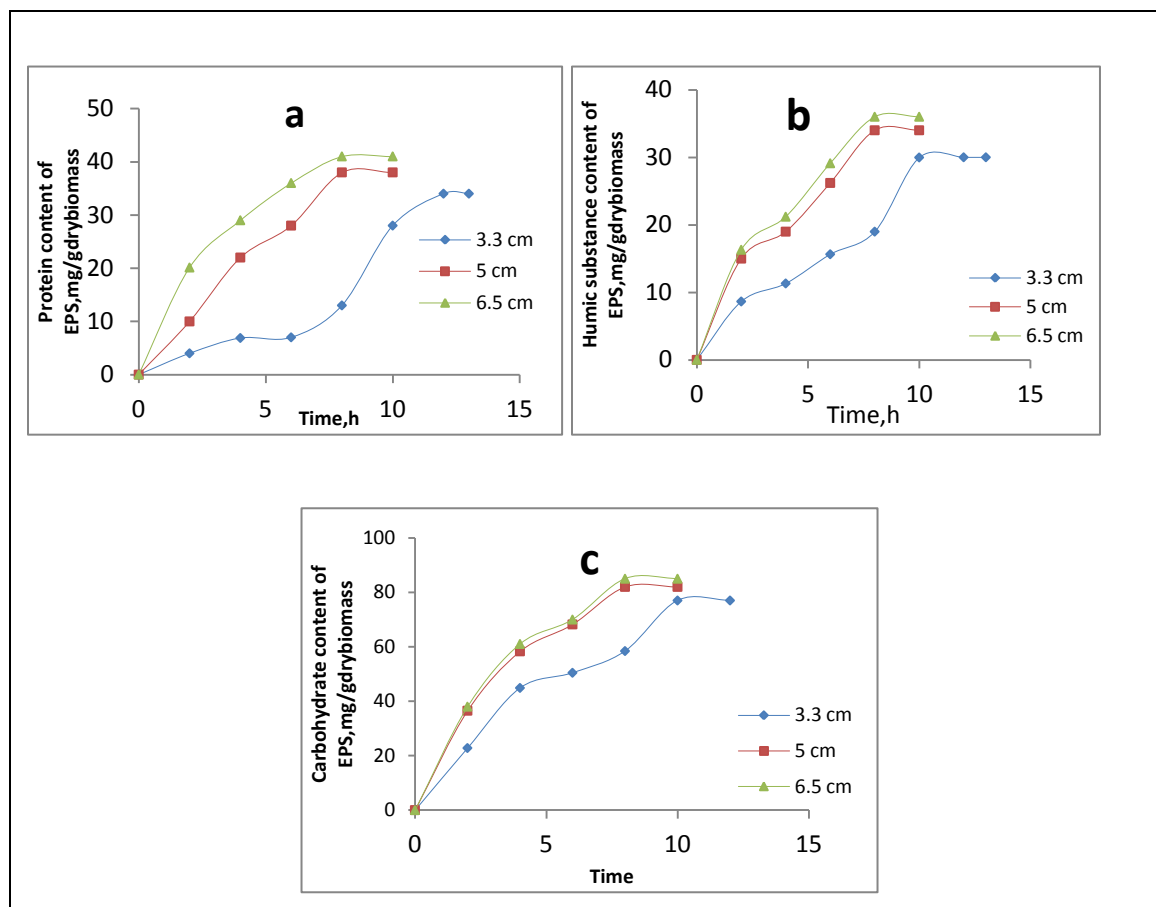


Fig.4.57. Effect of amplitude of pulsation on production of (a) Protein (b) Humic substance and (c) Carbohydrate contents of EPS during start up at influent phenol concentration of 800 ppm. Conditions: $f=0.08\text{ s}^{-1}$; $D=0.33\text{ h}^{-1}$; $S=80\text{ g}$.

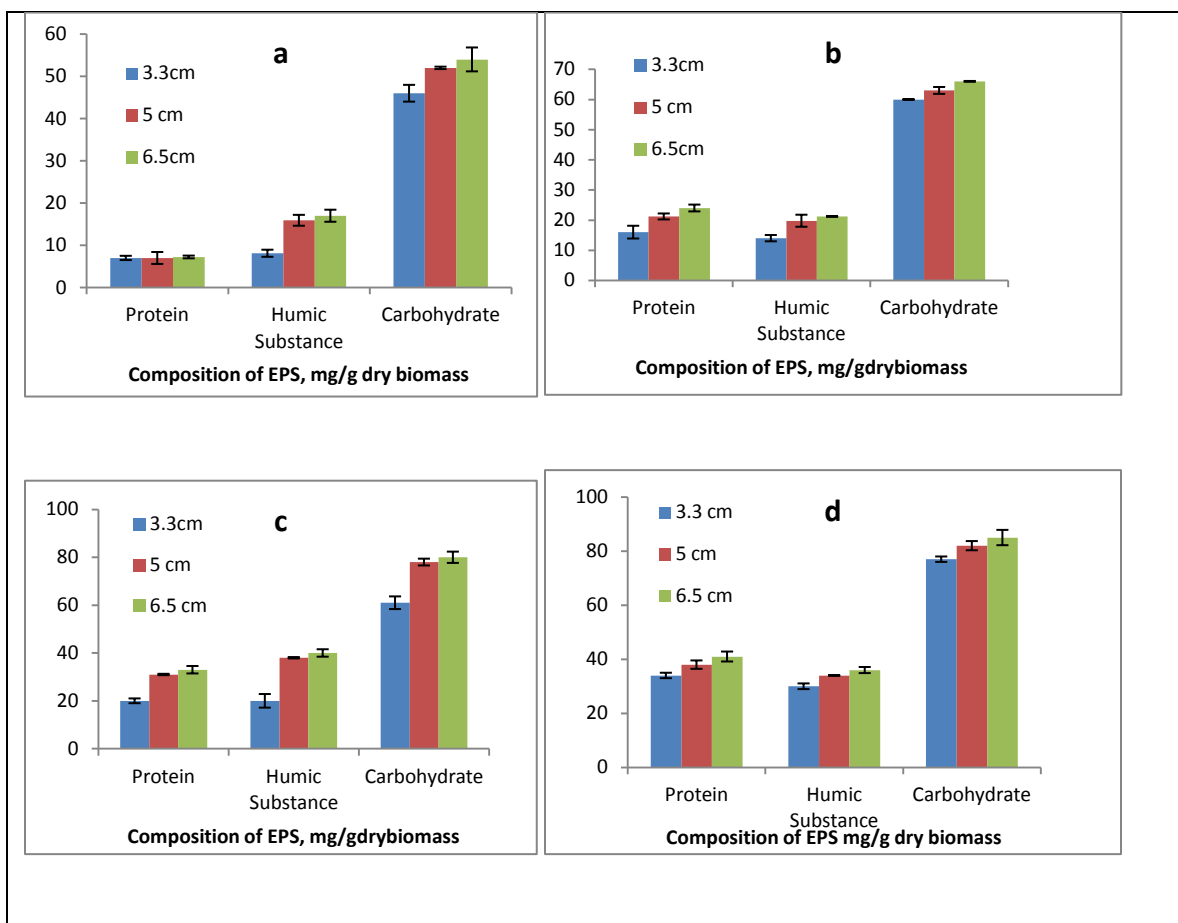


Fig 4.58 Effect of amplitude of pulsation on production of EPS components at steady state with influent phenol concentrations of a) 200 ppm b) 400 ppm c) 600 ppm and d) 800ppm. Conditions: $f = 0.08 \text{ s}^{-1}$; $D=0.33 \text{ h}^{-1}$; $S=80 \text{ g}$.

4.5.2.2. Effect of amplitude on biofilm physical characteristics

Fig.4.59 to 4.62 show the variation in biofilm thickness, attached dry biomass and biofilm dry density as a function of time during the start-up of the bioreactor at different amplitudes of pulsation with various influent phenol concentrations of 200, 400, 600 and 800 ppm respectively. The biofilm thickness, biomass dryweight and biofilm density increased with time owing to the formation of biofilm during the start-up.

As observed from Fig.4.59(a), the biofilm thickness increased when there is an

increase in amplitude from 3.5 to 5cm and remained almost same when the amplitude was increased from 5cm to 6.5 cm. When the reactor was operated at an amplitude of 3.5 cm, the availability of nutrients to the immobilized cells may be less owing to mass transfer limitations in the reactor, resulting in lower growth of microorganisms thus leading to lower biomass dryweight as observed in Fig.4.59(b), leading to thinner biofilm [Fig 4.59(a)]. When amplitude of pulsation was increased, mixing and mass transfer characteristics in the bioreactor improved eliminating the mass transfer limitations and leading to enhanced availability of nutrients, oxygen and phenol to the microbial cells present in biofilm matrix. This leads to higher growth rate leading to higher growth of biofilm [Fig.4.59(b)] and hence increase in thickness as shown in Fig.4.59 (a). However, the enhanced mixing intensity caused by increased amplitude appeared to provide no enhanced shear effects on the biofilm as revealed by increased biofilm thickness with increase in amplitude. However, as observed from Fig.4.59(a) and (b) the change in biofilm thickness and the dry biomass weight with increase in amplitude from 5cm to 6.5 cm is marginal owing to absence of mass transfer limitation for the transfer of nutrients to the surface of biofilm at amplitude ≥ 5 cm as explained earlier in Section 4.5.1.1. As observed from Fig.4.59(c), there is an increase in biofilm dry density when the amplitude was increased from 3.5 cm to 5cm and with further increase in amplitude to 6.5cm, the density change seems to be negligible. The increase in biofilm dry density indicates compaction of biofilm that would occur owing to enhanced EPS component production with increased amplitude. The increase in amplitude may provide dual fold effect of (i) High EPS component production in response to higher shear effects caused by higher mixing intensities (ii) High EPS production owing to higher rate of mass transfer and thus the phenol consumption to produce more of EPS along with cell growth. As observed in Fig.4.58(a),(b),(c) and (d), the protein, carbohydrate and humic substance content in EPS has increased with amplitude. These components of EPS contribute to strong cohesion of cells in the biofilm causing compaction of biofilm.

Fig.4.63 shows the physical characteristics of biofilm at steady state. The enhanced availability of nutrients and increase in mass transfer flux leading to penetration

of phenol deep in to the biofilm may also be resulting in denser biofilm at higher amplitudes. Figure 4.64 shows morphological characteristics of biofilm with different amplitude of pulsation. The SEM images indicate that the biofilm becomes more denser and compact with the increase in amplitude. Large number of loose single cells uncovered by EPS matrix is observed in the biofilm formed at amplitude of 3.5 cm. Small and deeper micropores are visible in the biofilm formed at 3.5 cm. However, as the amplitude was increased the visibility of single cells is not observed. The biofilm becomes more compact, smoother and denser with a the increase in amplitude. The cells seem to be bound tightly by the EPS matrix. The biofilm is very compact and dense at the highest amplitude of 6.5cm. A few wider but shallow crevices are observed on the biofilm formed at 5 cm rather than the micropores. These crevices may have resulted due to biofilm shear effect at higher amplitude. However, the biofilm formed at 6.5 cm amplitude is very smooth, compact with dense EPS matrix without the presence of any micropores or crevices. At very high amplitude, the shear effect due to high pulsing intensity results in the production of larger quantity of EPS and cells adhere among themselves tightly to withstand the shear, thus compacting themselves in the biofilm matrix, thus resulting in denser and compact biofilm. The pores in the biofilm for the diffusion of phenol may be very small and nanosized at high amplitudes.

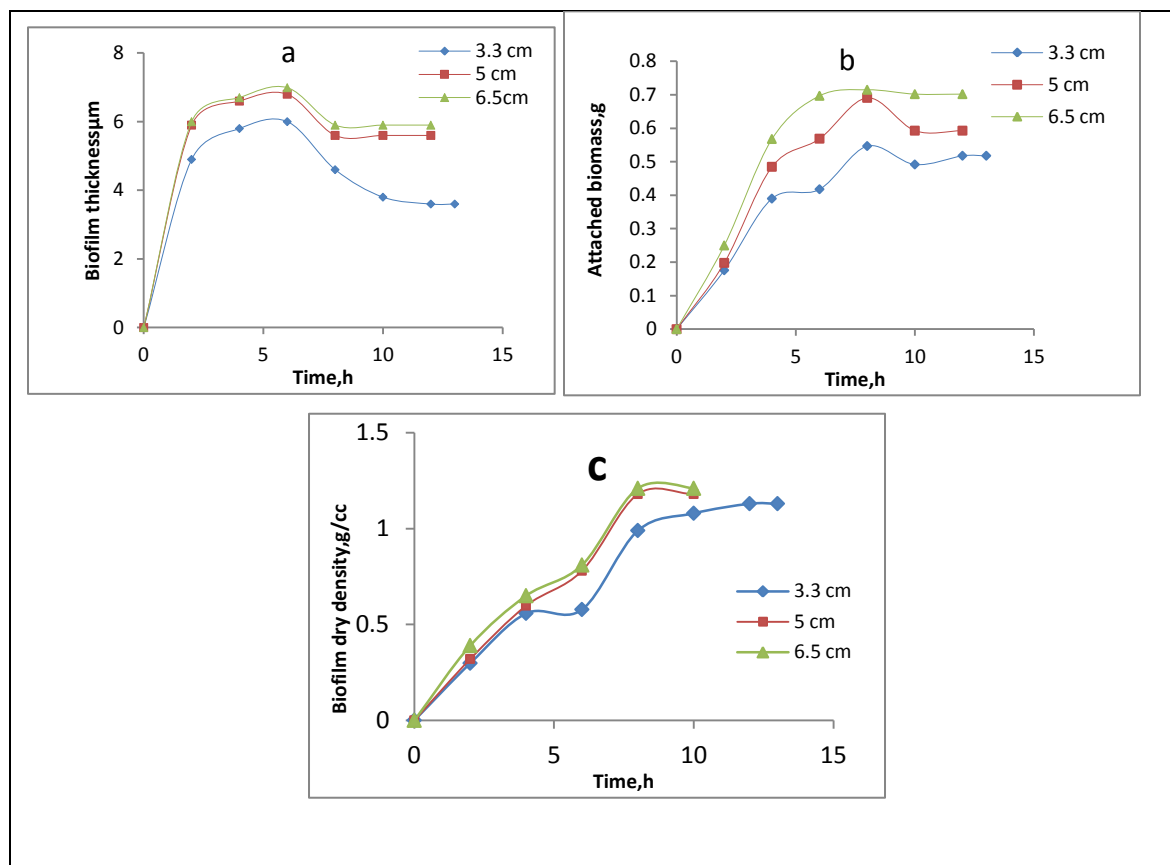


Fig. 4.59 Effect of amplitude of pulsation on physical characteristics of the biofilm during start-up a) biofilm thickness b) attached dry biomass and c) biofilm dry density for 200 ppm of influent phenol concentration . Conditions: $f=0.08\text{s}^{-1}$; $D=0.33\text{h}^{-1}$; $S=80\text{g}$.

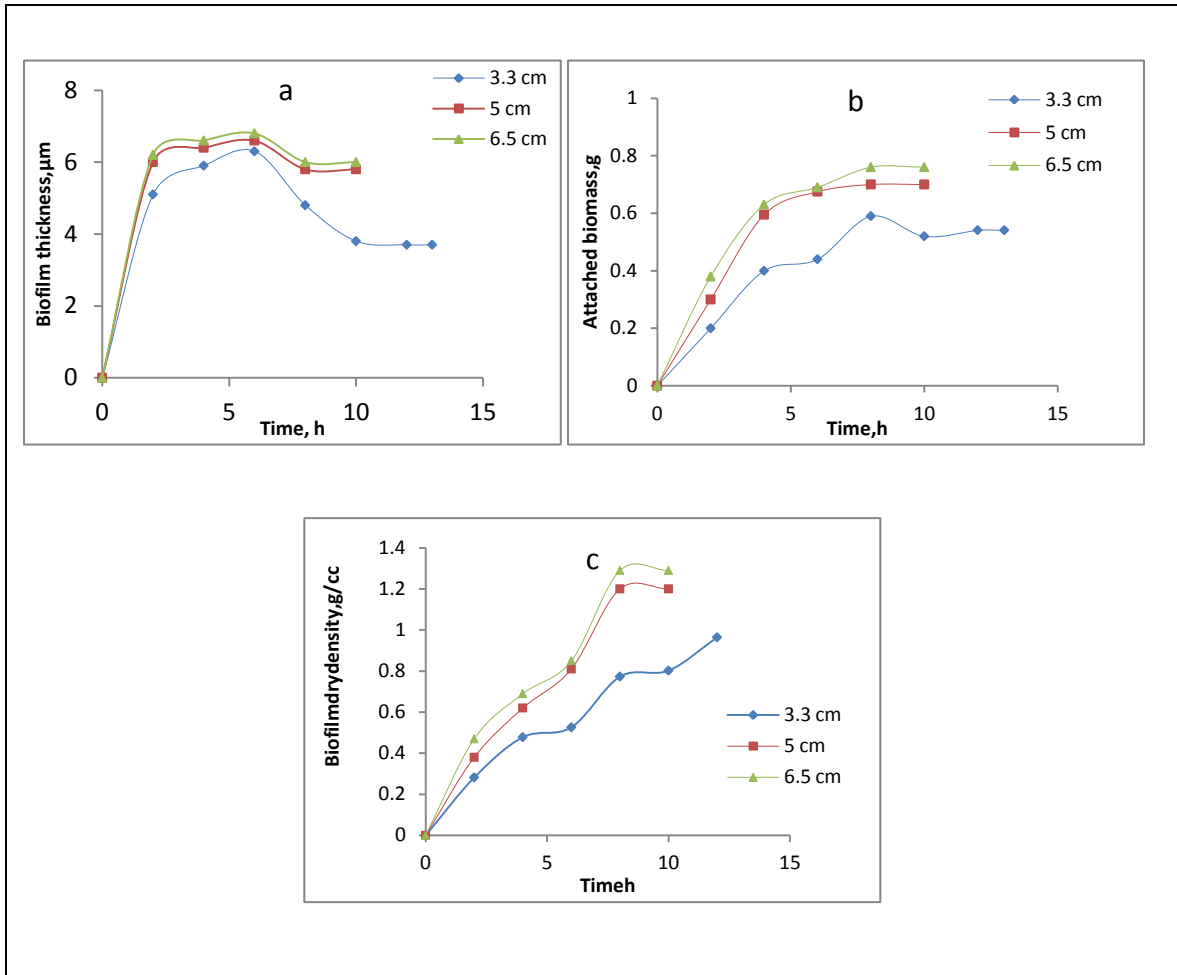


Fig. 4.60 Effect of amplitude of pulsation on physical characteristics of the biofilm during start-up a) biofilm thickness b) attached dry biomass and c) biofilm dry density for 400ppm of influent phenol concentration. Conditions: $f=0.08 \text{ s}^{-1}$; $D=0.33 \text{ h}^{-1}$; $S=80 \text{ g}$.

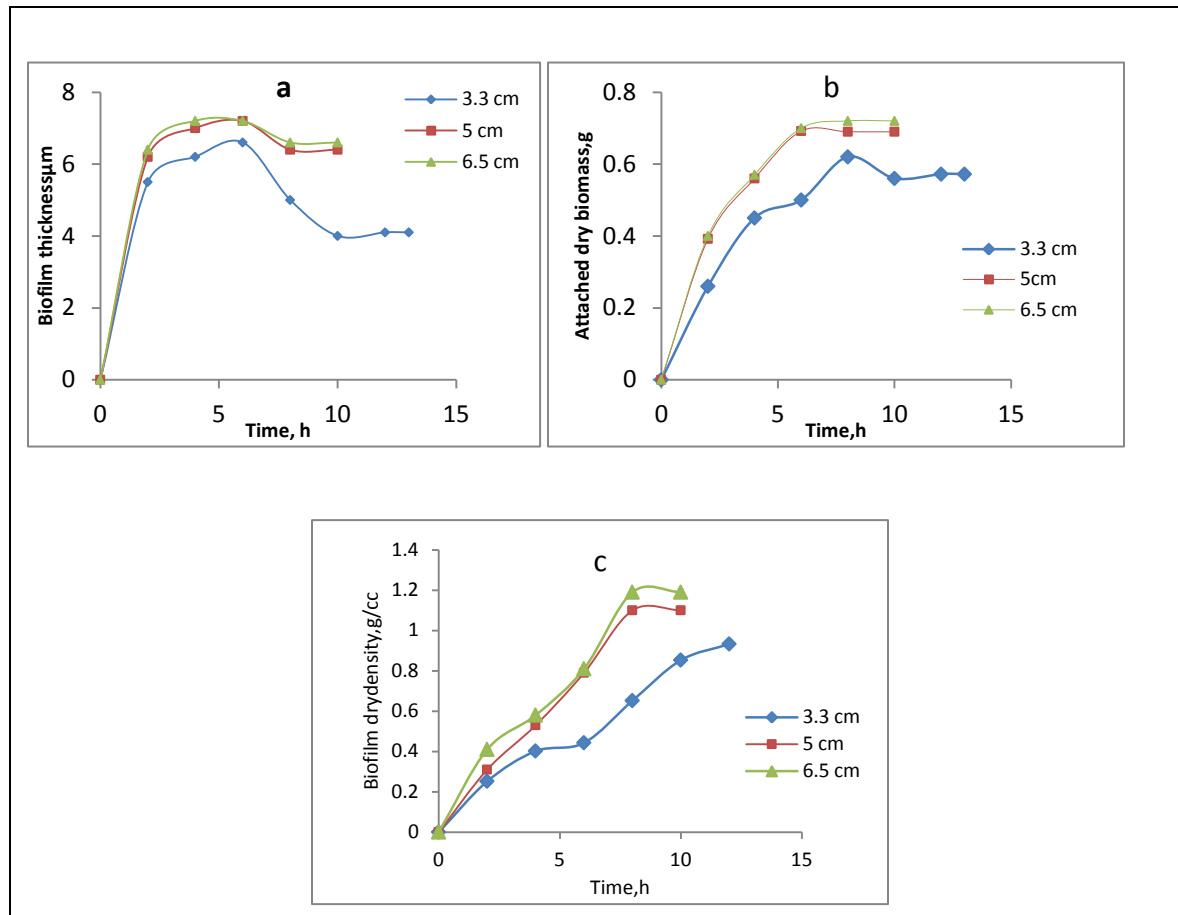


Fig. 4.61 Effect of amplitude of pulsation on physical characteristics of the biofilm during start-up a) biofilm thickness b) attached dry biomass and c) biofilm dry density for 600 ppm of influent phenol concentration . Conditions: $f=0.08 \text{ s}^{-1}$; $D=0.33 \text{ h}^{-1}$; $S=80 \text{ g}$.

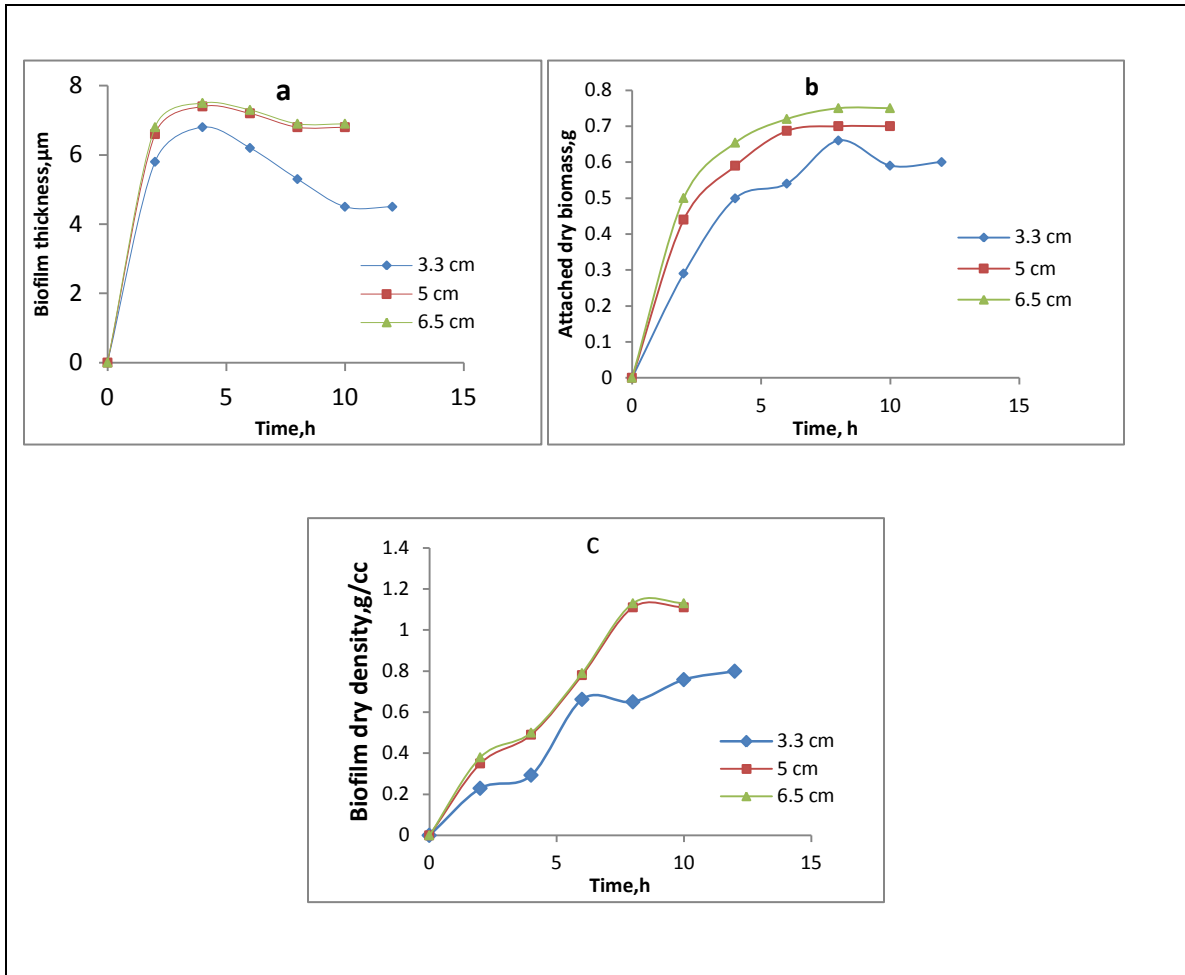


Fig. 4.62 Effect of amplitude of pulsation on physical characteristics of the biofilm during start-up a) biofilm thickness b) attached dry biomass and c) biofilm dry density for 800 ppm of influent phenol concentration . Conditions: $f=0.08 \text{ s}^{-1}$; $D=0.33 \text{ h}^{-1}$; $S=80 \text{ g}$.

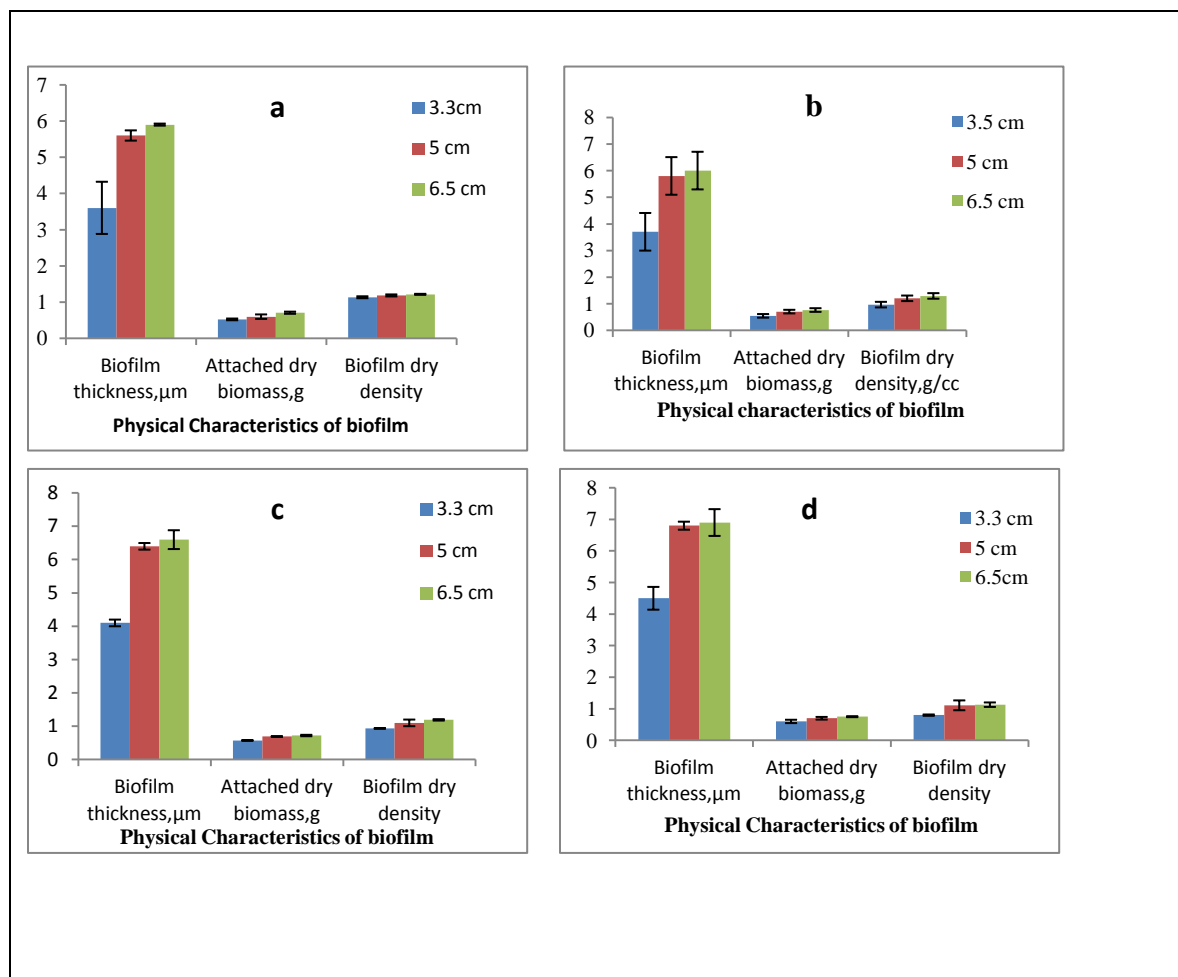


Fig.4. 63 Effect of amplitude of pulsation on physical characteristics of biofilm at steady state for various influent phenol concentration of a)200 ppm b) 400ppm c) 600ppm and d)800ppm. Conditions: $f=0.08 \text{ s}^{-1}$; $D=0.33 \text{ h}^{-1}$; $S=80 \text{ g}$.

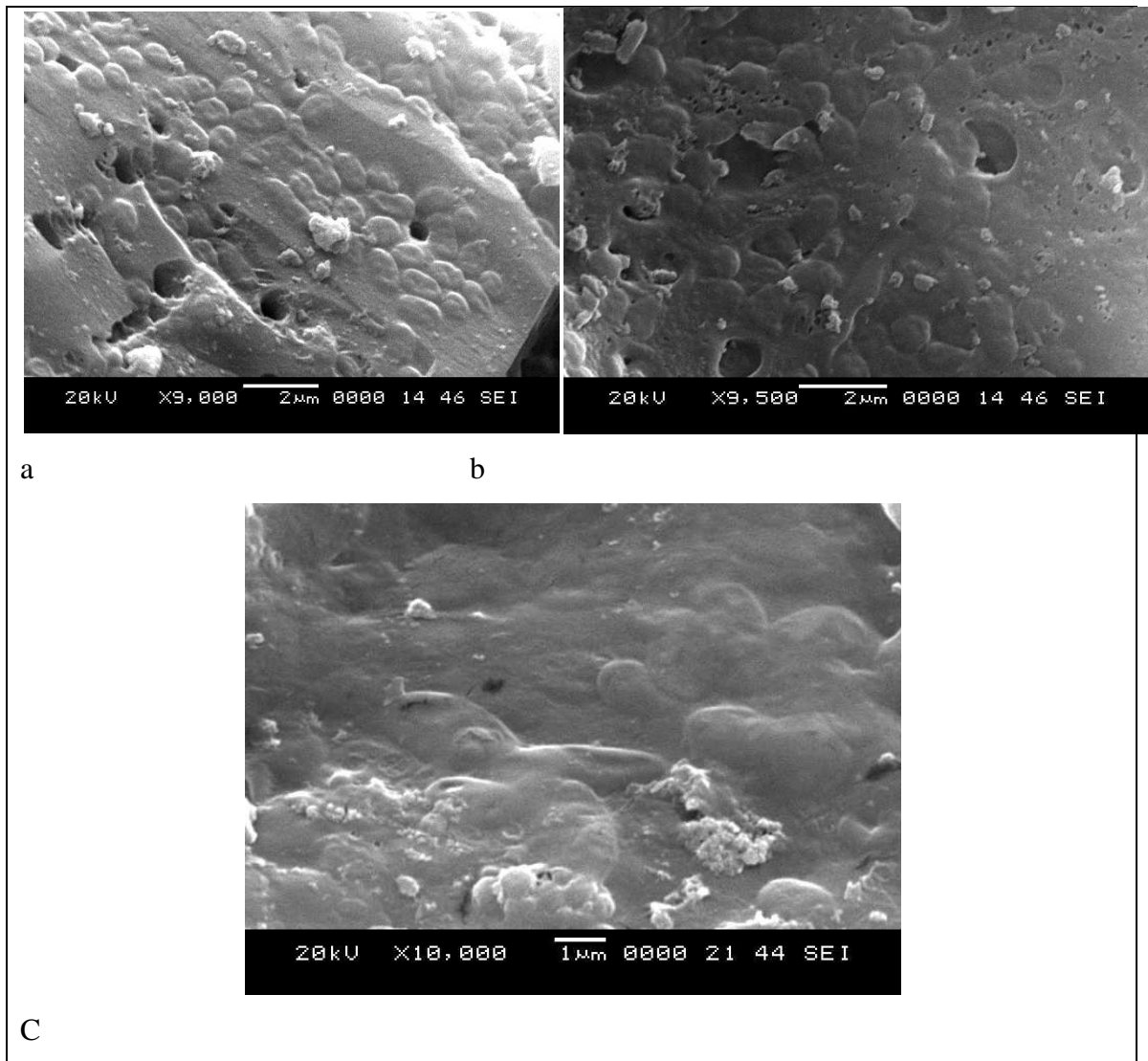


Fig.4.64 Effect of amplitude of pulsation on morphological characteristics of biofilm at steady state .(a) 3.5cm (b) 5cm and (c) 6.5 cm. Conditions:Influent phenol concentration =200 ppm $f=0.08\text{ s}^{-1}$; $D=0.33\text{ h}^{-1}$; $S=80\text{ g}$.

The studies on the effect of amplitude of pulsation showed that amplitude of pulsation greatly affects the start-up and steady state characteristics of the biofilm and the performance of PPBR in terms of phenol biodegradation. Almost complete degradation of 200 to 800 ppm influent phenol could be achieved at amplitudes of 5 cm or larger. These studies showed that the amplitude of pulsation has a profound effect on phenol

biodegradation and biofilm characteristics upto 5 cm amplitude. But at amplitude of pulsation of greater than 5 cm the influence of amplitude was marginal indicating that the mass transfer limitations in PPBR are completely overcome at amplitudes of 5 cm or greater. However, the effect of amplitude was profound at influent phenol concentration of 800 ppm.

CHAPTER 5

MODELLING OF BIOFILM CHARACTERISTICS

Biological systems are highly nonlinear in nature and are very complex. In order to understand the organization and function of microorganisms in biofilms better, a variety of models that capture the knowledge of biofilm systems have been developed over the last three decades (Klapper and Dockery 2010; Wanner and Gujer 1986; Chen *et al.* 1989; Horn and Lackner 2014). Such models represent a biofilm system by considering the physico-chemical phenomena such as the mechanisms of transport and shear, the mechanical strength in addition to the biochemical and environmental aspects of the microorganisms in biofilms. Thus, modeling of biofilm systems is a multidisciplinary effort (Horn and Lackner 2014). The mass transfer and detachment mechanisms in biofilms can be modeled separately with the available modeling tools but the situation in a full scale biofilm reactor cannot be predicted easily because the biofilm, the reactor geometry, carrier geometry and the surface characteristics has to be considered collectively. Owing to the non availability or partial availability of necessary data for the reactor model, the accurate predictions are difficult. Measurement of the necessary parameters in the model continues to be a challenging task and thus difficulties in model simulation and accurate predictions arise. To predict the performance of any bioreactor in terms of substrate conversion, mechanistic (theoretical) models such as reaction–diffusion models are used. However, solution of these mechanistic models require data on biofilm characteristics such as biofilm density, thickness etc. Knowledge on EPS composition may further improve the predictions from mechanistic models. However, determination of biofilm characteristics by using mechanistic models is a challenging task. Rittmann and McCarty (1980) have computed the steady-state-biofilm thickness by equating the available and maintenance energy rates. The model did not consider biomass losses due to sloughing or exchange with the bulk liquid and thus they cautioned that the model may overestimate the biofilm mass. They also reported that lack of knowledge

on biofilm dynamics or changes in bacterial density with growth is a disadvantage in modelling the biofilm systems. Rao *et al.* (2010) have hypothesized that the biofilm is composed of a static and a variable portion and the thickness of the variable portion was assumed to increase with the organic loading rate and decrease with the hydraulic loading rate. Thus, they postulated a linear regression model and estimated the coefficients of the model from the experimental data for packed bed reactor with gravel stones and Raschig ring packings. The coefficients for the model varied with the carrier material indicating the dependency of the biofilm thickness on the carrier characteristics. Kumar and Venkateswarulu (2012) adopted the model proposed by Rao *et al.* (2010) to predict the biofilm thickness in a fixed bed reactor with Raschig rings/gravel stones as the carrier material. These models however, do not take into account the detachment conditions and thus linear dependency is often questionable in cases where the detachment forces are strong. Very limited models on predicting the biofilm characteristics have been reported in literature. The characteristics of biofilm such as biofilm thickness, density, biomass dry weight and the EPS composition govern the bioreactor performance and their values are in turn dependent on the hydraulic loading, substrate loading and shear effects in the reactor. Development of mathematical models to predict the bioreactor performance and to facilitate the design requires the data on the biofilm characteristics. Most often these values are obtained from the experiments and used directly in the model (Wang *et al.* 2011; Livingston *et al.* 1989; Tang and Fan 1987, Shetty *et al.* 2011) and often constant values are used owing to nonavailability of the models to predict the biofilm characteristics in bioreactors.

Researchers have suggested hybrid models where biofilm characteristics under different operating conditions of the bioreactor may be predicted using black box models developed from pilot plant or lab scale experimental data. Hong (1998) has used a hybrid model to predict the performance of three phase fluidized bed biofilm reactor, wherein he used neuro fuzzy model to predict the biofilm thickness and density and coupled it with the reaction –diffusion model. He allowed biofilm thickness and density to vary with biofilm growth in the model to simulate the biofilm reactor performance. Artificial neural

network (ANN) techniques are recently being used as black box modelling tools for many chemical and biochemical processes. The main advantages of ANNs in process modelling are that, it can be used to model complex nonlinear relationships with limited prior knowledge of the process and it has the ability to infer the output for an unknown combination of input variables.

5.1. Artificial Neural Networks (ANN)

Artificial Neural network is a machine learning approach and is designed to function the way in which human brain functions. ANN consists of massively parallel and highly interconnected, simple processing units (neurons). It resembles brain in two ways (i) acquirement of knowledge from the environment through learning process and (ii) interneuron connection strengths that are known as synaptic weights used to store the acquired data. The procedure used for learning is called learning algorithm where synaptic weights are modified into more orderly fashion to attain a desired objective (Simon Haykin 2009). ANN proves useful due to its ability to deal efficiently with imprecise, noisy and highly complex nonlinear systems (Rene *et al.* 2008). Artificial neural network is used for solving engineering problems. They are highly adaptive in nature and hence can adapt to changes in the data and learn input signal characteristics.

A basic neural network structure consists of three layers namely input, hidden and output layer. The computation nodes of hidden layer are called hidden neurons. These hidden neurons intervene between external input and the network output in some useful manner. Higher number of hidden neurons extracts higher-order statistics from its input. Fig. 5.1 shows a typical architecture of a feed forward network with one hidden layer and one output layer. A neuron is considered to be an information processing unit during the operation of a neural network. The number of input variables and desired output correspond to number of neuron in input and the output layers respectively.

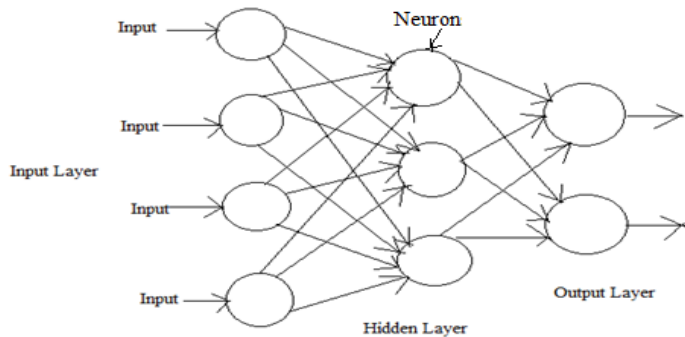
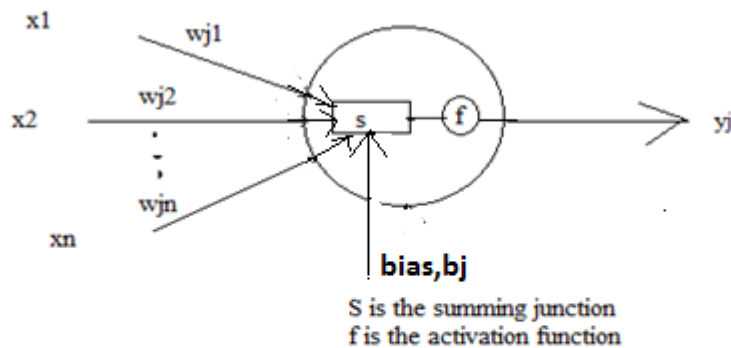


Fig. 5.1 Architecture of feed forward network.

The processed information passes from input neurons to output neurons via hidden neurons. Fig. 5.2 is the block diagram representing a neuron model which is considered for developing neural network systems. A set of synapses (connecting links) connects the neurons and each synapses is characterized by its own weight. These weights of synapses may include in the range of positive as well as negative values.



x_1, x_2, \dots, x_n are the output from the neuron in the preceding layer
 $w_{j1}, w_{j2}, \dots, w_{jn}$ are the weights of the synapses connecting neuron N_j to the preceding layer neurons
 y_j is the output from neuron N_j

Figure 5.2. Neuron model

Neuron processes the information as follows. The output from the summing junction is S_j and is given by Eq 5.1.

$$S_j = \sum_{i=1}^n W_{ji} x_i + b_j \quad \dots\dots\dots 5.1$$

The output y_j from the neuron is obtained through the activation function and is given by Eq 5.2.

$$y_j = f(S_j) \quad \dots\dots\dots 5.2$$

The activation functions used in neurons are generally Tan-sigmoid, log-sigmoid or linear. ANN has inherent learning capability that deals with noisy, imprecise and highly complex nonlinear data and the ability to process parallelly. The trained neural network can predict the output data for any given new set of inputs. The feedforward neural networks (FNNs) are the one most commonly used type that are called as multilayer perceptions with back propagation learning algorithm (Balan *et al.* 1999).

The input to the neural network is passed through the complete network by linear connection and transformation may be linear or nonlinear. Suitable algorithm is used to train the network with the given data by adjusting the connecting weights. Training may be of the type supervised learning or non-supervised learning. In the former, the target output will be provided during training, whereas in non-supervised learning no information is available on output or target value. Training with supervised learning targets to minimize the mean square error between the output from the network and the desired value (Shetty *et al.* 2011). Artificial neural network models have been developed by several researchers for different biotechnological applications as these are generally non-linear in nature. ANN models have been developed for batch Cr (VI) reduction by using immobilized cells of an isolated chromium resistant bacteria (Shetty *et al.* 2012), batch phenol biodegradation using suspended cells of microbial consortium

(Perpetuo *et al.* 2012), for the development of optimized complex medium for phenol degradation using *Pseudomonas pictorum* (NICM 2074) in batch reactor (Annadurai and Lee 2007), to predict the effect of glucose, yeast extract, $(\text{NH}_4)_2\text{SO}_4$ and NaCl on batch phenol degradation using *Pseudomonas pictorum* (Balan 1999) and batch biodegradation of p-cresol using a microbial consortia (Singh and Kumar 2014). Artificial neural network models have also been developed to predict the performance of continuous bioreactor systems such as for the continuous treatment of substituted phenol containing wastewater in packed bed bioreactor (Nandwana *et al.* 2014), continuous degradation of starch wastewater in Inverse Fluidized Bed Bioreactor (Raasimman *et al.* 2007) to optimize the dilution rate for maximization of cellular productivity of a continuous culture of baker's yeast in the presence of disturbances in environmental conditions and biofilm characteristics (Sarkar and Modak 1996). ANN has been developed for continuous biodegradation of phenol using the cells of *Nocardia hydrocarbonoxydans* in a spouted bed bioreactor with GAC as cell carrier material (Dabhade *et al.* 2008) and in pulsed plate bioreactor with glass beads as cell carrier material (Shetty *et al.* 2008). In these studies ANN was used to predict the steady state percentage biodegradation of phenol under different operating conditions of the bioreactor. In the present study, ANN has been developed to predict the steady state biofilm characteristics and the biofilm dynamics during start-up.

5.2. ANN model development to predict the biofilm characteristics at steady state and during start-up of pulsed plate bioreactor

In the present study ANN model has been developed to predict the biofilm characteristics associated with continuous phenol biodegradation during start-up and at steady state in a pulsed plate bioreactor under various operating conditions. Back propagation algorithm was adopted in the present study to train the network.

To predict the biofilm characteristics during start up, the input variables to the network were dilution rate, GAC loading, frequency of pulsation, amplitude of pulsation, influent phenol concentration and the time during start up. The output variables from the network are biofilm thickness (μm), biofilm density ($\text{g}\cdot\text{cm}^{-3}$), protein (mg/g biomass weight), humic substance (mg/g dry biomass) and carbohydrate (mg/g dry biomass) content of EPS. A three layer network with an input layer, one hidden layer and an output layer was chosen. The input layer consisted of six neurons and the output layer consisted five neurons. The input-output data obtained from various experimental runs during the start-up of the bioreactor were used for training, testing and validation. Totally 155 data sets (Table 5.1) were used to model the biofilm dynamics during the start-up. Among these 109 data sets (70 %) were used for training the ANN and 23 data sets (15%) each were used for testing and validation. Function 'nftool' of the Neural Network Toolbox of MATLAB R2015b was used for the development of neural network model. The data for training, testing and validation were randomly chosen by the Neural Network Toolbox software. The software used Levenberg-Marquardt Backpropagation Algorithm for training the network. The hidden neurons use tan-sigmoidal functions and the output neurons use linear functions. The software preprocesses the input-output data by using 'mapminmax' function and normalizes the data to produce outputs in the range $[-1, 1]$. The network training was carried out repeatedly by changing the number of neurons in the hidden layer until the values of R (Corrilation coefficient) for training, testing and validation are shown very near to '1'. The three layer network with one hidden layer containing 10 neurons was trained to give the best results for training, testing and validation. The weights and bias values of the network are presented in the MATLAB function script generated by the Neural Network Tool Box and is appended as Appendix 1.

The network was then saved and further was used with a blind test data (8 No.) for manual validation. These blind set data were not fed to the neural network tool box software during the development of the model. The plots of outputs (predicted values) vs targets (experimental values) for training, testing, validation and the total data set are

shown in Fig 5.3 with their corresponding R values. The plots indicates the good ness of fit of the developed neural network model and the validation of the model. The network was tested with a blind data set shown in Table 5.2 and the plot of the experimental and predicted values shown in Fig 5.4 indicate that the network predicts the results with a good accuracy for chemical characteristics and reasonably well for the physical characteristics. Thus, the neural network model with 10 neurons in the hidden layer, as developed in the present study can be used to predict the biofilm dynamics during start up in pulsed plate column during continuous biodegradation of phenol using the cells of *Pseudomonas desmolyticum* immobilized on granular activated carbon.

Table 5.1. Input Data for training artificial neural network system during start up period.

Sl.NO.	D, h^{-1}	S, gm	f, s^{-1}	A, cm	C_i, ppm	t, h	Thickness, μm	Density, g/cc	Protein, $mg/gdrybiomass$	HS, $mg/gdrybiomass$	CH, $mg/gdrybiomass$
1	0.33	80	0.08	3.5	200	2	4.8	0.298	0.88	3	10.49
2	0.33	80	0.08	3.5	200	4	5.1	0.558	1.48	4.11	24.5
3	0.33	80	0.08	3.5	200	6	6.1	0.579	1.78	6.85	30
4	0.33	80	0.08	3.5	200	8	4.1	0.88	3.4	7.31	34.6
5	0.33	80	0.08	3.5	200	12	3.2	1.13	7	8.6	48
6	0.66	80	0.08	3.5	200	2	4	0.272	0.65	1.8	7.65
7	0.66	80	0.08	3.5	200	4	4.2	0.31	0.70	2.7	14.8
8	0.66	80	0.08	3.5	200	6	4.6	0.294	0.7	4	20.1
9	0.66	80	0.08	3.5	200	8	4.1	0.378	1.9	4.8	21.2
10	0.66	80	0.08	3.5	200	12	3	0.56	3.5	4.8	24.9
11	0.66	80	0.08	3.5	200	16	2.9	0.589	3.3	5.9	30.9
12	0.66	80	0.08	3.5	200	20	2.9	0.608	4.2	5.1	32.2
13	0.66	80	0.08	3.5	200	24	2.9	0.607	3.2	5.21	32.1
14	0.66	80	0.08	3.5	200	30	2.9	0.607	3.09	5.2	32.1
15	0.99	80	0.08	3.5	200	2	3.8	0.24	0.4	1.2	5.14
16	0.99	80	0.08	3.5	200	4	3.91	0.248	0.6	2.4	11.2
17	0.99	80	0.08	3.5	200	8	3.51	0.261	0.99	4.03	18.0
18	0.99	80	0.08	3.5	200	10	3.11	0.343	1.6	4.7	20.1
19	0.99	80	0.08	3.5	200	12	2.45	0.444	1.44	5	20
20	0.99	80	0.08	3.5	200	16	2.22	0.551	1.99	4.7	24.3
21	0.99	80	0.08	3.5	200	20	2	0.503	2.33	4.9	25
22	0.99	80	0.08	3.5	200	30	1.8	0.501	1.87	3.5	25
23	0.99	80	0.08	3.5	200	38	1.81	0.523	1.88	3.49	26

Sl.NO.	D, h ⁻¹	S, gm	f, s ⁻¹	A, cm	Ci, ppm	t,h	Thickness,μm	Density ,g/cc	Protein, mg/gdrybiomass	HS, mg/gdrybiomass	CH, mg/gdrybiomass
24	0.33	80	0.08	3.5	1200	4	2.3	0.295	2	4.72	19
25	0.33	80	0.08	3.5	1200	6	2.21	0.299	2.5	5.31	16.6
26	0.33	80	0.08	3.5	1200	8	2.2	0.3	1.1	4.93	17
27	0.33	80	0.08	3.5	1200	10	2.2	0.321	2.87	4.69	19
28	0.33	80	0.08	3.5	1200	15	2.7	0.448	1.5	3.4	20.9
29	0.33	80	0.08	3.5	1200	30	2.3	0.549	1.7	4	22
30	0.33	80	0.08	3.5	1200	45	2.21	0.602	1.8	4.4	26
31	0.33	80	0.08	3.5	1200	47	2.2	0.592	1.82	4.45	28
32	0.33	80	0.08	3.5	1200	50	2.2	0.59	1.81	4.4	28
33	0.66	80	0.08	3.5	1200	15	2.3	0.382	1.31	2.89	17.9
34	0.66	80	0.08	3.5	1200	30	2	0.538	1.35	3	19.5
35	0.66	80	0.08	3.5	1200	47	1.8	0.572	1.53	3.59	22.5
36	0.66	80	0.08	3.5	1200	50	1.6	0.57	1.64	3.99	22.1
37	0.99	80	0.08	3.5	1200	15	1.8	0.361	0.98	2	13
38	0.99	80	0.08	3.5	1200	30	1.71	0.503	1	2.28	13.7
39	0.99	80	0.08	3.5	1200	45	1.61	0.494	1.1	2.56	14.4
40	0.99	80	0.08	3.5	1200	47	1.22	0.501	1.2	2.59	15.0
41	0.99	80	0.08	3.5	1200	50	1.15	0.499	1.22	2.88	16
42	0.99	80	0.08	3.5	1200	56	1.18	0.485	1.229	2.79	16.3
43	0.33	80	0.08	3.5	400	2	5.1	0.268	1.656	5	15
44	0.33	80	0.08	3.5	400	4	5.9	0.527	2.988	7.3	30.9
45	0.33	80	0.08	3.5	400	6	6.3	0.553	3.67	10	39.9
46	0.33	80	0.08	3.5	400	8	4.8	0.925	6.54	13	42.1
47	0.33	80	0.08	3.5	400	10	3.8	1.06	13	14	54
48	0.33	80	0.08	3.5	400	12	3.9	0.99	16	17	59.7

Sl.NO.	D, h ⁻¹	S, gm	f, s ⁻¹	A, cm	Ci, ppm	t,h	Thickness,μm	Density ,g/cc	Protein, mg/gdrybiomass	HS, mg/gdrybiomass	CH, mg/gdrybiomass
49	0.33	80	0.08	3.5	600	2	5.5	0.253	2.5	6	18.5
50	0.33	80	0.08	3.5	600	4	6.2	0.472	4.34	9.87	38.1
51	0.33	80	0.08	3.5	600	6	6.6	0.493	5.43	12.36	45.6
52	0.33	80	0.08	3.5	600	8	5	0.858	10	14.67	51.8
53	0.33	80	0.08	3.5	600	10	4	0.913	19	20	60.7
54	0.33	80	0.08	3.5	600	12	4.2	0.971	20.32	22	67.6
55	0.33	80	0.08	3.5	800	2	5.8	0.252	4	8.65	22.8
56	0.33	80	0.08	3.5	800	4	6.8	0.435	6.88	11.32	44.8
57	0.33	80	0.08	3.5	800	6	6.9	0.447	7	15.64	50.4
58	0.33	80	0.08	3.5	800	8	5.3	0.684	13	18.99	58.4
59	0.33	80	0.08	3.5	800	10	4.5	0.653	28	29.97	71
60	0.33	80	0.08	3.5	800	12	4.5	0.664	34	36.4	77
61	0.33	80	0.12	3.5	200	2	2.45	0.653	2.34	8.18	18.0
62	0.33	80	0.12	3.5	200	4	3.31	0.885	3.97	12.73	37.6
63	0.33	80	0.12	3.5	200	6	3.82	1.18	5.12	16.87	68.9
64	0.33	80	0.12	3.5	200	8	2.36	1.66	6.34	20.55	78.6
65	0.33	80	0.12	3.5	200	10	2.99	1.648	9.01	22.76	100
66	0.33	80	0.16	3.5	200	2	2.06	0.756	8.79	14.5	40
67	0.33	80	0.16	3.5	200	4	3.24	1.18	15.09	32.6	77
68	0.33	80	0.16	3.5	200	6	2.7	1.56	23	44.6	150
69	0.33	80	0.16	3.5	200	8	2.34	2.07	38.01	55	195
70	0.33	80	0.12	3.5	400	2	2.3	0.869	5.12	14.21	31
71	0.33	80	0.12	3.5	400	4	3.5	1.07	7	20	69
72	0.33	80	0.12	3.5	400	6	2.88	1.44	11	30	98.9
73	0.33	80	0.12	3.5	400	8	2.6	1.92	18	38	136

Sl.NO.	D, h ⁻¹	S, gm	f, s ⁻¹	A, cm	C _i , ppm	t,h	Thickness,μm	Density ,g/cc	Protein, mg/gdrybiomass	HS, mg/gdrybiomass	CH, mg/gdrybiomass
74	0.33	80	0.12	3.5	400	10	2.4	2.03	28	46.81	189
75	0.33	80	0.16	3.5	400	2	2.1	1.23	15	28	50
76	0.33	80	0.16	3.5	400	4	2.8	1.7	28.8	66	90
77	0.33	80	0.16	3.5	400	6	2.4	2.15	60.12	88	185
78	0.33	80	0.16	3.5	400	8	2.1	2.62	78.99	120	241
79	0.33	80	0.12	3.5	600	2	2.1	0.985	10.1	21	43
80	0.33	80	0.12	3.5	600	4	3.2	1.19	14.65	32	91
81	0.33	80	0.12	3.5	600	6	2.8	1.49	19.98	43.77	140
82	0.33	80	0.12	3.5	600	8	2.4	2.11	26	55.91	194
83	0.33	80	0.12	3.5	600	10	2.2	2.38	23	70.89	230
84	0.33	80	0.16	3.5	600	2	1.8	1.48	23	44	80
85	0.33	80	0.16	3.5	600	6	2.3	2.24	89.34	134	210
86	0.33	80	0.16	3.5	600	8	1.9	2.9	151.77	180	262
87	0.33	80	0.12	3.5	800	2	2	1.25	10.8	30	62
88	0.33	80	0.12	3.5	800	4	3	1.3	14.44	42	102
89	0.33	80	0.12	3.5	800	6	2.5	1.77	18	61	182
90	0.33	80	0.12	3.5	800	8	3	1.93	28.13	80	231
91	0.33	80	0.12	3.5	800	10	2.5	2.4	38	85	269
92	0.33	80	0.16	3.5	800	2	1.8	1.8	32	60	96
93	0.33	80	0.16	3.5	800	4	2.4	2.1	59	132	199
94	0.33	80	0.16	3.5	800	6	2.1	2.5	130.66	159	262
95	0.33	80	0.16	3.5	800	8	1.6	3.5	164.19	210	304
96	0.33	120	0.08	3.5	200	2	4.2	0.36	1.21	5.21	16
97	0.33	120	0.08	3.5	200	4	5.2	0.65	1.83	8.41	32
98	0.33	120	0.08	3.5	200	6	5.6	0.74	2.98	9.92	47

Sl.NO.	D, h ⁻¹	S, gm	f, s ⁻¹	A, cm	Ci, ppm	t,h	Thickness,μm	Density ,g/cc	Protein, mg/gdrybiomass	HS, mg/gdrybiomass	CH, mg/gdrybiomass
99	0.33	120	0.08	3.5	200	8	4.1	1.12	5.12	16	56
100	0.33	120	0.08	3.5	200	10	3.2	1.26	8.22	21.9	72
101	0.33	120	0.08	3.5	400	2	3.2	0.53	2.87	10.5	31
102	0.33	120	0.08	3.5	400	4	4.5	0.72	3.77	15.3	47
103	0.33	120	0.08	3.5	400	6	4	0.88	5.32	20	60
104	0.33	120	0.08	3.5	400	8	3.2	1.38	8.43	30	78
105	0.33	120	0.08	3.5	400	10	2.4	1.6	15	38	80
106	0.33	120	0.08	3.5	600	2	3	0.59	4.25	19.5	39
107	0.33	120	0.08	3.5	600	4	4	0.79	7.61	36	56
108	0.33	120	0.08	3.5	600	6	3.2	1.02	10.65	40	69
109	0.33	120	0.08	3.5	600	8	2.6	1.49	23	50	83
110	0.33	120	0.08	3.5	600	10	2	1.79	24	63	98
111	0.33	120	0.08	3.5	600	12	1.6	1.95	26	63	98
112	0.33	120	0.08	3.5	800	2	2.3	0.64	6.94	27	49
113	0.33	120	0.08	3.5	800	4	3.5	0.89	9.41	41	67
114	0.33	120	0.08	3.5	800	6	2.9	1.21	14	60	94
115	0.33	120	0.08	3.5	800	8	2.2	1.824	22.8	76	96
116	0.33	120	0.08	3.5	800	10	1.8	2.21	36	81	110
117	0.33	120	0.08	3.5	800	12	1.4	2.54	36	81	110
118	0.33	80	0.08	5	200	2	5.9	0.32	0.97	7	21
119	0.33	80	0.08	5	200	4	6.6	0.598	1.681	10	31
120	0.33	80	0.08	5	200	6	6.8	0.78	2.31	12	44
121	0.33	80	0.08	5	200	8	5.6	1.18	6.99	15.91	50
122	0.33	80	0.08	5	200	10	5.6	1.18	6.99	15.91	52
123	0.33	80	0.08	6.5	200	2	6	0.39	1.02	9.99	24

Sl.NO.	D, h ⁻¹	S, gm	f, s ⁻¹	A, cm	Ci, ppm	t,h	Thickness,μm	Density ,g/cc	Protein, mg/gdrybiomass	HS, mg/gdrybiomass	CH, mg/gdrybiomass
124	0.33	80	0.08	6.5	200	4	6.7	0.65	1.699	11.82	36
125	0.33	80	0.08	6.5	200	6	6.99	0.81	2.61	13.87	47
126	0.33	80	0.08	6.5	200	8	5.9	1.21	7.23	16.99	54
127	0.33	80	0.08	6.5	200	10	5.9	1.21	7.23	16.99	54
128	0.33	80	0.08	5	400	2	6	0.38	4.68	8.2	6
129	0.33	80	0.08	5	400	4	6.4	0.62	7.11	11.9	12
130	0.33	80	0.08	5	400	6	6.6	0.81	11	15	15
131	0.33	80	0.08	5	400	8	5.8	1.2	21.2	19.78	26
132	0.33	80	0.08	5	400	10	5.8	1.2	21.2	19.78	31
133	0.33	80	0.08	6.5	400	2	6.2	0.47	5.24	10	7.2
134	0.33	80	0.08	6.5	400	4	6.6	0.69	7.99	12.9	13.4
135	0.33	80	0.08	6.5	400	6	6.8	0.85	12	16	15.9
136	0.33	80	0.08	6.5	400	8	6	1.29	24	21.2	28
137	0.33	80	0.08	6.5	400	10	6	1.29	24	21.2	33
138	0.33	80	0.08	5	600	2	6.2	0.35	6	11.28	30.82
139	0.33	80	0.08	5	600	4	7	0.49	12	16.88	49
140	0.33	80	0.08	5	600	6	7.2	0.78	15	29	58
141	0.33	80	0.08	5	600	8	6.4	1.11	26	33.01	66.22
142	0.33	80	0.08	6.5	600	2	6.4	0.38	7.2	13.11	33
143	0.33	80	0.08	6.5	600	4	7.2	0.5	13.4	18	52
144	0.33	80	0.08	6.5	600	6	7.2	0.79	15.9	29.99	60
145	0.33	80	0.08	6.5	600	8	6.6	1.13	28	34	67
146	0.33	80	0.08	5	800	2	6.6	0.35	9.99	15	36.51
147	0.33	80	0.08	5	800	4	7.4	0.49	22	18.99	58.32
148	0.33	80	0.08	5	800	6	7.2	0.78	28	26.2	68.21

Sl.NO.	D, h ⁻¹	S, gm	f, s ⁻¹	A, cm	Ci, ppm	t,h	Thickness,μm	Density ,g/cc	Protein, mg/gdrybiomass	HS, mg/gdrybiomass	CH, mg/gdrybiomass
149	0.33	80	0.08	5	800	8	6.8	1.11	38	34	82
150	0.33	80	0.08	5	800	10	6.8	1.11	38	34	82
151	0.33	80	0.08	6.5	800	2	6.8	0.38	20.12	16.3	38
152	0.33	80	0.08	6.5	800	4	7.5	0.5	29	21.2	61.02
153	0.33	80	0.08	6.5	800	6	7.3	0.79	36	29.11	70
154	0.33	80	0.08	6.5	800	8	6.9	1.13	41	36	85
155	0.33	80	0.08	6.5	800	10	6.9	1.13	41	36	85

Table 5.2. Blind test Data for artificial neural network model to predict biofilm characteristics the during start up period

Sl. No.	D, h ⁻¹	S, gm	f, s ⁻¹	A, cm	C _i , ppm	t, h	Thickness, μm	density, g/cc	Protein, mg/gdrybiomass	Humic Substance, mg/gdry biomass	Carbohydrate, mg/gdry biomass
1	0.33	80	0.08	3.5	200	10	3.87	0.98	6.54	7.81	45.94
2	0.99	80	0.08	3.5	200	6	3.99	0.25	0.8	3.2	16.21
3	0.33	80	0.08	3.5	1200	12	2.2	0.341	1.8	2.66	20
4	0.33	80	0.08	3.5	1200	2	2.7	0.28	1	3	10
5	0.66	80	0.08	3.5	1200	45	1.9	0.562	1.46	3.25	20
6	0.33	80	0.08	3.5	600	4	6.2	0.472	4.34	9.87	38.11
7	0.33	80	0.16	3.5	600	4	2.7	1.8	44.91	100	139
8	0.33	80	0.08	6.5	800	6	7.3	0.79	36	29.11	70

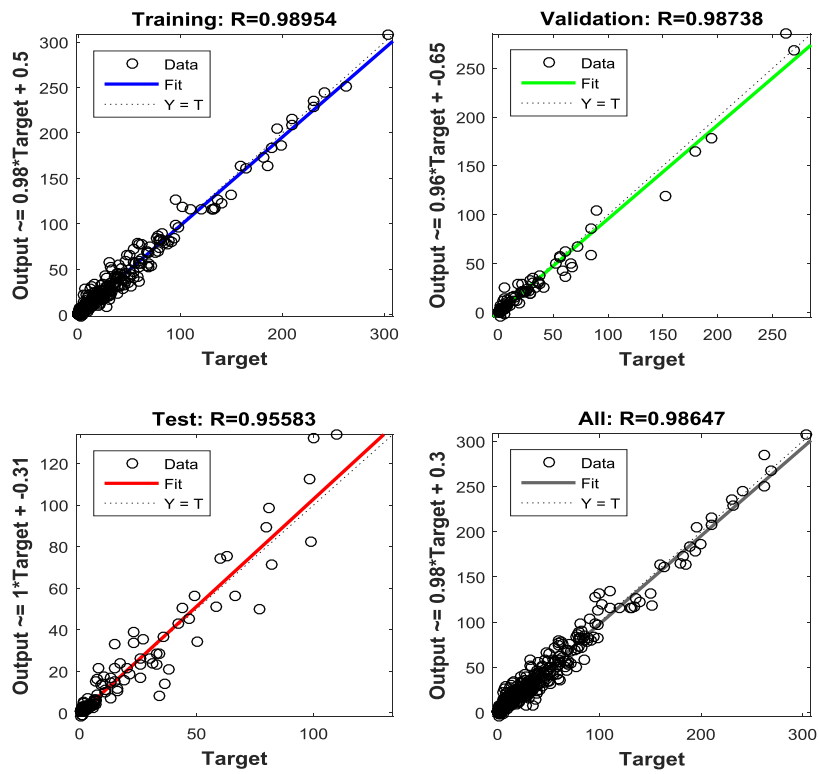


Fig.5.3 Output (model predicted) vs Target(experimental) values for training, testing, validation and the total data set points during Start up studies.

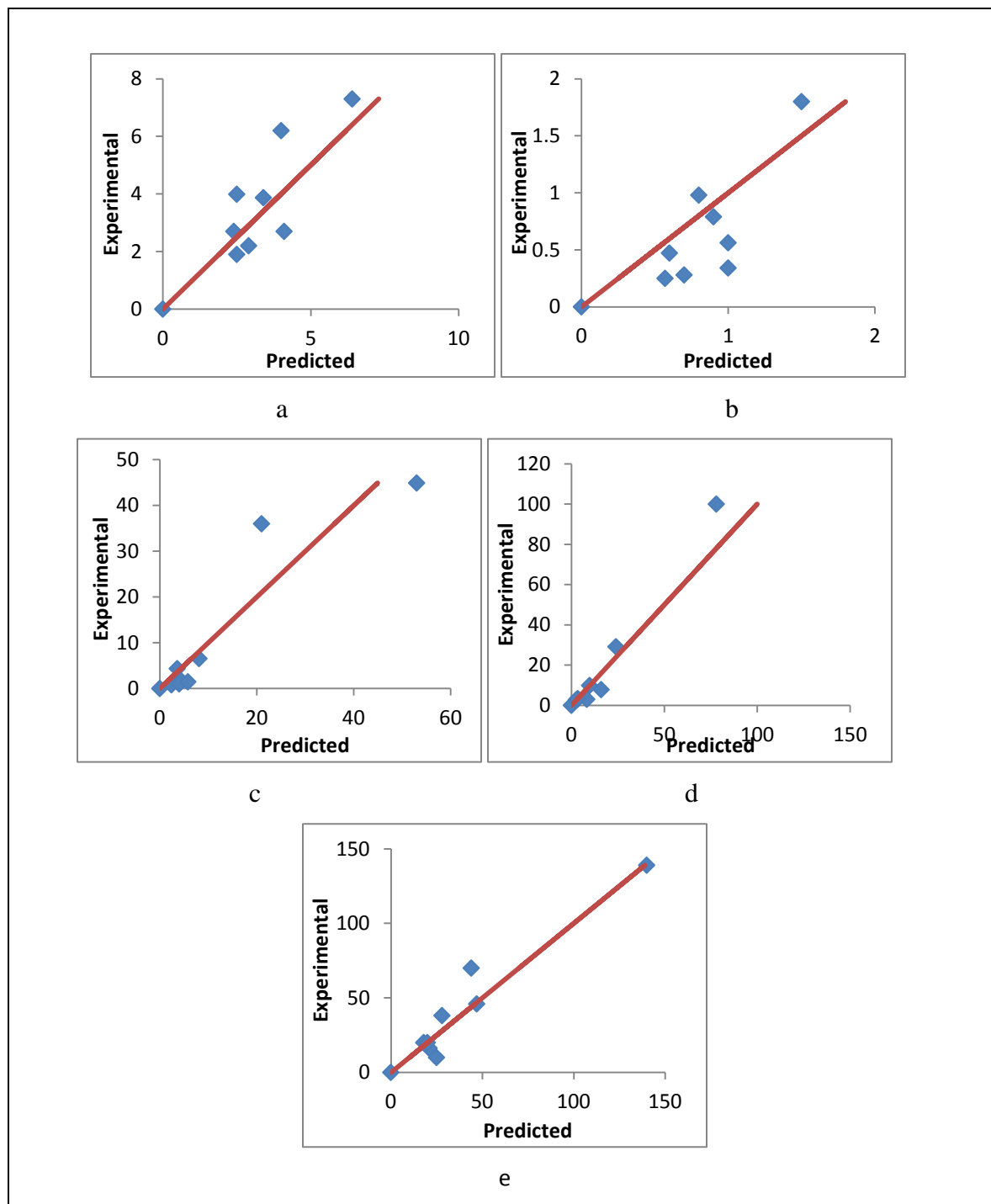


Fig. 5.4. Experimental vs predicted values of the ANN model with blind data set for Start up (a) Biofilm thickness, μm (b) Biofilm density, g/cc (c) Protein content of EPS, mg/g dry biomass (d) Humic substance content of EPS, mg/g dry biomass and (e) Carbohydrate content of EPS, mg/g dry biomass.

Similarly to predict the biofilm characteristics at steady state, the input variables to the network were dilution rate, GAC loading, frequency of pulsation, amplitude of pulsation and influent phenol concentration. The output variables from the network are biofilm thickness (μm), biofilm density ($\text{g}\cdot\text{cm}^{-3}$), protein (mg/g biomass weight), humic substance (mg/g dry biomass) and carbohydrate (mg/g dry biomass) content of EPS at steady state. A three layer network with an input layer, one hidden layer and an output layer was used. The input layer consisted of five neurons and the output layer consisted of five neurons. The input-output data obtained at steady state from various experimental runs were used for training, testing and validation. Totally 24 data sets (Table 5.3) were used to model the biofilm characteristics at steady state. Among these 16 data sets (70 %) were used for training the ANN and 4 data sets (15%) each were used for testing and validation. The data for training, testing and validation were randomly chosen by the Neural Network Toolbox software. The software used Levenberg-Marquardt backpropagation Algorithm for training the network, tan-sigmoidal functions for hidden neurons and the linear functions for output neurons. The network training was carried out repeatedly by changing the number of neurons in the hidden layer until the values of R (correlation coefficient) for training, testing and validation are shown very near to '1'. The three layer network with one hidden layer containing 5 neurons was trained to give the best results for training, testing and validation. The weights and bias values of the network are presented in the MATLAB script generated by the Neural Network Tool Box and is appended as Appendix 2.

The plots of outputs (predicted values) vs targets (experimental values) for training, testing, validation and the total data set are shown in Fig 5.5 with their corresponding R values. The equations relating the output and the target are also presented on the y-axis. The testing and validation results indicate that the network predicts chemical characteristics and physical characteristics of the biofilm accurately.

Table 5.3. Data for training artificial neural network system to predict the steady state biofilm characteristics.

Sl.NO.	C _i ,pp m	D, h ⁻¹	f, s ⁻¹	A,cm	S _g	Thickness ,μm	density, g/cc	Protein, mg/gdrybiomass	Humic Substance, mg/gdry biomass	Carbohydrate, mg/gdry biomass
1	200	0.33	0.08	5	80	3.6	0.979	7.06	8.11	48.4
2	200	0.66	0.08	5	80	2.94	0.607	3.08	5.2	32.11
3	200	0.99	0.08	5	80	1.81	0.523	1.88	3.48	26.09
4	1200	0.33	0.08	5	80	2.2	0.582	1.81	4.4	28
5	1200	0.66	0.08	5	80	1.29	0.573	1.62	4	22
6	1200	0.99	0.08	5	80	0.92	0.591	1.22	2.79	16.39
7	400	0.33	0.08	5	80	3.9	0.99	16	17	59.87
8	600	0.33	0.08	5	80	4.2	0.971	20	21.87	67
9	800	0.33	0.08	5	80	4.5	0.664	33.8	36	77
10	200	0.33	0.12	5	80	2.99	1.63	9.05	22.55	100
11	400	0.33	0.12	5	80	3.3	1.52	16	47	189
12	600	0.33	0.12	5	80	3.4	1.32	25.89	71	231
13	800	0.33	0.12	5	80	4.1	1.25	38	85	270
14	200	0.33	0.16	5	80	2.3	2.07	38	54.5	189
15	400	0.33	0.16	5	80	3.2	1.67	74	120.4	215
16	600	0.33	0.16	5	80	3.5	1.4	99.8	176	261
17	800	0.33	0.16	5	80	3.8	1.19	141.1	208	302.9
18	200	0.33	0.08	5	120	3.2	1.26	8.2	21.9	72
19	400	0.33	0.08	5	120	2	1.6	15	38	80
20	600	0.33	0.08	5	120	1.6	1.95	26	63	98
21	800	0.33	0.08	5	120	2.7	2.54	36	81	110
22	200	0.33	0.08	3.5	80	1.38	0.4	3.8	6.8	37
23	400	0.33	0.08	3.5	80	1.48	0.42	7.2	8.21	42

Sl.NO.	C,pp m	D, h ⁻¹	f, s ⁻¹	A,cm	S,g	Thickness ,μm	density, g/cc	Protein, mg/gdrybiomass	Humic Substance, mg/gdry biomass	Carbohydrate, mg/gdry biomass
24	600	0.33	0.08	3.5	80	1.58	0.44	12	10.5	53
25	800	0.33	0.08	3.5	80	2.4	0.48	15	11.74	42
26	200	0.33	0.08	6.5	80	3.66	1.19	7.77	8.81	47.21
27	400	0.33	0.08	6.5	80	3.8	0.998	17.64	14.55	62
28	600	0.33	0.08	6.5	80	4.15	0.954	21.55	21	67
29	800	0.33	0.08	6.5	80	4.6	0.82	34.73	32	79

The plots indicate the good ness of fit of the developed neural network model and the validation of the model. Thus, the neural network model with 5 neurons in the hidden layer, as developed in the present study can be used to predict steady state biofilm characteristics in a pulsed plate column during continuous biodegradation of phenol using the cells of *Pseudomonas desmolyticum* immobilized on granular activated carbon.

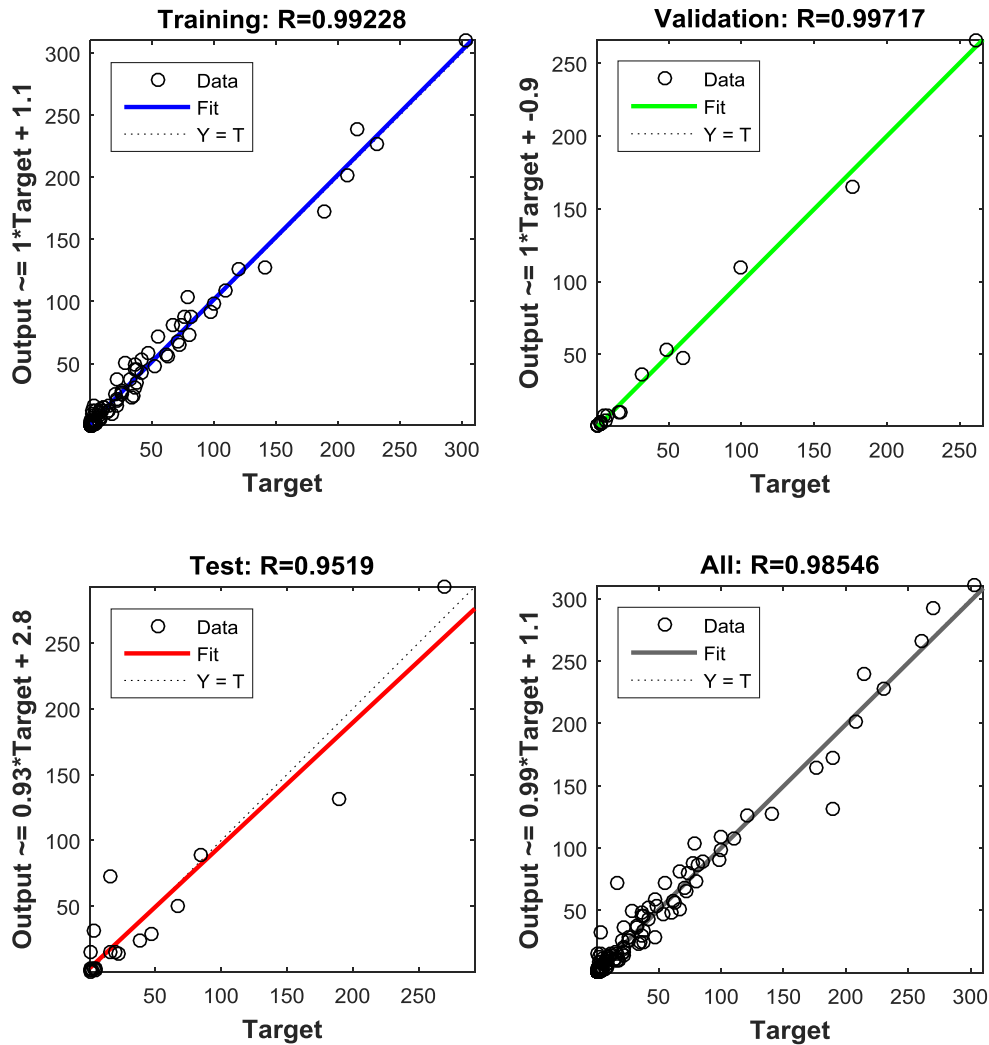


Fig.5.5 Output(predicted) vs Target (experimental) values for training, testing, validation and the total data set points by ANN for steady state.

The artificial neural network models developed in the present study can find applications in predicting the biofilm characteristics such as biofilm thickness, density and chemical composition of biofilm EPS in terms of protein, carbohydrate and humic substances. These models can be used in association with theoretical (mechanistic) models for pulsed plate bioreactor to predict the phenol biodegradation during the start-up and at steady state, thus in the development of hybrid models.

CHAPTER 6

SUMMARY AND CONCLUSIONS

The presently reported study was focused on evaluating the steady state and start-up performance of pulsed plate bioreactor in terms of its efficiency in degradation of phenol using the immobilized cells of *Pseudomonas desmolyticum* and the biofilm characteristics. The dynamics of biofilm formation during the start-up of the bioreactor was also studied.

The research work presented in this report, shows the efficacy of a continuous PPBR using bacterial strain *Pseudomonas desmolyticum* (NCIM2112) during the degradation of phenol from synthetic wastewater. The microorganisms were immobilized on granular activated carbon that acted as support for the formation of biofilm. The performance of bioreactor in phenol degradation and biofilm formation was evaluated under various operating conditions of the bioreactor such as frequency of pulsation; amplitude of pulsation; cell carrier material loadings; dilution rates and influent substrate concentration. The effect of these operating conditions was studied. Steady state and dynamic characteristics during start-up were also studied.

The findings of the present work is summarized as follows:

- Pulsed plate bioreactor can be effectively used for continuous biodegradation of phenol using the cells of *Pseudomonas desmolyticum* immobilized on GAC.
- During the start-up of the continuous bioreactor, initially adsorption is the dominant mechanism and during the later stages and at steady state biodegradation is the dominant mechanism of phenol removal.
- The production of EPS component and the protein, carbohydrate and humic substance content in the EPS component of the biofilm increased during the start-up which indicate that these components are synthesized to aid in adhesion and cohesion of cells in the biofilm

- The formation of biofilm in pulsed plate bioreactor during start up, dominantly included three phases of accumulation, compaction and plateau.
- Percentage degradation of phenol at steady state decreased with the increase in dilution rate showing that residence time in the reactor governs the phenol removal efficiency rather than the external mass transfer limitations. Thus, external mass transfer resistance is not the governing resistance in PPBR and is completely overcome by the high mixing and turbulence created due to pulsation of plates.
- Lower dilution rates favored the formation of uniform and thick biofilm in PPBR and thus in PPBR shear stress effects are more significant than mass transfer limitation effect.
- The EPS production and physical characteristics of the biofilm in PPBR at steady state are strongly influenced by the dilution rates and lower dilution rates favor higher production of biomass, EPS as well as the protein, carbohydrate and humic substances content of EPS.
- The stable operation of pulsed plate bioreactor is possible even at high influent concentrations of upto 1200 ppm, though the substrate inhibitory effect of phenol is predominant at 1200 ppm. To achieve higher efficiency of PPBR lower concentrations are favorable. The volumetric substrate loading of upto this concentration level is favorable in PPBR operating at a dilution rate of 0.33h^{-1} .
- The EPS production in the biofilm and the physical characteristics of the biofilm are strongly influenced by influent phenol concentration. The EPS and biomass production are favored at higher influent phenol concentration, upto the concentrations at which inhibitory effects are not predominant
- The biofilm structure changed from dense, smooth and uniform surface to rough, non uniform surface with fluffy outgrowth as the influent phenol concentrations increased from 200 ppm to 800 ppm. The biofilm structure integrity affected greatly when high inhibitory levels of phenol concentrations prevail in the bioreactor.

- Frequency of pulsation has a marginal influence on percentage degradation at lower influent phenol concentrations of 200 to 600 ppm. However, the influence of frequency on percentage degradation is higher at higher phenol concentrations as it enhances the mass transfer of phenol from the bulk liquid phase to the biofilm.
- Increasing the amplitude leads to higher phenol degradation at steady state. However, the amplitudes of 5cm and above could facilitate to effectively overcome any mass transfer limitations in the bioreactor, thus leading to almost complete degradation of phenol at all the influent phenol concentrations studied. Thus mass transfer rate does not remain as the rate limiting step in the process of phenol biodegradation at amplitudes of 5cm and above.
- The shear inducing parameters of the PPBR such as frequency and amplitude of pulsation lead to higher production of EPS components to keep the biofilm structure stronger, thus forming stable, thinner, denser, smoother, uniform and compact biofilms at higher frequencies and amplitudes.
- The increase in amplitude and frequency may provide dual fold effect of (i) High EPS component production in response to higher shear effects caused by higher mixing intensities (ii) High EPS component production owing to higher rate of mass transfer and thus the phenol consumption to produce more of EPS component along with cell growth.
- The frequencies of upto $0.16s^{-1}$ were found to be suitable for the stable operation of PPBR with the frequency of $0.16s^{-1}$ greatly favoring the bioreactor stability by forming thin and dense biofilms which are more stable. It indicates that the strain force is uniform throughout the biofilm and is lower than the tensile strength of the polymer matrix and thus avoiding the breakage of the matrix even at higher frequencies.
- The marginal increase in percentage degradation was achieved with the increase in cell carrier loading at the influent phenol concentrations of 200 ppm to 600 ppm. However, increase in cell carrier loading has a positive

influence on percentage degradation at high influent phenol concentrations.

- The EPS production and physical characteristics of the biofilm are greatly influenced by cell carrier loading with higher loading favoring the EPS production and formation of denser and thinner biofilm.
- The effect of enhancement in mass transfer due to particle movement at lower carrier loading seems marginal as compared to the effect of lower surface area available for phenol biodegradation and biomass production. Thus, higher available surface for microbial growth governs the bioreactor performance.
- Lower dilution rate, high cell carrier loading, higher frequency and amplitude of pulsation, favor the performance of bioreactor by reducing the start-up time owing to faster rate of growth of biofilm during start-up under these conditions.
- Start-up time is not influenced by the influent phenol concentrations at sub inhibitory levels. However, it is a strong function of inhibitory effect of substrate on microbial growth as observed from very large start-up time required for influent phenol concentration of 1200 ppm.
- Inhibitory substrate concentrations result in fluctuating reactor dynamics during the start-up which is attributed to higher detachments that occur due to fluffy and very porous biofilms formed as a result of lower growth rate.
- Higher frequencies also result in fluctuating reactor dynamics during the start-up owing to continuous growth and detachment of the biofilm at rates of higher magnitude before the attainment of steady state.
- Adsorption remains the dominant phenol removal phenomena for a longer time during the start-up at lower amplitudes of pulsation owing to slower rate of formation of biofilm.
- The artificial neural network models were developed to predict the biofilm dynamics during start-up as a function of influent phenol concentration, dilution rate, GAC loading and pulsing conditions (frequency and amplitude). ANN model was also developed to predict the steady state biofilm characteristics as a function of influent phenol concentration, dilution rate and pulsing conditions

(frequency and amplitude). These black box models were found to be valid and can predict the biofilm characteristics at steady state and during start-up . They can find their application in modeling and optimization of PPBR performance.

Thus, it may be concluded that pulsed plate bioreactor with immobilized cells of *Pseudomonas desmolyticum* on GAC can be continuously operated in efficient manner under stable conditions for degradation of phenol in wastewater with influent concentration of upto 800 ppm with dilution rate of 0.33h^{-1} at pulsing conditions of frequency 0.08 s^{-1} and amplitude 5 cm to achieve greater than 99.5% degradation. Though stable operation of PPBR is possible at higher inhibitory concentrations, it is not recommended to operate at these concentrations owing to lower efficiency of phenol degradation. The chemical , physical and morphological characteristics of biofilm have been found to be influenced by the PPBR operating conditions such as influent phenol concentration, dilution rate, GAC loading, frequency and amplitude of pulsation and they play dominant role in controlling the biofilm structure and integrity thus leading to stable operation of the bioreactor. Conditions which lead to the formation of thinner, denser, compact biofilms with uniform and smooth surface always lead to efficient operation of PPBR with better performance in terms of phenol biodegradation.

The present study has successfully demonstrated that PPBR with cells of *Pseudomonas desmolyticum* immobilized on GAC is an efficient biofilm reactor and can be employed in wastewater treatment for phenol degradation without much operational difficulties associated with controlling the biofilm thickness, structure , integrity and stability as encountered in other types of biofilm reactors such as fixed bed bioreactors. The study has been successful in adding a new knowledge in to the field of biofilm systems. Though this study was carried out at a laboratory scale, it has a high significance as it can advance us towards the development and optimal operation of an economical, large scale treatment system for continuous degradation of phenol from industrial wastewaters.

Apprnx 1

```
function [y1] = myNeuralNetworkFunction(x1)
%MYNEURALNETWORKFUNCTION neural network simulation function.
%
% Generated by Neural Network Toolbox function genFunction, 22-Aug-2016
20:19:19.
%
% [y1] = myNeuralNetworkFunction(x1) takes these arguments:
%   x = Qx6 matrix, input #1
% and returns:
%   y = Qx5 matrix, output #1
% where Q is the number of samples.

%#ok<*RPMT0>

% ===== NEURAL NETWORK CONSTANTS =====

% Input 1
x1_step1_xoffset = [0.33;80;0.08;3.5;200;2];
x1_step1_gain = [3.03030303030303;0.05;25;0.666666666666667;0.002;0.037037037037037];
x1_step1_ymin = -1;

% Layer 1
b1 = [2.0796733341726159;-
1.7541172915773211;1.0093091241487373;3.0485692131023598;-
0.32476564427354176;1.7031416956149386;0.88566510958203426;0.0379894963
26135457;1.4155536386862624;-2.3243039196947315];
IW1_1 = [-0.97585614688459132 -0.99715009146886635 -0.80086365516042124
-0.98749206815472212 0.21150338046529166 -
0.80964737087025085;1.697826759102953 1.3176053527102398 -
0.91208758130757928 2.0126368374164456 0.33448643093770325
1.0793025902424236;-3.7033812205777403 1.7348310565769571
0.4107066066452692 -0.32535597227165786 0.76836825963186894
4.3266049922382734;1.4599708714109274 0.69268338267410634
0.38956847057228833 -3.3979197862256592 -1.0968553410156059
1.5514931033182193;1.1052719298474689 3.441720552960907 -
0.12469616702902779 1.2850839629692217 0.46748103342340991
1.8419689555171346;-3.8653596470052354 3.9561506068450076 -
0.70819674814040268 -0.52005544845671403 0.97423487851848245
4.5423225992264511;-0.16303799271455768 -0.13563338190971869
3.9511390874637082 3.0708407744719679 0.54090668702910538
3.4085000130224214;-0.58046447720696748 -0.1911037948968492
3.6178493444374014 2.3061304085044063 0.003592847682022008
3.9534115555488216;2.2576825898440811 1.6942143902890658
0.82079061893249172 0.87764345916529529 -3.0172200320005218
0.10490844613058108;1.0355435906615031 0.22579259475640781 -
1.4701347966734983 -0.57639395510679658 -1.2425957349608492
0.59290427350407915];
```

```

% Layer 2
b2 = [-0.90023636525958672;-0.43888619188936151;1.0946320486886305;-
0.20171099444045137;0.94419723813461853];
LW2_1 = [-0.81909040565505598 -0.1039886625882316 -0.53636714587982237
-0.38623954337708144 0.10493738062059142 0.27694501442140745 -
1.8482758550398055 0.31090018668671654 0.12447411023360945 -
0.43280090817083078;-0.15610238563414927 -0.44503446569334071
0.86695069503957278 -0.056639534248156646 0.00060680447116273541 -
0.70525489781497253 0.47360389012538773 -0.044941467845391318
0.0047768264493606681 -0.0030018544690718803;-0.091558778478993574 -
0.97797295086686187 0.39835926158646767 -0.091123831998175364
0.49856959571178233 -0.37509595243519589 2.6299352066035904 -
0.28549939834236848 -0.088107374285098086
0.10587298376969781;1.2592228802092087 -0.78022765310436815
0.70600740867262002 -0.050319340027780324 1.1659381091155863 -
0.71739735980444153 2.031480989136945 -0.43193916953244726 -
0.044339117914102583 0.040468534486162187;-0.33014321519952483 -
0.27187556890456843 1.5520459329873892 -0.039077689384950098
0.95734251370868872 -1.5276406646778848 -1.4825041363699485
2.2640929365453069 0.03673895534511952 -0.010502827951505801];

% Output 1
y1_step1_ymin = -1;
y1_step1_gain =
[0.31496062992126;0.613496932515337;0.0122137404580153;0.00957854406130
268;0.00669209663387539];
y1_step1_xoffset = [1.15;0.24;0.44;1.2;5.14];

% ===== SIMULATION =====

% Dimensions
Q = size(x1,1); % samples

% Input 1
x1 = x1';
xp1 = mapminmax_apply(x1,x1_step1_gain,x1_step1_xoffset,x1_step1_ymin);

% Layer 1
a1 = tansig_apply(repmat(b1,1,Q) + IW1_1*xp1);

% Layer 2
a2 = repmat(b2,1,Q) + LW2_1*a1;

% Output 1
y1 =
mapminmax_reverse(a2,y1_step1_gain,y1_step1_xoffset,y1_step1_ymin);
y1 = y1';
end

% ===== MODULE FUNCTIONS =====

% Map Minimum and Maximum Input Processing Function

```

```

function y =
mapminmax_apply(x, settings_gain, settings_xoffset, settings_ymin)
y = bsxfun(@minus, x, settings_xoffset);
y = bsxfun(@times, y, settings_gain);
y = bsxfun(@plus, y, settings_ymin);
end

% Sigmoid Symmetric Transfer Function
function a = tansig_apply(n)
a = 2 ./ (1 + exp(-2*n)) - 1;
end

% Map Minimum and Maximum Output Reverse-Processing Function
function x =
mapminmax_reverse(y, settings_gain, settings_xoffset, settings_ymin)
x = bsxfun(@minus, y, settings_ymin);
x = bsxfun(@rdivide, x, settings_gain);
x = bsxfun(@plus, x, settings_xoffset);
end

```

Appendix 2

```
MYNEURALNETWORKFUNCTION neural network simulation function.
%
% Generated by Neural Network Toolbox function genFunction, 27-Aug-2016
23:23:31.
%
% [y1] = myNeuralNetworkFunction(x1) takes these arguments:
%   x = Qx5 matrix, input #1
% and returns:
%   y = Qx5 matrix, output #1
% where Q is the number of samples.

%#ok<*RPMT0>

% ===== NEURAL NETWORK CONSTANTS =====

% Input 1
x1_step1_xoffset = [200;0.33;0.08;3.5;80];
x1_step1_gain = [0.002;3.03030303030303;25;0.666666666666667;0.05];
x1_step1_ymin = -1;

% Layer 1
b1 = [1.171466062025351;-2.1926992951086959;-
0.59183456878509277;4.3188553087423811;-1.1291379587758457;-
1.713767771008285];
IW1_1 = [-1.1405044323208557 1.2060006755549562 -3.584597218713625
0.59001410930178622 -3.183977273123348;0.97533652634146351 -
2.1109169887299681 1.5677791677252109 0.36187999368211954
1.2765784984008826;3.5092212740372299 -0.40017215475159496
1.9818139213666164 1.0643130983069706 -1.6077914073870745;-
1.6465369567883541 0.44917370078745206 2.357474580398117 -
0.40767615875965818 0.5517004286088687;-2.1431053480681186
4.5748144278844656 -6.2848270183894233 -0.078060917802720842
1.9650249068179231;2.5685801927149186 0.77824258532552715 -
4.8913099882288424 -0.52210261992862383 0.36070605859177463];

% Layer 2
b2 = [0.6587262284951223;-0.29144737224250689;-0.25495657878275774;-
0.076951096659073584;-0.066121107930522616];
LW2_1 = [-0.547862707168426 -0.28197959569104686 0.12745602313449603 -
0.52180260256981204 0.17858265216366176 -
0.31880118916005173;0.21982090589731204 0.23128720082930113
0.15718888027133679 -0.18356075824259399 0.23718563660242631 -
0.46267519989450728;-1.7444175307586085 -1.0516797331931742
0.16452700859064198 0.22737596562225706 -0.09265384975174154
0.026282204466827268;0.1857632927793052 1.1476267836213043
0.27098758650768534 0.38851252806989189 -0.033326199879304123
0.011581983172914381;2.5601408603173978 3.4303347213818407
```

```

0.4269140237994245      0.64079970847728029      -0.10687105796729025      -
0.11315919503810964];

% Output 1
y1_step1_ymin = -1;
y1_step1_gain =
[0.543478260869565;0.934579439252336;0.0142979696883043;0.0097461137371
4731;0.00698055914278734];
y1_step1_xoffset = [0.92;0.4;1.22;2.79;16.39];

% ===== SIMULATION =====

% Dimensions
Q = size(x1,1); % samples

% Input 1
x1 = x1';
xp1 = mapminmax_apply(x1,x1_step1_gain,x1_step1_xoffset,x1_step1_ymin);

% Layer 1
a1 = tansig_apply(repmat(b1,1,Q) + IW1_1*xp1);

% Layer 2
a2 = repmat(b2,1,Q) + LW2_1*a1;

% Output 1
y1 =
mapminmax_reverse(a2,y1_step1_gain,y1_step1_xoffset,y1_step1_ymin);
y1 = y1';
end

% ===== MODULE FUNCTIONS =====

% Map Minimum and Maximum Input Processing Function
function y =
mapminmax_apply(x,settings_gain,settings_xoffset,settings_ymin)
y = bsxfun(@minus,x,settings_xoffset);
y = bsxfun(@times,y,settings_gain);
y = bsxfun(@plus,y,settings_ymin);
end

% Sigmoid Symmetric Transfer Function
function a = tansig_apply(n)
a = 2 ./ (1 + exp(-2*n)) - 1;
end

% Map Minimum and Maximum Output Reverse-Processing Function
function x =
mapminmax_reverse(y,settings_gain,settings_xoffset,settings_ymin)
x = bsxfun(@minus,y,settings_ymin);
x = bsxfun(@rdivide,x,settings_gain);

```



```
x = bsxfun(@plus,x,settings_xoffset);  
end
```

References

Abd-El-Haleem, Desouky, Usama Beshay, Abdu O. Abdelhamid, Hassan Moawad and Sahar Zaki (2003). "Effects of mixed nitrogen sources on biodegradation of phenol by immobilized *Acinetobacter* sp. strain W-17." *African Journal of Biotechnology* 2(1), 8-12.

Agarry, S. E., Solomon, B. O. and Layokun, S. K. (2008). "Kinetics of batch microbial degradation of phenols by indigenous binary mixed culture of *Pseudomonasaeruginosa* and *Pseudomonas fluorescens*." *African Journal of Biotechnology*. 7, 2417–2423.

Ahmed, A. M., Nakhla, G. F. and Farooq, S. (1995). "Phenol degradation by *Pseudomonas aeruginosa*." *Journal of Environmental Science & Health Part A*, 30(1), 99-107.

Al-Khalid, Taghreed and Muftah H. El-Naas (2012). "Aerobic biodegradation of phenols: a comprehensive review." *Critical reviews in environmental science and technology* 42, no. 16 : 1631-1690.

Alves, C. F., Melo, L. F. and Vieira, M. J. (2002). "Influence of Medium Composition on the Characteristics of a Denitrifying Biofilm formed by *Alcaligenes Denitrificans* in a Fluidised Bed Reactor." *Process Biochemistry*, 37(8), 837-845.

American Public Health Association (1995). "Standard Methods for the Examination of Water and Waste Water" 19th edition, Washington DC: American Water Works Association/WaterEnvironmentFederation.

Andersson, S., Dalhammar, G., Land, C. J. and Rajarao, G. K. (2009). "Characterization of extracellular polymeric substances from denitrifying organism *Comamonas denitrificans*." *Applied microbiology and biotechnology*, 82(3), 535-543.

Andrews, G. F. (1982). "Fluidized-bed fermenters: A steady-state analysis." *Biotechnology and bioengineering*, 24(9), 2013-2030.

Annadurai, G., and Lee, J. F. (2007). "Application of artificial neural network model for the development of optimized complex medium for phenol degradation using *Pseudomonas pictorum* (NICM 2074)." *Biodegradation*, 18(3), 383-392.

Annadurai, G., Balan, S. M. and Murugesan, T. (2000). "Design of experiments in the biodegradation of phenol using immobilized *Pseudomonas pictorum* (NICM-2077) on activated carbon." *Bioprocess Engineering*, 22(2), 101-107.

Ascon, M. A. and Lebeault, J. M. (1999). "High efficiency of a coupled aerobic-anaerobic recycling biofilm reactor system in the degradation of recalcitrant chloroaromatic xenobiotic compounds." *Applied microbiology and biotechnology*, 52(4), 592-599.

ATSDR (Agency for Toxic Substances and Disease Registry) (2008). "toxicological profile for phenol" U.S. department of health and human services Public Health Service, <http://www.atsdr.cdc.gov/toxprofiles/tp115.pdf>.

Audet, J., Thibault, J. and LeDuy, A. (1996). "Polysaccharide concentration and molecular weight effects on the oxygen mass transfer in a reciprocating plate bioreactor." *Biotechnology and bioengineering*, 52(4), 507-517.

Aygun, A., Nas, B. and Berkay, A. (2008). "Influence of high organic loading rates on COD removal and sludge production in moving bed biofilm reactor." *Environmental Engineering Science*, 25(9), 1311-1316. doi:10.1089/ees.2007.0071.

Bakke, R., Trulear, M. G., Robinson, J. A. and Characklis, W. G. (1984). "Activity of *Pseudomonas Aeruginosa* in Biofilms: Steady State". *Biotechnology and Bioengineering*, 26(12), 1418-1424.

Balan, S. M., Annadurai, G., Sheeja, R. Y., Srinivasamoorthy, V. R. and Murugesan, T. (1999). "Modeling of phenol degradation system using artificial neural networks." *Bioprocess Engineering*, 21(2), 129-134.

Banerjee, A., and Ghoshal, A. K. (2010). "Phenol degradation by *Bacillus cereus*: pathway and kinetic modeling." *Bioresource technology*, 101(14), 5501-5507.

Barbara Vu, Chen, M., Crawford, R. J. and Ivanova, E. P. (2009). "Bacterial extracellular polysaccharides involved in biofilm formation." *Molecules*, 14(7), 2535-2554.

Barker, J. and Bloomfield, S. F. (2000). "Survival of *Salmonella* in bathrooms and toilets in domestic homes following salmonellosis." *Journal of Applied Microbiology*, 89(1), 137-144

Barwal, A. and Chaudhary, R. (2014). "To study the performance of biocarriers in moving bed biofilm reactor (MBBR) technology and kinetics of biofilm for retrofitting the existing aerobic treatment systems: a review." *Reviews in Environmental Science and Bio/Technology*, 13(3), 285-299

Basha, Khazi Mahammedilyas, Aravindan Rajendran and Viruthagiri Thangavelu (2010). "Recent advances in the biodegradation of phenol: a review." *Asian Journal of Experimental Biological Sciences* 1(2) 219-234.

Beeftink, H. H. (1987). "Anaerobic bacterial aggregates. Variety and variation." Ph.D. Thesis, University of Amsterdam
[https://www.researchgate.net/publication/238523326 Anaerobic bacterial aggregates Variety and variation](https://www.researchgate.net/publication/238523326_Anaerobic_bacterial_aggregates_Variety_and_variation)

Begum, S. S. and Radha, K. V. (2015). "Hydrodynamic behavior of inverse fluidized bed biofilm reactor for phenol biodegradation using *Pseudomonas fluorescens*." *Korean Journal of Chemical Engineering*, 31(3), 436-445.

Begum, S. S., and Radha, K. V. (2013). "Biodegradation kinetic studies on phenol in internal draft tube (inverse fluidized bed) biofilm reactor using *Pseudomonas fluorescens*: performance evaluation of biofilm and biomass characteristics." *Bioremediation Journal*, 17(4), 264-277.

Beyenal, H. and Lewandowski, Z. (2002). "Internal and external mass transfer in biofilms grown at various flow velocities." *Biotechnology progress*, 18(1), 55-61.

Bhamidimarri, S. M. R., Greenfield, P. F. and Bell, P. R. F. (1988). "Biofilm characteristics in a fluidized-bed bioreactor." In *Proceedings of the 42nd Purdue industrial waste conference*. Lewis Publishers; Chelsea, MI (USA); West Lafayette, IN (USA); 12-14 May 1987, Book p. 103-112.

Bishop, P. L., Gibbs, J. T. and Cunningham, B. E. (1997). "Relationship between concentration and biofilm rheology." *Biotechnology Bioengineering*, 65, 83-92.

Bishop, P. L., Zhang, T. C., and Fu, Y. C. (1995). "Effects of biofilm structure, microbial distributions and mass transport on biodegradation processes." *Water Science and Technology*, 31(1), 143-152.

Boaventura, R. A. and Rodrigues, A. E. (1997). "Denitrification kinetics in a rotating disk biofilm reactor." *Chemical Engineering Journal*, 65(3), 227-235.

Bollinger, N., Hassett, D. J., Iglewski, B. H., Costerton, J. W. and McDermott, T. R. (2001). "Gene expression in *Pseudomonas aeruginosa*: evidence of iron override effects on quorum sensing and biofilm-specific gene regulation." *Journal of Bacteriology*, 183(6), 1990-1996.

Borkar, R. P., Gulhane, M. L. and Kotangale A. J. (2013). "Moving Bed Biofilm Reactor – A New Perspective in Wastewater Treatment." *Journal Of Environmental Science, Toxicology And Food Technology ISSN: 2319-2399. Volume 6, Issue. 15-21.*

Botchkova, E. A., Litti, Y. V., Kuznestov, B. B. and Nozhevnikova, A. N. (2014). "Microbial Biofilms formed in a laboratory-scale anammox bioreactor with flexible bursh carrier." *Journal of Biomaterials and Nanotechnology. DOI:10.4236/jbnb.2014.52010.*

Bott, T. R. (1998). "Techniques for reducing the amount of biocide necessary to counteract the effects of biofilm growth in cooling water systems." *Applied thermal engineering*, 18(11), 1059-1066.

Burghate, S. P., and Ingole, N. W. (2013). "Denitrification Potential of Fluidized Bed Biofilm Reactor." *International Journal of Research in Environmental Science and Technology*, 3(3), 78-85.

Bushnell, L. D., and Haas, H.F. (1941). "The utilization of certain hydrocarbons by microorganisms." *J Bacteriol* 41(5):653.

Cai, W., Li, J. and Zhang, Z. (2007). "The characteristics and mechanisms of phenol biodegradation by *Fusarium* sp." *Journal of hazardous materials*, 148(1), 38-42.

Calleja, G.B. (1984). "Microbial Aggregation." Florida: CRC Press. ISBN 0-84935708-X.

Casey, E. (1999). "The membrane-aerated biofilm reactor: fundamental reaction engineering aspects governing performance." Ph.D. thesis, National University of Ireland, Dublin, Ireland.

Chang, H. T., Rittmann, B. E., Amar, D., Heim, R., Ehlinger, O. and Lesty, Y. (1991). "Biofilm detachment mechanisms in a liquid-fluidized bed." *Biotechnology and Bioengineering*, 38(5), 499-506.

Chang, Y. H., Li, C. T., Chang, M. C. and Shieh, W. K. (1998). "Batch phenol degradation by *Candida tropicalis* and its fusant." *Biotechnology and bioengineering*, 60(3), 391-395.

Characklis, W. G., McFeters, G. A., and Marshall, K. C. (1990a). "Physiological ecology in biofilm systems." *Biofilms*, 37, 67-72.

Characklis, W. G. (1990b). "Biofilm processes." *Biofilms*, 195-231.

Characklis, W. G., Trulear, M. G., Bryers, J. D. and Zolver, N. (1982). "Dynamics of biofilm processes: methods." *Water Res* 16:1207-1216

Charaklis, W. G. (1981). "Fouling. Biofilm Development - A Process Analysis. Bioengineering Report;" *Biotech, and. Bioeng.* 23; pp 1923-1960.

Chavant, P., Martinie, B., Meylheuc, T., Bellon-Fontaine, M. N. and Hebraud, M. (2002). "Listeria monocytogenes LO28: surface physicochemical properties and ability to form biofilms at different temperatures and growth phases." *Applied and Environmental Microbiology*, 68(2), 728-737.

Chen, G. H., Ozaki, H. and Terashima, Y. (1989). "Modelling of the simultaneous removal of organic substances and nitrogen in a biofilm." *Water science and technology*, 21(8-9), 791-804.

Chen, M. J., Zhang, Z. and Bott, T. R. (1998). "Direct measurement of the adhesive strength of biofilms in pipes by micromanipulation." *Biotechnology Techniques*, 12(12), 875-880.

Chen, Y. M., Lin, T. F., Huang, C., Lin, J. C., and Hsieh, F. M. (2007). "Degradation of phenol and TCE using suspended and chitosan-bead immobilized *Pseudomonas putida*." *Journal of Hazardous Materials*, 148(3), 660-670.

Cheng, Kuan-Chen, Ali Demirci and Jeffrey M. Catchmark (2010). "Advances in biofilm reactors for production of value-added products." *Applied microbiology and biotechnology* 87(2), 445-456.

Cheng, S. S., Chen, W. C., and Hwang, H. H. (1997). "Biofilm formation: The effects of hydrodynamic and substrate feeding patterns in three phase draft-tube fluidized bed for nitrification process." *Water science and technology*, 36(12), 83-90.

Choi, Y. C. and Morgenroth, E. (2003). "Monitoring biofilm detachment under dynamic changes in shear stress using laser-based particle size analysis and mass fractionation." *Water Science and Technology*, 47(5), 69-76.

Choi, Y. C., Kim, D. S., Park, T. J., Park, K. K., and Song, S. K. (1995). "Wastewater treatment in a pilot scale inverse fluidized-bed biofilm reactor." *Biotechnology techniques*, 9(1), 35-40.

Choquette-Labbé, M., Shewa, W. A., Lalman, J. A. and Shanmugam, S. R. (2014). "Photocatalytic degradation of phenol and phenol derivatives using a nano-TiO₂ catalyst: Integrating quantitative and qualitative factors using response surface methodology." *Water*, 6(6), 1785-1806.

Christensen, BJORN E. and WILLIAM G. Characklis (1990). "Physical and chemical properties of biofilms." *Biofilms* 93 130.

Chung, T. P., Tseng, H. Y. and Juang, R. S. (2003). "Mass transfer effect and intermediate detection for phenol degradation in immobilized *Pseudomonas putida* systems." *Process Biochemistry*, 38(10), 1497-1507.

Clara, M., Strenn, B., Gans, O., Martinez, E., Kreuzinger, N. and Kroiss, H. (2005). "Removal of selected pharmaceuticals, fragrances and endocrine disrupting compounds in a membrane bioreactor and conventional wastewater treatment plants." *Water research*, 39(19), 4797-4807.

Coetser, S. E. and Cloete, T. E. (2005). "Biofouling and biocorrosion in industrial water systems." *Critical reviews in microbiology*, 31(4), 213-232.

Cortez, S., Teixeira, P., Oliveira, R., and Mota, M. (2008). Rotating biological contactors: a review on main factors affecting performance. *Reviews in Environmental Science and BioTechnology*, 7(2), 155-172.

Cresson, R., Carrere, H., Delgenes, J. P. and Bernet, N. (2006). "Biofilm formation during the start-up period of an anaerobic biofilm reactor—Impact of nutrient complementation." *Biochemical Engineering Journal*, 30(1), 55-62.

Crueger, W. and Crueger, C. (1989). "Biotechnology. A textbook of industrial microbiology." Sinauer Associates, Inc., Sunderland. MA; Organic acids

Czaczyk, K., and Myszka, K. (2007). "Biosynthesis of extracellular polymeric substances (EPS) and its role in microbial biofilm formation." *Polish Journal of Environmental Studies*, 16(6), 799.

Czaczyk, K., and Wojciechowska, K. (2003). "Formation of bacterial biofilms? the essence of the matter and mechanisms of interactions." *Biotechnologia*, 3, 180-192.

Dabhade, M. A., Saidutta, M. B., and Murthy, D. V. R. (2008). "Modeling of phenol degradation in spouted bed contactor using artificial neural network (ANN)." *Chemical Product and Process Modeling*, 3(2).

Dabhade, M. A., Saidutta, M. B., and Murthy, D. V. R. (2009). "Continuous phenol removal using *Nocardia hydrocarbonoxydans* in spouted bed contactor: Shock load study." *African Journal of Biotechnology* 8(4), 644-649. ISSN 1684–5315 © 2009 Academic Journals.

Daniels, S.L. (1980). "Mechanisms involved in sorption of microorganisms to solid surface." In Adsorption of Microorganisms, eds. Bitton, G. and Marshall, K.C., pp. 8-57. New York: John Wiley & Sons. ISBN 0-471-03157-7.

De Beer, D. and Stoodley, P. (1995). "Relation between the structure of an aerobic biofilm and transport phenomena." *Water Science and Technology*, 32(8), 11-18.

De Beer, D., Stoodley, P. and Lewandowski, Z. (1996). "Liquid flow and mass transport in heterogeneous biofilms." *Water Research*, 30(11), 2761-2765.

De Beer, D., Stoodley, P., Roe, F. and Lewandowski, Z. (1994). "Effects of biofilm structures on oxygen distribution and mass transport." *Biotechnology and bioengineering*, 43(11), 1131-1138.

Del Borghi, M., Palazzi, E., Parisi, F. and Ferraiolo, G. (1985). "Influence of process variables on the modelling and design of a rotating biological surface." *Water Research*, 19(5), 573-580.

Demirci, A., Pometto, A. L. III, Ho K-LC (1997). "Ethanol production by *Saccharomyces cerevisiae* in biofilm reactors." *Journal Ind Microbiol Biotechnol* 19:299-304

Denkhaus, E., Meisen, S., Telgheder, U. and Wingender, J. (2007). "Chemical and Physical Methods for Characterisation of Biofilms." *Microchimica Acta*, 158(1-2), 1-27.

Dey, S. and Mukherjee, S. (2013). "Performance study and kinetic modeling of hybrid bioreactor for treatment of bi-substrate mixture of phenol-m-cresol in wastewater: Process optimization with response surface methodology." *Journal of Environmental Sciences*, 25(4), 698-709.

Dey, Sudipta and Somnath Mukherjee (2010). "Performance and kinetic evaluation of phenol biodegradation by mixed microbial culture in a batch reactor." *International Journal of Water Resources and Environmental Engineering* 2, no. 3 (2010): 40-49.

Di Bonaventura, G., Piccolomini, R., Paludi, D., D'orio, V., Vergara, A., Conter, M. and Ianieri, A. (2008). "Influence of temperature on biofilm formation by *Listeria monocytogenes* on various food-contact surfaces: relationship with motility and cell surface hydrophobicity." *Journal of applied microbiology*,104(6), 1552-1561.

Dimitrov, Dimitar, Dimiter Hadjiev and Jordan Nikov (2007). "Optimisation of support medium for particle-based biofilm reactors." *Biochemical Engineering Journal* 37, no. 3 : 238-245.

Dixon, M. A. and Abbas, T. R. (2016). "Use of aerated magnetic biofilm reactor to treat wastewater." *Desalination and Water Treatment*, 57(18), 8061-8067.

Dong, B., Chen, H. Y., Yang, Y., He, Q. B. and Dai, X. H. (2015). "Biodegradation of Polychlorinated Biphenyls Using a Moving-Bed Biofilm Reactor." *CLEAN–Soil, Air, Water*, 43(7), 1078-1083.

Donlan, R. M. (2002). "Biofilms: microbial life on surfaces." *Emerging Infectious Diseases*, 8(9).

Dos Passos, C. T., Michelon, M., Burkert, J., Kalil, S. J. and Burkert, C. A. V. (2010). "Biodegradation of phenol by free and encapsulated cells of a new *Aspergillus* sp. isolated from a contaminated site in southern Brazil." *African Journal of Biotechnology*, 9(40), 6716-6720.

Duan, K. and Surette, M. G. (2007). "Environmental regulation of *Pseudomonas aeruginosa* PAO1 Las and Rhl quorum-sensing systems." *Journal of bacteriology*, 189(13), 4827-4836.

Dubois, M, Gilles, K.A, Hamilton, J.K, Rebers PT and Smith, F. (1956) “Colorimetric Method for Determination of Sugars and Related Substances.” *Analytical Chemistry* 28(3): 350-356.

Ebrahimi, S., Picioreanu, C., Xavier, J.B., Kleernenzem,R., Kreutzer, M., Kapteijn, F., Moulijn, J.A. and Loosdrecht, M.C.M. (2005). "Biofilm growth pattern in honeycomb monolith packings: Effect of shear rate and substrate transport limitations" *Catalysis Today*, 105, 448- 454..

Elawwad, A., Abdel-Halim, H. and Koeser, H. (2012). “The Start-Up of Aerated Submerged Fixed-Bed Biofilm Reactors for Steady State Nitrification.” *Journal ISSN, 1929, 2732*.

El-Naas, M. H., Al-Muhtaseb, S. and Makhlouf, S. (2009). “Biodegradation of phenol by *Pseudomonas putida* immobilized in polyvinyl alcohol (PVA) gel.” *Journal of Hazardous Materials*. 164, 720–725.

El-Naas, M., Al-Zuhair, S. and Makhlouf, S. (2010). “Batch degradation of phenol in a spouted bed bioreactor system.” *Journal of Industrial and Engineering Chemistry* 16, 267–272.

EPA (2014). “Priority Pollutant List.” <http://www.epa.gov/sites/production/files/2015-09/documents/priority-pollutant-list-epa.pdf> (date of access, Feb 01 2016)

Fajerweg, K., Foussard, J. N., Perrard, A., and Debellefontaine, H. (1997). “Wet oxidation of phenol by hydrogen peroxide: the key role of pH on the catalytic behaviour of Fe-ZSM-5.” *Water Science and Technology*, 35(4), 103-110.

Fan, L. S., Fujie, K., Long, T. R. and Tang, W. T. (1987). "Characteristics of draft tube gas-liquid-solid fluidized-bed bioreactor with immobilized living cells for phenol degradation." *Biotechnology and bioengineering*, 30(4), 498-504.

Fan, L. S., Hwang, S. J. and Matsuura, A. (1984). "Hydrodynamic behaviour of a draft tube gas-liquid-solid spouted bed." *Chemical engineering science*, 39(12), 1677-1688.

Fennell, D. E., Underhill, S. E. and Jewell, W. J. (1992). "Methanotrophic attached-film reactor development and biofilm characteristics." *Biotechnology and bioengineering*, 40(10), 1218-1232.

Fernández, I., Bravo, J. I., Mosquera-Corral, A., Pereira, A., Campos, J. L., Méndez, R. and Melo, L. F. (2014). "Influence of the shear stress and salinity on Anammox biofilms formation: modelling results." *Bioprocess and biosystems engineering*, 37(10), 1955-1961.

Fidel Toldra, Augustie Flors, Juan L. Lequerica and Salvador Valles (1986).

"Fluidized bed Biomethanation of acetic acid." *Applied Microbiology and Biotechnology*. 23,336-341.

Flemming, H. C. and Wingender, J. (2001). "Relevance of microbial extracellular polymeric substances (EPSs)-Part II: Technical aspects." *Water Science and Technology*, 43(6), 9-16

Fletcher, C. and Peto, R. (1977). "The natural history of chronic airflow obstruction." *British Medical Journal*, 1(6077), 1645-1648.

Förberg, C. and Häggström, L. (1985). "Control of cell adhesion and activity during continuous production of acetone and butanol with adsorbed cells." *Enzyme and microbial technology*, 7(5), 230-234.

Fox, Peter, Makram T. Suidan, and John T. Bandy.(1990). "A comparison of media types in acetate fed expanded-bed anaerobic reactors." *Water Research* 24(7), 827-835.

Freitas, C. and Teixeira, J. A. (1998). "Hydrodynamic studies in an airlift reactor with an enlarged degassing zone." *Bioprocess Engineering*, 18(4), 267-279.

Frolund, B., Griebe, T. and Nielsen, P. H. (1995). "Enzymatic activity in the activated-sludge floc matrix." *Applied Microbiology and Biotechnology*, 43(4), 755-761.

Fuqua, C., Parsek, M. R. and Greenberg, E. P. (2001). "Regulation of gene expression by cell-to-cell communication: acyl-homoserine lactone quorum sensing." *Annual review of genetics*, 35(1), 439-468

Furumai, H. and Rittmann, B. E. (1994). "Evaluation of multiple-species biofilm and floc processes using a simplified aggregate model." *Water Science and Technology*, 29(10-11), 439-446.

Gaber, IDRIS (a) and Medhat Moustafa(2004). "quantification of biofilm formed at a plan liquidliquid interface." *Eighth International Water Technology Conference, IWTC8, Alexandria, Egypt* 793.

Gad, N. S., and Saad, A. S. (2008). "Effect of environmental pollution by phenol on some physiological parameters of *Oreochromis niloticus*." *Global Vet*, 2, 312-319.

Gandhi, H. P., Ray, R. M. and Patel, R. M. (1997). "Exopolymer production by Bacillus species." *Carbohydrate polymers*, 34(4), 323-327.

Ganlzer, C. J. (1989). "Inhibitory substrate utilization by steady state biofilm." *Journal of Environmental Engineering*, 155, 302-319.

García, I. G., Venceslada, J. B., Peña, P. J. and Gómez, E. R. (1997). "Biodegradation of phenol compounds in vinasse using Aspergillus terreus and Geotrichum candidum." *Water Research*, 31(8), 2005-2011.

Garny, K., Horn, H. and Neu, T. R. (2008). "Interaction between Biofilm Development, Structure and Detachment in Rotating Annular Reactors." *Bioprocess and Biosystems Engineering*, 31(6), 619-629.

Garrett, T. R., Bhakoo, M. and Zhang, Z. (2008). "Bacterial adhesion and biofilms on surfaces." *Progress in Natural Science*, 18(9), 1049-1056.

Garrett, T. R., Bhakoo, M., & Zhang, Z. (2008). "Bacterial adhesion and biofilms on surfaces." *Progress in Natural Science*, 18(9), 1049-1056.

Garrido, J. M., Van Benthum, W. A. J., Van Loosdrecht, M. C. M. and Heijnen, J. J. (1997). "Influence of dissolved oxygen concentration on nitrite accumulation in a biofilm airlift suspension reactor." *Biotechnology and bioengineering*, 53(2), 168-178.

Gauthami, R. Shetty and Vidya, K. Shetty (2016). "Pathway identification, enzyme activity and kinetic study for the biodegradation of phenol by Nocardia hydrocarbonoxydans NCIM 2386." *Desalination and Water Treatment*, 57(19), 8789-8801.

Ghannadzadeh, M. J., Jonidi-Jafari, A., Rezaee, A. and Soltani, R. D. C. (2015). "Biodegradation of Phenol in Synthetic Wastewater Using a Fixed Bed Reactor With up Flow Sludge Blanket Filtration (FUSBF)." *Global journal of health science*, 7(7), 120.

Gibert, Oriol, Benoît Lefèvre, Marc Fernández, Xavier Bernat, Miquel Paraira, Montse Calderer and Xavier Martínez-Lladó (2013). "Characterising biofilm development on granular activated carbon used for drinking water production." *Water research* 47, no. 3 : 1101-1110.

Gjaltema, A., Van Loosdrecht, M. C. M. and Heijnen, J. J. (1997). "Abrasion of suspended biofilm pellets in airlift reactors: Effect of particle size." *Biotechnology and bioengineering*, 55(1), 206-215.

Goldberg, J. (2002). "Biofilms and antibiotic resistance: a genetic linkage." *Trends in Microbiology*, 10(6), 264.

Gomma, H.G. and Tawell, A. M. A. (2005). "Axial mixing in a novel pilot scale gas-liquid reciprocating plate column." *Chemical Engineering Process*, 44(12), 85-1295.

Gong, W. J., Liang, H., Li, W. Z. and Wang, Z. Z. (2011). "Selection and evaluation of biofilm carrier in anaerobic digestion treatment of cattle manure." *Energy*, 36(5), 3572-3578.

Gonzalez, G., Herrera, M. G., Garcia, M. T. and Pena, M. M. (2001). "Biodegradation of phenol in a continuous process: Comparative study of stirred tank and fluidized-bed bioreactors." *Bioresource Technology*, 76, 245-251.

Goudar, Chetan T., Shobha H. Ganji, Basayya G. Pujar and Keith A. Strevett (2000). "Substrate inhibition kinetics of phenol biodegradation." *Water environment research* 72(1), 50-55.

Grabow, W. O. K., Dohmann, M., Haas, C., Hall, E. R., Lesouef, A., Orhon, D., and Nagle, P. T. (1998). "Water Quality International'98. Part 7. Wastewater: biological processes." Selected proceedings of the 19th biennial conference of the International Association on Water Quality, Vancouver, Canada, 21-26 June 1998." *Water Science and Technology (United Kingdom)*.

Grady, C.P.L. Jr. (1985). "Biodegradation: Its measurement and microbiological basis." *Biotechnology and Bioengineering*, 27, 660-674.

Gross, R., Hauer, B., Otto, K. and Schmid, A. (2007). "Microbial biofilms: New catalysts for maximizing productivity of long-term biotransformations." *Biotechnology and bioengineering*, 98(6), 1123-1134.

Habouzit, F., Hamelin, J., Santa-Catalina, G., Steyer, J. P., and Bernet, N. (2014). "Biofilm development during the start-up period of anaerobic biofilm reactors: the biofilm Archaea community is highly dependent on the support material." *Microbial biotechnology*, 7(3), 257-264.

Halabi, M., Wiesholzer-Pittl, M., Schöberl, J. and Mittermayer, H. (2001). "Non-touch fittings in hospitals: a possible source of *Pseudomonas aeruginosa* and *Legionella* spp." *Journal of hospital infection*, 49(2), 117-121

Haribabu, K. and Sivasubramanian, V. (2013). "Determination of mass transfer coefficient in an inverse fluidized bed reactor using statistical and dynamic method for a non-Newtonian fluid." *Journal of Scientific and Industrial Research*, 72, 485-490.

He, Junguo., Hu, H., Qiu, W., Liu, J., Liu, M., Zhao, C. and Xu, J. (2015). "Community diversity and biofilm characteristic response to low temperature and low C/N ratio in a suspended carrier biofilm reactor." *Desalination and Water Treatment*, 1-11.

Hekmat, D., Bauer, R. and Neff, V. (2007). "Optimization of the microbial synthesis of dihydroxyacetone in a semi-continuous repeated-fed-batch process by in situ immobilization of *Gluconobacter oxydans*." *Process Biochemistry*, 42(1), 71-76.

Herald, P. J. and Zottola, E. A. (1988). "Attachment of *Listeria monocytogenes* to stainless steel surfaces at various temperatures and pH values." *Journal of Food science*, 53(5), 1549-1562.

Herbert-Guillou, D., Tribollet, B. and Festy, D. (2001). "Influence of the hydrodynamics on the biofilm formation by mass transport analysis." *Bioelectrochemistry*, 53(1), 119-125.

Herzberg, M., Dosoretz, C. G., Tarre, S., Beliaevski, M. and Green, M. (2004). "Biological granulated activated carbon fluidized bed reactor for atrazine remediation." *Water Science and Technology*, 49(11-12), 215-222.

Hidalgo, A., Jaureguibeitia, A., Prieto, M. B., Rodríguez-Fernández, C., Serra, J. L. and Llama, M. J. (2002). "Biological treatment of phenolic industrial wastewaters by *Rhodococcus erythropolis* UPV-1." *Enzyme and microbial technology*, 31(3), 221-226.

Hirata, A., Takemoto, T., Ogawa, K., Auresenia, J. and Tsuneda, S. (2000). "Evaluation of kinetic parameters of biochemical reaction in three-phase fluidized bed

biofilm reactor for wastewater treatment.” *Biochemical engineering journal*, 5(2), 165-171.

Hong, Y. S. (1998). “*Mechanistic, neural network, and intelligent hybrid models for a three-phase fluidised-bed biofilm reactor: a thesis presented in partial fulfillment of the requirements for the degree of Doctor of Philosophy in Environmental Engineering at Institute of Technology and Engineering, Massey University (Doctoral dissertation, Massey University).*”

Horn, H. and Hempel, D. C. (1998). “Modeling mass transfer and substrate utilization in the boundary layer of biofilm systems.” *Water Science and Technology*, 37(4-5), 139-147.

Horn, H. and Lackner, S. (2014). “Modeling of biofilm systems: a review. In *Productive Biofilms* (pp. 53-76).” *Springer International Publishing*. DOI: 10.1007/10_2014_275 © Springer-Verlag Berlin Heidelberg 2014 Published Online: 28 August 2014.

Horswill, A. R., Stoodley, P., Stewart, P. S. and Parsek, M. R. (2007). “The effect of the chemical, biological, and physical environment on quorum sensing in structured microbial communities.” *Analytical and bioanalytical chemistry*, 387(2), 371-380.

Howell, J. A. and Atkinson, B. (1976). “Influence of oxygen and substrate concentrations on the ideal film thickness and the maximum overall substrate uptake rate in microbial film fermenters.” *Biotechnology and Bioengineering*, 18(1), 15-35.

Hsien, T. Y. and Lin, Y. H. (2005). “Biodegradation of phenolic wastewater in a fixed biofilm reactor.” *Biochemical engineering journal*, 27(2), 95-103. <http://cdn.intechopen.com/pdfs-wm/40591.pdf>

Hui, Y. S., Amirul, A. A., Yahya R. M. A. and Azizan M. N. M. (2010). "Cellulase production by free and immobilized *Aspergillus terreus*." *World Journal of Microbiology and Biotechnology*, 26:79–84.

Idris, G. (2004). "Quantification of biofilm formed at a plan liquid-liquid interface." *Eighth International Water Technology Conference, IWTC8 2004, Alexandria, Egypt* 793

Iliuta, I. (2006). "Dynamics of cells attachment, aggregation, growth and detachment in trickle-bed bioreactors." *Chemical engineering science*, 61(15), 4893-4908. ISBN 978 92 4 154815 1 (Date of Access, 2 Feb 2016).

Immich, M. and Onken, U.(1992). "Prediction of minimum gas velocity in suspended bubble columns and airlift reactors." *Chemical engineering science*, 47(13), 3379-3386.

Jian-An, C. and Nieuwstad, T. J. (1992). "Modelling the three-phase flow in a pilot-scale airlift internal-loop reactor for wastewater treatment." *Environmental technology*, 13(2), 101-113.

Jiang, Y., Wen, J., Bai, J., Jia, X. and Hu, Z. (2007). "Biodegradation of phenol at high initial concentration by *Alcaligenes faecalis*." *Journal of Hazardous Materials*, 147(1), 672-676.

Kar, S., Swaminathan, T. and Baradarajan, A. (1997). "Biodegradation of phenol and cresol isomer mixtures by *Arthrobacter*." *World Journal of Microbiology and Biotechnology*, 13(6), 659-663.

Karel, S.F., Libicki, S.B. and Roberston, C.R. (1985). "The immobilization of whole cells; Engineering principles." *Chemical engineering Science* , 40(8), 1321-1354.

Kargi, F. and Eker, S. (2003). "Performance of rotating perforated tubes biofilm reactor in biological wastewater treatment." *Enzyme and microbial technology*, 32(3), 464-471.

Karigar, C., Mahesh, A., Nagenahalli, M. and Yun, D. J. (2006). "Phenol degradation by immobilized cells of *Arthrobacter citreus*." *Biodegradation*, 17(1), 47-55.

Kawase, Y. and Uchiyama, S. (1993). "Hydrodynamics and mixing in three-phase fluidized bed bioreactors." *Applied biochemistry and biotechnology*, 38(1-2), 41-55.

Karr, A. E. (1959). "Performance of a reciprocating-plate extraction column." *AIChE Journal*, 5(4), 446-452. **DOI:** 10.1002/aic.690050410.

Kennelly, C., Clifford, E., Gerrity, S., Walsh, R., Rodgers, M. and Collins, G. (2012). "A horizontal flow biofilm reactor (HFBR) technology for the removal of methane and hydrogen sulphide at low temperatures." *Water Science and Technology*, 66(9), 1997-2006.

Kennes, C. and Lema, J.M. (1994). "Simultaneous biodegradation of p-cresol and phenol by the basidiomycete *Phanerochaete chrysosporium*." *Journal of Industrial Microbiology*, 13:311-314.

Kim, J., Park, H. D. and Chung, S. (2012). "Microfluidic approaches to bacterial biofilm formation." *Molecules*, 17(8), 9818-9834.

Kirisits, M. J., Margolis, J. J., Purevdorj-Gage, B. L., Vaughan, B., Chopp, D. L., Stoodley, P., and Parsek, M. R. (2007). "Influence of the hydrodynamic environment

on quorum sensing in *Pseudomonas aeruginosa* biofilms.” *Journal of bacteriology*, 189(22), 8357-8360.

Klahre, J. and Flemming, H. C. (2000). “Monitoring of biofouling in papermill process waters.” *Water Research*, 34(14), 3657-3665.

Klapper, I. and Dockery, J. (2010). “Mathematical description of microbial biofilms.” *SIAM review*, 52(2), 221-265

Klein, J., Szijjarto, A., Vicente, A. A. and Teixeira, J. A. (2002). “Hydrodynamic considerations in three-phase internal-loop airlift bioreactors: effect of dual separator and draught tube design.” <http://hdl.handle.net/1822/3573>

Koch, B., Ostermann, M., Höke, H. and Hempel, D. C. (1991). “Sand and activated carbon as biofilm carriers for microbial degradation of phenols and nitrogen-containing aromatic compounds.” *Water research*, 25(1), 1-8.

Kodialbail, V. S. and Srinikethan, G. (2011). “Mixing and solid-liquid mass transfer characteristics in a three phase pulsed plate column with packed bed of solids in interplate spaces—a novel aerobic immobilized cell bioreactor.” *Journal of Chemical Technology and Biotechnology*, 86(10), 1310-1320.

Kommedal, R. and Bakke, R. (2003). “Modeling *Pseudomonas aeruginosa* biofilm detachment.” <http://hdl.handle.net/2282/222>.

Kotresha, D. and Vidyasagar, G.M. (2008). “Isolation and characterization of phenol-degrading *Pseudomonasaeruginosa* MTCC 4996.” *World Journal of Microbiology Biotechnology*, 24:541-547.

Kourkoutas, Y., A. Bekatorou, I. Mm Banat, Roger Marchant and A. A. Koutinas (2004). "Immobilization technologies and support materials suitable in alcohol beverages production: a review." *Food Microbiology* 21, no. 4 : 377-397.

Kreft, J. U. and Wimpenny, J. W. (2001). "Effect of EPS on biofilm structure and function as revealed by an individual-based model of biofilm growth." *Water Science and Technology*, 43(6), 135-135.

Krug, M., H. Ziegler and G. Straube (1985). "Degradation of phenolic compounds by the yeast *Candida tropicalis* HP 15 I. Physiology of growth and substrate utilization." *Journal of basic microbiology* 25, no. 2 : 103-110.

Kryst, K., and Karamanev, D. G. (2001). "Aerobic phenol biodegradation in an inverse fluidized-bed biofilm reactor." *Industrial & engineering chemistry research*, 40(23), 5436-5439.

Kumar, M. A., Anandapandian, K. T. K. and Parthiban, K. (2011). "Production and Characterization of Exopolysaccharides (EPS) from Biofilm forming Marine Bacterium." *Brazilian Archives of Biology and Technology*, 54(2), 259-265.

Kumar, B. S., and Venkateswarlu, C. (2012). "Estimating biofilm reaction kinetics using hybrid mechanistic-neural network rate function model." *Bioresourcetechnology*, 103(1), 300-308.

Kunduru, M.R. and Pometto, A.L. (1983). "Continuous ethanol production by *Zymomonas mobilis* immobilized on ion exchange resin." *Biotechnology* ,5, 159-164.

Kwok, W. K., Picioreanu, C., Ong, S. L., Van Loosdrecht, M. C. M., Ng, W. J. and Heijnen, J. J. (1998). "Influence of biomass production and detachment forces on

biofilm structures in a biofilm airlift suspension reactor.”*Biotechnology and bioengineering*, 58(4), 400-407.

Landau, J., Dim, A. and Houlihan, R. (1973). “A reciprocating-plate extraction column for hydrometallurgical applications.” *Metallurgical Transactions*, 4(12), 2827-2832.

Langer, S., Schropp, D., Bengelsdorf, F. R., Othman, M. and Kazda, M. (2014). “Dynamics of biofilm formation during anaerobic digestion of organic waste.” *Anaerobe*, 29, 44-51.

Lazarova, V. and Manem, J. (1994). “Advances in biofilm aerobic reactors ensuring effective biofilm activity control.” *Water Science and Technology*, 29(10-11), 319-327.

Lazarova, V., Bellahcen, D., Rybacki, D., Rittmann, B. and Manem, J. (1998). “Population dynamics and biofilm composition in a new three-phase circulating bed reactor.” *Water Science and Technology*, 37(4-5), 149-158.

Le Cloirec, P., André, Y., Faur-Brasquet, C. and Gerente, C. (2003). “Engineered biofilms for metal ion removal.” *Reviews in Environmental Science and Biotechnology*, 2(2-4), 177-192

Lembre, P., Lorentz, C., Di Martino, P., and Di Martino, P. (2012). “Exopolysaccharides of the biofilm matrix: A complex biophysical world.” *INTECH Open Access Publisher*. <http://dx.doi.org/10.5772/51213>.

Lesko, T., Colussi, A. J. and Hoffmann, M. R. (2006). “Sonochemical decomposition of phenol: evidence for a synergistic effect of ozone and ultrasound for the elimination of total organic carbon from water.” *Environmental science & technology*, 40(21), 6818-6823.

Lettinga, G. A. F. M., Van Velsen, A. F. M., Hobma, S. W., De Zeeuw, W. and Klapwijk, A. (1980). "Use of the upflow sludge blanket (USB) reactor concept for biological wastewater treatment, especially for anaerobic treatment." *Biotechnology and bioengineering*, 22(4), 699-734. doi: 10.1002/bit.260220402.

Lettinga, G., Roersma, R. and Grin, P. (1983). "Anaerobic treatment of raw domestic sewage at ambient temperatures using a granular bed UASB reactor." *Biotechnology and bioengineering*, 25(7), 1701-1723. 10.1002/bit.260250703. : DOI 10.1016/S0960-8524(98)00046-7.

Lewandowski, Z., Stoodley, P., Altobelli, S. and Fukushima, E. (1994). "Hydrodynamics and kinetics in biofilm systems-recent advances and new problems." *Water Science and Technology*, 29(10-11), 223-229.

Liesegang, T. J. (1997). "Contact lens-related microbial keratitis: Part II: athophysiology." *Cornea*, 16(3), 265-273.

Liu, Y. Q., Liu, Y. and Tay, J. H. (2004). "The effects of extracellular polymeric substances on the formation and stability of biogranules." *Applied Microbiology and Biotechnology*, 65(2), 143-148.

Liu, Hong, and Herbert H.P. Fang (2002). "Extraction of extracellular polymeric substances (EPS) of sludges." *Journal of Biotechnology* 95(3), 249-256.

Liu, Y. and Wang, Q.D. (1996). "Surface modification of bio-carrier by plasma oxidation-ferric ions coating technique to enhance bacterial adhesion." *Journal of Environmental Science and Health A31*, 869-878.

Liu, Y. J., Zhang, A. N. and Wang, X. C. (2009). "Biodegradation of phenol by using free and immobilized cells of *Acinetobacter* sp. XA05 and *Sphingomonas* sp. FG03." *Biochemical Engineering Journal*, 44, 187–192.

Liu, Y. Q., Liu, Y. and Tay, J. H. (2004). "The effects of extracellular polymeric substances on the formation and stability of biogranules." *Applied Microbiology and Biotechnology*, 65(2), 143-148.

Liu, Y., & Tay, J. H. (2002). "The essential role of hydrodynamic shear force in the formation of biofilm and granular sludge." *Water research*, 36(7), 1653-1665.

Liu, Y., and Tay, J. H. (2001). "Detachment forces and their influence on the structure and metabolic behaviour of biofilms." *World Journal of Microbiology and Biotechnology*, 17(2), 111-117.

Livingston, A. G. and Chase, H. A. (1989). "Modeling phenol degradation in a fluidized-bed bioreactor." *AIChE journal*, 35(12), 1980-1992.

Looijesteijn, P. J., Boels, I. C., Kleerebezem, M. and Hugenholtz, J. (1999). "Regulation of Exopolysaccharide Production by *Lactococcus lactis* subsp. *cremoris* by the Sugar Source." *Applied and environmental microbiology*, 65(11), 5003-5008.

Lopes, F. A., Vieira, M. J. and Melo, L. F. (2000). "Chemical Composition and Activity of a Biofilm during the Start-up of an Airlift Reactor." *Water Science and Technology Vol 41 No 4-5*, 105–111.

Lounes, M., and Thibault, J. (1993). "Hydrodynamics and power consumption of a reciprocating plate gas-liquid column." *The Canadian Journal of Chemical Engineering*, 71(4), 497-506. DOI: 10.1002/cjce.5450710401.

Lounes, M., Audet, J., Thibault, J., and LeDuy, A. (1995). "Description and evaluation of reciprocating plate bioreactors." *Bioprocess Engineering*, 13(1), 1-11.

Lowry, O.H., Rosebrough, N.J., Farr, A.L. and Randall, R.J. (1951) "Protein Measurement with the Folin Phenol Reagent." *Journal Biological Chemistry* 193(1), 265-275.

Maddox, I. S. (1989). "The acetone-butanol-ethanol fermentation: recent progress in technology." *Biotechnology and Genetic Engineering Reviews*,7(1), 189-220.

Mahiudddin, M. and Fakhruddin, A. N. M. (2012). "Degradation of phenol via meta cleavage pathway by *Pseudomonas fluorescens* PU1." *ISRN microbiology*.

Maric S., Vranes (2007). "Characteristics and Significance of Microbial Biofilm Formation." *Periodicals Biologica*, 109, 115-121.

Marotta, M., Martino, A., De Rosa, A., Farina, E., Carteni, M. and De Rosa, M. (2002). "Degradation of dental plaque glucans and prevention of glucan formation using commercial enzymes." *Process Biochemistry*, 38(1), 101-108

Marshall, K.C., Stout, R. and Mitchell, S.R. (1971). "Mechanism of initial events in the adsorption of marine bacteria to surface." *Journal of General Microbiology* 68 , 337-348.

Marvasi, M., Visscher, P. T. and Martinez, L. C. (2010). "Exopolymeric substances (EPS) from *Bacillus subtilis*: polymers and genes encoding their synthesis." *FEMS microbiology letters*, 313(1), 1-9.

McNaught, H. and Wert, E. C. (2015). "Evaluation of Chemical and Environmental Methods to Optimize Performance of Fixed Bed Biofilm Reactors to Remove Ozonation By-Products." *Ozone: Science and Engineering*, 37(3), 227-239.

Medel, A., Bustos, E., Esquivel, K., Godínez, L. A. and Meas, Y. (2012). "Electrochemical incineration of phenolic compounds from the hydrocarbon industry using boron-doped diamond electrodes." *International Journal of Photoenergy*.

Menniti, Adrienne, Seoktae Kang, Menachem Elimelech and Eberhard Morgenroth (2009). "Influence of shear on the production of extracellular polymeric substances in membrane bioreactors." *Water research* 43(17), 4305-4315.

Miller, M. B. and Bassler, B. L. (2001). "Quorum sensing in bacteria." *Annual Reviews in Microbiology*, 55(1), 165-199.

Molin, G. O. R. A. N. and Nilsson, I. (1985). "Degradation of phenol by *Pseudomonas putida* ATCC 11172 in continuous culture at different ratios of biofilm surface to culture volume." *Applied and environmental microbiology*, 50(4), 946-950.

Monteiro, Álvaro AMG., Rui, AR., Boaventura and Alírio, E. Rodrigues (2000). "Phenol biodegradation by *Pseudomonas putida* DSM 548 in a batch reactor." *Biochemical Engineering Journal* 6, no. 1 : 45-49.

More, T. T., Yadav, J.S.S., Yan, S., Tyagi, R. D. and Surampalli, R. Y. (2014). "Extracellular Polymeric Substances of Bacteria and their Potential Environmental Applications." *Journal of Environmental Management*, 144, 1-25.

More, T. T., Yadav, J.S.S., Yan, S., Tyagi, R. D. and Surampalli, R. Y. (2014). "Extracellular Polymeric Substances of Bacteria and their Potential Environmental Applications." *Journal of Environmental Management*, 144, 1-25.

Moreira, J. M. R., Teodósio, J. S., Silva, F. C., Simões, M., Melo, L. F. and Mergulhão, F. J. (2013). "Influence of flow rate variation on the development of *Escherichia coli* biofilms." *Bioprocess and biosystems engineering*, 36(11), 1787-1796.

Morgenroth, E. and Wilderer, P.A. (2000). "Influence of detachment mechanisms on competition in biofilms." *Wat. Res.*, 34(2), 417-426.

Moussavi, G., Khavanin, A. and Alizadeh, R. (2009). "The investigation of catalytic ozonation and integrated catalytic ozonation/biological processes for the removal of phenol from saline wastewaters." *Journal of hazardous materials*, 171(1), 175-181.

Mshandete, A., Murto, M., Kivaisi, A. K., Rubindamayugi, M. S. T. and Mattiasson, B. (2004). "Influence of recirculation flow rate on the performance of anaerobic packed-bed bioreactors treating potato-waste leachate." *Environmental technology*, 25(8), 929-936.

Mulder, A. and Heijnen, J. J. (1988). "The effect of carrier characteristics on the biofilm development in airlift suspension reactors." In *Proceedings, Netherland Biotechnology Congress NBC* (2), 102-110.

Nair, C. I., Jayachandran, K. and Shashidhar, S. (2008). "Biodegradation of phenol." *African Journal of Biotechnology*, 7(25).

Najafpour, G. D., Zinatizadeh, A. A. L. and Lee, L. K. (2006). "Performance of a three-stage aerobic RBC reactor in food canning wastewater treatment." *Biochemical engineering journal*, 30(3), 297-302.

Nandwana, T., Pakshirajan, K. and Sahoo, N. K.(2014) "Artificial Neural Network (ANN) Modelling of a Packed Bed Bioreactor System Treating Substituted Phenol Containing Wastewater." <http://www.iitg.ernet.in/biotech/K.Pakshirajan.html>

Nam, Teresa K., Michael B. Timmons, Carlo D. Montemagno and Scott M. Tsukuda (2000). "Biofilm characteristics as affected by sand size and location in fluidized bed vessels." *Aquacultural engineering* 22, no. 3 : 213-224.

Napoli, F., Olivieri, G., Russo, M. E., Marzocchella, A. and Salatino, P. (2010). "Butanol production by *Clostridium acetobutylicum* in a continuous packed bed reactor." *Journal of Industrial Microbiology Biotechnology*. doi:10.1007/s10295-010-0707-8.

Naresh, B., Honey, P. and Vaishali, S. (2012). "Biodegradation of phenol by a bacterial strain isolated from a phenol contaminated site in India." *Research Journal of Environment Sciences*, 1, 46-49.

Nemati, M., Jenneman, G. E. and Voordouw, G. (2001). "Mechanistic study of microbial control of hydrogen sulfide production in oil reservoirs." *Biotechnology and bioengineering*, 74(5), 424-434

Nicolella, C., Van Loosdrecht, M. C. M. and Heijnen, J. J. (2000). "Wastewater treatment with particulate biofilm reactors." *Journal of biotechnology*, 80(1), 1-33.

Nikolaev, Y. A. and Plakunov, V. K. (2007). "Biofilm—"City of microbes" or an analogue of multicellular organisms?." *Microbiology*, 76(2), 125-138.

Nikolov, Ludmil N. and Dimitar G. Karamanev(1990). "The inverse fluidized bed biofilm reactor: a new laboratory scale apparatus for biofilm research." *Journal of Fermentation and Bioengineering* 69(4), 265-267.

Ochoa, J. C., Coufort, C., Escudié, R., Liné, A. and Paul, E. (2007). "Influence of non-uniform distribution of shear stress on aerobic biofilms." *Chemical engineering science*, 62(14), 3672-3684.

Ogbonna, J. C., Amano, Y., Nakamura, K., Yokotsuka, K., Shimazu, Y., Watanabe, M. and Hara, S. (1989). "A multistage bioreactor with replaceable bioplates for continuous wine fermentation." *American journal of enology and viticulture*, 40(4), 292-298.

Ohashi A, Harada H. (1994). "Adhesion strength of biofilm developed in an attached growth reactor." *Water Sci Technol* 29(10-11):281-288.

Ohashi A, Harada H. (1994). "Adhesion strength of biofilm developed in an attached growth reactor." *Water Science and Technology* 29(10-11):281-288.

Ohashi A, Harada H. (1996). "A novel concept for evaluation of biofilm adhesion strength by applying tensile force and shear force." *Water Science and Technology* 34(5-6):201-211.

Ohashi, A., Koyama, T., Syutsubo, K., and Harada, H. (1999). "A novel method for evaluation of biofilm tensile strength resisting erosion." *Water science and technology*, 39(7), 261-268.

Olivares, R. C., Iglesias, L. M. P. and Ohlbaum, R. B. (2010). "U.S. Patent Application No. 12/859,083." US Patent No.US 20110045581 A1, Publication date 24 Feb 2011

Oliveira, A. C., Rosa, M. F., Aires-Barros, M. R. and Cabral, J. M. S. (2000). "Enzymatic esterification of ethanol by an immobilised *Rhizomucor miehei* lipase in a perforated rotating disc bioreactor." *Enzyme and microbial technology*, 26(5), 446-450.

Pai, S. L., Hsu, Y. L., Chong, N. M., Sheu, C. S. and Chen, C. H. (1995). "Continuous degradation of phenol by *Rhodococcus* sp. immobilized on granular activated carbon and in calcium alginate." *Bioresource Technology*, 51(1), 37-42.

Pakula, A. N. N. A., Bieszkiewicz, E., Boszczyk-Maleszak, H. A. N. K. A., & Mycielski, R. O. M. A. N. (1998). "Biodegradation of phenol by bacterial strains from petroleum-refining wastewater purification plant." *Acta Microbiologica Polonica*, 48(4), 373-380.

Paller, G., Hommel, R. K. and Kleber, H. P. (1995). "Phenol degradation by *Acinetobacter calcoaceticus* NCIB 8250." *Journal of basic microbiology*, 35(5), 325-335.

Park, A., Jeong, H. H., Lee, J., Kim, K. P. and Lee, C. S. (2011). "Effect of shear stress on the formation of bacterial biofilm in a microfluidic channel." *BioChip Journal*, 5(3), 236-241.

Pei-Shi, Q., Wen-bin, W. and Zheng, Q. I. (2008). "Effect of Shear Stress on Biofilm Morphological Characteristics and the Secretion of Extracellular Polymeric Substances. In *Bioinformatics and Biomedical Engineering, 2008. ICBBE 2008.*" *The 2nd International Conference on IEEE*, 3438-3441.

Pellicer-Nàcher, C. and Smets, B. F. (2014). "Structure, composition and strength of nitrifying membrane-aerated biofilms." *Water research*, 57, 151-161.

Peng, J. S., Tsai, W. C., and Chou, C. C. (2002). "Inactivation and removal of *Bacillus cereus* by sanitizer and detergent." *International journal of food microbiology*, 77(1), 11-18.

Peyton, B. M. (1996). "Effects of shear stress and substrate loading rate on *Pseudomonas aeruginosa* biofilm thickness and density." *Water Research*, 30(1), 29-36.

Peyton, B. M., and Characklis, W. G. (1993). "A statistical analysis of the effect of substrate utilization and shear stress on the kinetics of biofilm detachment." *Biotechnology and Bioengineering*, 41(7), 728-735.

Pham, Duy . K., Ivanova, E. P., Wright, J. P. and Nicolau, D. V. (2003). "AFM analysis of the extracellular polymeric substances (EPS) released during bacterial attachment on polymeric surfaces." In *Biomedical Optics 2003* (pp. 151-159). International Society for Optics and Photonics. phenolic compounds by *Aspergillus awamori* NRRI 3112. *Int. Biodeterior. Biodegrad.*, 60:342-365

Picioreanu, C., M. C. M. van Loosdrecht, and J. J. Heijnen. (2000). "Modelling and predicting biofilm structure, p. 129–166." In D. G. Allison, P. Gilbert, H. M. Lappin-Scott, and M. Wilson (ed.), *Community structure and cooperation in biofilms*. 59th Symposium of the Society for General Microbiology. Cambridge University Press, Cambridge, United Kingdom.

Picioreanu, C., Van Loosdrecht, M. C. M. and Heijnen, J. J. (1999). "Discrete-differential modelling of biofilm structure." *Water Science and Technology*, 39(7), 115-122.

Pimentel, M., Oturan, N., Dezotti, M. and Oturan, M. A. (2008). "Phenol degradation by advanced electrochemical oxidation process electro-Fenton using a carbon felt cathode." *Applied Catalysis B: Environmental*, 83(1), 140-149.

Pishgar, R., Najafpour, G., Neyra, B. N., Mousavi, N. and Bakhshi, Z. (2011). "Anaerobic biodegradation of phenol: Comparative study of free and immobilized growth." *Iranica Journal of Energy and Environment (IJEE)*, 2(4), 348-355.

Pishgar, R., Najafpour, G., Neyra, B. N., Mousavi, N. and Bakhshi, Z. (2011). "Anaerobic biodegradation of phenol: Comparative study of free and immobilized growth." *Iranica Journal of Energy and Environment (IJEE)*, 2(4), 348-355.

Pizarro, C., Donoso-Bravo, A., Jeison, D., Ruiz-Filippi, G. and Chamy, R. (2011). "Biofilm formation for organic matter and sulphate removal in gas-lift reactors." *Electronic Journal of Biotechnology*, 14(4), 3-3.

Popat, R., Cornforth, D. M., McNally, L. and Brown, S. P. (2015). "Collective sensing and collective responses in quorum-sensing bacteria." *Journal of the Royal Society Interface*, 12(103), 20140882.

Prieto, M. B., Hidalgo, A., Serra, J. L. and Llama, M. J. (2002). "Degradation of phenol by *Rhodococcus erythropolis* UPV-1 immobilized on Biolite® in a packed-bed reactor." *Journal of Biotechnology*, 97(1), 1-11.

Quan, X., Shi, H., Zhang, Y., Wang, J., and Qian, Y. (2004). "Biodegradation of 2, 4-dichlorophenol and phenol in an airlift inner-loop bioreactor immobilized with *Achromobacter sp.*" *Separation and Purification Technology*, 34(1), 97-103.

Qureshi, N. and Blaschek, H. (2001). "Evaluation of recent advances in butanol fermentation, upstream, and downstream processing." *Bioprocess and Biosystems Engineering*, 24(4), 219-226.

Qureshi, N. and Maddox, I. S. (1987). "Continuous solvent production from whey permeate using cells of *Clostridium acetobutylicum* immobilized by adsorption onto bonechar." *Enzyme and microbial technology*, 9(11), 668-671

Qureshi, N., Annous, B. A., Ezeji, T. C., Karcher, P., and Maddox, I. S. (2005). "Biofilm reactors for industrial bioconversion processes: employing potential of enhanced reaction rates." *Microbial Cell Factories*, 4(1), 1.

Raasimman, M., Govindarajan, I. and Karthikeyan, C. (2007). "Artificial neural network modeling of an inverse fluidized bed bioreactor." *Journal of Applied Sciences and Environmental Management*, 11(2). 65 – 69.

Rabah, F. K., and Dahab, M. F. (2004). "Biofilm and biomass characteristics in high-performance fluidized-bed biofilm reactors." *Water research*, 38(19), 4262-4270.

Radwan, S. S., Al-Hasan, R. H., Salamah, S. and Al-Dabbous, S. (2002). "Bioremediation of oily sea water by bacteria immobilized in biofilms coating macroalgae." *International biodeterioration & biodegradation*, 50(1), 55-59

Raganati, F., Procentese, A., Olivieri, G., Russo, M. E., Gotz, P., Salatino, P. and Marzocchella, A. (2016). "Butanol production by *Clostridium acetobutylicum* in a series of packed bed biofilm reactors." *Chemical Engineering Science*, 152, 678-688.

Rama Rao, N. V., and Baird, M. H. I. (2003). "Gas-liquid mass transfer in a 15 cm diameter reciprocating plate column." *Journal of Chemical Technology and Biotechnology*, 78(2-3), 134-137.

Rama Rao, N. V., Srinivas, N. S., & Varma, Y. B. G. (1983). "Dispersed phase holdup and drop size distributions in reciprocating plate columns." *The Canadian Journal of Chemical Engineering*, 61(2), 168-177.

Rao, K. R., Srinivasan, T. and Venkateswarlu, C. (2010). "Mathematical and kinetic modeling of biofilm reactor based on ant colony optimization." *Process Biochemistry*, 45(6), 961-972.

Read, S. T., Dutta, P., Bond, P. L., Keller, J. and Rabaey, K. (2010). "Initial development and structure of biofilms on microbial fuel cell anodes." *BMC microbiology*, 10(1), 1.

Rene, E. R., Kim, J. H. and Park, H. S. (2008). "An intelligent neural network model for evaluating performance of immobilized cell biofilter treating hydrogen sulphide vapors." *International Journal of Environmental Science & Technology*, 5(3), 287-296.

Rim, J. M., Kim, B. U. and Kwon, J. H. (2004). "Attachment characteristics of biofilms in fixed-lock media for swine wastewater treatment." *Journal of Environmental Science Health A Toxic Hazard Substances Environmental Engineering*. 39(7); 1843-52.

Rittman, B. E. (1982a). "The effect of shear stress on biofilm loss rate." *Biotechnology and Bioengineering*, 24(2), 501-506

Rittmann, B. E. (1982b). "Comparative performance of biofilm reactor types." *Biotechnology and bioengineering*, 24(6), 1341-1370

Rittmann, B. E., Trinet, F., Amar, D. and Chang, H. T. (1992). "Measurement of the activity of a biofilm: Effects of surface loading and detachment on a three-phase, liquid-fluidized-bed reactor." *Water Science and Technology*, 26(3-4), 585-594.

Roca, E., Ferrari, D., Nunez, M. J. and Lema, J. M. (1994). "Alcoholic Fermentation in a pulsed semi-pilot bioreactor-start-up and preliminary-results." *Afinidad*, 51(450), 103-108.

Rochex, A. and Lebeault, J. M. (2007). "Effects of nutrients on biofilm formation and detachment of a *Pseudomonas putida* strain isolated from a paper machine." *Water research*, 41(13), 2885-2892.

Rochex, A., Godon, J. J., Bernet, N. and Escudié, R. (2008). "Role of shear stress on composition, diversity and dynamics of biofilm bacterial communities." *Water Research*, 42(20), 4915-4922.

Rouxhet, P. G. and Mozes, N. (1990). "Physical chemistry of the interface between attached micro-organisms and their support." *Water science and technology*, 22(1-2), 1-16.

Sancinetti, G. P., Sader, L. T., Varesche, M. B. A., Amorim, E. L. C. D., Omena, S. P. F. D. and Silva, E. L. (2012). "Phenol degradation in an anaerobic fluidized bed reactor packed with low density support materials." *Brazilian Journal of Chemical Engineering*, 29(1), 87-98.

Sanromán, A., Roca, E., Núñez, M. J. and Lema, J. M. (1994). "A pulsing device for packed-bed bioreactors: II. Application to alcoholic fermentation." *Bioprocess Engineering*, 10(2), 75-81.

Sarkar, D. and Modak, J. M. (1996). "Adaptive optimization of continuous bioreactor using neural network model." *Chemical Engineering Communications*, 143(1), 99-116.

Sarti, A., Silva, A. J., Zaiat, M., and Foresti, E. (2011). "Full-scale anaerobic sequencing batch biofilm reactor for sulfate-rich wastewater treatment." *Desalination and Water treatment*, 25(1-3), 13-19.

Sawyer, L. K. and Hermanowicz, S. W. (2000). "Detachment of *Aeromonas hydrophila* and *Pseudomonas aeruginosa* due to variations in nutrient supply." *Water science and technology*, 41(4-5), 139-145.

Schaedler, S., Bukhardt, C., Kappler, A.(2008). "Evaluation of electron microscopic sample preparation methods and imaging techniques for characterization of cell-mineral aggregates." *Geomicrobiology Journal*,25(5), 228-239

Scott, J. P. and Ollis, D. F. (1995). "Integration of chemical and biological oxidation processes for water treatment: review and recommendations." *Environmental Progress*, 14(2), 88-103.

Seghezzi, L., Zeeman, G., van Lier, J. B., Hamelers, H. V. M. and Lettinga, G. (1998). "A review: the anaerobic treatment of sewage in UASB and EGSB reactors." *Bioresource Technology*, 65(3), 175-190.

Şeker, Ş., Beyenal, H., Salih, B. and Tanyolac, A. (1997). "Multi-substrate growth kinetics of *Pseudomonas putida* for phenol removal." *Applied microbiology and biotechnology*, 47(5), 610-614.

Şeker, Şule, Haluk Beyenal and Abdurrahman Tanyolaç (1995): "The effects of biofilm thickness on biofilm density and substrate consumption rate in a differential fluidized bed biofilm reactor (DFBBR)." *Journal of biotechnology* 41, no. 1 39-47.

Sekoulov, I. and Brinke-Seiferth, S. (1999). "Application of biofiltration in the crude oil processing industry." *Water science and technology*, 39(8), 71-76.

Setyawati, M.I., Chien, L.J. and Lee, C.K. (2009). "Self-immobilized recombinant *Acetobacter xylinum* for biotransformation". *Biochemical Engineering Journal* ,43, 78-84.

Seyed Alireza Mousavi Shirazi (2011). "The New Methods for Purifying the Industrial Effluents by Submerged Biofilm Reactors." *Journal of Environmental Protection*, 2, 996-1001.

Shah, M. P. (2014). "Microbiological Removal of Phenol by an Application of *Pseudomonas* spp. ETL-: An Innovative Biotechnological Approach Providing Answers to the Problems of FETP." *Journal of Applied & Environmental Microbiology*, 2(1), 6-11.

Shen, Z. J., Rama Rao, N. V. and Baird, M. H. I. (1985). "Mass transfer in a reciprocating plate extraction column—effects of mass transfer direction and plate material." *The Canadian Journal of Chemical Engineering*, 63(1), 29-36.

Sheng, G. P., Yu, H. Q. and Li, X. Y. (2010). "Extracellular Polymeric Substances (EPS) of Microbial Aggregates in Biological Wastewater Treatment Systems: A Review." *Biotechnology Advances*. 28(6), 882-894.

Sheng, G. P., Yu, H. Q. and Li, X. Y. (2010). "Extracellular Polymeric Substances (EPS) of Microbial Aggregates in Biological Wastewater Treatment Systems: A Review." *Biotechnology Advances* 28(6), 882-894.

Shetty, K. V., Kedargol, M. R. and Srinikethan, G. (2008). "Combined effect of plate pulsation parameters and phenol concentrations on the phenol removal efficiency of a pulsed plate bioreactor with immobilized cells." *Water Science and Technology*, 58(6), 1253-1259.

Shetty, G. R. and Shetty, V. K. (2016). "Pathway identification, enzyme activity and kinetic study for the biodegradation of phenol by *Nocardia hydrocarbonoxydans* NCIM 2386." *Desalination and Water Treatment*, 57(19), 8789-8801.

Shetty, K. V. and Srinikethan, G. (2010). "Oxygen mass transfer coefficients in a three-phase pulsed plate bioreactor." *International Journal of Chemical Reactor Engineering*, 8(1).

Shetty, K. V., Kalifathulla, I., and Srinikethan, G. (2007a). Performance of pulsed plate bioreactor for biodegradation of phenol. *Journal of Hazardous Materials*, 140(1), 346-352.

Shetty, K. V., Yarangali, S. B. and Srinikethan, G. (2013). "Biodegradation of phenol using immobilized nocardia hydrocarbonoxydans in a pulsed plate bioreactor: effect of packed stages, cell carrier loading, and cell acclimatization on startup and steady-state behavior." *Bioremediation Journal*, 17(4), 252-263.

Shetty, K. Vidya, R. Ramanjaneyulu, and G. Srinikethan(2007b). "Biological phenol removal using immobilized cells in a pulsed plate bioreactor: Effect of dilution rate and influent phenol concentration." *Journal of hazardous materials* 149(2), 452-459.

Shieh, W. K. and Keenan, J. D. (1986). "Fluidized bed biofilm reactor for wastewater treatment." In *Bioproducts* (pp. 131-169). Springer Berlin Heidelberg.

Shirazi, S. A. M. (2011). "The new methods for purifying the industrial effluents by submerged biofilm reactors." *Journal of Environmental Protection*, 2(07), 996.

Shreve, G. S., Olsen, R. H. and Vogel, T. M. (1991). "Development of pure culture biofilms of *Pseudomonas putida* on solid supports." *Biotechnology and bioengineering*, 37(6), 512-518.

Shreve, G. S., Olsen, R. H. and Vogel, T. M. (1991). "Development of pure culture biofilms of *Pseudomonas putida* on solid supports." *Biotechnology and bioengineering*, 37(6), 512-518.

Siegel, M.H., Hallaile, M., Herskowitz, M. and Merchuk, J.C. (1988). "Hydrodynamics and Mass Transfer in a Three-Phase Airlift Reactor." In: R. King (Ed.): *2nd International Conference on Bioreactor Fluid Dynamics*, pp. 21-23.

Simon Haykin (2009). "Neural Networks and Learning Machines." 3rd edition *EEE Pearson Prentice Hall New Jersey 07458 USA*.

Singh, R. K., and Kumar, P. R. (2014). "Development of artificial neural network modeling of p-cresol biodegradation." *cresol*, 12, 26. *International Journal of Advanced Biotechnology and Research*

Skala, D. U., Janjić, V. V., Veljković, V. B., Lazić, M. L. and Banković-ILIĆ, I. B. (1993). "Gas holdup in a gas-liquid-solid reciprocating plate column." *The Canadian Journal of Chemical Engineering*, 71(5), 817-820.

Slamet, Heri Hermansyah, Agung Sri Hendarsa and Miranda Hasanah (2015). "Biofilm composite design on pumice stone for phenol degradation in batik industrial waste." *International Journal of Environment and Waste Management* 16, no. 3 : 209-220.

Smirnova, T. A., Didenko, L. V., Azizbekyan, R. R. and Romanova, Y. M. (2010). "Structural and functional characteristics of bacterial biofilms." *Microbiology*, 79(4), 413-423.

Smith, K. H., Bowser, T. and Stevens, G. W. (2008). "Performance and scale-up of Karr reciprocating plate extraction columns." *Industrial & Engineering Chemistry Research*, 47(21), 8368-8375.

Sokół, W. (2003). "Treatment of refinery wastewater in a three-phase fluidised bed bioreactor with a low density biomass support." *Biochemical Engineering Journal*, 15(1), 1-10.

Sokół, W. and Korpál, W. (2004). "Determination of the optimal operational parameters for a three-phase fluidised bed bioreactor with a light biomass support when used in treatment of phenolic wastewaters." *Biochemical Engineering Journal*, 20(1), 49-56.

Sowinska, A., and Makowska, M. (2016). "Suspended and immobilized biomass in individual wastewater treatment systems SBR and SBBR." *Desalination and Water Treatment*, 1-12.

Speitel Jr, G. E., and DiGiano, F. A. (1987). "Biofilm shearing under dynamic conditions." *Journal of Environmental Engineering*, 113(3), 464-475.

Sridevi, V., and Lakshmi, M. C. (2009). "Effect of pH and inoculum size on phenol degradation by *Pseudomonas desmolyticum* (NCIM 2028)." *Biosciences, Biotechnology Research Asia*, 6(2), 791-795.

Sridevi, V., Chandana Lakshami, M. V. V., Manasa, M. and Sravani, M. (2012). "Metabolic pathways for the biodegradation of phenol." *International Journal of Engineering Science and Advanced Technology*, 2 : 695-705.

Srinikethan, G., Prabhakar, M. A., and Varma, Y. B. G. (1987). "Axial dispersion in plate-pulsed columns." *Bioprocess Engineering*, 2(4), 161-168.

Stamenković, I. S., Stamenković, O. S., Banković-Ilić, I. B., Lazić, M. L., Veljković, V. B. and Skala, D. U. (2005). "The gas holdup in a multiphase reciprocating plate column filled with carboxymethylcellulose solutions." *Journal of the Serbian Chemical Society*, 70(12), 1533-1544.

Stella, A., Mensforth, K. H., Bowser, T., Stevens, G. W. and Pratt, H. C. (2008). "Mass transfer performance in Karr reciprocating plate extraction columns." *Industrial & Engineering Chemistry Research*, 47(11), 3996-4007.

Stevens, G. W. and Baird, M. H. I. (1990). "A model for axial mixing in reciprocating plate columns." *Chemical engineering science*, 45(2), 457-465.

Stewart, P. S. (1998). "A review of experimental measurements of effective diffusive permeabilities and effective diffusion coefficients in biofilms." *Biotechnology Bioengineering* 59:261-272.

Stoodley, P., Boyle, J. D., DeBeer, D. and Lappin-Scott, H. M. (1999b). "Evolving perspectives of biofilm structure." *Biofouling*, 14(1), 75-90.

Stoodley, P., Boyle, J. D., Dodds, I., and Lappin-Scott, H. M. (1997). "Consensus model of biofilm structure." In: Wimpenny, J.W.T., Handley, P.S., Gilbert, P., Lappin-Scott, H.M., and Jones, M.(eds.) *Biofilms: Community Interactions and Control: 3rd meeting of the Biofilm Club*, 1-9. <http://eprints.soton.ac.uk/id/eprint/157629>

Stoodley, P., Dodds, I., Boyle, J. D. and Lappin-Scott, H. M. (1999a). "Influence of hydrodynamics and nutrients on biofilm structure." *Journal of Applied Microbiology*, 85, 19-28.

Stoodley, P., Lewandowski, Z., Boyle, J. D. and Lappin-Scott, H. M. (1998). "Oscillation characteristics of biofilm streamers in turbulent flowing water as related to drag and pressure drop." *Biotechnology and bioengineering*, 57(5), 536-544.

Subramanian, S. B., Yan, S., Tyagi, R. D. and Surampalli, R. Y. (2010). "Extracellular polymeric substances (EPS) producing bacterial strains of municipal wastewater sludge: isolation, molecular identification, EPS characterization and performance for sludge settling and dewatering." *Water research*, 44(7), 2253-2266.

Sundaresan, A., and Varma, Y.B.G. (1990). "Dispersed Phase and Holdup in Bubble size Distribution in Gas-Liquid Countercurrent Flow in Reciprocating Plate Column." *The Canadian Journal of Chemical Engineering*, 68, 560-568.

Sutherland, I. W. (2001). "Biofilm exopolysaccharides: a strong and sticky framework." *Microbiology*, 147(1), 3-9

Tang, B., Yu, C., Bin, L., Zhao, Y., Feng, X., Huang, S., and Chen, Q. (2016). "Essential factors of an integrated moving bed biofilm reactor–membrane bioreactor: Adhesion characteristics and microbial community of the biofilm." *Bioresourcetechnology*, 211, 574-583.

Tang, W. T., and Fan, L. S. (1987). "Steady state phenol degradation in a draft-tube, gas-liquid-solid fluidized-bed bioreactor." *AIChE journal*, 33(2), 239-249.

Tanyolaç, A. and Beyenal, H. (1996). "Predicting average biofilm density of a fully active spherical bioparticle." *Journal of biotechnology*, 52(1), 39-49.

Tanyolaç, A. and Beyenal, H. (1998). "Prediction of substrate consumption rate, average biofilm density and active thickness for a thin spherical biofilm at pseudo-steady state." *Biochemical engineering journal*, 2(3), 207-216.

The Environment (Protection) Rules 1986a "<http://cpcb.nic.in/GeneralStandards.pdf>"

The Environment (Protection) Rules 1986b "<http://www.cpcb.nic.in/Industry-Specific-Standards/Effluent/402.pdf>" (Date of Access, 02Feb 2016)

Tijhuis, L., Hijman, B., Van Loosdrecht, M. V. and Heijnen, J. J. (1995). "Influence of detachment, substrate loading and reactor scale on the formation of biofilms in airlift reactors." *Applied microbiology and biotechnology*, 45(1-2), 7-17.

Tijhuis, L., M. C. M. Van Loosdrecht and J. J. Heijnen (1994). "Formation and growth of heterotrophic aerobic biofilms on small suspended particles in airlift reactors." *Biotechnology and bioengineering* 44, no. 5 : 595-608.

Tolker-Nielsen, T. and Molin, S. (2000). "Spatial organization of microbial biofilm communities." *Microbial ecology*, 40(2), 75-84.

Trulear, M. G., and Characklis, W. G. (1982). "Dynamics of biofilm processes." *Journal (Water Pollution Control Federation)*, 1288-1301.

Tyagi, R. D. and Ghose, T. K. (1982). "Studies on immobilized *Saccharomyces cerevisiae*. I. Analysis of continuous rapid ethanol fermentation in immobilized cell reactor." *Biotechnology and bioengineering*, 24(4), 781-795. doi: 10.1002/bit.260240403.

Unell, M., Nordin, K., Jernberg, C., Stenström, J. and Jansson, J. K. (2008). "Degradation of mixtures of phenolic compounds by *Arthrobacter chlorophenicus* A6." *Biodegradation*, 19(4), 495-505.

Usman, M. R., Sattar, H., Hussain, S. N., Muhammad, H., Asghar, A. and Afzal, W. (2009). "Drop size in a liquid pulsed sieve-plate extraction column." *Brazilian Journal of Chemical Engineering*, 26(4), 677-683.

Van Benthum, W. A. J., Van Loosdrecht, M. C. M. and Heijnen, J. J. (1997). "Control of heterotrophic layer formation on nitrifying biofilms in a biofilm airlift suspension reactor." *Biotechnology and bioengineering*, 53(4), 397-405.

Van Loosdrecht, M. C. M., Eikelboom, D., Gjaltema, A., Mulder, A., Tjihuis, L. and Heijnen, J. J. (1995). "Biofilm Structures." *Water Science and Technology*, 32(8), 35-43.

Van Loosdrecht, M. C., Lyklema, J., Norde, W., Schraa, G. and Zehnder, A. J. (1987). "The role of bacterial cell wall hydrophobicity in adhesion." *Applied and environmental microbiology*, 53(8), 1893-1897.

Van Loosdrecht, Mark C. M., and Sef J. Heijnen (1993). "Biofilm bioreactors for waste-water treatment." *Trends in Biotechnology* 11(4), 117-121.

Vanysacker L, Denis C, Declerk P, Piasecka A and Vankelecom I F J (2013). "Microbial Adhesion and Biofilm Formation on Microfiltration Membranes: A Detailed Characterization Using Model Organisms with Increasing Complexity." *BioMed Research International* (2013) <http://dx.doi.org/10.1155/2013/470867>.

Vasić, L. S., Banković-Ilić, I. B., Lazić, M. L., Veljković, V. B. and Skala, D. U. (2007). "Oxygen mass transfer in a 16.6 cm id multiphase reciprocating plate column." *Journal of the Serbian Chemical Society*, 72(5), 523-531.

Vicente, A.A., Mota, M. and Teixeira, J.A. (2001). "Flocculation Bioreactors." In: *Multiphase Bioreactor Design*, J.M.S. Cabral, M. Mota, J. Tramper (Eds.), Harwood Academic Publishers, London.

Vieira, M. J., Melo, L. F. and Pinheiro, M. M. (1993). "Biofilm formation: hydrodynamic effects on internal diffusion and structure." *Biofouling*, 7(1), 67-80.

Viggiani, A., Olivieri, G., Siani, L., Di Donato, A., Marzocchella, A., Salatino, P., and Galli, E. (2006). "An airlift biofilm reactor for the biodegradation of phenol by *Pseudomonas stutzeri* OX1." *Journal of biotechnology*, 123(4), 464-477.

Vijayagopal, V., & Sabarathinam, P. L. (2008). “ Kinetics of biological treatment of phenolic wastewater in a three phase draft tube fluidized bed bioreactor containing biofilm.” *African journal of biotechnology*, 7(6).

Villasenor, J. C., Van Loosdrecht, M. C. M., Picioreanu, C. and Heijnen, J. J. (2000). “Influence of Different Substrates on the Formation of Biofilms in a Biofilm Airlift Suspension Reactor.” *Water Science & Technology*, 41(4), 323-330.

Wang, C., and Li, Y. (2007). “Incorporation of granular activated carbon in an immobilized membrane bioreactor for the biodegradation of phenol by *Pseudomonas putida*.” *Biotechnology letters*, 29(9), 1353-1356.

Wang, F., Wang, W. G., Wang, X. J., Wang, H. Y., Tung, C. H. and Wu, L. Z. (2011). “A highly efficient photocatalytic system for hydrogen production by a robust hydrogenase mimic in an aqueous solution.” *Angewandte Chemie International Edition*, 50(14), 3193-3197.

Wang, Z. W., Hamilton-Brehm, S. D., Lochner, A., Elkins, J. G. and Morrell-Falvey, J. L. (2011). “Mathematical modeling of hydrolysate diffusion and utilization in cellulolytic biofilms of the extreme thermophile *Caldicellulosiruptor obsidiansis*.” *Bioresource technology*, 102(3), 3155-3162.

Wang, Z., Cai, W., Hong, X., Zhao, X., Xu, F., and Cai, C. (2005). “Photocatalytic degradation of phenol in aqueous nitrogen-doped TiO₂ suspensions with various light sources.” *Applied Catalysis B: Environmental*, 57(3), 223-231.

Wanner, O. and Gujer, W. (1986). “A multispecies biofilm model.” *Biotechnology and bioengineering*, 28(3), 314-328.

Wäsche, S., Horn, H. and Hempel, D. C. (2000). "Mass Transfer Phenomena in Biofilm Systems." *Water Science and Technology*, 41(4-5), 357-360.

WHO (2011) "Guidelines for Drinking-water Quality" 4th ed.
http://apps.who.int/iris/bitstream/10665/44584/1/9789241548151_eng.pdf

Wijeyekoon, S., Mino, T., Satoh, H. and Matsuo, T. (2004). "Effects of substrate loading rate on biofilm structure." *Water research*, 38(10), 2479-2488.

Wilderer, P. A., Arnz, P. and Arnold, E. (2000). "Application of biofilms and biofilm support materials as a temporary sink and source." *Water, air, and soil pollution*, 123(1-4), 147-158.

Williamson, K. and McCarty, P. L. (1976). "A model of substrate utilization by bacterial films." *Journal (Water Pollution Control Federation)*, 9-24.

Wimpenny, J. W. T. and Colasanti, R. (1997). "A unifying hypothesis for the structure of microbial biofilms based on cellular automaton models." *FEMS Microbiology Ecology*, 22, 1-16.

Xiao, J. and Chu, S. (2015). "A novel bamboo fiber biofilm carrier and its utilization in the upgrade of wastewater treatment plant." *Desalination and Water Treatment*, 56(3), 574-582.

Xu, H. and Liu, Y. (2011). "D-Amino acid mitigated membrane biofouling and promoted biofilm detachment." *Journal of membrane science*, 376(1), 266-274.

Yan, J., Jianping, W., Hongmei, L., Suliang, Y. and Zongding, H. (2005). "The biodegradation of phenol at high initial concentration by the yeast *Candida tropicalis*." *Biochemical Engineering Journal*, 24(3), 243-247.

Yang, C., Qian, Y., Zhang, L. and Feng, J. (2006). "Solvent extraction process development and on-site trial-plant for phenol removal from industrial coal-gasification wastewater." *Chemical Engineering Journal*, 117(2), 179-185.

Yang, S. and Lewandowski, Z. (1995). "Measurement of local mass transfer coefficient in biofilms." *Biotechnology and bioengineering*, 48(6), 737-744.

Yavuz, Y., Savas Koparal, A. and Bakir Ögütveren, Ü. (2007). "Phenol removal through chemical oxidation using Fenton reagent." *Chemical engineering and technology*, 30(5), 583-586.

Ying, W., Ye, T., Bin, H., ZHAO, H. B., BI, J. N. and CAI, B. L. (2007). "Biodegradation of phenol by free and immobilized *Acinetobacter* sp. strain PD12." *Journal of Environmental Sciences*, 19(2), 222-225.

Yotova, L., D. Marinkova, V. Mironova and R. Dulgerova (2009). "Investigation of Formation, Development and Application of *Arthrobacter Oxydans* 1388 Biofilm." *Biotechnology and Biotechnological Equipment* 23 (1), 823-826.

Yousef, R. I., El-Eswed, B. and Ala'a, H. (2011). "Adsorption characteristics of natural zeolites as solid adsorbents for phenol removal from aqueous solutions: kinetics, mechanism, and thermodynamics studies." *Chemical Engineering Journal*, 171(3), 1143-1149.

Yu Liu (2002). “ The accumulation of fixed biomass increases the observed growth yield of a nitrifying biofilm.” *Biotechnology Letters* **24**: 391–394.

Yung, K. K., Smith, C. D., Bowser, T., Perera, J. M. and Stevens, G. W. (2012). “The use of an ionic liquid in a Karr reciprocating plate extraction column.” *Chemical Engineering Research and Design*, 90(11), 2034-2040.

Zafarzadeh, A., Bina, B., Nikaeen, M., Attar, H. M. and Nejad, M. H. (2010). “Performance of moving bed biofilm reactors for biological nitrogen compounds removal from wastewater by partial nitrification-denitrification process.” *Iranian Journal of Environmental Health Science and Engineering*, 7(4), 353.

Zhang, T. C., Bishop, P. L. and Gibbs, J. T. (1994). “Effect of roughness and thickness of biofilms on external mass transfer resistance.” *In: Critical Issues in Water and Wastewater Treatment National*.

Zhang, T. C., Fu, Y. C., & Bishop, P. L. (1995). “Competition for substrate and space in biofilms.” *Water Environment Research*, 67(6), 992-1003.

Zhang, W., Seminara, A., Suaris, M., Brenner, M. P., Weitz, D. A. and Angelini, T. E. (2014). “Nutrient depletion in *Bacillus subtilis* biofilms triggers matrix production.” *New Journal of Physics*, 16(1).

Zhang, X. Q., Bishop, P. L. and Kupferle, M. J. (1998). “Measurement of polysaccharides and proteins in biofilm extracellular polymers.” *Water Science and Technology* 37, 345-348.

Zhang, X., Chen, X., Zhang, C., Wen, H., Guo, W. and Ngo, H. H. (2016). “Effect of filling fraction on the performance of sponge-based moving bed biofilm reactor.” *Bioresource Technology*.

Zune, Q., Toye, D., Delvigne, F., Brognaux, A., Ongena, M. and Thonart, P. (2013). “Biofilm formation on metal structured packing for the production of high added value biomolecules.” *Récents Progrès en Génie des Procédés*. ISSN: 1775-335X ; ISBN: 978-2-910239-78-7, Ed. SFGP, Paris, France.

List of Publications based on PhD Research Work

1. Veena, B. R., Shetty K. Vidya and Saidutta, M. B. (2015). "Shear Stress Effects on Production of Exopolymeric Substances and Biofilm Characteristics During Phenol Biodegradation by Immobilized *Pseudomonas desmolyticum* (NCIM2112) Cells in a Pulsed Plate Bioreactor." *Preparative Biochemistry and Biotechnology*.
ISSN: 1082-6068 (Print) 1532-2297 (Online) Journal homepage:
<http://www.tandfonline.com/loi/lpbb20>
2. Veena B. R., Vidya, S.K. and Vidya and Saidutta, M. B. (2016). "Effect of dilution rate on dynamic and steady-state biofilm characteristics during phenol biodegradation by immobilized *Pseudomonas desmolyticum* cells in a pulsed plate bioreactor." *Frontiers in Environmental Science and Engineering*. 10(4): 16 DOI :10.1007/s11783-016-0863-9.

BIODATA

1	Name	B.R.Veena
2	Date of Birth	19.12.1966
3	Education Qulification	B.E.(Chemical Engineering) M.E. (Chemical Engineering)
4	Designation	Associate Professor
5	Address	Department of Chemical Engineering DSCE, Bangalore-78
6	Contact Details	Email: veenabr@hotmail.com veenasridhara@gmail.com Mob: +9448804370
7	Teaching Experience	25 years
8	Membership of Professional bodies	ISTE-LM IChE-LM
9	Area of Research Work	Environmental and Biochemical Engineering